Towards understanding the role of membrane cholesterol and sialic acid in the function of immune cells: studies with monoclonal antibodies

PhD Thesis

Andrea Balogh

2010

Supervisors:
Prof. János Matkó D.Sc.
Glória László Ph.D.

Immunology Programme
Programme leader: Prof. Anna Erdei D.Sc.

Department of Immunology
Institute of Biology
Eötvös Loránd University, Budapest, Hungary

Contents

Abbreviations

Ab	antibody
ACHA	anti-cholesterol antibody
APC	antigen-presenting cell
BCR	B cell receptor
BLNK	B cell linker protein
CD	cluster of differentiation
CRAC	cholesterol recognition/interaction amino acid consensus
CTX-B	cholera toxin-B
DAP-12	DNAX-activating protein of 12 kDa
DRM	detergent resistant membrane
ER	endoplasmic reticulum
Fab	Fragment antigen binding
Fas	TNF superfamily receptor 6
FCS	fluoresence correlation spectroscopy
FRET	föster/fluorescnence resonance energy transfer
Gal	galactose
Glc	glucose
GlcNAc	N-acetylglucosamine
GPI	glycosylphosphatidylinositol
HCV	hepatitis C virus
HEV	high endothelial venule
HIV-1	human immunodeficiency virus type I
HSA	heat stabile antigen
IL	interleukine
ITAM	immunoreceptor tyrosine-based activation motif
ITIM	immunoreceptor tyrosine-based inhibitory motif
LAT	linker for activation of T cells
Lck	leukocyte-specific protein tyrosine kinase
Lyn	an src family tyrosine-protein kinase
MHC	major histocompatibility gene complex
PBMC	peripheral blood mononuclear cell
$PI(4,5)P_2$	phosphatidylinositol 4,5-bisphosphate
PKCθ	protein kinase c theta
Sia	sialic acid
Siglecs	sialic acid binding immunoglobulin-like lectins
SNA	Sambucus nigra agglutinin
SLP-76	SH2-domain-containing leukocyte protein of 76 kDa
Syk	spleen tyrosine kinase
TCR	T cell receptor
Th	T helper
Tc	T cytotoxic
TNF	tumor necrosis factor
YIYF	tyrosine-isoleucine-tyrosine-phenylalanine
ZAP-70	zeta-chain-associated protein kinase 70

Chapter 1

Introduction

The immune system is a remarkably adaptive defense apparatus that has evolved in vertebrates to protect them from invading pathogenic microorganisms and cancer, preserving this way the consistency of the genetic code. This unique apparatus is able to generate an enormous variety and numbers of cells and molecules capable of recognizing and eliminating foreign invaders. Either the innate immunity, providing immediate and non-specific response, or the adaptive immunity which is capable of specific recognition and selective elimination of pathogenic agents upon activation by the innate response, consist of both soluble and cellular components. The cell membrane physically separates the intracellular components from the extracellular environment, keeping thereby the integrity of cells and serving also as a communication platform. Therefore, intact plasma membrane is required for cell viability and normal cell functions. Plasma membrane of immune cells consists of proteins, lipids and carbohydrates attached to the previous ones. Distribution and glycosylation of membrane molecules is highly inhomogeneous.

Simons and Ikonen formulated the ‘lipid raft hypothesis’, according to which the lateral assembly of glycosphingolipids, sphingomyelin and cholesterol creates ordered microdomains floating in a glycerophospholipid-rich fluid environment and able to recruit a specific set of proteins while excluding others. (Simons and Ikonen, 1997). Many studies explored various roles of lipid rafts in immunocyte signalling, membrane trafficking and in entry of various pathogens into target cells, demonstrating their importance in the function of immune cells (Horejsi, 2003; Matko and Szollosi, 2002).

Glycosylation of raft-associated or non-raft membrane components is another critical factor that controls cell functions. Sialic acid and its derivatives are ligands of Sia-binding proteins, many of them expressed by cells of hematopoietic origin. These receptors, involving siglecs and selectins, play role in cell-cell interactions, cell signalling or endocytosis. In this way, they regulate the homing and activation of lymphoid and myeloid cells.

Since the details of lipid raft- and glycosylation-dependent immune functions remained in many cases (e.g. infection by pathogens, cellular activation, motility, homing, maturation etc.) controversial or unclear, studying the role of cholesterol and sialic acid in the membrane of immune cells can certainly broaden our knowledge about these processes.

1.1. Lipid rafts and the immune system

1.1.1. Composition and heterogeneity of lipid rafts

Lipid rafts of mammalian cells have unique lipid and protein composition. Sphingomyelin and glycosphingolipids with saturated acyl chains associate with each other and are more tightly packed than the surrounding bilayer (Simons and Ikonen, 1997). Cholesterol, the major structural component of these domains, fills gaps between saturated fatty acids and is required in establishing proper membrane fluidity over the range of physiological temperatures (Brown and London, 2000). Raftophilic lipids, due to their biophysical properties, are in a liquid-ordered (L_o) type of organization in the membrane, while other parts of the plasma membrane are in liquid-disordered phase (L_d) (Mukherjee and Maxfield, 2004). The interaction of cholesterol with lipids is dictated to a large extent by fitting of its planar steroid ring to the fully saturated acyl chains of neighbouring lipids, supporting van der Waals attractive forces. Moreover, hydrogen bonding between the hydroxyl group of cholesterol and the amide group of sphingomyelin could further stabilize the interaction between these raft-resident lipids (Veiga et al., 2001). In model membrane vesicles it has been demonstrated that small modifications of cholesterol structure have moderately deleterious effects on the ability to support raft formation (Wang et al., 2004). For example, the free 3-β-hydroxyl group is important, but not absolutely necessary, for the promotion of ordered domain formation by steroids. Ceramide can accumulate in detergent-resistant membrane domains upon sphingomyelinase action (Megha et al., 2006), leading to formation of large platforms in certain types of apoptosis and bacterial infections. Cholesterol is displaced in these ceramide-rich domains and that is likely to have consequences for raft functions based on altered association of cholesterol-bound proteins with rafts (Megha and London, 2004).

Different types of protein-lipidations can direct proteins to raft microdomains. GPI-linkage targets proteins exclusively to lipid rafts, because phosphoinositide anchors usually have saturated acyl chains (Schroeder et al., 1998). On leukocytes, many GPI-anchored proteins have been revealed to be detergent resistant, e.g. CD14, HSA (CD24), CD48, CD55, CD59, Thy-1 (CD90) (Horejsi et al., 1999). These glycoproteins are members of adhesion molecules, pathogen receptors, ectoenzymes, complement-regulatory proteins etc. In the cytomplasmic leaflet, palmitoylated and myristoylated proteins partition into ordered domains. Most prominent members are

src-family protein tyrosine kinases, containing palmitic and/or myristic acid moieties, that are implicated in relaying signals downstream of a wide variety of cell-surface receptors to evoke and regulate diverse cellular responses including proliferation, differentiation and cell survival (Lowell, 2004). In contrast, the uneven surface of a prenyl group commonly excludes proteins from raft domains (Melkonian et al., 1999). The nature and length of the transmembrane helical segment might also be factors critically determining sorting of integral membrane proteins into raft or non-raft regions (McIntosh et al., 2003). Dozen's of proteins, including TCR and BCR, can be recruited to lipid rafts upon multimerization or conformational changes. In addition, **CRAC** motif and **YIYF** amino acid sequence in the juxtamembrane segment are thought to play role in recognizing cholesterol, thereby keeping proteins in raft regions (Kuwabara and Labouesse, 2002; Li et al., 2001).

Caveolae is a special group of rafts that are small, flask-shaped invaginations (25-150 nm) stabilized by caveolin, a cholesterol-binding protein (Thorn et al., 2003). Caveolin-1 contains three sites of palmitoylation at cysteine residues. When palmitoylation sites were mutated, the resulting protein still translocated to caveolae (Dietzen et al., 1995). CRAC motif occurs in caveolin-1 that can partition the mutated protein into rafts (Williams and Lisanti, 2004). The HIV-1 gp41 protein has been also shown to contain a segment with a CRAC motif adjacent to its transmembrane helix that promotes membrane fusion (Salzwedel et al., 1999). CCR7, which is an important chemokine receptor of lymphocyte homing to peripheral lymph nodes and spleen, have both CRAC and YIYF motifs (Epand, 2006). In spite of this, raft-association of CCR7 is still elusive (Molon et al., 2005), suggesting that other parts of the protein might interfere with localization to detergent resistant membranes (DRMs).

The rafts in cells appear to be heterogeneous both in terms of their protein and lipid content, and can be localized to different regions of the cell. They are 10-200 nm sized dynamic membrane structures that can extend up to 1 μm sized stabile microdomains upon cross-linking or different stimuli. Therefore, the activation and differentiation state of a given cell type determines the raft size and composition. Different methods provide evidence for raft heterogeneity. These are the differential detergent-sensitivity, separation of raft proteins by immunoaffinity chromatography and direct visualization of raft proteins and lipids in spatially distinct regions of the cell (Pike, 2004). For example, the GPI-anchored CD24 was found in detergent

resistant membrane fractions by Triton X-100 solubilization, but only 42% of this protein was in the rafts fractions if murine T-lymphoma cells were extracted with 60mM octylglucoside (Ilangumaran et al., 1999). Thy-1 did not show this difference. Immunopurification of Thy-1 or CD3ε by monoclonal antibodies in another cell line, also suggest that CD3ε is present only a small subset of lipid rafts, whereas the bulk of the Thy-1 is distributed into other detergent-resistant domains (Drevot et al., 2002). Gomez-Mouton et al. demonstrated that ganglioside G_{M3} and the GPI-anchored protein, urokinase plasminogen activator receptor, were localized exclusively at the leading edge of the polarized T cells. Conversely, ganglioside G_{M1} and the raft-localized transmembrane domain protein, CD44, were localized at the trailing edge of the cells. All four of these components were present in the low-density detergent-insoluble fraction of Jurkat T cells (Gomez-Mouton et al., 2001). Thus, in intact cells the investigated raft markers were physically distinct and spatially segregated from each other. Analysis of early events of T cell activation also provided evidence for raft heterogeneity. Colocalization of Lck kinase and LAT adaptor protein to distinct raft domains was shown by electron microscopy (Schade and Levine, 2002).

Consequently, not only lipid-lipid, but lipid-protein and protein-protein interactions can also essentially influence formation and composition of lipid rafts. In *Figure 1* the structure of cholesterol and a schematic representation of lipid raft organization can be seen.

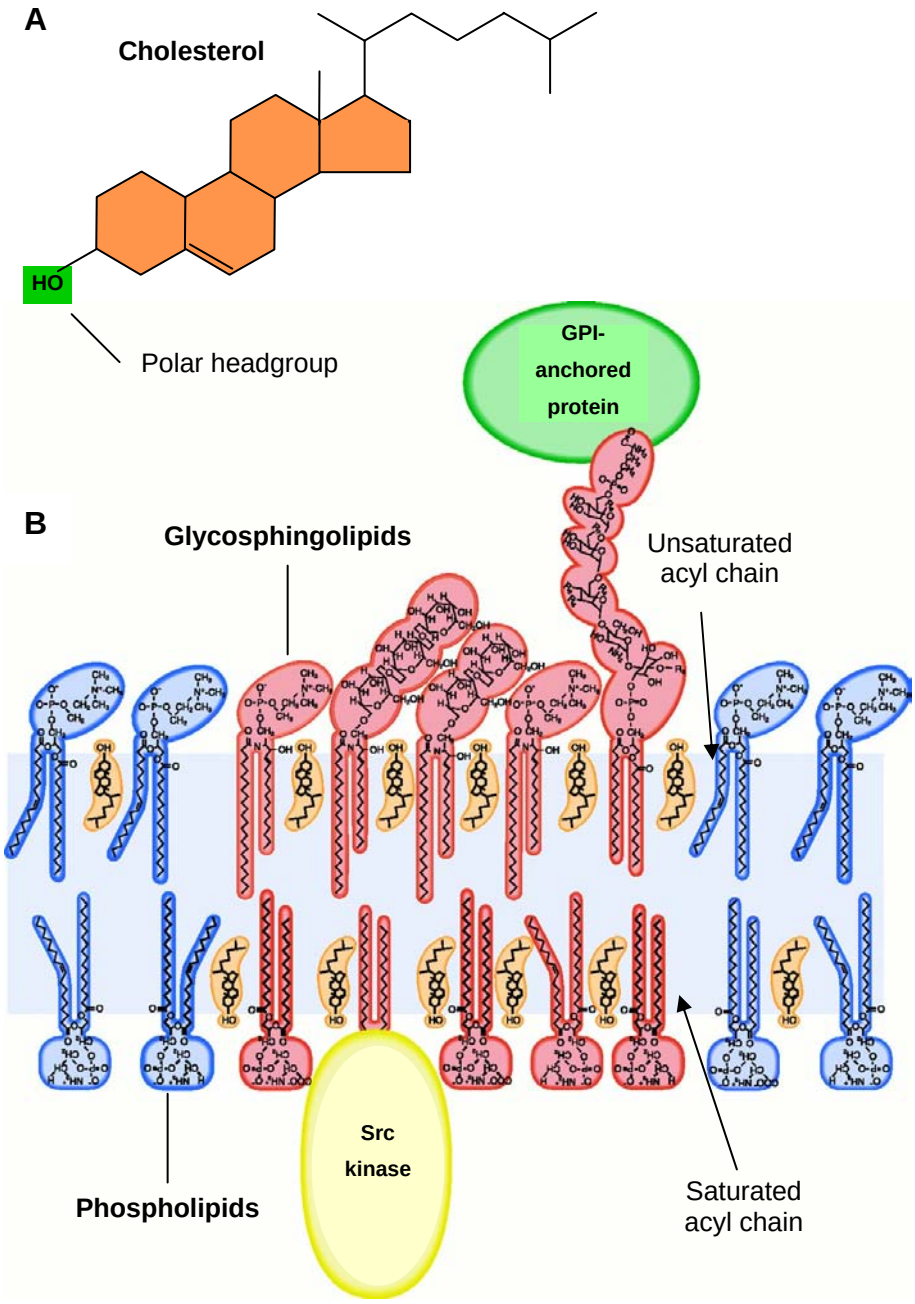

Figure 1. (A) Structure of cholesterol. *The body of cholesterol consists of a series of fused rings, which make that part of the molecule quite rigid. At one end of this planar ring system is a hydroxyl group and at the other end is a hydrocarbon tail, so cholesterol, like other membrane lipids, has both hydrophilic and hydrophobic poles that determine its positioning within the lipid bilayer.* ***(B) Schematic representation of lipid raft organization in the cell membrane.*** *The outer leaflet of the membrane rafts (liquid-ordered phase; L_o) is enriched in glycosphingolipids and sphingomyelin and the corresponding inner leaflet is illustrated as containing glycerolipids with predominantly saturated fatty acyls. Cholesterol partitions preferentially into the L_o phase. GPI-anchored proteins are attached to the exoplasmic leaflet, and a doubly acylated Src-kinases to the cytoplasmic leaflet (Simons and Ikonen, 2000).*

1.1.2. What is the function of lipid rafts in the membrane of immune cells?

Functions of lipid rafts have been widely studied in the last 15 years. Caveolin$^+$ and caveolin$^-$ lipid rafts play an important role in many cellular processes, including signal transduction, membrane sorting and trafficking, cell polarization, immunological synapse formation, cell movement or pathogen entry *(Figure 2)*. Next, I will mention several examples without the claim of completeness.

The spatial organization of immune receptors and components of their signalling cascades plays a central role in the initiation and regulation of signal transduction. The abundance of signalling molecules in lipid rafts suggests that these domains are key organizing elements of signal transduction (Brown and London, 1998). Many antigen receptors of the immune system belong to the family of multichain immune recognition receptors (MIRRs). Binding of ligand (antigen) to MIRR results in receptor phosphorylation, triggering downstream signalling pathways and cellular activation (Sigalov, 2005). TCR on T lymphocytes, BCR on B cells or FcεRI expressed by mast cells belong to this family. It has been shown by detergent resistance measurements or confocal microscopic colocalization studies that rafts are critical in signalling of these receptors. In resting lymphocytes TCR is excluded from rafts, while other signalling components, such as Lck, LAT or CD4/CD8 co-receptors are concentrated to them (Dykstra et al., 2003). Upon engagement, TCR becomes raft-associated and other members of the 'signalosome' including the kinase ZAP-70, the adaptor protein SLP-76 and PKCθ, are also recruited to lipid rafts following TCR activation (Dykstra et al., 2003). Indeed, more than seventy raft-associated proteins have been identified in resting and activated Jurkat T cells by proteomic analysis (von Haller et al., 2001). Similar events take place during B cell activation, just in this case, the BCR, kinases Lyn and Syk or BLNK adaptor protein are the key signal elements (Cheng et al., 1999). The raft proteome of B cells involves cytoskeletal proteins, transmembrane receptors, cell surface glycoproteins, Src-family kinases, small G proteins, heterotrimeric G proteins, motor proteins and trafficking proteins as analyzed by mass spectrometry of isolated DRMs (Gupta et al., 2006).

The role of lipid rafts in spatial organization and compartmentalization of receptors other than MIRRs and downstream signalling elements has also been proven. For instance, cross-linking of MHC class II molecules on APCs with specific antibody was followed by its colocalization with G_{M1} gangliosides and partition into

insoluble membranes (Huby et al., 1999). Other studies demonstrated a constitutive raft-association of class II molecules (Anderson et al., 2000; Gombos et al., 2004). Furthermore, coengagement of CD28, co-receptor known to lower the threshold for TCR activation, resulted in both an increase of raft-localization and its redistribution to the immunological synapse (Martin et al., 2001; Viola et al., 1999). Thus, formation of clustered rafts in T cells and APCs is needed to the formation of the immunological synapse (Gombos et al., 2004).

Lipid rafts play role, beside cell activation, in other signalling events, such as apoptosis, cell growth or differentiation. Recruitment of TNF receptor 1 or Fas receptor to these microdomains was revealed by different groups (Legler et al., 2003; Scheel-Toellner et al., 2002). In addition, the disruption of lipid rafts has led to the inhibition of ligand-induced apoptosis. Differences in raft composition and abundance have been implicated in regulating responses in the T cell subsets (Th1, Th2, Tc) and in naïve or effector T cells (Balamuth et al., 2001; de Mello Coelho et al., 2004; Tuosto et al., 2001). The response of B lymphocytes to BCR stimuli depends on their differentiation state as well. In pre-B cells, the pre-BCR constantly resides in lipid rafts and signals for survival. BCR is excluded from rafts in immature and mature resting B cells. However, upon cross-linking, BCR became stably raft-associated only in mature cells, but not in immature or tolerant ones (Chung et al., 2001; Weintraub et al., 2000).

Not just immune synapse formation, but chemotaxis also requires asymmetric redistribution of membrane receptors, signalling molecules and the actin cytoskeleton. (Manes and Viola, 2006). The spatial segregation of different raft-associated molecules in polarized T lymphocytes is described in the previous section. Another example is the morphologic polarization of human hematopoietic stem cells, where redistribution of several lipid raft markers, including cholesterol-binding protein prominin-1 (CD133), during migration has been observed (Giebel et al., 2004).

The endocytic role of caveolae and lipid rafts has been substantially investigated by Fivaz et al. (Fivaz et al., 2002). They concluded that trafficking of GPI-anchored proteins (GPI-APs) is controlled by their residence time in rafts, and hence that raft partitioning regulates GPI-APs sorting in the endocytic pathway. However, caveolae/raft ligands can also be internalized by other endocytic pathway. For instance, cholera and shiga toxins bind to cell surface raft domains and yet are internalized *via* clathrin-dependent pathways (Sandvig et al., 1989; Shogomori and

Futerman, 2001). Various bacteria, viruses and even parasites use lipid rafts/caveolae as portals of entry into target cells. For example, the FimH (mannose-binding fimbrial adhesin) expressing form of *Escherichia coli* is taken up by mast cells and macrophages *via* an endocytic route that does not include fusion with lysosomes and thus, the intracellular bacteria remain in viable state. The receptor for it was identified as CD48, a GPI-anchored protein (Shin and Abraham, 2001). Another interesting finding is that the parasitophorous vacuole of *Plasmodium falciparum* and *Toxoplasma gondii* is enriched in GPI-anchored proteins and raftophilic lipids (Lauer et al., 2000; Mordue et al., 1999). In the following section, I will focus on a specific case, the role of lipid microdomains in the infection by HIV-1, a member of the retrovirus family.

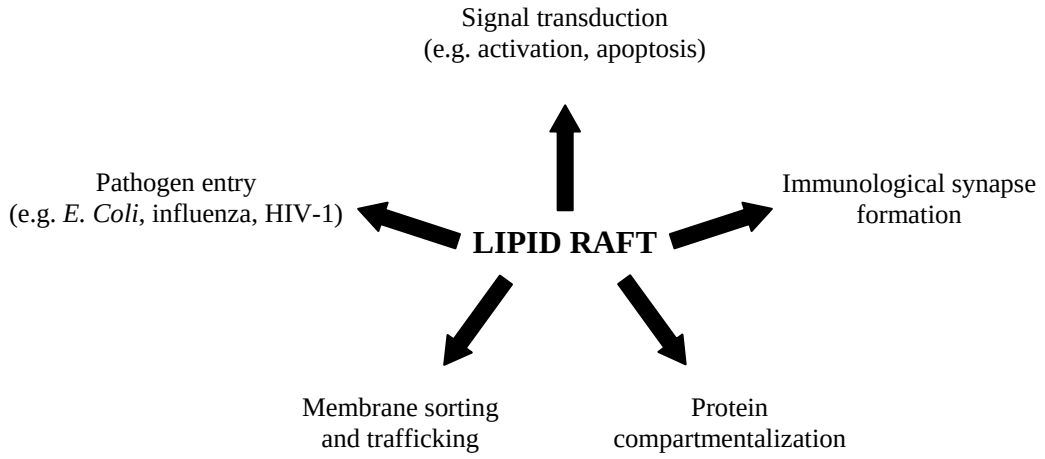

Figure 2. Role of lipid rafts in immune cell functions. *Cholesterol- and sphingolipid-rich lipid rafts are capable to spatio-temporally organize membrane proteins and thereby regulate various functions of immunocytes including signal transduction, membrane trafficking and pathogen uptake.*

1.1.3. Lipid rafts and the pathogenesis of HIV-1

Role of lipid rafts in the pathogenesis of HIV-1 is an important area of nowadays' biology. Many papers have reported on cholesterol- and lipid raft-requirement for the entry of the virus into the target cells. This is compatible with the finding that CD4, the primary receptor of HIV-1, is a palmitoylated protein, and thus it is constitutively present in raft microdomains (Fragoso et al., 2003). The CCR5 and CXCR4 chemokine receptors, known as co-receptors of the virus, are at least raft-partitioned and can dynamically associate to DRMs upon various stimuli (Baker et al., 2007; Nguyen and Taub, 2002; Xiao et al., 2000). HIV-1 entry into the host cell is a multistep process that comprises viral attachment, co-receptor interactions and fusion *(Figure 3)*. Initial interactions between gp120 (an abundant glycoprotein in the virus shell) and CD4 are followed by conformational changes in Env viral protein, permitting the interaction of the gp120-CD4 complex with the co-receptor leading to a further barrage of conformational changes that eventually lead to gp41 six-helix bundle formation and fusion (Gallo et al., 2003). Cholesterol is indeed required to this process. Depletion of the host membrane cholesterol strongly decreased HIV-1 infectivity by diminished binding of the virus (Guyader et al., 2002; Liao et al., 2001). Another group has also confirmed this observation by using cholesterol oxidase to sequester cholesterol from lipid rafts (Nguyen and Taub, 2003), instead of β-cyclodextrin, known to form soluble inclusion complexes with cholesterol, thereby removing it from the membrane. Furthermore, cross-linking HIV-1 particles by antibodies has led to the coaggregation of various raft-associated proteins, like CD59 and CD90 (Nisole et al., 2002). The presence of gp120 glycoprotein in membrane microdomains has also been reported. Recombinant gp120 highly colocalized with the raft component G_{M1} ganglioside and could be detected in DRM fractions (Popik et al., 2002). The proximity of gp120 and G_{M1} was shown by fluorescence resonance energy transfer (FRET) imaging as well (Yi et al., 2006).

On the other hand, cholesterol-rich membrane microdomains proved to be also critical in HIV-1 assembly/budding *(Figure 4)*. Gag is a structural component of the viral particle driving virion assembly. The protein is myristoylated on the N-terminal, therefore it favours tightly packed part of the plasma membrane where it is directed post-synthesis (Kawada et al., 2008). Gag also interacts with $PI(4,5)P_2$ and annexin2, two raft-localized molecules (Harrist et al., 2009; Lindwasser and Resh, 2001). The

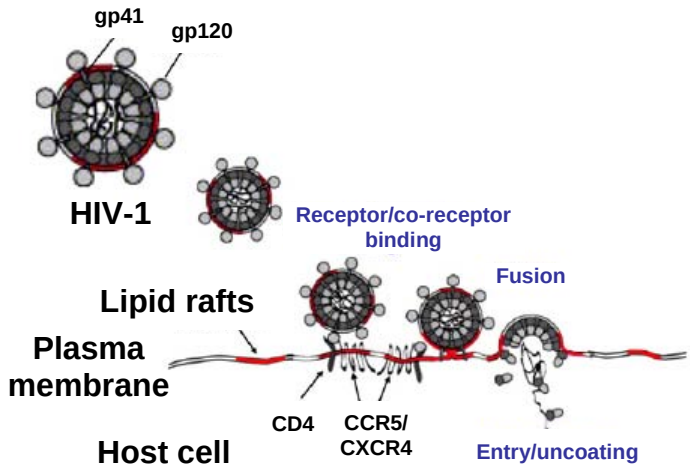

Figure 3. HIV-1 entry into the target cell. *Env glycoprotein, gp120, on the surface of HIV-1 virion binds to CD4 receptor in the lipid raft region of HIV-1 permissive cells. This binding induces conformational changes in the glycoprotein leading to interaction with CCR5/CXCR4 co-receptor. The glycoprotein gp41-mediated membrane fusion between viral and plasma membrane results in viral entry and uncoating (Waheed and Freed, 2009).*

annexin2-Gag protein interaction is PI(4,5)P_2-dependent, since depletion of PI(4,5)P_2 caused failure of Gag trafficking to the plasma membrane (Harrist et al., 2009). Two other viral proteins, Env and Nef, were described to be palmitoylated and myristoylated, respectively (Bhattacharya et al., 2004; Wang et al., 2000). The cytoplasmic domain of gp41, an Env protein, contains cysteine residues (C764 and C837) which are targets for palmitoylation and when these cysteine residues were mutated, gp41 was not able to associate with lipid rafts (Bhattacharya et al., 2004). Furthermore, Gag regulates the raft-association of Env, since in the absence of Gag, Env proteins failed to associate with DRMs (Bhattacharya et al., 2006). It has been shown by confocal microscopy that HIV-1 incorporated GPI-linked host cell proteins, CD59 and CD90, and G_{M1} ganglioside in its membrane (Nguyen and Hildreth, 2000). Analysis of the HIV-1 'lipidome' showed that cholesterol and sphingomyelin is accumulated in the viral membrane, and inhibition of sphingomyelin synthesis reduced virus infectivity (Brugger et al., 2006). HIV-1 can also spread by direct contact of infected cells with non-infected ones. High colocalization of Gag and Env proteins with G_{M1} in the virological synapse has been reported by Jolly et al. (Jolly and Sattentau, 2005). All these investigations can contribute to our understanding how HIV-1 infection and spread take place, and could be the basis of finding new targets for vaccines.

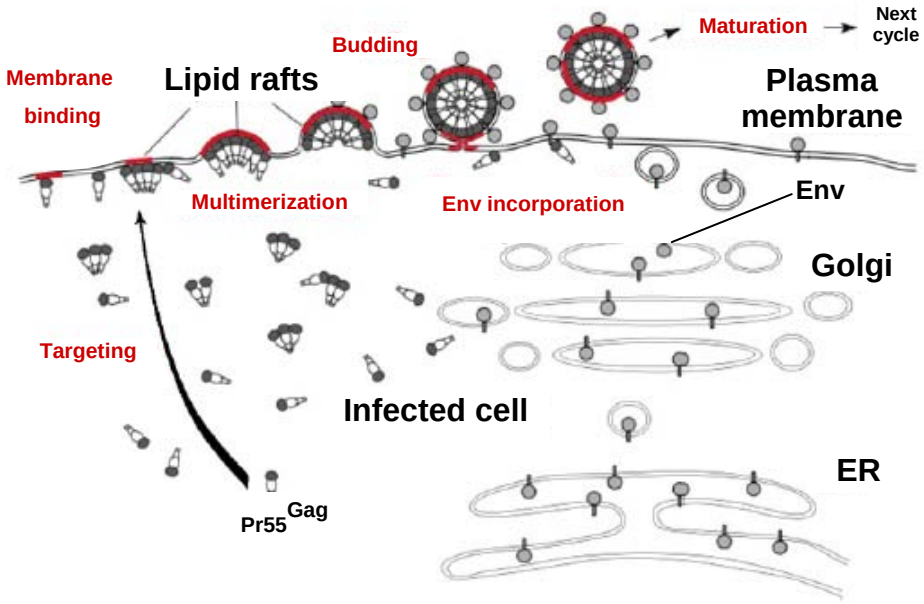

Figure 4. HIV-1 assembly and release from infected cells. *$Pr55^{Gag}$ viral protein is directed to the plasma membrane where it associates with lipid raft microdomains. Viral Env glycoproteins are incorporated into multimerized Gag complexes. After assembly of viral particles virions ultimately pinch off from the cell surface (Waheed and Freed, 2009).*

1.2. Sialic acid and Sia binding proteins

1.2.1. Introduction to sialic acid biology

Amongst the major classes of conjugated macromolecules in biology, the glycoconjugates are the most complex ones. Their complexity is comprised of a large variety of monosaccharides, linkages and branching structures, as well as a remarkable degree of intra- and interspecies diversity (Bishop and Gagneux, 2007). Glycosylation is an enzymatic process producing a diverse repertoire of glycans linked to proteins, lipids or other saccharides. An increasing number of studies show the importance of glycans in different biological functions such as protein maturation and turnover, cell adhesion and trafficking, receptor binding and activation, and also pathogen recognition (Marth and Grewal, 2008; van Kooyk and Rabinovich, 2008).

Sialic acid (Sia) is a general term for a diverse family of nine-carbon sugar containing α-2 acid group that are all derived from neuraminic acid (Neu) or keto-deoxynonulosonic acid (KDN) (Taylor and Drickamer, 2003). They are typically found on the exposed termini of mammalian oligosaccharide chains attached to cell surface proteins or lipids. Sialic acids are transferred using α2-3, α2-6 or α2-8 linkages to subterminal sugars by a family of about twenty sialyltransferases (STs). These sialyltransferases are grouped into four families according to the carbohydrate linkages they synthesize: β-galactoside α2-3 STs (ST3Gal I-VI), β-galactoside α2-6 STs (ST6Gal I, II), N-acetylgalactosamine α2-6 STs (ST6GalNAc I-VI) and α2-8 STs (ST8Sia I-VI) (Harduin-Lepers et al., 2001; Takashima, 2008). More than fifty different sialic acid structures have been found in nature including Neu, KDN, and their acetylated, methylated, lactylated, sulfated, and phosphorylated derivatives (Angata and Varki, 2002). One prominent Sia detected in many mammals is N-glycolylneuraminic acid (Neu5Gc) which differs from the other common Sia, N-acetylneuraminic acid (Neu5Ac), in one additional oxygen atom in the acyl group at the C5 position (Varki, 2001) *(Figure 5A).* Schauer and co-workers discovered and studied in details CMP-Neu5Ac-hydroxylase (CMAH) *(Figure 5B),* the enzyme converting CMP-Neu5Ac to CMP-Neu5Gc (Schoop et al., 1969). Due to a mutation occurred in the *Cmah* gene during evolution (Chou et al., 2002; Chou et al., 1998; Hayakawa et al., 2001) human have only Neu5Ac. The loss of Neu5Gc resulted in relaxation of the specificity of Sia-binding proteins (e.g. Siglec-7, Siglec-9) described to prefer Neu5Gc in chimpanzees and gorillas (Sonnenburg et al., 2004). This means

adjustments in the binding pockets of these Siglecs, allowing the binding of Neu5Ac, without loss of NeuGc binding. Additional human-specific changes have been also found, affecting at least ten genes known to be involved in the biology of sialic acids (Altheide et al., 2006). Most of these changes affected members of the Siglec protein family and include gene inactivation, amino acid changes altering function, and expression differences (Varki, 2009).

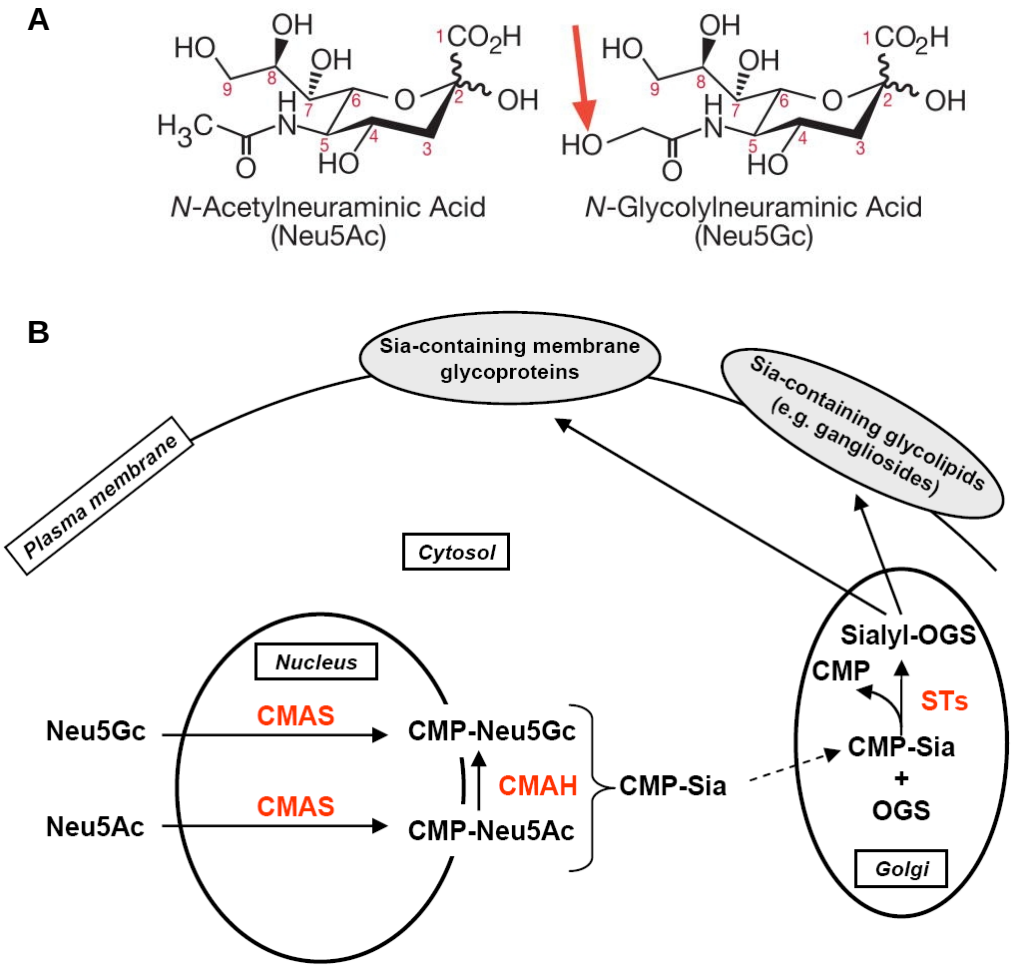

Figure 5. (A) Structural differences between two major molecular species of sialic acid (Sia). *The metabolic precursor N-acetylneuraminic acid (Neu5Ac) and its modified form N-glycolylneuraminic acid (Neu5Gc) differing only by an oxygen atom at the C5 position.* ***(B) Biosynthesis of sialylated glycoproteins in mouse.*** *Cytidine monophosphate (CMP)-Neu5Ac synthetase (CMAS) catalyzes the activation of Sia to CMP-Sia. The enzyme CMP-Neu5AC hydroxylase (CMAH) is responsible for the conversion of CMP-Neu5Ac to CMP-Neu5Gc. CMP-Sia is imported into the Golgi apparatus and used by sialyltransferases (STs). These enzymes attach CMP-Sia to oligoglycosaccharides (OGS) found on glycoproteins and glycolipids. The synthesized biomolecules are then transferred to the plasma membrane.*

1.2.2. Sia-binding proteins: essential membrane receptors in the immune system

Leukocyte extravasation is an important process in inflammation and in lymphocyte homing (Fabbri et al., 1999; Hogan and Foster, 1996). Selectins belong to the C-type lectin family of adhesion molecules *(Figure 6A)* that are involved in leukocyte-endothelial cell adhesion. Three types of selectins have been discovered so far. L-selectins are expressed by leukocytes, the expression of E- and P-selectins is inducible on vascular endothelium upon cytokine stimuli, and P-selectins were also found on platelets (Kansas, 1996; Keelan et al., 1994). Their ligands was described as sialic acid-containing tetrasaccharides, called sialyl-Lewis^x and sialyl-Lewis^a (Galustian et al., 1999; Welply et al., 1994). The main ligand for P-selectin is P-selectin glycoprotein ligand-1 (PSGL-1). This receptor is primarily expressed in hematopoietic cells such as granulocytes, monocytes, and certain subsets of T cells, and is also expressed by activated endothelial cells. PSGL-1 can be recognized, but with lower affinity, by the other two selectins as well. E-selectin has been described to bind to several glycoconjugates on various hematopoietic and cancer cells in affinity or binding assay. These ligands may include L-selectin, E-selectin ligand-1, CD43, CD44, β2 integrins and glycolipids (Barthel et al., 2007). All these ligands can promote tethering and rolling of activated leukocytes or tumour cells on the endothelium. Glycosylation-dependent cell adhesion molecule-1, CD34, and mucosal addressin cell-adhesion molecule-1 have been discovered as ligands for L-selectin (Rosen, 2004). They are sialomucins, belonging to vascular addressins expressed on HEVs, which can present O-linked sugar chains to the lectin domain of L-selectin.

The other important group of Sia-binding proteins is the Siglec family belonging to type I membrane proteins. Siglecs are sialic acid binding immunoglobulin-like lectins *(Figure 6B)* that are known to influence various functions of mammalian immune cells, such as regulation of cellular signalling, cell-cell interactions and endocytosis (Crocker et al., 2007). Most of them contain ITIM- and/or ITIM-like motifs that can negatively regulate signal transduction. Some non-ITIM containing Siglecs have been shown to interact with DAP-12, an ITAM-containing adaptor that triggers both activating and inhibitory signalling (Crocker and Redelinghuys, 2008). Siglec-1 (Sialoadhesin), Siglec-2 (CD22), Siglec-3 (CD33) and Siglec-4 were the original members of the family. Many new members were identified in the last ten years and are called CD33-related Siglecs based on their high homology with CD33. Until now, 14 different siglecs have been described in human. Siglec

expression has been found mainly in the hematopoietic and immune system (Crocker et al., 2007). Sialoadhesin is a macrophage-specific adhesion molecule and CD22 is a well studied protein known to play role in regulation of B cell signalling (O'Keefe et al., 1996) and homing of B cells to the bone marrow (Floyd et al., 2000; Nitschke et al., 1997). In contrast, the CD33-related Siglecs show more complex expression patterns on innate immune cells. Most cell types in the human and mouse express at least one Siglec, while others express several. Siglecs can bind to either *cis* or *trans* ligands. *Cis* interactions with sialic acids in the same plasma membrane could potentially regulate their function by 'masking' them from ligands presented on the surface of other cells or pathogens. The 'unmasking' of the Siglecs could be mediated by a variety of possible mechanisms, including a cell surface sialidase, *via* altered glycosilation or by reorganization of plasma membrane domains (Crocker et al., 2007; Crocker and Varki, 2001). Determination of the sialic acid-bearing molecules that could be feasible ligands of Siglecs is a developing area of biological research. Binding of Siglec-4 to gangliosides was already shown by Schnaar et al (Schnaar et al., 1998). The CD22-Ig Fc fusion protein has been reported to bind to CD45, serum IgM and many other B cell (and T cell) glycoproteins *in vitro* (Law et al., 1995; Stamenkovic et al., 1991). However, defining the precise function of Siglecs upon binding to biologically relevant ligands raise an important challenge.

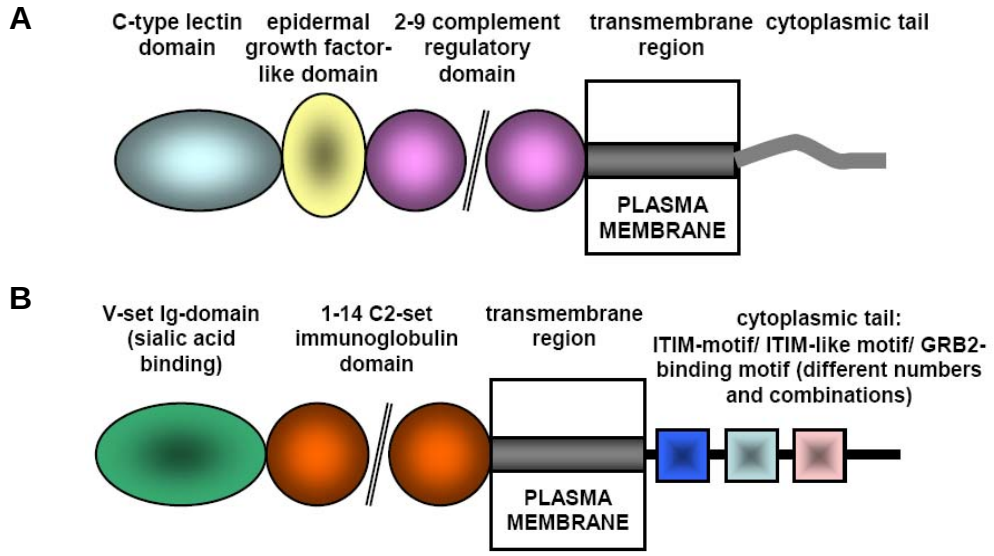

Figure 6. Structure of mammalian Sia-binding proteins. ***(A)*** *Selectins are type 1 membrane proteins with different functional domains. They have role in leukocyte extravasation through endothelial wall.* ***(B)*** *Siglecs are sialic acid binding immunoglobulin-like lectin transmembrane receptors known to function as adhesion molecules and regulators of immune cell functions.*

1.2.3. Brief history of the sialic acid-containing GL7 epitope

GL7, a rat monoclonal IgM antibody (developed previously in the NIH) was produced against *in vitro* stimulated mouse B lymphoblasts and proposed to bind to a 35 kDa late activation antigen expressed by mouse B and T lymphocytes (Laszlo et al., 1993). GL7 antibody bound to only 0-9% of freshly separated splenic B cells and 0-1% of splenic T lymphocytes. The GL7 epitope density increased to approximately 70% on activated lymphocytes. All the tested DNA, RNA and protein synthesis inhibitors strongly prevented the expression of the GL7 epitope. The GL7 Ab staining pattern was found very similar to that of peanut agglutinin (PNA) in mouse lymph node and spleen, namely the epitope is strongly expressed by IgD^- B cells in the germinal center (Cervenak et al., 2001). The epitope also had been found on a small subpopulation (~9-22%) of 'TCR-bright' thymocytes (Hathcock et al., 1995). In the mouse bone marrow the GL7 epitope is detectable as early as on the pro-B/early pre-B cell stages and its expression becomes very high on large pre-B cells but it is completely down regulated on mature naive resting B cells, so it may define the cycling stage of B cell maturation (Murasawa et al., 2002). In a study that analysed functional capacities of activated and sorted lymph node B lymphocytes, only $GL7^+$ cells had high antigen presenting capacity and produced antibodies (Cervenak et al., 2001). Comparative study of thymocyte subpopulations showed, that $GL7^+$ cells proliferated vigorously and produced more cytokines (IL-2, IL-4) compared to the $GL7^{-/low}$ fraction. Later the antibody was shown to recognize the Neu5Acα2-6Galβ1-4GlcNAcβ1-3Galβ1-4Glc carbohydrate epitope that is also expressed by different human B cell lines (Naito et al., 2007). Furthermore, two enzymes was shown to regulate the expression of GL7 (Naito et al., 2007). CMP-Neu5Ac hydroxylase enzyme (CMAH) was found to be down-regulated in activated mouse B cells in negative correlation with GL7 expression. Another enzyme, ST6Gal I sialyltransferase was revealed to positively regulate the expression of the epitope, since its gene expression and GL7 Ab reactivity positively and strongly correlated in different human B cell lines. All these results indicate that the GL7 epitope may have role in lymphocyte functions.

Reference list

Altheide T. K., Hayakawa T., Mikkelsen T. S., Diaz S., Varki N. and Varki A. (2006) System-wide genomic and biochemical comparisons of sialic acid biology among primates and rodents: Evidence for two modes of rapid evolution. *J Biol Chem* **281**, 25689-702.

Anderson H. A., Hiltbold E. M. and Roche P. A. (2000) Concentration of MHC class II molecules in lipid rafts facilitates antigen presentation. *Nat Immunol* **1**, 156-62.

Angata T. and Varki A. (2002) Chemical diversity in the sialic acids and related alpha-keto acids: an evolutionary perspective. *Chem Rev* **102**, 439-69.

Baker A. M., Sauliere A., Gaibelet G., Lagane B., Mazeres S., Fourage M., Bachelerie F., Salome L., Lopez A. and Dumas F. (2007) CD4 interacts constitutively with multiple CCR5 at the plasma membrane of living cells. A fluorescence recovery after photobleaching at variable radii approach. *J Biol Chem* **282**, 35163-8.

Balamuth F., Leitenberg D., Unternaehrer J., Mellman I. and Bottomly K. (2001) Distinct patterns of membrane microdomain partitioning in Th1 and th2 cells. *Immunity* **15**, 729-38.

Barthel S. R., Gavino J. D., Descheny L. and Dimitroff C. J. (2007) Targeting selectins and selectin ligands in inflammation and cancer. *Expert Opin Ther Targets* **11**, 1473-91.

Bhattacharya J., Peters P. J. and Clapham P. R. (2004) Human immunodeficiency virus type 1 envelope glycoproteins that lack cytoplasmic domain cysteines: impact on association with membrane lipid rafts and incorporation onto budding virus particles. *J Virol* **78**, 5500-6.

Bhattacharya J., Repik A. and Clapham P. R. (2006) Gag regulates association of human immunodeficiency virus type 1 envelope with detergent-resistant membranes. *J Virol* **80**, 5292-300.

Bishop J. R. and Gagneux P. (2007) Evolution of carbohydrate antigens--microbial forces shaping host glycomes? *Glycobiology* **17**, 23R-34R.

Brown D. A. and London E. (1998) Functions of lipid rafts in biological membranes. *Annu Rev Cell Dev Biol* **14**, 111-36.

Brown D. A. and London E. (2000) Structure and function of sphingolipid- and cholesterol-rich membrane rafts. *J Biol Chem* **275**, 17221-4.

Brugger B., Glass B., Haberkant P., Leibrecht I., Wieland F. T. and Krausslich H. G. (2006) The HIV lipidome: a raft with an unusual composition. *Proc Natl Acad Sci U S A* **103**, 2641-6.

Cervenak L., Magyar A., Boja R. and Laszlo G. (2001) Differential expression of GL7 activation antigen on bone marrow B cell subpopulations and peripheral B cells. *Immunol Lett* **78**, 89-96.

Cheng P. C., Dykstra M. L., Mitchell R. N. and Pierce S. K. (1999) A role for lipid rafts in B cell antigen receptor signaling and antigen targeting. *J Exp Med* **190**, 1549-60.

Chou H. H., Hayakawa T., Diaz S., Krings M., Indriati E., Leakey M., Paabo S., Satta Y., Takahata N. and Varki A. (2002) Inactivation of CMP-N-acetylneuraminic acid hydroxylase occurred prior to brain expansion during human evolution. *Proc Natl Acad Sci U S A* **99**, 11736-41.

Chou H. H., Takematsu H., Diaz S., Iber J., Nickerson E., Wright K. L., Muchmore E. A., Nelson D. L., Warren S. T. and Varki A. (1998) A mutation in human CMP-sialic acid hydroxylase occurred after the Homo-Pan divergence. *Proc Natl Acad Sci U S A* **95**, 11751-6.

Chung J. B., Baumeister M. A. and Monroe J. G. (2001) Cutting edge: differential sequestration of plasma membrane-associated B cell antigen receptor in mature and immature B cells into glycosphingolipid-enriched domains. *J Immunol* **166**, 736-40.

Crocker P. R., Paulson J. C. and Varki A. (2007) Siglecs and their roles in the immune system. *Nat Rev Immunol* **7**, 255-66.

Crocker P. R. and Redelinghuys P. (2008) Siglecs as positive and negative regulators of the immune system. *Biochem Soc Trans* **36**, 1467-71.

Crocker P. R. and Varki A. (2001) Siglecs in the immune system. *Immunology* **103**, 137-45.

de Mello Coelho V., Nguyen D., Giri B., Bunbury A., Schaffer E. and Taub D. D. (2004) Quantitative differences in lipid raft components between murine CD4+ and CD8+ T cells. *BMC Immunol* **5**, 2.

Dietzen D. J., Hastings W. R. and Lublin D. M. (1995) Caveolin is palmitoylated on multiple cysteine residues. Palmitoylation is not necessary for localization of caveolin to caveolae. *J Biol Chem* **270**, 6838-42.

Drevot P., Langlet C., Guo X. J., Bernard A. M., Colard O., Chauvin J. P., Lasserre R. and He H. T. (2002) TCR signal initiation machinery is pre-assembled and activated in a subset of membrane rafts. *Embo J* **21**, 1899-908.

Dykstra M., Cherukuri A., Sohn H. W., Tzeng S. J. and Pierce S. K. (2003) Location is everything: lipid rafts and immune cell signaling. *Annu Rev Immunol* **21**, 457-81.

Epand R. M. (2006) Cholesterol and the interaction of proteins with membrane domains. *Prog Lipid Res* **45**, 279-94.

Fabbri M., Bianchi E., Fumagalli L. and Pardi R. (1999) Regulation of lymphocyte traffic by adhesion molecules. *Inflamm Res* **48**, 239-46.

Fivaz M., Vilbois F., Thurnheer S., Pasquali C., Abrami L., Bickel P. E., Parton R. G. and van der Goot F. G. (2002) Differential sorting and fate of endocytosed GPI-anchored proteins. *Embo J* **21**, 3989-4000.

Floyd H., Nitschke L. and Crocker P. R. (2000) A novel subset of murine B cells that expresses unmasked forms of CD22 is enriched in the bone marrow: implications for B-cell homing to the bone marrow. *Immunology* **101**, 342-7.

Fragoso R., Ren D., Zhang X., Su M. W., Burakoff S. J. and Jin Y. J. (2003) Lipid raft distribution of CD4 depends on its palmitoylation and association with Lck, and evidence for CD4-induced lipid raft aggregation as an additional mechanism to enhance CD3 signaling. *J Immunol* **170**, 913-21.

Gallo S. A., Finnegan C. M., Viard M., Raviv Y., Dimitrov A., Rawat S. S., Puri A., Durell S. and Blumenthal R. (2003) The HIV Env-mediated fusion reaction. *Biochim Biophys Acta* **1614**, 36-50.

Galustian C., Lubineau A., le Narvor C., Kiso M., Brown G. and Feizi T. (1999) L-selectin interactions with novel mono- and multisulfated Lewisx sequences in comparison with the potent ligand 3'-sulfated Lewisa. *J Biol Chem* **274**, 18213-7.

Giebel B., Corbeil D., Beckmann J., Hohn J., Freund D., Giesen K., Fischer J., Kogler G. and Wernet P. (2004) Segregation of lipid raft markers including CD133 in polarized human hematopoietic stem and progenitor cells. *Blood* **104**, 2332-8.

Gombos I., Detre C., Vamosi G. and Matko J. (2004) Rafting MHC-II domains in the APC (presynaptic) plasma membrane and the thresholds for T-cell activation and immunological synapse formation. *Immunol Lett* **92**, 117-24.

Gomez-Mouton C., Abad J. L., Mira E., Lacalle R. A., Gallardo E., Jimenez-Baranda S., Illa I., Bernad A., Manes S. and Martinez A. C. (2001) Segregation of leading-edge and uropod components into specific lipid rafts during T cell polarization. *Proc Natl Acad Sci U S A* **98**, 9642-7.

Gupta N., Wollscheid B., Watts J. D., Scheer B., Aebersold R. and DeFranco A. L. (2006) Quantitative proteomic analysis of B cell lipid rafts reveals that ezrin regulates antigen receptor-mediated lipid raft dynamics. *Nat Immunol* **7**, 625-33.

Guyader M., Kiyokawa E., Abrami L., Turelli P. and Trono D. (2002) Role for human immunodeficiency virus type 1 membrane cholesterol in viral internalization. *J Virol* **76**, 10356-64.

Harduin-Lepers A., Vallejo-Ruiz V., Krzewinski-Recchi M. A., Samyn-Petit B., Julien S. and Delannoy P. (2001) The human sialyltransferase family. *Biochimie* **83**, 727-37.

Harrist A. V., Ryzhova E. V., Harvey T. and Gonzalez-Scarano F. (2009) Anx2 interacts with HIV-1 Gag at phosphatidylinositol (4,5) bisphosphate-containing lipid rafts and increases viral production in 293T cells. *PLoS One* **4**, e5020.

Hathcock K. S., Pucillo C. E., Laszlo G., Lai L. and Hodes R. J. (1995) Analysis of thymic subpopulations expressing the activation antigen GL7. Expression, genetics, and function. *J Immunol* **155**, 4575-81.

Hayakawa T., Satta Y., Gagneux P., Varki A. and Takahata N. (2001) Alu-mediated inactivation of the human CMP- N-acetylneuraminic acid hydroxylase gene. *Proc Natl Acad Sci U S A* **98**, 11399-404.

Hogan S. P. and Foster P. S. (1996) Cellular and molecular mechanisms involved in the regulation of eosinophil trafficking in vivo. *Med Res Rev* **16**, 407-32.

Horejsi V. (2003) The roles of membrane microdomains (rafts) in T cell activation. *Immunol Rev* **191**, 148-64.

Horejsi V., Drbal K., Cebecauer M., Cerny J., Brdicka T., Angelisova P. and Stockinger H. (1999) GPI-microdomains: a role in signalling via immunoreceptors. *Immunol Today* **20**, 356-61.

Huby R. D., Dearman R. J. and Kimber I. (1999) Intracellular phosphotyrosine induction by major histocompatibility complex class II requires co-aggregation with membrane rafts. *J Biol Chem* **274**, 22591-6.

Ilangumaran S., Arni S., van Echten-Deckert G., Borisch B. and Hoessli D. C. (1999) Microdomain-dependent regulation of Lck and Fyn protein-tyrosine kinases in T lymphocyte plasma membranes. *Mol Biol Cell* **10**, 891-905.

Jolly C. and Sattentau Q. J. (2005) Human immunodeficiency virus type 1 virological synapse formation in T cells requires lipid raft integrity. *J Virol* **79**, 12088-94.

Kansas G. S. (1996) Selectins and their ligands: current concepts and controversies. *Blood* **88**, 3259-87.
Kawada S., Goto T., Haraguchi H., Ono A. and Morikawa Y. (2008) Dominant negative inhibition of human immunodeficiency virus particle production by the nonmyristoylated form of gag. *J Virol* **82**, 4384-99.
Keelan E. T., Licence S. T., Peters A. M., Binns R. M. and Haskard D. O. (1994) Characterization of E-selectin expression in vivo with use of a radiolabeled monoclonal antibody. *Am J Physiol* **266**, H278-90.
Kuwabara P. E. and Labouesse M. (2002) The sterol-sensing domain: multiple families, a unique role? *Trends Genet* **18**, 193-201.
Laszlo G., Hathcock K. S., Dickler H. B. and Hodes R. J. (1993) Characterization of a novel cell-surface molecule expressed on subpopulations of activated T and B cells. *J Immunol* **150**, 5252-62.
Lauer S., VanWye J., Harrison T., McManus H., Samuel B. U., Hiller N. L., Mohandas N. and Haldar K. (2000) Vacuolar uptake of host components, and a role for cholesterol and sphingomyelin in malarial infection. *Embo J* **19**, 3556-64.
Law C. L., Aruffo A., Chandran K. A., Doty R. T. and Clark E. A. (1995) Ig domains 1 and 2 of murine CD22 constitute the ligand-binding domain and bind multiple sialylated ligands expressed on B and T cells. *J Immunol* **155**, 3368-76.
Legler D. F., Micheau O., Doucey M. A., Tschopp J. and Bron C. (2003) Recruitment of TNF receptor 1 to lipid rafts is essential for TNFalpha-mediated NF-kappaB activation. *Immunity* **18**, 655-64.
Li H., Yao Z., Degenhardt B., Teper G. and Papadopoulos V. (2001) Cholesterol binding at the cholesterol recognition/ interaction amino acid consensus (CRAC) of the peripheral-type benzodiazepine receptor and inhibition of steroidogenesis by an HIV TAT-CRAC peptide. *Proc Natl Acad Sci U S A* **98**, 1267-72.
Liao Z., Cimakasky L. M., Hampton R., Nguyen D. H. and Hildreth J. E. (2001) Lipid rafts and HIV pathogenesis: host membrane cholesterol is required for infection by HIV type 1. *AIDS Res Hum Retroviruses* **17**, 1009-19.
Lindwasser O. W. and Resh M. D. (2001) Multimerization of human immunodeficiency virus type 1 Gag promotes its localization to barges, raft-like membrane microdomains. *J Virol* **75**, 7913-24.
Lowell C. A. (2004) Src-family kinases: rheostats of immune cell signaling. *Mol Immunol* **41**, 631-43.
Manes S. and Viola A. (2006) Lipid rafts in lymphocyte activation and migration. *Mol Membr Biol* **23**, 59-69.
Marth J. D. and Grewal P. K. (2008) Mammalian glycosylation in immunity. *Nat Rev Immunol* **8**, 874-87.
Martin M., Schneider H., Azouz A. and Rudd C. E. (2001) Cytotoxic T lymphocyte antigen 4 and CD28 modulate cell surface raft expression in their regulation of T cell function. *J Exp Med* **194**, 1675-81.
Matko J. and Szollosi J. (2002) Landing of immune receptors and signal proteins on lipid rafts: a safe way to be spatio-temporally coordinated? *Immunol Lett* **82**, 3-15.
McIntosh T. J., Vidal A. and Simon S. A. (2003) Sorting of lipids and transmembrane peptides between detergent-soluble bilayers and detergent-resistant rafts. *Biophys J* **85**, 1656-66.
Megha, Bakht O. and London E. (2006) Cholesterol precursors stabilize ordinary and ceramide-rich ordered lipid domains (lipid rafts) to different degrees. Implications for the Bloch hypothesis and sterol biosynthesis disorders. *J Biol Chem* **281**, 21903-13.
Megha and London E. (2004) Ceramide selectively displaces cholesterol from ordered lipid domains (rafts): implications for lipid raft structure and function. *J Biol Chem* **279**, 9997-10004.
Melkonian K. A., Ostermeyer A. G., Chen J. Z., Roth M. G. and Brown D. A. (1999) Role of lipid modifications in targeting proteins to detergent-resistant membrane rafts. Many raft proteins are acylated, while few are prenylated. *J Biol Chem* **274**, 3910-7.
Molon B., Gri G., Bettella M., Gomez-Mouton C., Lanzavecchia A., Martinez A. C., Manes S. and Viola A. (2005) T cell costimulation by chemokine receptors. *Nat Immunol* **6**, 465-71.
Mordue D. G., Desai N., Dustin M. and Sibley L. D. (1999) Invasion by Toxoplasma gondii establishes a moving junction that selectively excludes host cell plasma membrane proteins on the basis of their membrane anchoring. *J Exp Med* **190**, 1783-92.
Mukherjee S. and Maxfield F. R. (2004) Membrane domains. *Annu Rev Cell Dev Biol* **20**, 839-66.
Murasawa M., Okada S., Obata S., Hatano M., Moriya H. and Tokuhisa T. (2002) GL7 defines the cycling stage of pre-B cells in murine bone marrow. *Eur J Immunol* **32**, 291-8.

Naito Y., Takematsu H., Koyama S., Miyake S., Yamamoto H., Fujinawa R., Sugai M., Okuno Y., Tsujimoto G., Yamaji T., Hashimoto Y., Itohara S., Kawasaki T., Suzuki A. and Kozutsumi Y. (2007) Germinal center marker GL7 probes activation-dependent repression of N-glycolylneuraminic acid, a sialic acid species involved in the negative modulation of B-cell activation. *Mol Cell Biol* **27**, 3008-22.

Nguyen D. H. and Hildreth J. E. (2000) Evidence for budding of human immunodeficiency virus type 1 selectively from glycolipid-enriched membrane lipid rafts. *J Virol* **74**, 3264-72.

Nguyen D. H. and Taub D. (2002) Cholesterol is essential for macrophage inflammatory protein 1 beta binding and conformational integrity of CC chemokine receptor 5. *Blood* **99**, 4298-306.

Nguyen D. H. and Taub D. D. (2003) Inhibition of chemokine receptor function by membrane cholesterol oxidation. *Exp Cell Res* **291**, 36-45.

Nisole S., Krust B. and Hovanessian A. G. (2002) Anchorage of HIV on permissive cells leads to coaggregation of viral particles with surface nucleolin at membrane raft microdomains. *Exp Cell Res* **276**, 155-73.

Nitschke L., Carsetti R., Ocker B., Kohler G. and Lamers M. C. (1997) CD22 is a negative regulator of B-cell receptor signalling. *Curr Biol* **7**, 133-43.

O'Keefe T. L., Williams G. T., Davies S. L. and Neuberger M. S. (1996) Hyperresponsive B cells in CD22-deficient mice. *Science* **274**, 798-801.

Pike L. J. (2004) Lipid rafts: heterogeneity on the high seas. *Biochem J* **378**, 281-92.

Popik W., Alce T. M. and Au W. C. (2002) Human immunodeficiency virus type 1 uses lipid raft-colocalized CD4 and chemokine receptors for productive entry into CD4(+) T cells. *J Virol* **76**, 4709-22.

Rosen S. D. (2004) Ligands for L-selectin: homing, inflammation, and beyond. *Annu Rev Immunol* **22**, 129-56.

Salzwedel K., West J. T. and Hunter E. (1999) A conserved tryptophan-rich motif in the membrane-proximal region of the human immunodeficiency virus type 1 gp41 ectodomain is important for Env-mediated fusion and virus infectivity. *J Virol* **73**, 2469-80.

Sandvig K., Olsnes S., Brown J. E., Petersen O. W. and van Deurs B. (1989) Endocytosis from coated pits of Shiga toxin: a glycolipid-binding protein from Shigella dysenteriae 1. *J Cell Biol* **108**, 1331-43.

Schade A. E. and Levine A. D. (2002) Lipid raft heterogeneity in human peripheral blood T lymphoblasts: a mechanism for regulating the initiation of TCR signal transduction. *J Immunol* **168**, 2233-9.

Scheel-Toellner D., Wang K., Singh R., Majeed S., Raza K., Curnow S. J., Salmon M. and Lord J. M. (2002) The death-inducing signalling complex is recruited to lipid rafts in Fas-induced apoptosis. *Biochem Biophys Res Commun* **297**, 876-9.

Schnaar R. L., Collins B. E., Wright L. P., Kiso M., Tropak M. B., Roder J. C. and Crocker P. R. (1998) Myelin-associated glycoprotein binding to gangliosides. Structural specificity and functional implications. *Ann N Y Acad Sci* **845**, 92-105.

Schoop H. J., Schauer R. and Faillard H. (1969) [On the biosynthesis of N-glycolyneuraminic acid. Oxidative formation of N-glycolylneuraminic acid from N-acetylneuraminic acid]. *Hoppe Seylers Z Physiol Chem* **350**, 155-62.

Schroeder R. J., Ahmed S. N., Zhu Y., London E. and Brown D. A. (1998) Cholesterol and sphingolipid enhance the Triton X-100 insolubility of glycosylphosphatidylinositol-anchored proteins by promoting the formation of detergent-insoluble ordered membrane domains. *J Biol Chem* **273**, 1150-7.

Shin J. S. and Abraham S. N. (2001) Caveolae as portals of entry for microbes. *Microbes Infect* **3**, 755-61.

Shogomori H. and Futerman A. H. (2001) Cholera toxin is found in detergent-insoluble rafts/domains at the cell surface of hippocampal neurons but is internalized via a raft-independent mechanism. *J Biol Chem* **276**, 9182-8.

Sigalov A. (2005) Multi-chain immune recognition receptors: spatial organization and signal transduction. *Semin Immunol* **17**, 51-64.

Simons K. and Ikonen E. (1997) Functional rafts in cell membranes. *Nature* **387**, 569-72.

Simons K. and Ikonen E. (2000) How cells handle cholesterol. *Science* **290**, 1721-6.

Sonnenburg J. L., Altheide T. K. and Varki A. (2004) A uniquely human consequence of domain-specific functional adaptation in a sialic acid-binding receptor. *Glycobiology* **14**, 339-46.

Stamenkovic I., Sgroi D., Aruffo A., Sy M. S. and Anderson T. (1991) The B lymphocyte adhesion molecule CD22 interacts with leukocyte common antigen CD45RO on T cells and alpha 2-6 sialyltransferase, CD75, on B cells. *Cell* **66**, 1133-44.

Takashima S. (2008) Characterization of mouse sialyltransferase genes: their evolution and diversity. *Biosci Biotechnol Biochem* **72**, 1155-67.

Taylor M. and Drickamer K. (2003) *Introduction to glycobiology*. University Press, Oxford.

Thorn H., Stenkula K. G., Karlsson M., Ortegren U., Nystrom F. H., Gustavsson J. and Stralfors P. (2003) Cell surface orifices of caveolae and localization of caveolin to the necks of caveolae in adipocytes. *Mol Biol Cell* **14**, 3967-76.

Tuosto L., Parolini I., Schroder S., Sargiacomo M., Lanzavecchia A. and Viola A. (2001) Organization of plasma membrane functional rafts upon T cell activation. *Eur J Immunol* **31**, 345-9.

van Kooyk Y. and Rabinovich G. A. (2008) Protein-glycan interactions in the control of innate and adaptive immune responses. *Nat Immunol* **9**, 593-601.

Varki A. (2001) Loss of N-glycolylneuraminic acid in humans: Mechanisms, consequences, and implications for hominid evolution. *Am J Phys Anthropol* **Suppl 33**, 54-69.

Varki A. (2009) Multiple changes in sialic acid biology during human evolution. *Glycoconj J* **26**, 231-45.

Veiga M. P., Arrondo J. L., Goni F. M., Alonso A. and Marsh D. (2001) Interaction of cholesterol with sphingomyelin in mixed membranes containing phosphatidylcholine, studied by spin-label ESR and IR spectroscopies. A possible stabilization of gel-phase sphingolipid domains by cholesterol. *Biochemistry* **40**, 2614-22.

Viola A., Schroeder S., Sakakibara Y. and Lanzavecchia A. (1999) T lymphocyte costimulation mediated by reorganization of membrane microdomains. *Science* **283**, 680-2.

von Haller P. D., Donohoe S., Goodlett D. R., Aebersold R. and Watts J. D. (2001) Mass spectrometric characterization of proteins extracted from Jurkat T cell detergent-resistant membrane domains. *Proteomics* **1**, 1010-21.

Waheed A. A. and Freed E. O. (2009) Lipids and membrane microdomains in HIV-1 replication. *Virus Res* **143**, 162-76.

Wang J., Megha and London E. (2004) Relationship between sterol/steroid structure and participation in ordered lipid domains (lipid rafts): implications for lipid raft structure and function. *Biochemistry* **43**, 1010-8.

Wang J. K., Kiyokawa E., Verdin E. and Trono D. (2000) The Nef protein of HIV-1 associates with rafts and primes T cells for activation. *Proc Natl Acad Sci U S A* **97**, 394-9.

Weintraub B. C., Jun J. E., Bishop A. C., Shokat K. M., Thomas M. L. and Goodnow C. C. (2000) Entry of B cell receptor into signaling domains is inhibited in tolerant B cells. *J Exp Med* **191**, 1443-8.

Welply J. K., Abbas S. Z., Scudder P., Keene J. L., Broschat K., Casnocha S., Gorka C., Steininger C., Howard S. C., Schmuke J. J. and et al. (1994) Multivalent sialyl-LeX: potent inhibitors of E-selectin-mediated cell adhesion; reagent for staining activated endothelial cells. *Glycobiology* **4**, 259-65.

Williams T. M. and Lisanti M. P. (2004) The caveolin proteins. *Genome Biol* **5**, 214.

Xiao X., Kinter A., Broder C. C. and Dimitrov D. S. (2000) Interactions of CCR5 and CXCR4 with CD4 and gp120 in human blood monocyte-derived dendritic cells. *Exp Mol Pathol* **68**, 133-8.

Yi L., Fang J., Isik N., Chim J. and Jin T. (2006) HIV gp120-induced interaction between CD4 and CCR5 requires cholesterol-rich microenvironments revealed by live cell fluorescence resonance energy transfer imaging. *J Biol Chem* **281**, 35446-53.

Chapter 2

Objectives

Cholesterol is a key, stabilizing molecule of membrane microdomains. Therefore, studying its role in lipid raft-mediated immune processes may help better understanding how lipid rafts function. Furthermore, based on these properties, membrane cholesterol and other raft components became potential new targets for immunotherapies. In spite of the considerable knowledge on lipid rafts, there are still only a few reliable and properly selective markers for these microdomains. No *in situ* modulators of rafts are available so far either, which could affect biological role of rafts in immune processes without depleting/deprivating cholesterol from the membrane. Having in hand two novel IgG type anti-cholesterol monoclonal antibodies (ACHAs), developed in our laboratory, we set the following goals and questions:

1. **Characterization of the novel cholesterol-specific monoclonal antibodies (ACHAs) in terms of their specificity, affinity and plasma membrane or intracellular binding sites.**

   Monoclonal IgG3-type cholesterol-specific antibodies (AC1, AC8) have recently been developed in our laboratory by immunizing mice with cholesterol-rich liposomes. Our aim was to characterize in details their binding to membrane cholesterol in liposomes and various immune cells. We investigated the potential of monoclonal IgG ACHAs as selective markers of lipid rafts/caveolae, as well.

2. **What is the molecular background behind the capacity of monoclonal ACHAs to inhibit *in vitro* HIV infection/production?**

   Our collaboration partners (Z. Beck and co-workers: University of Debrecen, Hungary/Walter Reed Army Institute of Research, Rockville, MD, USA) found that treatment of HIV-1 target cells, but not of the virus, with AC1 or AC8 antibodies prior to *in vitro* infection significantly diminished the virus production. Our goal was to study the background mechanism of this inhibitory potential of ACHAs, with special attention to their effects on distribution/interaction pattern, accessibility, mobility or raft association of the primary (CD4) and co-receptors (CXCR4) of HIV-1.

Another important membrane component is sialic acid, a carbohydrate, attached to glycoconjugates (glycoproteins and glycolipids), serving as ligands to Sia-binding proteins that are known to regulate cell signalling and cell-cell interactions. GL7 antibody has been shown to bind to the surface of mouse lymphocytes and human B cell lines. It has been also revealed that the antibody's epitope have a Sia moiety. The cell specific expression and membrane localization of the GL7 epitope on immune cells as well as the functional role of the molecule(s) bearing the epitope still remained unresolved. Therefore, here we set the following goal:

3. Characterization of the GL7 epitope: its expression and localization in human immunocytes.

The expression of GL7 epitope by human immune cells has not yet been sufficiently characterized. Therefore, we propose to characterize the expression of the epitope by various human lymphoid and myeloid cells and the localization of the epitope-bearing cells in lymphoid organs. Furthermore, we analysed the membrane localization and the nature of the GL7 epitope. These investigations may contribute to identify GL7 epitope-bearing molecule(s) and, in this way, assign a function to the epitope.

Chapter 3

Summary of new scientific results

1. **Characterization of the novel cholesterol-specific monoclonal antibodies (ACHAs) in terms of their specificity, affinity and plasma membrane or intracellular binding sites.** (Chapters 4, 5, 7 and reviewed in Chapter 6)

- Binding properties of the generated monoclonal ACHAs to cells were determined by flow cytometry and confocal microscopy. AC1 and AC8 antibodies bound to different murine and human intact lymphocyte and monocyte-macrophage cell lines, which was enhanced substantially by a limited papain digestion of the cell surface that removes most of the largely protruding extracellular protein domains.
- The AC8 antibody strongly colocalized with markers of caveolin^{+} and caveolin^{-} cholesterol-rich lipid rafts at the cell surface and intracellularly with markers of ER and Golgi apparatus, suggesting that monoclonal ACHAs recognize clustered cholesterol in live cells.
- Specificity was further confirmed by cholesterol modulating agents, cholesterol oxidase or filipin III antibiotics, by which treatments the binding of our antibodies could be decreased either to cells or to isolated DRMs.
- Using surface plasmon resonance (SPR) technique, a medium affinity (K_d = 7.8 x 10^{-10} M) binding of AC8 monoclonal ACHA to cholesterol-rich liposomes was found.

3. **What is the molecular background behind the capacity of monoclonal ACHAs to inhibit *in vitro* HIV infection/production?** (Chapter 7)

- Upon binding to human T cells or monocytes, AC8 induced lateral lipid raft clustering, assessed by confocal microscopy. This clustering was characterized with an increased average raft-size (from 200-300 to 500-1000 nm) and elevated number (by five-fold) of highly 'patchy' cells.
- AC8 monoclonal ACHA promoted the association of CXCR4 with both CD4 and lipid rafts, as shown by the increased (by approximately two-fold) colocalization or FRET efficiency between CXCR4 and CD4 or CTX, calculated from confocal images. Consistent with this, the lateral mobility of CXCR4, measured by FCS microscopy, also significantly decreased. Fab fragments of ACHAs and antibodies against non-raft membrane proteins did not show these effects.

3. Characterization of the GL7 epitope: its expression and localization in human immunocytes. (Chapter 8)

- Our results clearly demonstrate that the sialic acid-containing GL7 epitope is exclusively expressed by lymphocytes among human blood cells, similarly to mouse and rat. However, an important difference is that while in rodents the GL7 epitope appears only after 48h activation of T and B cells, in human the epitope is constitutively expressed.
- Fluorescence immunohistochemical staining of human tonsil showed that GL7 epitope is maximally highly expressed in the B cell follicles by $CD19^{+}$ IgD^{+} IgM^{low} naïve B lymphocytes. Other B cell subpopulations and T cells have lower expression level of the epitope.
- The GL7 epitope strongly colocalized with the lipid raft marker G_{M1} ganglioside in human primary lymphocytes and B or T cell lines, whereas the non-raft protein CD71 showed only a moderate colocalization with GL7. Flow cytometric detergent resistance measurements (FCDR) further confirmed this raft-association.

Chapter 4

Adrienn Bíró, László Cervenak, Andrea Balogh, András Lőrincz, Katalin Uray, Anna Horváth, László Romics, János Matkó, George Füst, Glória László

Novel anti-cholesterol monoclonal immunoglobulin G antibodies as probes and potential modulators of membrane raft-dependent immune functions

Journal of Lipid Research 2007. 48(1):19-29.

Novel anti-cholesterol monoclonal immunoglobulin G antibodies as probes and potential modulators of membrane raft-dependent immune functions

Adrienn Bíró,[1,*,†] László Cervenak,[1,†] Andrea Balogh,[1,§] András Lőrincz,[§] Katalin Uray,[**] Anna Horváth,[*] László Romics,[*,†] János Matkó,[§] George Füst,[*,†] and Glória László[2,§]

Third Department of Internal Medicine,* Research Laboratory, Semmelweis University, Budapest, Hungary; Research Group on Metabolism and Atherosclerosis,† Hungarian Academy of Sciences-Semmelweis University, Budapest, Hungary; and Departments of Immunology,§ and Organic Chemistry,** Eötvös Lorand University, Budapest, Hungary

Abstract Natural autoantibodies against cholesterol are present in the sera of all healthy individuals; their function, production, and regulation, however, are still unclear. Here, we managed to produce two monoclonal anti-cholesterol antibodies (ACHAs) by immunizing mice with cholesterol-rich liposomes. The new ACHAs were specific to cholesterol and to some structurally closely related 3β-hydroxyl sterols, and they reacted with human lipoproteins VLDL, LDL, and HDL. They bound, usually with low avidity, to live human or murine lymphocyte and monocyte-macrophage cell lines, which was enhanced substantially by a moderate papain digestion of the cell surface, removing some protruding extracellular protein domains. Cell-bound ACHAs strongly colocalized with markers of cholesterol-rich lipid rafts and caveolae at the cell surface and intracellularly with markers of the endoplasmic reticulum and Golgi complex. These data suggest that these IgG ACHAs may serve as probes of clustered cholesterol (e.g., different lipid rafts) in live cells and thus may also have immunomodulatory potential.—Bíró, A., L. Cervenak, A. Balogh, A. Lőrincz, K. Uray, A. Horváth, L. Romics, J. Matkó, G. Füst, and G. László. **Novel anti-cholesterol monoclonal immunoglobulin G antibodies as probes and potential modulators of membrane raft-dependent immune functions. *J. Lipid Res.* 2007.** 48: **19–29.**

Supplementary key words membrane cholesterol • lymphocytes • monocyte-macrophage cells • lipoproteins • lipid rafts • caveolae

Because of its widespread distribution and important biological roles, cholesterol has long been assumed to be a nonimmunogenic or poorly immunogenic molecule. However, several laboratories reported the activation of the classical and alternative pathways of the complement system by cholesterol (1–4). Natural autoantibodies of both IgM and IgG isotypes against cholesterol were shown to be present ubiquitously in the sera of healthy individuals (2, 3). Because cholesterol is an evolutionally conserved, abundant structural lipid in the plasma membrane of mammalian cells, it was tempting to speculate whether naturally occurring antibodies against cholesterol could bind to the surface of cells. Under physiological conditions, antibodies against lipids, such as phospholipids or cholesterol, are not expected to bind with high affinity to intact cell membranes, because of the small size of the antigen epitope and the steric hindrance by surrounding glycolipids or large, protruding glycoproteins (3). However, when either the affinity of anti-lipid antibodies or the molecular pattern/morphology of the cell surface is altered, such interaction between antibodies and lipids may take place (e.g., under pathological conditions).

Monoclonal anti-cholesterol antibodies (ACHAs) were first reported in 1988 by Swartz et al. (1) after immunizing mice with cholesterol-containing liposomes, together with lipid A as adjuvant. They found cholesterol to be a surprisingly excellent immunogen, and murine monoclonal IgM-type complement-fixing antibodies to cholesterol were easily obtained (1). Perl-Treves et al. (4) developed and examined monoclonal IgM antibodies against cholesterol monohydrate crystals by implantation of cholesterol crystals in the spleen of mice. This choice was motivated by the fact that cholesterol, in the living organism, may aggregate or precipitate in pathological situations as microcrystals (gallstones, atherosclerotic plaques). These IgM antibodies did not seem to recognize the cholesterol molecule itself but rather a de-

Manuscript received 5 April 2006 and in revised form 11 August 2006 and in re-revised form 3 October 2006.

Published, JLR Papers in Press, October 5, 2006.
DOI 10.1194/jlr.M600158-JLR200

[1] A. Bíró, L. Cervenak, and A. Balogh contributed equally to this work.
[2] To whom correspondence should be addressed.
e-mail: glorial@elte.hu

fined, extended pattern of molecular motifs exposed on the cholesterol crystal surfaces. Kruth et al. (5) directly visualized plasma membrane cholesterol clusters with a monoclonal antibody that specifically detects ordered cholesterol arrays, but only when the cells were previously enriched with cholesterol. This antibody detected a specific plasma membrane pool of cholesterol, responsive to agents that modulate cholesterol trafficking. The cholesterol-rich domains they detected in the plasma membrane did not seem equivalent to the so-called lipid rafts (6), because they were highly sensitive to ice-cold Triton X-100 extraction, whereas lipid rafts are not.

The presence of ACHAs in normal serum raised another important question: do these antibodies against cholesterol play a role in the regulation of cholesterol levels, and by extension, in atherosclerosis, in vivo? A putative role of ACHAs in atherosclerosis, induced by a cholesterol-rich diet, can be postulated from results of experiments with rabbit models (7).

Altered serum levels of ACHA were reported in patients with atherosclerosis (8, 9) and with chronic viral infections (8, 10). Although IgG isotype ACHAs can be detected in the sera of both healthy individuals and patients with several diseases, only IgM isotype ACHA has been produced and characterized to date. Thus, the question emerged whether it is possible to produce IgG isotype monoclonal antibody against cholesterol by immunization. From a practical point of view, an IgG isotype antibody would be much more convenient in most immunological techniques, such as immunohistochemistry, flow cytometry, and ELISA.

Furthermore, generation and in vitro characterization of the biological activity of IgG-type ACHAs seem critically important steps toward understanding their physiological roles. On the other hand, various cholesterol- and sphingolipid-rich membrane microdomains (e.g., the caveolar and noncaveolar lipid rafts) were implicated in controlling/regulating numerous cellular functions (6, 11–15), including activatory and inhibitory signal transduction events and the cellular uptake of various pathogens (viruses, bacteria, protozoa) and toxins (16, 17). Thus, IgG-type ACHAs might have significance in probing or functional modulation of such membrane microdomains.

Therefore, the aim of this study was to produce IgG isotype monoclonal ACHAs by immunizing mice with cholesterol-enriched liposomes. We managed to produce two IgG isotype monoclonal antibodies against cholesterol (AC1 and AC8) and found that they specifically detect cholesterol and several structurally closely related sterols in cell-free assays, as well as specifically bind to human lipoprotein fractions. The IgG-type ACHAs also bound to various cellular compartments, both extracellularly and intracellularly, identified as clustered plasma membrane cholesterol, lipid rafts, caveolae or intracellular lipid vesicle membranes, endoplasmic reticulum, and Golgi compartments. The basic properties, selectivity, and cellular and subcellular localization of the novel IgG3 ACHAs, as well as their potential application areas, are described and discussed.

MATERIALS AND METHODS

Cells

Jurkat [American Type Culture Collection (ATCC)] and MT-4 (HTLV-1+; a generous gift from Z. Beck, University of Debrecen, Hungary) human T-cell lymphomas and MonoMac6 (a kind gift of Z. Bajtay, Eötvös University, Budapest) and U937 (ATCC) human monocyte-macrophage cell lines were cultured in RPMI 1640 supplemented with 10% fetal calf serum. Murine P388D1 and J774A.1 monocyte-macrophage cell lines, A20 (ATCC) B lymphoma cells, and the Keyhole Limpet Haemocyanin-specific murine T_H hybridoma (2/13), produced as described previously (18), were all cultured in RPMI 1640 supplemented with 10% fetal calf serum and 2-mercaptoethanol.

Cholesterol liposomes

Cholesterol-rich multilamellar vesicles (71 mol% cholesterol) used for the induction of antibody production to cholesterol were composed as described by Dijkstra et al. (19). Briefly, they were made of 1,2-dimyristoyl-*sn*-glycero-3-phosphocholine (DMPC), 1,2-dimyristoyl-*sn*-glycero-3-phosphoglycerol, and cholesterol in a molar ratio of 9:1:25, and for immunization they were completed with adjuvant monophosphoryl lipid A at 25 μg/μmol phospholipid. Reagents were purchased from Sigma-Aldrich (St. Louis, MO). The lipids were divided into aliquots from stock solutions in chloroform in a pyrogen-free, round-bottom flask, and the solvent was removed by rotary evaporation. Sterile deionized water was added to the dry lipid film, achieving 50 mM total phospholipid, and vortexed until all of the lipids were resuspended. The material was subsequently incubated for 2 h at room temperature. Aliquots of the liposomal preparations were lyophilized in vaccine vials, stored at −70°C, and reconstructed before use in PBS to 10 mM final concentration of total phospholipids.

Immunization with cholesterol-rich liposomes

For the induction of antibodies to cholesterol, four male inbred mice (BALB/c) were immunized with 100 μl of the cholesterol-rich multilamellar vesicles (2.5 μmol of cholesterol) intraperitoneally and subcutaneously. After 4 weeks, the mice were given a boost injection of 2.5 μmol of cholesterol. Two weeks later, the mice were bled from the tail vein to collect immune sera. Preimmune sera were collected just before the primary inoculation; a 1:50 dilution was used to measure reactivity. ELISA for cholesterol was used to determine serum titer change in mice, and one of them was selected to be used for cell fusion. The animal studies were reviewed and approved by the appropriate institutional review committee.

Production of monoclonal antibodies against cholesterol

Monoclonal antibodies were generated by hybridizing Sp2/0-Ag14 myeloma cells with the splenocytes of immunized mice. Hybridomas were selected by growth in hypoxanthine-aminopterin thymidine medium. Initial screening was performed by ELISA on cholesterol. Two IgG and eight IgM clones were selected for expansion and initial characterization. Isotyping was carried out by anti-mouse IgG1, IgG2a, IgG2b, IgG3, IgM, κ, and λ horseradish peroxidase-conjugated antibodies (SouthernBiotech, Birmingham, AL).

The two IgG3 subclones, AC1 and AC8, were further characterized in detail. The IgGs were purified on Protein-G Sepharose

4 Fast Flow (Amersham Pharmacia Biotech AB, Uppsala, Sweden) columns by affinity chromatography from the supernatant of the hybridoma cells. The purity of antibodies was analyzed by SDS-PAGE.

Enzyme-linked immunoassay of antibody binding to cholesterol and other lipids

Polystyrene plates (Greiner, Frickhausen, Germany) were coated with cholesterol (0.01–10 μg/well), ergosterol, coprostane, 7-ketocholesterol, cholesteryl oleate, 25-hydroxy-cholesterol, cholic acid, DMPC, DL-alpha-dipalmitoyl-phosphatidylcholine (DPPC), or L-alpha-dipalmitoyl-phosphatidylethanolamine (DPPE) (10 μg/well for all lipids) (Sigma) dissolved in 100 μl of absolute ethanol and incubated at 4°C for 24 h. After washing with PBS and blocking with 0.1% casein (Reanal, Budapest, Hungary) in PBS, wells were incubated with 100 μl of serum samples or purified IgG diluted in PBS containing 0.1% casein. Binding of ACHAs was detected by anti-mouse horseradish peroxidase-conjugated γ-chain-specific goat antibodies (DAKO, Glostrup, Denmark), with *o*-phenylenediamine (Sigma) and H_2O_2 as substrates. The optical density was measured at 490 nm (reference at 600 nm). Concentrations of monoclonal antibodies at which an optical density of 0.2 (490–600 nm) was reached are demonstrated by the following symbols in **Table 1**: −, no reaction (at 100 μg/ml); +, low reaction (10–100 μg/ml); ++, medium reaction (1–10 μg/ml); +++, strong reaction (<1 μg/ml).

Competitive ELISA with human lipoproteins

Purified monoclonal IgG was mixed with different concentrations of human lipoproteins VLDL, LDL, and HDL (Calbiochem, San Diego, CA), or with 0.1% casein as a control, and incubated at 37°C for 60 min. The preincubated mixtures were applied to cholesterol-coated plates, and IgG binding was detected as described previously. Lipoprotein concentrations were normalized to the same surface area using the following data. For particle mass: VLDL, 40,000 kDa/mol; LDL, 2,300 kDa/mol; HDL, 200 kDa/mol. For particle diameter: VLDL, 50 nm; LDL, 20 nm; HDL, 10 nm. Initial concentrations used for the serial dilutions were determined based on normalization for the surface area corresponding to 20 μg of HDL.

TABLE 1. Cross-reactivity of monoclonal anti-cholesterol IgG3 antibodies AC1 and AC8 with other lipids

Lipid Type	Name	AC1	AC8
Sterols containing free 3β-hydroxyl	Cholesterol	++	+++
	Ergosterol	+	+++
	7-Ketocholesterol	++	+++
	25-Hydroxy-cholesterol	−	−
Sterols lacking free 3β-hydroxyl	Cholesteryl oleate	−	−
	Coprostane	−	−
	Cholic acid	−	−
Nonsterol lipids	1,2-Dimyristoyl-*sn*-glycero-3-phosphocholine	−	−
	DPPC	−	−
	DPPE	−	−
	1,2-Dimyristoyl-*sn*-glycero-3-phosphoglycerol	−	−

DPPC, DL-alpha-dipalmitoyl-phosphatidylcholine; DPPE, L-alpha-dipalmitoyl-phosphatidylethanolamine. ELISA plates were coated with cholesterol, ergosterol, 7-ketocholesterol, 25-hydroxy-cholesterol, cholesteryl oleate, coprostane, cholic acid, 1,2-dimyristoyl-*sn*-glycero-3-phosphocholine, 1,2-dimyristoyl-*sn*-glycero-3-phosphoglycerol, DPPC, or DPPE. AC1 and AC8 antibodies were serially diluted and added to the plates. Concentrations of monoclonal antibodies at which an optical density of 0.2 (490–600 nm) was reached are demonstrated by the following symbols: −, no reaction (at 100 μg/ml); +, low reaction (10–100 μg/ml); ++, medium reaction (1–10 μg/ml); +++, strong reaction (<1 μg/ml).

Measurement of fluorescence resonance energy transfer

2-(4,4,-Difluoro-5,7-dimethyl-4-bora-3a,4a-diaza-s-indacene-3-pentanoyl)-1-hexadecanoyl-*sn*-glycero-3-phospho-choline (BODIPY-FL C_5-HPC) was purchased from Molecular Probes-Invitrogen (Eugene, OR). Fluorescence resonance energy transfer (FRET) from BODIPY-FL C_5-HPC (donor) bound to HDL and LDL to Alexa555-conjugated AC8 antibody (acceptor) was measured by recording the emission spectra of BODIPY-FL C_5-HPC-labeled lipoproteins in the absence or presence of fluorescent AC8 on an Edinburgh Instruments F900 fluorescence spectrometer (Livingston, UK), using 460 nm excitation wavelength. Anti-human CD11a/LFA-1α antibody (MEM-25; a kind gift from Vaclav Horejsi, Prague, Czech Republic) was used as a negative control. The efficiency of FRET was estimated from both the quenching of donor fluorescence and the sensitization of acceptor fluorescence (20).

Detection of cell-bound ACHA by flow cytometry and confocal microscopy

The lymphoid and human monocyte-macrophage cell lines were incubated with 1–10 μg/ml monoclonal ACHA for 30 min on ice, washed and incubated with Alexa488-conjugated goat anti-mouse IgG secondary antibody (Molecular Probes-Invitrogen), and assayed by flow cytometry. Alternatively, directly labeled Alexa488-ACHA was also used to label cells for flow cytometry or confocal laser scanning microscopy, using Ka40 tobacco mosaic virus-specific mouse monoclonal antibody (produced in our laboratory) as an isotype control. For intracellular staining, cells were incubated with Alexa488-AC8 after fixation by 2% formaldehyde and permeabilization by 0.1% saponin plus 0.1% BSA. Cells (5×10^5 cells/sample) were labeled for all experiments. In flow cytometric experiments, 10,000 cells were collected and analyzed in a Becton-Dickinson FACSCalibur flow cytometer using CellQuest Pro software. In confocal laser scanning microscopy imaging experiments, the labeled cells were placed onto 0.15 mm thin coverslips in a chamber and assayed with an Olympus (Hamburg, Germany) Fluoview500 confocal microscope equipped with four optical channels using a 60×, high-numerical aperture oil-immersion objective.

Papain treatment of cells

Cells were exposed to a limited digestion by 5 or 10 U/ml papain (Sigma) with 10 U/mg specific activity for 5 and 10 min at 37°C in HBSS (Gibco). Cells were then washed extensively with ice-cold FACS buffer (Becton-Dickinson) supplemented with 0.1% BSA and labeled with antibodies as described previously.

Modification of membrane cholesterol level/distribution

Membrane cholesterol level was modulated by depletion with methyl-β-cyclodextrin (RAMEB, CycloLab), treating the cells with 2–10 mM methyl-β-cyclodextrin for 15 min at 37°C, as described previously (21), or with cholesterol oxidase (Sigma) (22). Briefly, cells were incubated with 0.5 or 1 U/ml cholesterol oxidase (from *Pseudomonas fluorescens*) for 2 h at 37°C and washed extensively. For complexing and segregating membrane cholesterol, 1–10 μg/ml concentrations of filipin III antibiotics (Sigma) were applied for a 45 min incubation at 37°C (23).

Isolation of detergent-insoluble buoyant membrane from T_H cells and immunodot blot analysis

Detergent-resistant and -soluble membrane fractions were isolated from T_H cells by a cold Triton X-100 lysis and subsequent

separation using sucrose density gradient (5–40%) ultracentrifugation, as described previously (24). Immunodot blots were developed on nitrocellulose membranes (Bio-Rad Laboratories, Hercules, CA). Cholesterol was diluted from stock solution in absolute ethanol to 50 μg/ml using PBS, and detergent-resistant (low buoyant density: 5% sucrose) and detergent-soluble (high buoyant density: 36–40% sucrose) membrane fractions were dropped onto the membrane in small amounts (2 μl) either directly or at 2× dilution and dried. Pretreatment of the samples with cholesterol oxidase was performed as described above. After blocking with 0.1% casein in PBS for 1 h, AC8 was added (1.5 μg/ml) for 1 h and then washed three times with PBS. The dot blots were finally developed by incubating with horseradish peroxidase-conjugated GAM IgG3 (SouthernBiotech) for 1 h, followed by washing six times with PBS, and evaluated using enhanced chemiluminescence reagent (Pierce Chemicals, Rockford, IL) and X-ray film (Agfa, Mortsel, Belgium).

Confocal microscopic colocalization assay

Cells were stained for lipid raft markers (GM1 gangliosides) with Alexa488- or Alexa647-cholera toxin B (Molecular Probes-Invitrogen), according to the manufacturer's instructions; FITC-anti-caveolin-1 antibody (rabbit IgG; Santa Cruz Biotechnology, Inc., Santa Cruz, CA) was used to label caveolae after a mild permeabilization of the plasma membrane (25). The long-chain diIC18 (3) (Molecular Probes-Invitrogen) lipid probe partitioning into liquid-ordered/gel-phase membrane regions was used according to the manufacturer's instructions. Human CD71-specific Cy3-MEM-75 (mouse IgG1 antibody) was a kind gift from Vaclav Horejsi, and FITC-conjugated rat anti-mouse antibody G7.4 (IgG2c; from ATCC) was used to label Thy1. CD2 on T-cells were labeled with FITC-conjugated anti-human CD2 monoclonal antibody (Sigma). ACHAs were applied either as Alexa488-conjugated AC8 or biotinylated AC8 plus Alexa647-conjugated neutravidin. For all antibodies, appropriate isotype control antibodies or cell lines were used as negative controls. BODIPY-brefeldin A558 (fixed/permeabilized cells, 100 nM, 30 min, 37°C) and BODIPY FL C_5-ceramide (live cells, 5 μM, 30 min, 4°C; Molecular Probes-Invitrogen) were used as markers of the endoplasmic reticulum/Golgi complex, whereas LysoTracker 568 (live cells, 75 nM, 30 min, 37°C; Molecular Probes-Invitrogen) served as a marker of lysosomes. Cell nuclei and mitochondria were stained with Draq5 (live cells, 2.5 μM, 10 min, room temperature; Biostatus, Ltd., Leicestershire, UK) and MitoTracker (live cells, 50 nM, 30 min, 37°C; Molecular Probes-Invitrogen), respectively. All of these markers were applied for cell labeling as described in the manufacturer's protocol. For plasma membrane cholesterol staining, live cells were used; to identify the subcellular localization of cholesterol, however, cells were fixed/permeabilized, as described above. Colocalization indices were determined with ImageJ software using appropriate plug-ins (Image Correlator Plus), from >100 regions of interest per sample, selected from at least 20 cells.

Statistical analysis and image processing

GraphPad Prism 4 for Windows (version 4.02) software (GraphPad Software, San Diego, CA) was used for the statistical analyses. Inhibitory effects of lipoproteins were compared by two-way ANOVA. Confocal microscopic images were further processed and analyzed with ImageJ software (Wayne Rasband, National Institutes of Health, Bethesda, MD), available at the website of the Wright Cell Imaging Facility (Toronto, Ontario, Canada; www.uhnres.utoronto.ca/facilities/wcif.htm).

RESULTS

Monoclonal antibody production

Preimmune sera reacted with cholesterol very weakly, similar to healthy mouse control sera (Sigma). After immunizing with liposomes containing 71% cholesterol, both IgG and IgM ACHA titers were largely increased (data not shown). Monoclonal antibodies were generated by hybridizing Sp2/0-Ag14 myeloma cells with spleen cells from immunized mice of the highest antibody titer. After subcloning, three IgG- and eight IgM-secreting hybridomas were selected based on their capacity to produce antibodies reacting with cholesterol. All of the IgG antibodies were of the IgG3 isotype, and all of the IgG and IgM antibodies had κ light chains. Several IgMs specific to cholesterol had already been generated and characterized (1, 4, 19); therefore, we focused our investigations on the IgGs. Two selected clones (AC1 and AC8) were further analyzed in terms of their specificity and binding to intact cells (plasma membrane/subcellular localization).

Reactivity of monoclonal IgG ACHAs to cholesterol and other lipids

When applied in solid phase to ELISA plates, cholesterol has been reported to show a concentration-dependent aggregation (4). At 1 μg of cholesterol per well, cholesterol dominantly exists in noncrystalline form, except for a few microscopic crystals, whereas a significant amount of microcrystals exists at 10 μg of cholesterol per well. To determine whether the clustering or crystal structure of cholesterol has an effect on the binding of our monoclonal antibodies, plates were coated with 0.01–10 μg/well cholesterol, and ACHA binding was tested in an ELISA system. Both AC1 and AC8 monoclonal antibodies bound in a dose-dependent manner to cholesterol adsorbed on polystyrene plates. The binding of both monoclonal antibodies was fairly independent of cholesterol concentration between 0.1 and 10 μg/well cholesterol. Their binding capacity, however, declined sharply to <0.1 μg/well (**Fig. 1**). The isotype control antibody (Ka40) did not bind to the coat (Fig. 1B).

The binding of ACHAs to various structurally related sterols and to other lipids was also tested by ELISA. The 3β-hydroxyl group was proposed previously as a critical structural motif in the binding of anti-cholesterol IgMs (9). To investigate the fine specificities of AC1 and AC8, six structurally related sterols (ergosterol, coprostane, cholesteryl oleate, 25-hydroxy-cholesterol, 7-ketocholesterol, and cholic acid) and three other nonsterol lipids (DMPC, DPPC, and DPPE) were tested as coated antigens. Like cholesterol, ergosterol, 7-ketocholesterol, and 25-hydroxy-cholesterol contain a free 3β-hydroxyl group, whereas cholic acid, coprostane, and cholesteryl oleate do not. ELISA results showed a more efficient binding of AC8 to cholesterol, ergosterol, and 7-ketocholesterol than to the other sterols. AC1 consistently showed a lower affinity to all sterols than did AC8, and the sterols to which they bound with the highest affinity were different (cholesterol for AC1 and 7-ketocholesterol for AC8). This indicates that the molec-

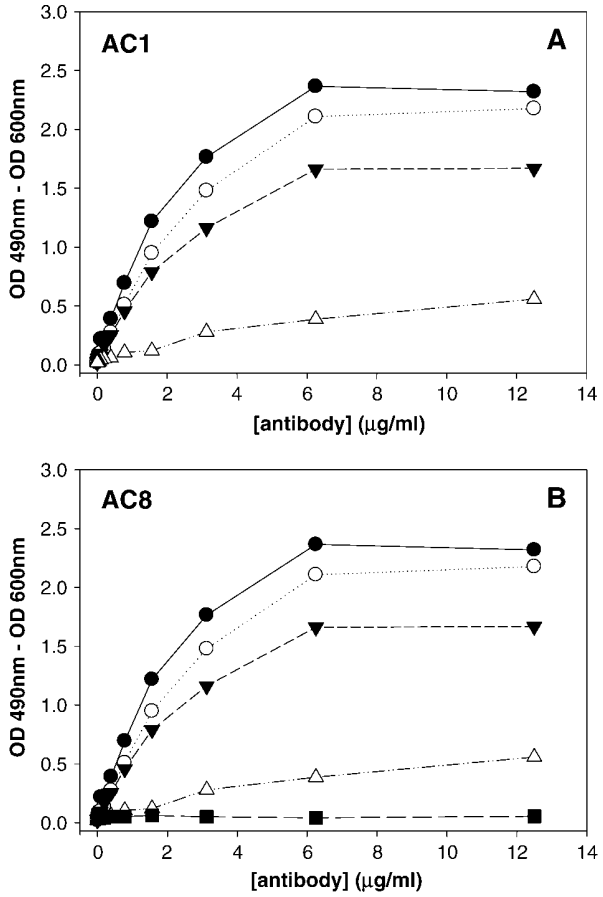

Fig. 1. Binding of monoclonal antibodies to cholesterol. Cholesterol was adsorbed to polystyrene plates at concentrations of 0.01 (open triangles), 0.1 (closed inverted triangles), 1.0 (open circles), and 10 (closed circles) μg/well. ELISA was carried out with serially diluted purified monoclonal IgG [initial concentrations: AC1 IgG, 100 μg/ml (A); AC8 IgG, 25 μg/ml (B)], then goat anti-mouse IgG labeled with horseradish peroxidase was applied. In B, binding of the isotype control Ka40 antibody (closed squares) is also displayed. Representative results from three independent experiments are shown. OD, optical density.

ular determinants may be slightly different for AC8 and AC1. In spite of the presence of a 3β-hydroxyl group of 25-hydroxy-cholesterol, the ACHAs did not bind to it. On the other hand, there was no detectable binding to other sterols lacking the 3β-hydroxyl group (Table 1). These results together suggest that the epitope recognized by ACHAs comprises the 3β-hydroxyl group in sterols, although other parts of the structure (not present in 25-hydroxy-cholesterol) cannot be excluded. As a control, no significant binding of IgG3 ACHAs to three other selected phospholipids was observed (Table 1).

The IgG3 ACHAs specifically bind to lipoproteins

Lipoproteins contain a significant amount of cholesterol in both the free and esterified forms. To assess the ability of ACHAs to interact with the human lipoproteins VLDL, LDL, and HDL, purified ACHAs were premixed with different concentrations of lipoproteins. After incubation at 37°C for 60 min, the mixture was applied to cholesterol-coated plates. All of the human lipoproteins (VLDL, LDL, and HDL) inhibited the binding of ACHAs to cholesterol in a dose-dependent manner (**Fig. 2A**). The lipoproteins did not bind to the cholesterol coat under the same conditions (data not shown). When the results were normalized to the surface areas (corresponding to the available binding sites for antibody) of the various lipoproteins, binding of ACHA to HDL was found to be only

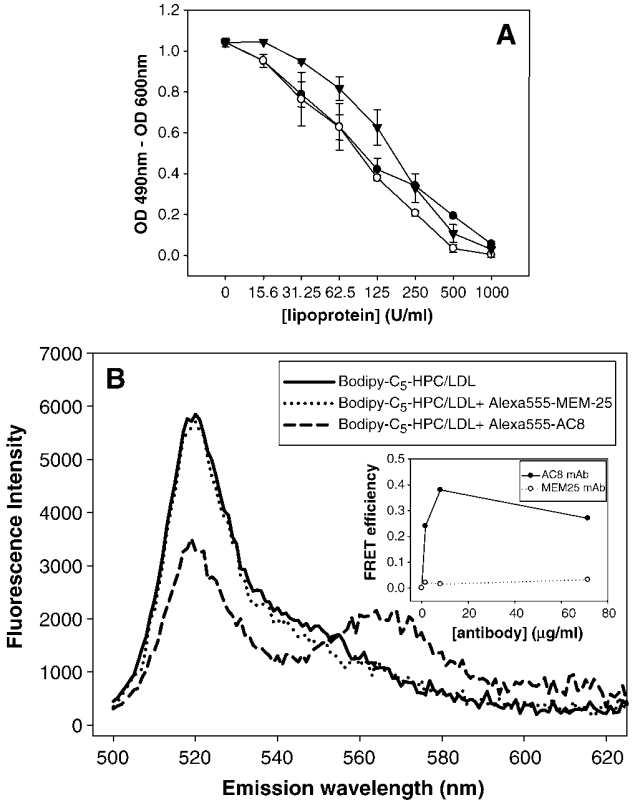

Fig. 2. Binding of anti-cholesterol IgG3 antibodies (ACHAs) to lipoproteins. A: Inhibition of the ACHA-cholesterol interaction by human lipoproteins. Serially diluted liposomes or human VLDL (closed circles), LDL (open circles), and HDL (closed inverted triangles) were mixed with anti-cholesterol IgG, AC8 (10 μg/ml). The surface of 20 μg is equal to 1.8×10^{-2} m^2. All the concentrations of lipoproteins (HDL, LDL, VLDL) were adjusted to this surface. The mixture was incubated at 37°C for 60 min, then dropped onto cholesterol-coated ELISA plates. Bound IgG was detected by goat anti-mouse IgG labeled with horseradish peroxidase. Means of three independent experiments ± SEM are shown. No significant differences were found between the inhibitory effects of the three lipoproteins using two-way ANOVA. OD, optical density. B: In fluorescence resonance energy transfer (FRET) measurements, LDL (500 μg total lipid/ml) with or without 2-(4,4,-difluoro-5,7-dimethyl-4-bora-3a,4a-diaza-s-indacene-3-pentanoyl)-1-hexadecanoyl-*sn*-glycero-3-phospho-choline (BODIPY-FL C_5-HPC; 110 nM) was titrated with increasing concentrations (X axis) of Alexa555-AC8 or Alexa555-anti-CD11a (as a negative control). FRET efficiencies (see inset) with AC8 (solid line) or anti-CD11a (dotted line) acceptors were calculated from either the decrease of corrected donor emission intensities at 519 nm or the acceptor sensitization at 570 nm, upon excitation at 460 nm. mAb, monoclonal antibody.

slightly weaker than to VLDL or LDL, in contrast to earlier findings with IgM ACHAs. Binding of AC8 to lipoproteins (LDL and HDL) was further confirmed by direct FRET measurements between BODIPY FL C_5-HPC lipid probe and Alexa555-AC8. A highly efficient ($E_{max} \sim 0.4$) and concentration-dependent FRET was observed in LDL (Fig. 2B). Similar, but less efficient ($E_{max} \sim 0.3$), FRET was obtained with HDL (data not shown). No FRET was detected when Alexa555-anti-CD11a antibody was used as the acceptor.

IgG3 ACHAs bind to various intact cells both extracellularly and intracellularly

Several cell types of different origin, expressing lipid rafts or caveola microdomains enriched in cholesterol, were selected to investigate the binding of monoclonal ACHAs to the cell surface or to intracellular compartments: mouse helper T-cell hybridoma (2/13), human T-lymphoma cell lines (Jurkat, MT-4), human monocyte-macrophage cell lines (MonoMac6, U937), and murine B- and macrophage cell lines (A20 and P388D1, respectively). A low-avidity spontaneous binding of both IgG3 ACHAs was observed in all cell lines, which was cell type-dependent (**Fig. 3A–D**). The expression pattern of long, protruding glycoproteins or glycolipids, which may shield the presumably small antigen determinant(s) of ACHAs, may vary among cell types. Therefore, we tested whether a limited papain digestion of the cell surface, expected to remove some long external protein domains, affects the binding of our ACHAs. Indeed, an optimized papain treatment significantly decreased the magnitude of immunofluorescence arising from several long cell surface glycoproteins, such as CD45R/B220 on B-cells and CD44 on T-lymphocytes (Fig. 3E, F). Binding of AC8 antibody substantially increased in all cell types upon papain digestion, proportionally with the papain dose (Fig. 3A–D), and the differences in the extent of ACHA binding among cell types also became more pronounced. This suggests that a limited digestion of the cells by papain (10 U/ml, 10 min, 37°C) may serve as an "epitope exposition tool" for ACHAs on either fixed or unfixed cells of different origin, allowing "snapshot imaging" of clustered cholesterol at the surface of cells under various physiological or pathological conditions (**Fig. 4**).

Confocal microscopy showed that AC8 IgG intensely stained the plasma membrane of murine T_H cells after papain digestion (Fig. 4B, C), whereas no or very weak staining was observed with the fluorescent isotype control antibody Ka40 (Fig. 4A) or in the absence of epitope exposition by papain (data not shown), respectively, in accordance with the flow cytometric data (Fig. 3A–D). The plasma membranes of various cells were labeled by AC8 uniformly, in a strongly patchy manner, with an approximate average patch size of 200–400 nm (Fig. 4C).

Membrane ganglioside (raft) expression, assessed by flow cytometric analysis of fluorescent cholera toxin B binding, showed a fairly good correlation with the magnitude of ACHA binding on various murine and human cell types (Fig. 3G). Notably, monocyte-macrophage cells were represented mostly in the high double expression region (Fig. 3G, right side), possibly because of their caveolar raft expression. In contrast, an IgM isotype ACHA, displaying cholesterol selectivity in cell-free assays, did not show detectable binding to any of the tested cell types, even after papain digestion (data not shown).

AC8 antibody also bound intracellularly in mouse or human T_H cells, after their formaldehyde fixation/saponin permeabilization. The intracellular staining may be attributed largely to cholesterol-containing membranes of lipid vesicles of varying size (Fig. 4D). Colocalization of ACHA with different intracellular organelle markers was also analyzed and quantified in mouse and human T-cells and macrophages. Intracellularly bound ACHA colocalized with fluorescent brefeldin A [colocalization coefficient (cc), 0.30] (Fig. 4E), a marker of the endoplasmic reticulum and Golgi complex, with the Golgi complex-specific BODIPY-ceramide$_5$ (cc, 0.32), and more weakly with a marker of lysosomes, LysoTracker (cc, 0.25), but not with markers of mitochondria or cell nuclei (cc, < 0.1) (Fig. 4J).

Cell surface-bound ACHA and the cholesterol-rich lipid raft microdomains

Because cholesterol is known to be enriched in various caveolar or noncaveolar lipid rafts, we intended to investigate how the surface-bound IgG3 ACHAs relate to these membrane microdomains, using snapshot imaging after epitope exposition by papain, as described above. ACHA AC8 strongly colocalized in T-cell membranes with cholera toxin B bound to GM_1 gangliosides (cc, 0.69) (Fig. 4F) and with a protein marker of lipid rafts, Thy1 (cc, 0.55) (Fig. 4G), and, although slightly weaker (cc, 0.39), with transferrin receptors (CD71) marking preferentially the chlathrin-coated pit membrane structures (Fig. 4H). In addition, AC8 antibody colocalized substantially with the diIC18 (3) lipid probe (cc, 0.48) as well, reported to preferentially partition into liquid-ordered or gel-phase membrane regions (26) (data not shown), indicating that ACHAs may bind to various cholesterol-rich, ordered microdomains/compartments of the cellular plasma membranes. This is further confirmed by the strong colocalization (cc, 0.63) between AC8 and caveolin-1 in macrophages (Fig. 4I). In contrast, in T-cells, ACHA did not colocalize with CD2 (Fig. 4J), reported as a nonraft protein in unstimulated T-lymphocytes (27).

In addition, AC8 bound to the detergent-resistant membrane fractions isolated from T_H cells and did not bind or bound very weakly to soluble membrane fractions of the same cells, as demonstrated by immunodot blot technique (**Fig. 5C**). Furthermore, treatment with cholesterol oxidase (COase) resulted in decreased binding of AC8 to both cholesterol and the detergent-resistant fraction on the dot blots. In contrast, no binding was observed to the cold Triton X-100-soluble membrane fraction (Fig. 5C). Deprivation of membrane cholesterol by cholesterol oxidase decreased ACHA binding in both T-helper cells and monocyte-macrophage cells, as assessed by flow cytometry (Fig. 5A, B). Filipin, an antibiotic known to selectively complex membrane cholesterol (23), also slightly decreased AC8 antibody binding to T-cells (Fig. 5A); at the same time, AC8 staining showed the filipin concentration-dependent segregation of cholesterol into large clusters

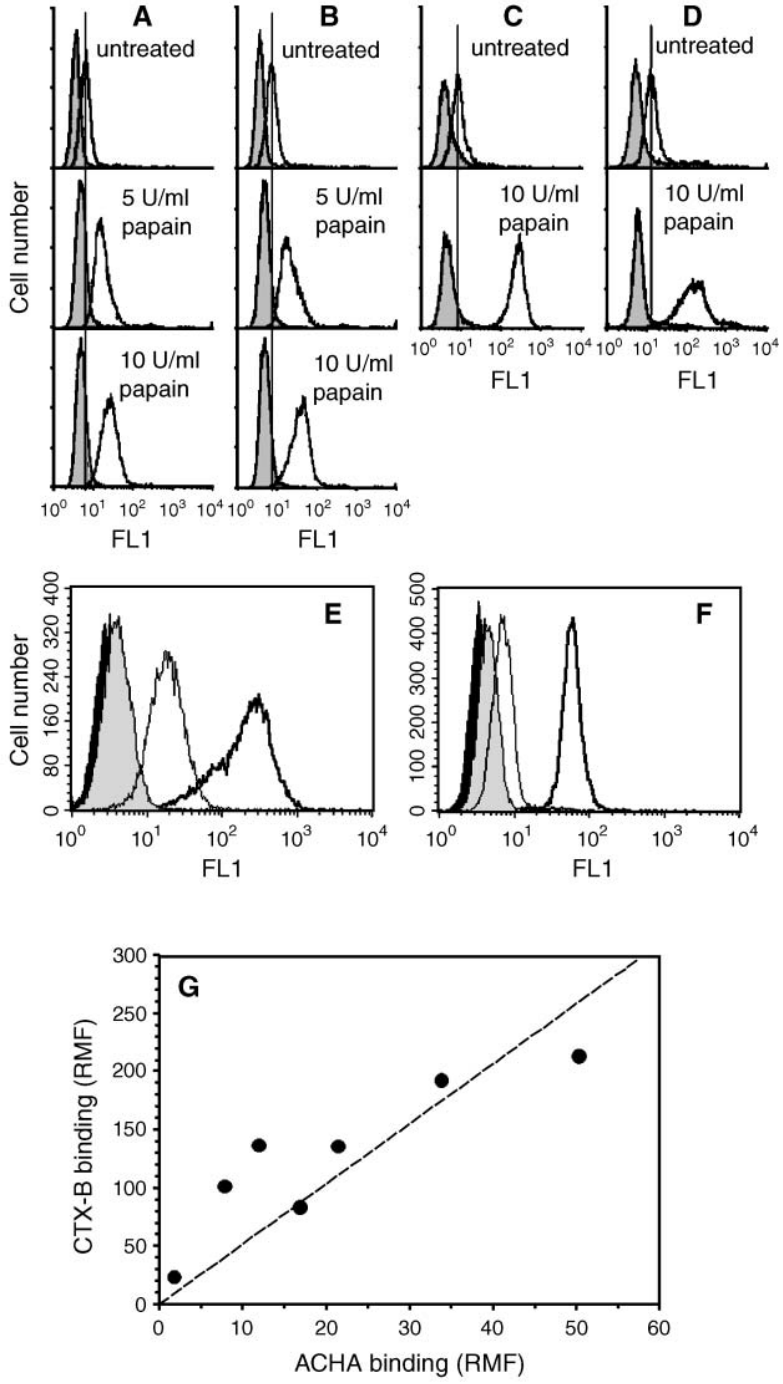

Fig. 3. Flow cytometric analysis of the binding of ACHAs to live murine and human lymphoid and monocyte-macrophage cell lines. A, B: Binding of AC1 (A) and AC8 (B) to murine T-helper cells (2/13), as detected by flow cytometry using Alexa488-conjugated ACHA. Histograms of isotype control (gray areas), ACHA binding to cells without (top) or with 5 U/ml (middle) and 10 U/ml (bottom) papain treatment are displayed. C, D: Binding of AC8 to the MonoMac6 human monocyte-macrophage cell line (C) and the MT-4 (HTLV-1+) human T-lymphoma cell line (D), without or with 10 U/ml papain treatment. Symbols are the same as those used in A and B. E, F: Papain digestion results in a decreased expression of long, protruding proteins, such as CD45R (B220) in B-cells (E) and CD44 in T-cells (F). Isotype controls in the absence (black areas) or presence of papain (gray areas) and immunofluorescence in the absence (thick lines) or presence of papain treatment (thin lines) are shown. G: AC8 binding to various cell types (human and murine B- and T-cells, macrophages) correlates well with GM_1 ganglioside expression of the cells. The correlation between AC8 and CTX binding was strong ($r = 0.89$) among seven different cell types. CTX, cholera toxin B; RMF, relative mean fluroescence.

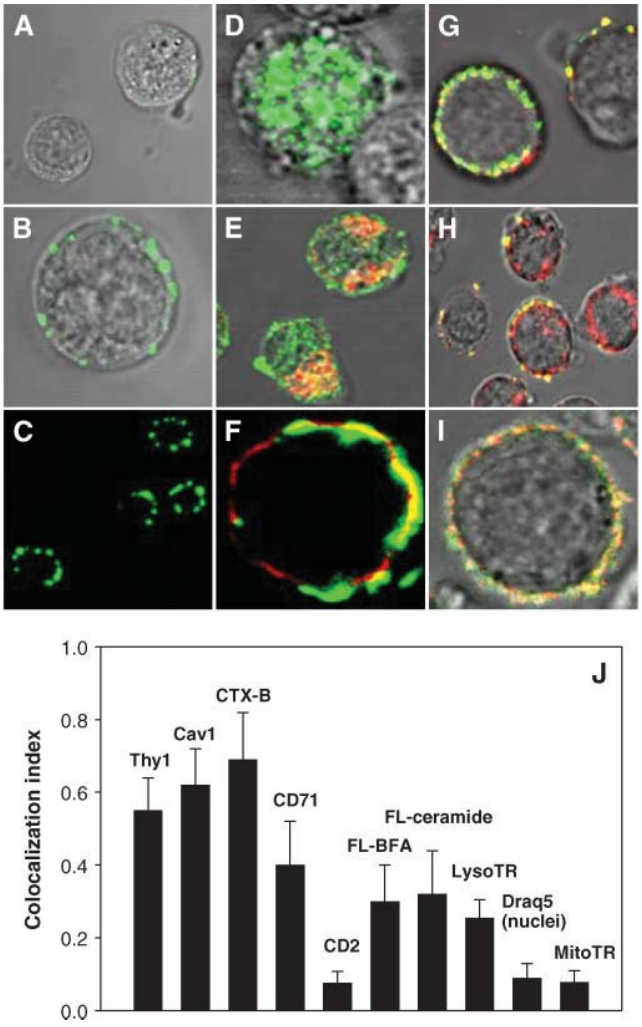

Fig. 4. Binding of AC8 antibody to live cells, by confocal microscopic analysis. Representative images of 2/13 mouse T_H cells labeled with isotype control antibody (A) and Alexa488-AC8 at high (B) or low (C) zoom are shown. The images were acquired using a 60× oil-immersion objective (numerical aperture, 1.45). Panels A, B, D, E, G, H, and I are composites of the equatorial fluorescent image slices and the differential interference contrast images of the cells, and panels C and F are fluorescent images. Intracellular staining of saponin-permeabilized 2/13 T_H cells by AC8 is shown in (D). Intracellular bound AC8 showed partial colocalization with a marker of endoplasmic reticulum and the Golgi complex, BODIPY-brefeldin A (E). Representative images show that AC8 colocalizes strongly with CTX-B (GM_1) (F), Thy1 antigen (G), and to a smaller extent with anti-CD71/transferrin receptor (H) in T-cells, as well as strongly with caveolin-1 (I) in macrophages. Colocalization indices of fluorescent AC8 with various fluorescent membrane and intracellular markers are summarized in (J) and expressed as means ± SD from at least 100 regions of interest. CTX-B, cholera toxin-B.

(Fig. 5D–F). Depletion of membrane cholesterol by methyl-β-cyclodextrin similarly reduced AC8 binding (data not shown).

In quiescent 2/13 mouse T_H cells, the patchy staining by AC8 was uniform (ring-like) along the plasma membrane (Fig. 5D), similar to cholera toxin B staining (Fig. 5G), with a substantial colocalization of the two labels (Fig. 4J). Activation of the T_H cells with mitogen (concanavalin A) had no effect on the amount of bound cholera toxin B or ACHA (data not shown), although it resulted in a remarkable cell surface redistribution of cholera toxin B, indicating polarization of rafts in the plasma membrane. More than 60% of the T-cells showed highly patchy or cap-like ganglioside/cholera toxin distribution after 24 h of activation (Fig. 5H). AC8 antibody was found highly co-polarized with the rafts (cc, >0.85) in activated T-cells (Fig. 5I), indicating that the novel IgG3 ACHAs can monitor the redistribution of cholesterol-rich microdomains in the plasma membranes of intact lymphoid cells upon activation signals.

These data together suggest that the AC8 IgG3-type monoclonal antibody, in addition to its preferential binding to cholesterol-rich raft microdomains at the cell surface, is able to monitor the dynamic redistribution of clustered cholesterol in the plasma membranes of immunocytes during their activation or signal transduction.

DISCUSSION

In this study, we demonstrated that production of not only IgM but also IgG ACHAs can be induced in mice by immunizing them with cholesterol-rich liposomes. In general, IgG3 is primarily produced against antigens with carbohydrate or repeated epitopes. Although the set of 11 generated ACHA clones is statistically insufficient, the fact that we produced exclusively IgM and IgG3 but no other IgG subtypes may indicate that the immunogenicity of cholesterol is somehow related to these classes of epitopes. This is supported by the structural similarities between the 3β-hydroxyl group and its environment in cholesterol and some surface-associated carbohydrate structures of pathogens, as well as by the periodically repeated (clustered) arrangement of cholesterol.

An earlier monoclonal IgM-type ACHA (monoclonal antibody 2C5-6) showed selectivity in its binding to aggregated cholesterol but not to strictly defined and organized surfaces of cholesterol monohydrate crystals. In contrast, other monoclonal IgMs selected against cholesterol crystals, recognizing a given pattern of epitopes present on the crystal faces. A cholesterol concentration of 10 μg/ml was reported as a critical threshold for obtaining a significant amount of microcrystals (4). Although no direct binding studies have been performed on crystalline cholesterol, the affinity of our two novel IgG ACHAs did not significantly depend on the cholesterol concentration being in the range of 0.1–10 μg/ml. This suggests that the IgG-type ACHAs AC8 and AC1 are less sensitive to the aggregation state of cholesterol than the previously developed IgM isotype ACHAs.

Dijkstra and coworkers (19) reported that cholesterol-immunreactive sera and a monoclonal anti-cholesterol IgM (2C5-6) were both specific to cholesterol and structurally similar sterols containing a 3β-hydroxyl group. In accordance with this observation, we found that the anti-

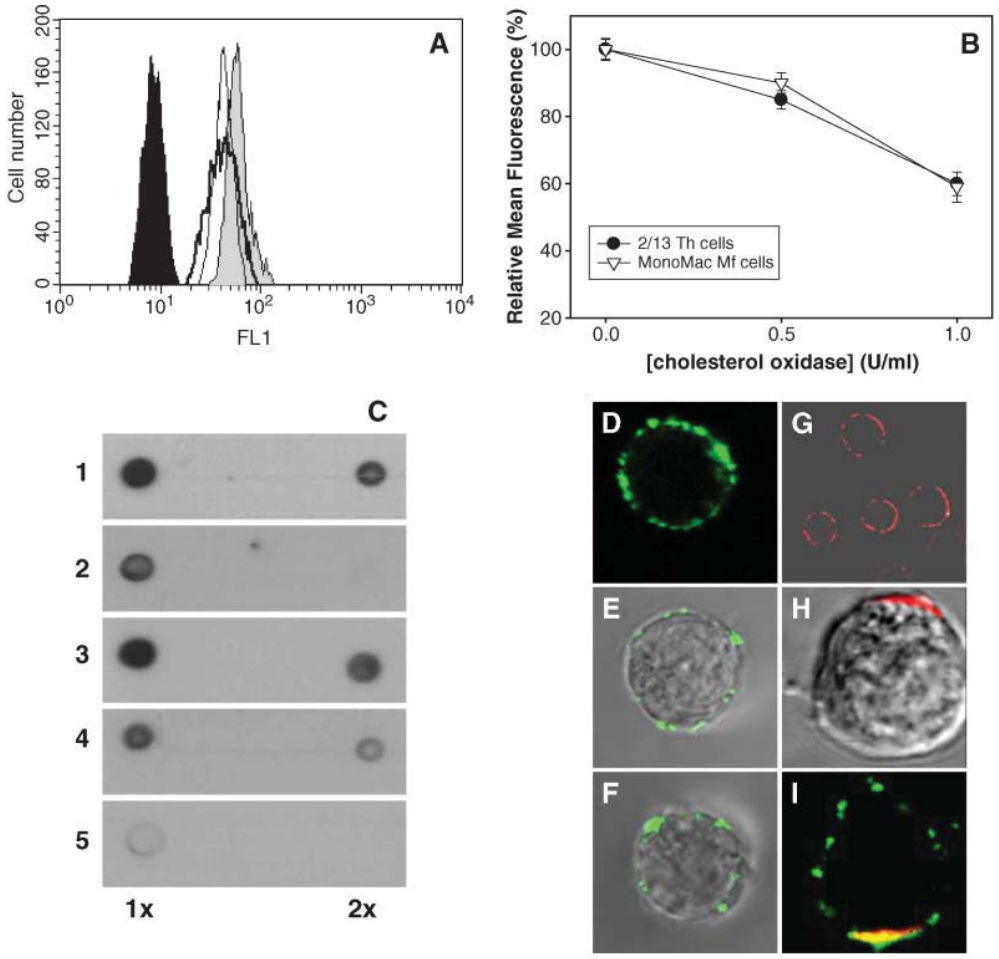

Fig. 5. AC8 binding to T-cells and macrophage cells is sensitive to membrane cholesterol/raft modulations. A: Filipin (10 μg/ml; thick line) or cholesterol oxidase (1 U/ml; thin line) reduces AC8 binding to the surface of papain-treated 2/13 T_H cells. Immunofluorescence of isotype control (black area) or AC8-labeled (gray area), papain-treated cells is also shown. B: Cholesterol oxidase dose-dependently reduces AC8 binding to papain-treated 2/13 T_H lymphocytes (closed diamonds) and MonoMac6 (open inverted triangles) human monocyte-macrophage cells. C: Immunodot blot analysis of detergent-resistant (gels 3, 4) and detergent-soluble (gel 5) fractions isolated from T_H cells and cholesterol (gels 1, 2) as a control. Samples were untreated (gels 1, 3, 5) or treated with cholesterol oxidase (gels 2, 4) and dropped onto the nitrocellulose membrane in small (2 μl) amounts either directly or at 2× dilution. D–I: Treatment of T-cells with 5 μg/ml (E) and 10 μg/ml (F) filipin results in a gradual segregation of membrane cholesterol relative to untreated control cells (D). 2/13 T_H cells are stained in a uniformly ring-like, patchy manner with cholera toxin B (G). Activation of T_H cells with concanavalin A mitogen results in capping of cholera toxin B, as shown by the representative image in (H). AC8 is strongly copolarized with cholera toxin B in the membrane of mitogen-activated T-cells (I). Error bars represent SEM.

cholesterol IgG monoclonal antibodies bound efficiently only to those cholesterol-like sterols that contain a 3β-hydroxyl group. However, additional chemical moieties or the polarity of the sterols may also influence antibody binding, consistent with the lack of binding to 25-hydroxycholesterol bearing the free 3β-hydroxyl moiety. The two monoclonal ACHAs (AC8 and AC1) differed slightly in their binding preference to the tested sterols, suggesting that, in spite of the small epitope size, two antibodies with different fine specificities could be generated.

Our monoclonal IgG ACHAs bound to human lipoproteins HDL, LDL, and VLDL alike. In contrast to previous studies with IgM, no strict selectivity was found in the binding to LDL and VLDL over HDL. Dijkstra et al. (19) reached their conclusion about binding selectivity on the basis of bound antibody per total (or free) cholesterol. However, the total cholesterol content (free plus esterified cholesterol) per particle mass, the particle size, the ratio of surface free cholesterol to total cholesterol, and the protein-to-lipid ratio may all vary strongly among the different lipoproteins. Moreover, these factors together may influence the available surface area for antibody binding. When the binding of our IgG ACHAs to the different lipoproteins was normalized for equivalent surface area, we obtained similar values, and the avidity to HDL was only slightly lower than that to LDL or VLDL. This is consistent

with the higher surface density of proteins in HDL, because the proteins may shield part of the surface cholesterol epitopes, and is also indicative of an important difference between IgM- and IgG-type ACHAs.

High serum levels of low density lipoproteins and low serum concentrations of HDL are independent risk factors for atherosclerotic diseases (28–32). The previously reported monoclonal ACHA binding to LDL and VLDL but not to HDL (19) led to the hypothesis (33) that naturally occurring ACHAs may have a role in the selective clearance of LDLs ("bad cholesterol"). That the IgG ACHAs generated in this work also bind to HDL, however, suggests that the role of natural ACHAs in the pathogenesis of atherosclerosis cannot be simplified. This is further supported by the clinical findings of high ACHA serum levels in patients with coronary heart disease (9) but low ACHA levels in patients with cerebrovascular diseases (29, 31) compared with healthy individuals.

As cholesterol is a fundamental component of cell membranes, it is an intriguing question whether natural ACHAs can bind to cell surfaces under physiological or pathological conditions. Previously, monoclonal IgM ACHAs were reported to react with plasma membrane cholesterol microdomains of macrophages responsive to changes in cholesterol trafficking. These IgMs bound to the cells only after artificial cholesterol enrichment by various treatments, suggesting that they define cholesterol arrays that are presumably not identical to lipid rafts (5, 24).

The novel IgG monoclonal antibodies AC1 and AC8 bound spontaneously, although weakly, to intact human and murine lymphoid or monocyte-macrophage cells. A limited papain digestion, removing some long extracellular protein domains from the cell surface, strongly enhanced their avidity, indicating that the IgG ACHAs bind to "extremely small epitopes" that are mostly shielded by the long, protruding membrane proteins. The higher level of AC8 binding to monocyte-macrophage cells versus lymphoid cells is likely attributable to the easier access to cholesterol epitopes in "opened" caveolar structures compared with the crowded surface of lymphocytes.

Exposure of cholesterol epitopes, however, may also change during apoptosis and the budding of enveloped viruses or under pathological conditions (e.g., tumors), because all of these processes may alter molecular composition, curvature, or the "surface smoothness" of the involved membrane regions. Recognition of the exposed cholesterol epitopes by naturally occurring cholesterol-specific antibodies may have further physiological consequences, such as activation of the complement and/or phagocytic system to eliminate dead cells as well as virus particles. Such altered cholesterol exposure may also be relevant in the increased level of ACHAs observed under pathological conditions (8–10, 34).

The high degree of colocalization between the IgG ACHA and cholera toxin B, anti-Thy1, or anti-caveolin-1 antibodies indicates that rafts or caveolae can be considered preferential binding sites for ACHAs in the plasma membrane. Although in lymphocytes and macrophages cholesterol can be found in fluid-phase membrane regions as well, it is locally enriched (clustered) in the noncaveolar and caveolar rafts or, to a lesser extent, in other functional membrane domains, such as chlathrin-coated pit structures (6), consistent with our findings. Aggregation of lipid rafts by T-cell activation signals has been described (6). Thus, the strongly patchy nature of membrane staining by ACHA and its copolarization (capping) with the lipid raft marker cholera toxin B upon T-cell activation, together with a substantial degree of colocalization between ACHA and other lipid raft markers, all suggest that AC8 antibody is capable of marking lipid raft microdomains and even monitoring their activation-induced redistribution in the plasma membranes of live lymphoid cells.

In contrast to the IgM antibodies reported by Kruth et al. (5), our data show that the IgG ACHAs bind to T- or B-cell membrane microdomains displaying detergent resistance and enriched in known markers of lipid rafts. These properties of the new IgG ACHAs allow further possible applications in the study of lipid raft functions.

In addition, the structural integrity of raft/caveola microdomains, stabilized by cholesterol, is essential in various immunological functions, such as antigen presentation (35–37), T-cell receptor-mediated signal transduction (36), and the uptake of viral (e.g., human immunodeficiency virus) and other pathogens or particles by phagocytes (16, 37). This raises the question of whether binding of ACHAs to the membrane microdomains of these cells can modulate these processes and, if so, how. Our preliminary results obtained with an antigen-presenting cell (APC)-T_H cell immunological synapse model (21), showing AC8-augmented antigen presentation and an enhanced phagocytosis of opsonized yeast cells by macrophages upon AC8 antibody binding, suggest that AC8 may have potential to modulate various immune functions dependent somehow on cholesterol-rich lipid rafts. Such modulatory effects are limited to those immunocytes to which ACHAs can bind spontaneously to a sufficient extent (e.g., APCs, macrophages). Indeed, no modulatory effect of ACHA on T-cell activation was observed in the APC-T_H cell immunological synapse if the T_H cells were preincubated with ACHAs instead of the APCs (38).

In conclusion, we generated two IgG3 isotype clones of ACHAs, AC1 and AC8, that were characterized in detail in both cell-free and cellular systems and have shown their potential to mark and monitor changes in the cell surface distribution of cholesterol-rich caveolar or noncaveolar lipid rafts. Consistent with their substantially enhanced binding to the surface of various immunocytes upon moderate papain digestion, we propose that IgG ACHAs, in contrast to IgM isotypes, may function by directly modulating several lipid raft-dependent immune functions, especially under specific physiological or pathological conditions, altering the epitope accessibility of their target cells. Further detailed investigations are required, however, to validate this and other possible functions of ACHAs in modulating the immune response; these are currently running in our laboratories.

The authors gratefully acknowledge Árpád Mikessy for his contribution to the immunization experiments and Dr. Zoltán Prohaszka for valuable discussions. This work was supported by Hugarian National Science Fund Grants TS044711 (J.M., G.L.), T043613 (G.L.), T049696 (J.M.), and F049164 (L.C.) and by Grant ETT 195/2003 from the Hungarian Ministry of Health (L.R., G.F.).

REFERENCES

1. Swartz, G. M., M. K. Gentry, L. M. Amende, E. J. Blanchette-Mackie, and C. R. Alving. 1988. Antibodies to cholesterol. *Proc. Natl. Acad. Sci. USA.* **85:** 1902–1906.
2. Alving, C. R., G. M. Swartz, and N. M. Wassef. 1989. Naturally occurring autoantibodies to cholesterol in humans. *Biochem. Soc. Trans.* **629:** 637–639.
3. Alving, C. R., N. M. Wassef, and M. Potter. 1995. Antibodies to cholesterol: biological implications of antibodies to lipids. *Curr. Top. Microbiol. Immunol.* **210:** 181–186.
4. Perl-Treves, D., N. Kessler, D. Izhaky, and L. Addadi. 1996. Monoclonal antibody recognition of cholesterol monohydrate crystal faces. *Chem. Biol.* **3:** 567–577.
5. Kruth, H. S., I. Ifrim, J. Chang, L. Addadi, D. Perl-Treves, and W. Y. Yhang. 2001. Monoclonal antibody detection of plasma membrane cholesterol microdomains responsive to cholesterol trafficking. *J. Lipid Res.* **42:** 1492–1500.
6. Matkó, J., and J. Szöllősi. 2004. Regulatory aspects of membrane microdomain (raft) dynamics in live cells: a biophysical approach. *In* Membrane Microdomain Signaling: Lipid Rafts in Biology and Medicine. M. Mattson, editor. Humana Press, Totowa, NJ. 15–46.
7. Alving, C. R., G. M. Swartz, N. M. Wassef, J. L. Ribas, E. E. Herderick, R. Virmani, F. D. Kolodgie, G. R. Matyas, and J. F. Cornhill. 1996. Immunisation with cholesterol-rich liposomes induces anti-cholesterol antibodies and reduces diet-induced hypercholesterolaemia and plaque formation. *J. Lab. Clin. Med.* **127:** 40–49.
8. Horváth, A., G. Füst, I. Horváth, G. Vallus, J. Duba, P. Harcos, Z. Prohaszka, E. Rajnavolgyi, L. Janoskuti, M. Kovacs, et al. 2001. Anti-cholesterol antibody (ACHA) levels in patients with different atherosclerotic vascular diseases. Characterization of human ACHA. *Atherosclerosis.* **156:** 185–192.
9. Veres, A., G. Füst, M. Smieja, M. McQueen, A. Horvath, Q. Yi, A. Biro, J. Pogue, L. Romics, I. Karadi, et al. 2002. Relationship of anti-60kDa heat shock protein and anti-cholesterol antibodies to cardiovascular events. *Circulation.* **106:** 2775–2780.
10. Biro, A., A. Horvath, L. Varga, E. Nemesanszky, A. Csepregi, K. David, G. Tolvaj, E. Ibranyi, L. Telegdy, A. Par, et al. 2003. Serum anti-cholesterol antibodies in chronic hepatitis-C patients during IFN-α-2b treatment. *Immunobiology.* **207:** 161–168.
11. Haks, M. C., S. M. Belkowski, M. Ciofani, M. Rhodes, J. M. Lefebvre, S. Trop, P. Hugo, J. C. Zuniga-Pflucker, and D. L. Wiest. 2003. Low activation threshold as a mechanism for ligand-independent signaling in pre-T-cells. *J. Immunol.* **170:** 2853–2861.
12. Guo, B., R. M. Kato, M. Garcia-Lloret, M. I. Wahl, and D. J. Rawlings. 2000. Engagement of the human pre-B cell receptor generates a lipid raft-dependent calcium signaling complex. *Immunity.* **13:** 243–253.
13. Poloso, N. J., and P. A. Roche. 2004. Association of MHC class II-peptide complexes with plasma membrane lipid microdomains. *Curr. Opin. Immunol.* **16:** 103–107.
14. Friedl, P., and J. Storim. 2004. Diversity in immune-cell interactions: states and functions of the immunological synapse. *Trends Cell Biol.* **14:** 557–567.
15. Holowka, D., and B. Baird. 2001. Fc(epsilon)RI as a paradigm for a lipid raft-dependent receptor in hematopoietic cells. *Semin. Immunol.* **13:** 99–105.
16. Rosenberger, C. M., J. H. Brumell, and B. B. Finlay. 2000. Microbial pathogenesis: lipid rafts as pathogen portals. *Curr. Biol.* **10:** R823–R825.
17. Gombos, I., E. Kiss, C. Detre, G. László, and J. Matkó. 2006. Cholesterol and sphingolipids as lipid organizers of the immune cells' plasma membrane: their impact on the function of MHC molecules, effector T-lymphocytes and cell death. *Immunol. Lett.* **104:** 59–69.
18. Rajnavölgyi, É., A. Horváth, P. Gogolák, G. K. Tóth, G. Fazakas, M. Fridkin, and I. Pecht. 1997. Characterizing immunodominant and protective influenza hemagglutinin epitopes by functional activity and relative binding to major histocompatibility complex class II sites. *Eur. J. Immunol.* **27:** 3105–3114.
19. Dijkstra, J., G. M. Swartz, J. J. Raney, J. Aniagolu, L. Toro, C. A. Nacy, and S. J. Green. 1996. Interactions of anti-cholesterol antibodies with human lipoproteins. *J. Immunol.* **157:** 2006–2013.
20. Szöllősi, J., J. Matkó, and G. Vereb. 2004. Cytometry of fluorescence resonance energy transfer (FRET). *Methods Cell Biol.* **75:** 105–152.
21. Gombos, I., C. Detre, G. Vamosi, and J. Matko. 2004. Rafting MHC-II domains in the APC (presynaptic) plasma membrane and the thresholds for T-cell activation and immunological synapse formation. *Immunol. Lett.* **92:** 117–124.
22. Rouquette-Jazdanian, A. K., C. Pelassy, J. P. Breittmayer, and C. Aussel. 2006. Revaluation of the role of cholesterol in stabilizing rafts implicated in T cell receptor signaling. *Cell. Signal.* **18:** 105–122.
23. Vereb, G., J. Matko, G. Vamosi, S. M. Ibrahim, E. Magyar, S. Varga, J. Szollosi, A. Jenei, R. Gaspar, Jr., T. A. Waldmann, et al. 2000. Cholesterol dependent clustering of IL-2Rα and its colocalization with HLA and CD48 on T lymphoma cells suggest their functional association with lipid rafts. *Proc. Natl. Acad. Sci. USA.* **97:** 6013–6018.
24. Gombos, I., Z. Bacso, C. Detre, H. Nagy, K. Goda, M. Andrasfalvy, G. Szabo, and J. Matko. 2004. Cholesterol sensitivity of detergent resistance: a rapid flow cytometric test for detecting constitutive or induced raft association of membrane proteins. *Cytometry.* **61:** 117–126.
25. Lupu, C., C. A. Goodwin, A. D. Westmuckett, J. J. Emeis, M. F. Scully, V. V. Kakkar, and F. Lupu. 1997. Tissue factor pathway inhibitor in endothelial cells colocalizes with glycolipid microdomains/caveolae. Regulatory mechanism(s) of the anticoagulant properties of the endothelium. *Arterioscler. Thromb. Vasc. Biol.* **17:** 2964–2974.
26. Bacia, K., D. Scherfeld, N. Kahya, and P. Schwille. 2004. Fluorescence correlation spectroscopy relates rafts in model and native membranes. *Biophys. J.* **87:** 1034–1043.
27. Hiltbold, E. M., N. J. Poloso, and P. A. Roche. 2003. MHC class II-peptide complexes and APC lipid rafts accumulate at the immunological synapse. *J. Immunol.* **170:** 1329–1338.
28. Steinberg, D. 1978. The rediscovery of high density lipoprotein: a negative risk factor in atherosclerosis. *Eur. J. Clin. Invest.* **8:** 107–109.
29. Rossner, S., K. G. Kjellin, K. L. Mettinger, A. Siden, and C. E. Soderstrom. 1978. Normal serum-cholesterol but low H.D.L.-cholesterol concentration in young patients with ischaemic cerebrovascular disease. *Lancet.* **18:** 577–579.
30. Newman, W. P., D. S. Freedman, A. W. Voors, P. D. Gard, S. R. Srinivasan, J. L. Cresanta, G. D. Williamson, L. S. Webber, and G. S. Berenson. 1986. Relation of serum lipoprotein levels and systolic blood pressure to early atherosclerosis. *N. Engl. J. Med.* **16:** 138–144.
31. Rossner, S., K. G. Kjellin, K. L. Mettinger, A. Siden, and C. E. Soderstrom. 1978. Dyslipoproteinemia in patients with ischemic cerebrovascular disease: a study of stroke before the age of 55. *Atherosclerosis.* **30:** 199–209.
32. Kruth, H. S. 2001. Lipoprotein cholesterol and atherosclerosis. *Curr. Mol. Med.* **1:** 633–653.
33. Alving, C. R., and N. M. Wassef. 1999. Naturally occurring antibodies to cholesterol: a new theory of LDL cholesterol metabolism. *Immunol. Today.* **20:** 362–366.
34. Bíró, A., E. Dósa, A. Horváth, Z. Prohászka, S. Rugonfalvi-Kiss, A. Szabó, I. Karadi, G. Acsady, L. Selmeczi, L. Entz, et al. 2005. Dramatic changes in the serum levels of anti-cholesterol antibodies after endarterectomy in patients with severe carotid atherosclerosis. *Immunol. Lett.* **99:** 51–56.
35. Tuosto, L., I. Parolini, S. Schroder, M. Sargiacomo, A. Lanzavecchia, and A. Viola. 2001. Organization of plasma membrane functional rafts upon T-cell activation. *Eur. J. Immunol.* **31:** 345–349.
36. Alonso, M. A., and J. Millan. 2001. The role of lipid rafts in signalling and membrane trafficking in T-lymphocytes. *J. Cell Sci.* **114:** 3957–3965.
37. Shin, J. S., Z. Gao, and S. N. Abraham. 1999. Bacteria-host cell interaction mediated by cellular cholesterol/glycolipid-enriched microdomains. *Biosci. Rep.* **19:** 421–432.
38. Balogh, A., A. Lőrincz, A. Bíró, L. Cervenák, G. Füst, G. László, and J. Matkó. 2006. Anti-cholesterol IgGs: probes and functional modulators of cholesterol-rich membrane microdomains (Abstract in 16th European Congress of Immunology. Paris, France, September 6–9, 2006).

Chapter 5

Imre Gombos, Gábor Steinbach, István Pomozi, Andrea Balogh, György Vámosi, Alexander Gansen, Glória László, Győző Garab, János Matkó

Some new faces of membrane microdomains: a complex confocal fluorescence, differential polarization, and FCS imaging study on live immune cells

Cytometry A 2008. 73(3):220-229.

ORIGINAL ARTICLE

Cytometry PART A
Journal of the International Society for Analytical Cytology

Some New Faces of Membrane Microdomains: A Complex Confocal Fluorescence, Differential Polarization, and FCS Imaging Study on Live Immune Cells

Imre Gombos,[1] Gábor Steinbach,[2] István Pomozi,[3] Andrea Balogh,[1] György Vámosi,[4] Alexander Gansen,[5] Glória László,[1] Győző Garab,[2] János Matkó[1]*

[1]Department of Immunology, Institute of Biology, Eotvos Lorand University, Budapest, Hungary

[2]Biologial Research Center, Hungarian Academy of Sciences, Szeged, Hungary

[3]Pi Vision Partnership, Budapest, Hungary

[4]Cell Biophysics Group of the Hungarian Academy of Sciences, University of Debrecen, Debrecen, Hungary

[5]Division Biophysics of Macromolecules, German Cancer Research Center, Heidelberg, Germany

Received 21 July 2007; Revision Received 12 October 2007; Accepted 16 November 2007

Grant sponsor: Hungarian National Science Fund OTKA; Grant numbers: T-034393, T-049696, K-63252, T48745, NK61412; Grant sponsor: Health Science Committee ETT; Grant numbers: 2006/070, 2006/065; Grant sponsor: EU FP6; Grant number: MCRTN-CT-2003-505069; Grant sponsor: OMFB; Grant number: OMFB-00194/2004; Grant sponsor: DAAD-MÖB; Grant number: 2006/34.

*Correspondence to: Janos Matko, Department of Immunology, Institute of Biology, Eotvos Lorand University, Budapest, Hungary.

Email: matko@elte.hu

Published online 28 December 2007 in Wiley InterScience (www.interscience.wiley.com)

DOI: 10.1002/cyto.a.20516

Abstract

Lipid rafts are cholesterol- and glycosphingolipid-rich plasma membrane microdomains, which control signal transduction, cellular contacts, pathogen recognition, and internalization processes. Their stability/lifetime, heterogeneity remained still controversial, mostly due to the high diversity of raft markers and cellular models. The correspondence of the rafts of living cells to liquid ordered (Lo) domains of model membranes and the effect of modulating rafts on the structural dynamics of their bulk membrane environment are also yet unresolved questions. Spatial overlap of various lipid and protein raft markers on live cells was studied by confocal laser scanning microscopy, while fluorescence polarization of DiIC18(3) and Bodipy-phosphatidylcholine was imaged with differential polarization CLSM (DP-CLSM). Mobility of the diI probe under different conditions was assessed by fluorescence correlation spectroscopic (FCS). GM1 gangliosides highly colocalized with GPI-linked protein markers of rafts and a new anti-cholesterol antibody (AC8) in various immune cells. On the same cells, albeit not fully excluded from rafts, diI colocalized much less with raft markers of both lipid and protein nature, suggesting the Lo membrane regions are not equivalents to lipid rafts. The DP-CLSM technique was capable of imaging probe orientation and heterogeneity of polarization in the plasma membrane of live cells, reflecting differences in lipid order/packing. This property—in accordance with diI mobility assessed by FCS—was sensitive to modulation of rafts either through their lipids or proteins. Our complex imaging analysis demonstrated that two lipid probes—G_{M1} and a new anti-cholesterol antibody—equivocally label the membrane rafts on a variety of cell types, while some raft-associated proteins (MHC-II, CD48, CD59, or CD90) do not colocalize with each other. This indicates the compositional heterogeneity of rafts. Usefulness of the DP-CLSM technique in imaging immune cell surface, in terms of lipid order/packing heterogeneities, was also shown together with its sensitivity to monitor biological modulation of lipid rafts.

Key terms

lipid rafts; live lymphoid cells; confocal polarization imaging; FCS; raft modulation

MICRODOMAINS enriched in cholesterol and glycosphingolipids (so called lipid rafts) are expressed in the plasma membrane of most mammalian cells (1–6) and involved in numerous membrane-associated cellular functions. Compartmentation, spatiotemporal coordination and coupling or isolation of receptor-, signal-transducing, or regulatory proteins were shown to be controlled, in some ways, by lipid rafts (3–6). Furthermore, these microdomains are supposed to be involved in the capturing and internalization of some viruses (e.g. human immunodeficiency virus, HIV and influenza virus), bacteria, or bacterial inflammatory molecules (e.g. toxins or lipopolysaccharides) by host cells (6,7) in the immune system and in regulation of

signal transduction in neuronal synapses (8). Moreover, a correlation between cholesterol homeostasis and appearance/composition of membrane microdomains in human monocyte-macrophage cells (9), as well as a differential regulatory role of E-LDL and Ox-LDL in the cholesterol- and ceramide-rich microdomains of these cells have recently been shown (10). Thus, lipid raft and caveola membrane microdomains gained a widespread attention in the research of cellular communication and signal transduction in general, and in the immunological, virological, and neurobiological research areas in particular.

Despite the extensive biochemical and biophysical characterization on model membranes and cells, several basic properties of these membrane microdomains on live cells (e.g. size, stability, fine structure, or compositional diversity), as well as the regulatory mechanisms controlling these properties still remained controversial and less understood (2,6,11–13). Since there is an ongoing debate on the size, size-distribution, lifetime and stability of microdomains, many groups are devoted to characterize different aspects of rafts by using various versions of optical fluorescence or scanning probe imaging. These approaches, focusing mostly on model membranes with less complexity, include, among others, confocal fluorescence (FRET-) microscopy (11); single particle tracking video-imaging (13); fluorescence correlation (FCS) microscopy (14,15); two-photon microscopic imaging of laurdan generalized polarization domains (16) and atomic force imaging of model membranes (17,18).

Various probes are used to mark these microdomains, such as fluorescent antibodies against GPI-anchored proteins (e.g. CD48, CD55, CD59, CD14, HA-R, AP, FR, etc.), GPI-GFP reporters, the cholera toxin β subunit binding selectively to $G_{M1,3}$ gangliosides or fluorescent lipid analogs (6). We have recently developed new IgG type monoclonal antibodies reactive to clustered cholesterol in both cell-free systems, such as lipoproteins, and in live immune cells (e.g. lymphocytes, macrophages). These antibodies were shown capable of marking cholesterol-rich membrane microdomains (rafts or caveolas) or even their redistribution in the plasma membrane of activated lymphocytes (19).

The phase separation of Lo (liquid ordered) and Ld (liquid disordered, fluid) domains has been quite extensively studied earlier in various model membrane systems (6,20–22). The imaging studies on such systems often applied fluorescent lipid probes to mark these domains, such as the diIC18 or diIC20 indocarbocyanine probes (diI) for Lo domains or Bodipy-phosphatidylcholine (B-PC) for the Ld domains (20–22). Although lipid rafts are often depicted as ordered lipid domains, the diI probe, partitioning well into Lo domains in model membranes of simple composition (e.g. GUVs) (20), has been assumed as a non-raft lipid probe (23,24), based on its weak miscibility with sphingomyelin (SM)-enriched regions. In these GUV (Giant Unilamellar Vesicle) models cholesterol was shown to increase separation of the Lo and Ld phases in a concentration dependent manner, demonstrating its capability to fine-tune dynamics of membrane phases and microdomains. The question whether the phase-relations and raft dynamics is similar in the plasma membrane of live cells, however, is still debated (24).

The lateral contacts of raft microdomains to their neighboring membrane areas, as well as the domain boundaries of Lo phase regions are both poorly understood in live cells. In order to investigate these questions we applied here a recently introduced novel differential polarization laser scanning confocal microscopic approach (DP-CLSM) (25,26) to further analyze the ordering of plasma membranes and lipid packing of live lymphoid cells. For this purpose we used the aforementioned indocarbocyanine lipid probe, diIC18(3). The expected membrane perturbation caused by this probe is certainly lower than those appearing when a large fluorescent IgG antibody, the very specific, but pentameric polypeptide, CTX-B, or large immunogold labels are used. Moreover its dipole orientation relative to the membrane surface was experimentally established and shown to be preferentially tangential, at least in red blood cells (27). Therefore it seems a suitable probe to study changes of lipid order/packing and the effects of raft modulations on their lipid neighborhood in live cells.

In the present study we addressed the following questions: (i) to what extent does the new marker of clustered cholesterol (AC8 antibody) overlap with $G_{M1,3}$ ganglioside-enriched domains and with the diI lipid probe in a variety of live immune cells; (ii) to what extent do the different protein markers of rafts overlap with the above two lipid probes and with each other; (iii) what can the differential polarization (DP-CLSM) images of diI tell us about lipid raft dynamics and the coupling of rafts with their lipid neighborhood. Our data demonstrate that cholera toxin B and the new anti-cholesterol antibody, AC8, as two lipid probes of membrane rafts, show a highly matching membrane localization in all cell types investigated, confirming that the gangliosides and cholesterol may indeed form a stable "nucleus/molecular skeleton" for membrane rafts. In contrast, several raft-associated proteins (e.g. MHC-II, CD48, or CD90) show a differential colocalization, reflecting a compositional heterogeneity in the protein content of co-existing lipid rafts on live immune cells. Usefulness of the differential polarization CLSM method in imaging immune cell surface in terms of lipid order/packing heterogeneities and detection of biological modulation of lipid rafts are also demonstrated and discussed.

Materials and Methods

Cells and Reagents

The human Kit225 K6 T-lymphoma cell line (kindly provided by T.A. Waldmann, Bethesda, MD) was cultured in RPMI 1640 medium supplemented with 10% fetal calf serum (FCS), penicillin, streptomycin, Na_2CO_3, and sodium pyruvate. Recombinant IL-2 (20 U/ml) was added in every 48 h (28). For the experiments, cells were harvested, washed, and resuspended in PBS, pH 7.4. JY human B lymphoblasts (HLA-A2,B7+) (29) were grown in RPMI 1640 + 10% FCS medium, while 2PK3 (I-Ed +, I-Ad +) murine B-lymphoma cell line of BALB/c origin (ATCC, TIB-203) and the L929 C3H/An mouse fibroblasts (ATCC, CCL-1) were cultured in RPMI

1640 medium with 0.05 mM 2-mercaptoethanol and 5% FCS, in 5% CO_2 atmosphere, at 37°C (30). Ten-week-old male Sprague-Dawley rats were decapitated, hearts were removed, rinsed in isotonic saline solution (0.9% NaCl), blotted dry, and chambers were separated from each other. Left ventricular tissue samples were sliced and stained right before they were assayed.

MβCD and MγCD (random methylated β and γ cyclodextrin) was purchased from CycloLab (Budapest, Hungary). Alexa 488-(or 647-) cholera toxin B, diIC18(3) and Bodipy-phosphatidylcholine were obtained from Molecular Probes-Invitrogen (Eugene, OR). MEM-75 (against transferrin receptor/CD71) and MEM-102 (against CD48) mAbs were kindly provided by V. Horejsi (Institute of Immunogenetics, ASCR, Prague, Czech Republic) and they were conjugated with Alexa fluorophores according to the manufacturer's instructions (Molecular Probes-Invitrogen).

Cell Labeling

Cells were labeled with Alexa488-conjugated cholera toxin B according to the manufacturer's (Molecular Probes-Invitrogen) instruction. Staining with diI (1.5 μg/ml) was performed by incubating the cells for 2–3 min., at 37°C, in HBSS (+5 mM glucose + 1% BSA), using a sonicated, air-fuged, and filtered stock solution of diI in ethanol. In case of double labeling, cells were incubated sequentially in diIC18(3) and then CTX-B for 10 min on ice. Cells were labeled with fluorescent antibodies for 40 min, on ice, and then washed twice before measurement. Human CD71 specific Cy3-MEM-75 (mouse IgG1 Ab) and FITC-conjugated rat anti-mouse antibody G7.4 (IgG2c, from ATCC) was used to label transferrin receptor and Thy1 (CD90), respectively. CD2 on T-cells were labeled with FITC-conjugated anti-human CD2 mAb (Sigma, St. Louis, MO, USA). ACHAs were applied either as Alexa488-conjugated AC8 or biotinylated AC8 followed by Alexa647-conjugated neutravidin and the cells were stained as described recently (19). In case of double labeling, the lipid probes and the antibodies were usually added to the cells simultaneously for the appropriate time intervals. No competition or mutual blocking of binding was observed with any pairs. For the fluorescent antibodies appropriate isotype control antibodies (or cell lines) were used as negative controls.

Depletion of Membrane Cholesterol by MβCD

Freshly harvested cells (1×10^6/ml) were incubated with 10 mM MβCD or MγCD (control) (Cyclolab, Budapest, Hungary) for 15 min, at 37°C, in PBS pH 7.4 and then washed. Forty to fifty percent of plasma membrane cholesterol could be removed with this treatment (28). MγCD a conformational isomer incapable of cholesterol extraction was used as control. After washing, the cells were labeled accordingly for further analysis.

Membrane Modulation by Crosslinking of Membrane Proteins

Cells were incubated with unconjugated MEM-75 (reactive with transferrin receptor, CD71) or MEM-102 (reactive with CD48) monoclonal antibodies on ice, for 40 min. After washing, samples were incubated with polyclonal goat anti mouse IgG for 30 min, on 37°C, to crosslink the primary antibodies.

CLSM Measurements

The stained cells or tissue sections were mounted on coverslip and imaged by Olympus FluoView500 confocal laser scanning microscope, using the 488 nm argon-ion laser line to excite Alexa 488 dye and the 543 nm He-Ne laser line for the diIC18(3). In case of long wavelength probes, a 632 laser line (He-Ne) was applied. The images (512 × 512 pixels) were recorded by using a 60× oil-immersion objective (N.A.:1.25). An SDM560 dichroic mirror and a BA505-525 bandpass emission filter was used for detecting Alexa 488 fluorescence (channel 1), SDM630 dichroic mirror and BA560-600 bandpass filter was used in channel 2 for detecting diIC18(3) emission and a 660IF long pass filter was used in channel 3 for detecting the fluorescence of long-wavelength probes Cy5 or Alexa647. A sequential scanning mode was applied in colocalization experiments to minimize the crosstalk between channels.

Pearson's colocalization coefficients were calculated by using the ImageJ software. The same experimental setup and strategy was applied to investigate colocalization of various double-stained lymphoid cells by CLSM.

FRET Measurements

FRET between membrane proteins, after their fluorescent immunocytochemical labeling, was measured either by the acceptor photobleaching FRET or the intensity-based FRET method (31). FITC-Cy3, Cy3-Cy5, or Alexa546-Cy5 dye pairs served as donors and acceptors, respectively. FRET efficiencies were measured by recording 512 × 512 pixels images of the double- or single (donor- or acceptor-) labeled cells in the optical channels of the FluoView 500 CLSM system, selected properly for the given dye pair by the appropriate emission filter combinations and dichroic mirrors. The images were evaluated for FRET efficiency as described previously (31,32).

FCS Measurements

FCS measurements were carried out on the fluorescence fluctuation microscope (FFM) constructed by Prof. Jörg Langowski's group at the DKFZ, Heidelberg. The setup combines an FCS/FCCS module with a galvanometric laser scanner attached to the video port of an inverted IX-70 microscope (Olympus, Hamburg, Germany) with a UplanApo 60×, 1.2 NA water immersion objective (33,34). Measurements were performed at room temperature. DiI fluorescence was excited with the 568 nm line of an Ar-Kr laser from Omnichrome (Wessling, Germany). Emission was detected through a 590–750 nm bandpass filter (OG590+700CSFP, Omega Optical, Brattlerborn, VT) by an avalanche photodiode (SPCM-AQR-13, Perkin-Elmer, Wellesley, MA). Confocal images of the cell membrane were acquired, and the laser beam was positioned at selected points of the membrane for FCS measurements. Laser power at the objective was ∼ 0.8 μW. For calculating the autocorrelation function from the signal of the photodiode, an ALV-5000/E correlator card (ALV Laser GmbH, Langen,

Germany) was used. Data acquisition time was always 60 s, corresponding to 10 runs of 6 s, which were averaged. From each sample ~10 cells were measured. Autocorrelation functions were fitted to a single component 2D diffusion model with triplet term using the program QuickFit (written in the laboratory of J. Langowski, DKFZ, Heidelberg):

$$G(\tau) = \frac{1}{N}\frac{\left(1 - T + Te^{-\tau/\tau_{tr}}\right)}{1 - T}\left[\left(1 + \frac{\tau}{\tau_d}\right)^{-1}\right],$$

where N is the average number of molecules in the detection volume, T is the fraction of diIC18(3) molecules being in the triplet state within the detection volume, τ_{tr} is the phosphorescence lifetime of diIC18(3) and τ_d is the diffusion time, which is the average time spent by the dye in the detection volume. The diffusion coefficient, D can then be derived as: $D = \omega_{xy}^2/4\tau_D$, where ω_{xy} is the lateral radius of the sensitive volume. ω_{xy} at 568 nm excitation was estimated by measuring the diffusion time of Alexa Fluor 568 dissolved in PBS ($\tau_d = 60 \pm 2$ μs at 25°C). Assuming inverse proportionality between the MW and D, and using Rhodamine 6G as reference (Culbertson et al., 2002, Talanta 56:365), we assessed the diffusion coefficient of Alexa Fluor 568 as $D_{Alexa\ 568} \sim D_{R6G} \times MW_{R6G}/MW_{Alexa\ 568} = 4.14 \times 10^{-6}$ cm^2/s $\times$ 471/716 $= 2.72 \times 10^{-6}$ cm^2/s. From this the radius was estimated to be $\omega_{xy} = \sqrt{4D\tau_D} \sim 255 \pm 5$ nm.

Differential Polarization Laser Scanning Microscopy

For recording P (the degree of polarization of the fluorescence emission) images we used a Zeiss LSM 410 laser scanning microscope equipped with DP (differential polarization) attachments. The overall schemes and technical details, including calibration and correction procedures, taking into account the polarization characteristics of the dichroic beam splitter, have been published elsewhere (25,26). For P imaging of the lymphocyte cells in the DP-CLSM (differential polarization confocal laser scanning microscope), the sample was excited with either the 488 or 514 nm linearly polarized beams of an Ar-ion laser. The polarization content of the fluorescence emission was analyzed with the aid of a photoelastic modulator (PEM, Hinds International) and a demodulation circuit, which consisted of a programmable, gated digital phase-sensitive detector (DPSD) constructed by Pawel Kamasza (SZFKI KFKI, Budapest). The DPSD was locked at the modulation frequency of PEM, at 100 kHz, and a low pass analog-digital converter amplifier (ADC) was used to determine the average intensity, I_a. The analyzer unit was adjusted in a manner to detect the intensity difference $\Delta I = I_1 - I_2$, where the polarized components are parallel (I_1) and perpendicular (I_2) to the polarization direction of the laser beam. P was calculated as $\Delta I/2I_a$, with $I_a = (I_1 + I_2)/2$.

5×10^5 Kit225 K6 T-lymphoma or JY human B lymphoma cells suspended in PBS were labeled with diIC18(3). After washing, cells were resuspended in PBS and mounted on coverslip. The 514 nm laser line was used for excitation, an FT560 dichroic beamsplitter and an additional long pass 560 nm color filter was used to separate the fluorescence; the PEM was adjusted to 586 nm, which is the emission peak of diIC18(3). When labeling with Bodipy-phosphatidylcholine, cells were incubated at the same density with the probe (1.5 μg/ml) for 10 min, at room temperature. After washing, cells were mounted on coverslip. Excitation of Bodipy fluorescence was at 488 nm, using an FT510 beamsplitter and a long pass 510 nm filter; PEM was adjusted to the emission peak (520 nm) of Bodipy-PC.

Results

Staining Patterns of the Fluorescent Lipid Membrane-Probes on Live Lymphoid Cells

In earlier studies the large diversity of the applied, supposed raft markers, and cellular models resulted in a broad spectrum of their localization and physicochemical properties (6). Therefore here we tried to perform a systemic study on cell types phenotypically closely related to each other, such as T- and B-lymphoma cells of human or murine origin and to apply the same lipid raft markers to all. First, we tested how the staining pattern of these cells with various well defined markers of lipid rafts (e.g. CTX-B, a new anti-cholesterol antibody, AC8) or with diIC18(3) and Bodipy-PC, lipid probes of Lo and Ld phase domains, respectively (12,20,21). As the representative intensity surface plots on Figure 1 show, the human T lymphoma cells (Kit 225 K6) displayed a differential staining pattern with these probes. While CTX-B, AC8, and diIC18(3) all stained these cells in a pattern of discrete small patches (Figs. 1A–1C), while the Bodipy-PC probe, enriched in the fluid membrane regions, as expected, stained the plasma membrane more homogenously (Fig. 1D). Similar staining patterns were observed for these probes in human B lymphoblast (JY) and macrophage (U937) cell lines (data not shown).

Membrane Domains Defined by diIC18(3) Match the Domains of Classical Lipid Raft Markers Only Partially in Lymphoid Cells

Despite that diIC18(3) was defined by model membrane studies as nonraft marker (enriched in Lo phase domains) (23,24), showed a typical patchy staining pattern on the surface of lymphoid cells (see Fig. 1C), suggesting that these 200–300 nm diameter patches define a certain type of membrane microdomain in these cells. A substantial colocalization was found between the new fluorescent AC8 anti-cholesterol antibody (19), and the CTX-B labeled G_{M1} gangliodies, the classical markers of rafts. A high level of matching of the AC8-labeled and G_{M1}-CTX-B + domains was observed in both B- and T-lymphocytes of human origin (cross correlation (cc): 0.68 and 0.67, respectively), similarly to murine T_H cells and macrophages (Table 1). The colocalization between diIC18(3) and AC8, however, was significantly lower (cc: 0.4) in the same cells. The spatial correlation between diIC18(3) and the G_{M1}/CTX-B domains was the lowest (28–34%), as assessed by a CLSM analysis on cells of different origin (Figs. 1E–1H), and it was independent of the cell type. These data suggest, that the "clustered" cholesterol and G_{M1} have a high spatial correlation in all cell types investigated, but the membrane regions

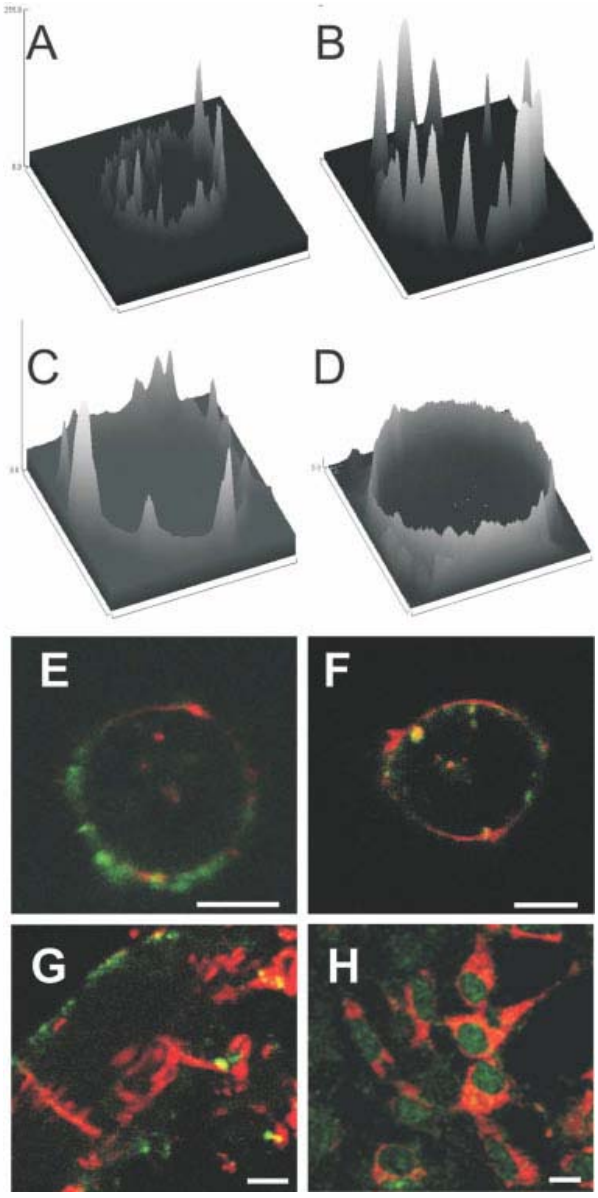

Figure 1. Staining pattern of various lipid probes on human T lymphoma cells and the colocalization of diIC18(3) with cholera toxin B on various cell types. Alexa488-Cholera toxin B labeling $GM_{1,3}$ gangliosides (**A**), Alexa488-AC8 anticholesterol antibody (**B**) and diIC18(3) (**C**) all stained Kit225 K6 T cells in a patchy fashion, defining discrete microdomains. Membrane staining by Bodipy-C5-phosphatidylcholine of the same cells (**D**) is much more homogenous. The fluorescence intensity surface plots were derived from representative confocal microscopic equatorial optical sections (width: 0.3 μm) recorded by a 60× oil immersion objective (N.A: 1.25). Colocalization of Alexa488-CTX B with diIC18(3) is shown on 2PK3 murine B lymphoma (**E**), JY human B lymphoblast (**F**), left ventricular tissue sections of raft heart (**G**), and L929 murine fibroblast (**H**) cells. The images were recorded by confocal microscope as described earlier, the white bars indicate 10 μm. The colocalization indices were 0.30 ± 0.12 (E), 0.34 ± 0.1(F), 0.26 ± 0.12 (G), and 0.32 ± 0.18 (H), respectively.

defined by diIC18(3) have a poor, but still non-negligible overlap with lipid rafts labeled with these two markers, on cells of lymphoid origin.

Lipid Rafts of Lymphoid Cells' Plasma Membrane Show Some Compositional Heterogeneity

Among the GPI-anchored lipid raft marker proteins, CD90 and CD59 are found mostly in T cells, while CD48 is expressed on both T and B cells of lymphoid origin (4,6). In contrast, CD2 is an abundant nonraft protein in T cells (35). Key molecules of antigen presentation, the class I and class II major histocompatibility antigens (MHC-I, MHC-II) are expressed on both T- and B-lymphoma cells and a substantial fraction of MHC-II was shown raft-associated on these cells (30,36). Here we tried to map the mutual colocalization/proximity of these membrane proteins with each other and with the aforementioned lipid markers of raft domains, using CLSM/FRET and colocalization analysis. As expected, CD48 and CD90 are firmly associated with the membrane domains defined by both G_{M1}/CTX-B and the anti-CHOL antibody, AC8 (19), while the nonraft CD2 protein did not associate with these domains (Table 1).

Concerning the MHC glycoproteins, colocalization and FRET data consonantly show that MHC-II is associated with raft marker G_{M1}, in a much higher extent than MHC-I, in the B- and T-lymphoma cells (Table 1). In addition, earlier data have shown that MHC-II is partially detergent resistant and that its homoassociation (clustering) on murine B lymphoma cells was cholesterol-sensitive (30). In contrast, MHC-I clusters on B lymphoma cells proved to be less sensitive to cholesterol, but rather dictated by β2m-dependent protein–protein affinity (37), consistent also with their very weak association with the G_{M1}/CTX-B-rich domains.

Despite its raft-association, MHC-II molecules show rather weak if any colocalization/proximity with CD48. A somewhat stronger colocalization with CD59 was observed on the same cells. Taking these data together, the MHC-II enriched lipid rafts of B and T lymphoma cells seem to be separate microdomains from those enriched in CD48, but show some degree of mutual compartmentalization with CD59. This can be regarded as a piece of evidence for heterogeneity in protein-composition of lipid rafts in lymphoid cells.

P-Imaging of dil-Stained Lymphoid Plasma Membranes with Differential Polarization Microscopy

By combining the technique of differential polarization (DP) with confocal microscopy a method has become available for imaging not only the fluorescence intensity but also the polarization or anisotropy DP parameters. For linearly polarized light, these include *P*, the degree of polarization of the fluorescence emission, which characterizes the depolarization e.g. due to rotation of the molecules and/or due to excitation energy transfer or migration in the system, linear dichroism (LD) and fluorescence detected LD, which are given rise by the anisotropic distribution of the absorbance dipoles, and *r*, the anisotropy of the fluorescence emission, a quantity which originates from the nonrandom distribution of the

Table 1. Colocalization/proximity of some membrane microdomain constituents in lymphoid cells

MEMBRANE MOLECULE I	MEMBRANE MOLECULE II	CELL TYPE	COLOCALIZATION INDEX	FRET EFFICIENCY (%)	REFS.[a]
GM_1 (CTX-B)	AC8 mAb	Murine T_H-cells, macrophages	0.65 ± 0.01	n.d.	(19)
GM_1 (CTX-B)	CD48	Kit225 K6, T_H-cells	0.64 ± 0.02	0.29 ± 0.06	
GM_1 (CTX-B)	CD48	Kit225 K6, T_H-cells (CHOL-depleted)	0.17 ± 0.01	0.06 ± 0.01	
GM_1 (CTX-B)	CD2	Kit225 K6, T_H-cells	0.04 ± 0.02	n.d.	
AC8 mAb	Thy.1(CD90)	Murine T_H cells	0.56 ± 0.09	n.d.	(19)
AC8 mAb	CD2	Murine T_H cells	0.06 ± 0.03	n.d.	(19)
MHC-I/β2-microglobulin	GM_1 (CTX-B)	JY B-, Jurkat T-lymphoma cells	0.11 ± 0.04	0.09 ± 0.04	
MHC-II	GM_1 (CTX-B)	JY B-, Jurkat T-lymphoma cells	0.54 ± 0.05	n.d.	
MHC-II	CD48	JY B-, Jurkat T-lymphoma cells	0.1 ± 0.06	0.07 ± 0.03	
MHC-II	CD59	JY B-, Jurkat T-lymphoma cells	0.37 ± 0.07	n.d.	

[a]Some data from our recent work published in Ref. 19 are given for comparison.

emission dipoles with respect to a coordinate system fixed to the laboratory or the sample (26).

We applied diIC18 and Bodipy-PC to probe Lo and fluid membrane regions (Fig. 2A) on live cells by DP-CLSM. As shown by Axelrod et al. (27) on red blood cells, the long fatty acyl chains of diIC18(3) are aligned preferentially parallel with the membrane normal, keeping the orientation of the indocarbocyanin's absorption dipole uniformly tangential with respect to the surface of the plasma membrane. In perfect accordance with the expectations, diIC18(3) probe shows a similar orientational behavior in both B and T lymphoblastoid cells (JY and Kit225 K6, respectively). In microscopic samples containing nonrandom orientation of the emission dipoles, i.e. in samples which exhibit nonzero *r*, *P* contains information both on the anisotropic distribution of the emission dipoles with respect to the membrane plane and on the depolarization due to the motional freedom of the lipid-dye molecular assemblies. This is demonstrated by the color-coded *P*-images of JY cells, which in the vertical and horizontal directions are dominated by the preferentially parallel and perpendicular orientation of the emission dipoles, resulting in positive and negative *P* values, respectively (Fig. 2B). (Note: in macroscopic samples this information is lost due to spatial averaging; in highly anisotropic samples, however, *P* might contain contributions from the residual anisotropy e.g. due to photoselection and/or due to gravitational alignment of the particles (38)).

In contrast to diIC18, Bodipy-PC is preferentially inserted into the fluid (Ld) regions of the plasma membrane through much shorter fatty acyl chains and the fluorophore ring is attached only to one of them. Thus, its absorption dipole is expected to be aligned in a less ordered fashion with respect to the membrane surface. The color-coded representative *P*-images of B-PC in JY B cells (Fig. 2B) indeed show that B-PC fluorescence is much less polarized throughout the membrane surface than that of the diIC18. Interestingly, as shown by the intensity and *P*-images of diIC18 recorded on membrane cholesterol-depleted JY cells, the diI staining became less patchy/more uniform, but a few large diI clusters are formed on the cells. The averaged *P* values became lower upon cholesterol depletion.

A large scale statistical analysis of Bodipy-PC and diIC18 P-images recorded on large human T lymphoma cells (Kit225 K6) resulted in similar, heterogenous *P*-distributions (Fig. 3). These distributions correspond to spatial averaging, at least for the selected sections, and thus the mean values can be compared with macroscopic measurements. The Bodipy-PC *P*-histogram is quite narrow, and at the same time the mean value (0.09) is rather small. This reflects a highly depolarized emission from Bodipy-PC all over the cells, and indicates a high rotational freedom with respect to the membrane normal and small contribution from *r*. In contrast, the diIC18(3) *P*-histograms are significantly broadened due to large contributions from the anisotropic distribution of the emission dipoles with respect to the membrane planes, and inhomogeneities in the local microenvironment of the probe over the cell surface. This difference is consistent with the intensity surface plots of the probes (see Figs. 1C and 1D).

Depletion of membrane cholesterol slightly decreased the width of *P*-distribution and shifted its mean value toward 0, consistent with results of macroscopic steady-state polarization data with DPH probes on the same Kit225 K6 T cells (28). Extensive crosslinking of either raft-associated CD48 GPI-anchored proteins or a nonraft protein, the transferrin receptor (CD71) both resulted in a significant positive shift in the mean value of *P*-distributions (smaller rotational freedom) of DiIC18(3) in the Kit225 K6 T cells.

FCS Analysis of the Mobility of diIC18(3) in the Plasma Membrane. Effects of Lipid Raft Modulations

The lateral mobility of diIC18(3) was analyzed by fluorescence correlation microscopy (23,33,34) upon various lipid raft modulation treatments in human Kit 225 K6 T lymphoma cells. Typical autocorrelation curves fitted to a single component diffusion model including triplet correction are shown in Figure 4. The average diffusion correlation time (τ_D, determined from 11 cells) was 24.1 ± 13.4 ms for control cells (Fig. 4A) and increased to 33.7 ± 7.8 ms ($n = 12$) upon crosslinking CD48, a constitutively raft-localized membrane protein (Fig. 4C). These values of τ_D correspond to diffusion coefficients of $(6.8 \pm 4) \times 10^{-9}$ cm^2/s and $(4.8 \pm 1.1) \times 10^{-9}$ cm^2/s,

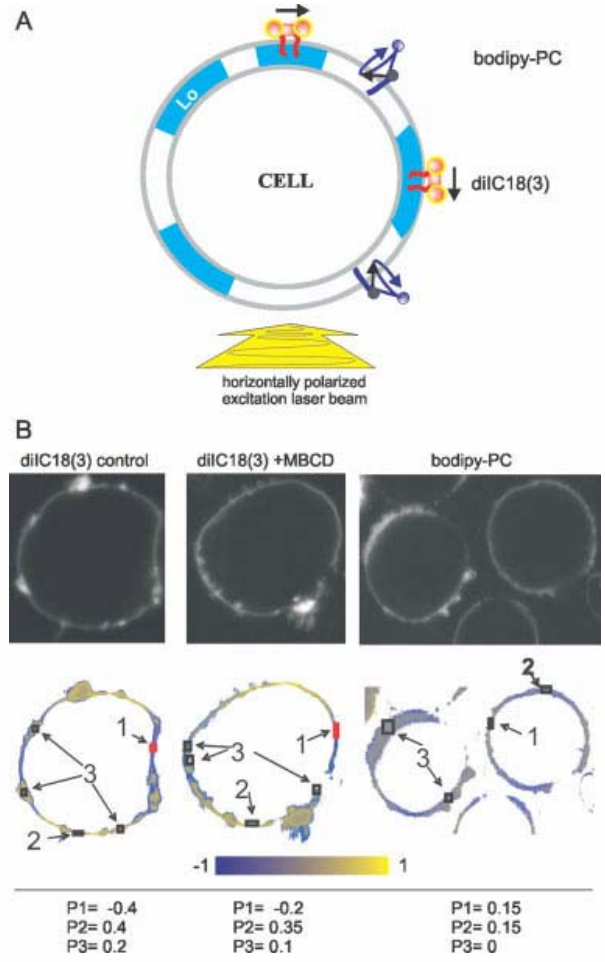

Figure 2. Model system and analysis strategy of P-imaging on live lymphoid cells by DP-CLSM. (**A**) Cells are excited by horizontally polarized laser beam. The scheme shows the preferred (tangential) orientation of diIC18 dipoles with respect to the membrane plane. For Bodipy-PC free conical rotation with respect to the tangential axis is allowed. (**B**) shows the fluorescence (gray scale, upper panels) and P (yellow-blue, lower panels) images of diIC18(3) in control (left), and MBCD-treated (middle) JY cells and the Bodipy-PC stained JY cells (right). In the *P* patterns the yellow color codes the horizontal, while the blue the vertical dipole orientations; the more saturated the color the higher the *P* value is; some quantitative *P* values derived from the numbered ROIs are shown as an example. The indices of *P* values correspond to the indicated membrane regions: in the diIC18(3) images the dipoles are aligned tangentially to the membrane (horizontal and vertical orientations from horizontal and vertical membrane regions, respectively) with relatively high values, while the *P* values in the Bodipy-PC image are rather small.

respectively. The average τ_D was even higher, 62.9 $\pm$ 42 ms corresponding to $D = (2.6 \pm 1.7) \times 10^{-9}$ cm^2/s ($n = 10$) when cholesterol was depleted from the plasma membrane by MBCD treatment (Fig. 4B). We note here that in some of the cholesterol-depleted cells the diffusion of diIC18 was extremely slowed down ($\tau_D > 100$ ms), while in other cells τ_D was close to that of the control cells, resulting altogether in an elevated average value. These data reflect decreased local diffusion rates of diIC18(3) upon both types of lipid raft modulation in randomly selected membrane areas of T cells.

Discussion

In the present work, first we demonstrated that a new anti-cholesterol antibody (AC8) labeling the clustered cell membrane cholesterol is highly enriched in the membrane domains defined by $G_{M1,3}$ gangliosides (cholera toxin labels) in human B- and T-lymphoid cells. Although quantitative cell surface staining with AC8 can be assessed only by a standard limited papain digestion, snapshot imaging of cells stained by AC8 could monitor not only the level of membrane cholesterol, but even redistribution of rafts in the plasma membrane, such as raft polarization upon T cell activation (19). Thus, $G_{M1,3}$ gangliosides and clustered cholesterol seem to be two essential "nucleating molecular skeletal elements" of lipid rafts existing in various lymphoid (T- and B-lymphocytes) or myeloid (e.g. monocyte-macrophage) cells of the immune system. The strong correlation between CTX-B and AC8 binding (expression) in seven different immune cells (19) indicates that regulation of their expression might be complex and not independent of each other, as proposed recently (9). Their simultaneous application might be a useful tool in a reliable detection of raft (or caveola) microdomains by fluorescence imaging.

Our results have also shown that some protein markers of rafts, such as CD48, CD59, or CD90 GPI-anchored proteins all highly colocalize with both CTX-B and AC8 in B- and T-lymphoid cells of mouse and human origin. On the other hand, these GPI proteins differentially colocalize with each other and with some transmembrane proteins, such as MHC-II or MHC-I glycoproteins. While the MHC-II-enriched raft domains (30,36) do not overlap with the CD48-enriched rafts, some CD59 was found in these MHC-II-clusters. Microcompartmentation of MHC-II by rafts may have important functional consequences, both in controlling the efficiency of antigen presentation (30) or through their raft/dependent and raft/independent signaling pathways (39). Similarly, Fas receptor/CD95 signaling was found differentially regulated, depending on the receptor localization in CD48-rich rafts or CD55-, CD59-rich microdomains (40). These results together provided a piece of evidence for coexisting lipid rafts with protein compositional diversity in lymphocytes. Similar compositional heterogeneity of membrane microdomains was reported on myeloid (monocyte-macrophage) cells (41) and even lipid domains distinct from cholesterol/SM-rich rafts were described on fibroblasts (42). Such compositional heterogeneity of rafts and their differential cellular localization may serve as a compartmentation mechanism providing a tool for spatiotemporal coordination of protein functions in the plasma membrane and various subcellular structures.

A detailed confocal colocalization analysis has also shown that the microdomains defined by both $G_{M1,3}$ gangliosides/CTX-B and the AC8 anti-cholesterol antibody overlap only partially (weakly) with membrane domains defined by the diIC18 probe, proposed as a nonraft marker enriched in Lo phase domains in model membranes (8,12,20–23). This low, but not negligible (20–30%) colocalization of diI with both

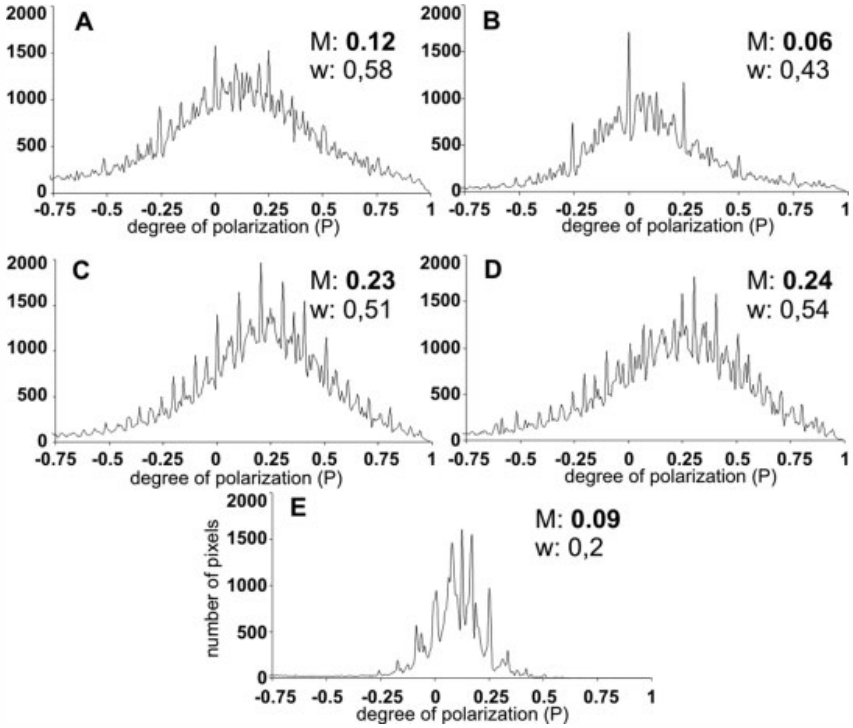

Figure 3. Distribution of *P* values detected for diIC18(3) and Bodipy-PC on Kit225 K6 T lymphoma cells: effect of membrane raft modifications. The *P* values, indicated on the *X* axis, were measured for selected cells (8–10/graph) by recording DP-CLSM images. The *Y* axis shows the normalized number of pixels with a given *P* value. Panels **A**–**D** display diIC18(3) fluorescence *P*-histograms in control, MBCD treated, CD48-crosslinked, and CD71-crosslinked T cells, respectively. Panel **E** shows *P*-histogram of Bodipy-PC probe in control, untreated K6 T cells. The *M* values on all panels display the mean *P* value while the *w* values display the width of Gaussian from a Gauss-Marquardt fitting of data.

classic lipid markers of rafts could be observed on lymphoid and myeloid cells, as well as on other cell types, such as fibroblasts or heart muscle cells and did not show cell type-dependence. This might mean that, in contrast to model membrane systems, in live cells the raft domains may differ in their SM content and a fraction of diI may partition into SM-poor raft domains. Another alternative explanation is that the constitutive protein content of rafts may partially shield the molecular immiscibility of diIC18 and SM within these domains. Taking all these together, we can say that in live cells the Lo-Ld phase separation is likely smoothened relative to model membranes by the numerous proteins interacting with the lipid components of these domains.

The recently introduced DP-CLSM technique (25,26) proved to be useful so far in detecting macroscopic ultrastructural changes in different plant (membrane) structures using various measuring modalities offered by the method. Here we used the *P*-imaging modality of DP confocal microscopy and, by applying diIC18 probe, we concluded that technically DP-CLSM is capable of monitoring either probe orientations or pixel by pixel emission polarization heterogeneities all over the cell surface in intact lymphoid cells. While the statistical analysis of *P*-images for the fluid phase probe Bodipy-PC has shown a relatively narrow and quite depolarized *P*-distribution over tens of T lymphoma cells, the *P*-distributions for diIC18 were substantially broadened with a higher mean value. This can be accounted for by the contributions from *r* and possibly also from the existence of small scale ordered membrane regions (including partly rafts), as compared with B-PC which is homogenously labeling the fluid membrane regions.

Modification of lipid raft microdomains by either cholesterol depletion (domain disruption) or by crosslinking of raft-localized proteins, such as CD48 (domain aggregation), both sensitively influenced the *P*-distributions derived from *P*-images recorded on T cells. Aggregation of rafts through CD48 crosslinking and interestingly crosslinking of a nonraft protein transferrin receptor (CD71), both shifted the mean of the *P*-distribution toward a higher value (restricted rotational freedom). These changes might arise partially from the reduced rotational freedom of "raft-captured" diI molecules and/or from a dynamic coupling between the coalesced rafts and their partially ordered lipid neighborhood, where binding of diIC18 to certain proteins may increase upon their aggregation. Such phenomenon was reported earlier for FcεRI on mast cells, where antigens could induce a large scale coaggregation of lipids with the clustered receptors (43).

This mechanism, as a model of raft-mediated membrane reorganization was studied later in a relatively simple model membrane system (44) and it was shown that crosslinking of a raft lipid (such as G_{M1}) or a single raft protein (such as Thy1/

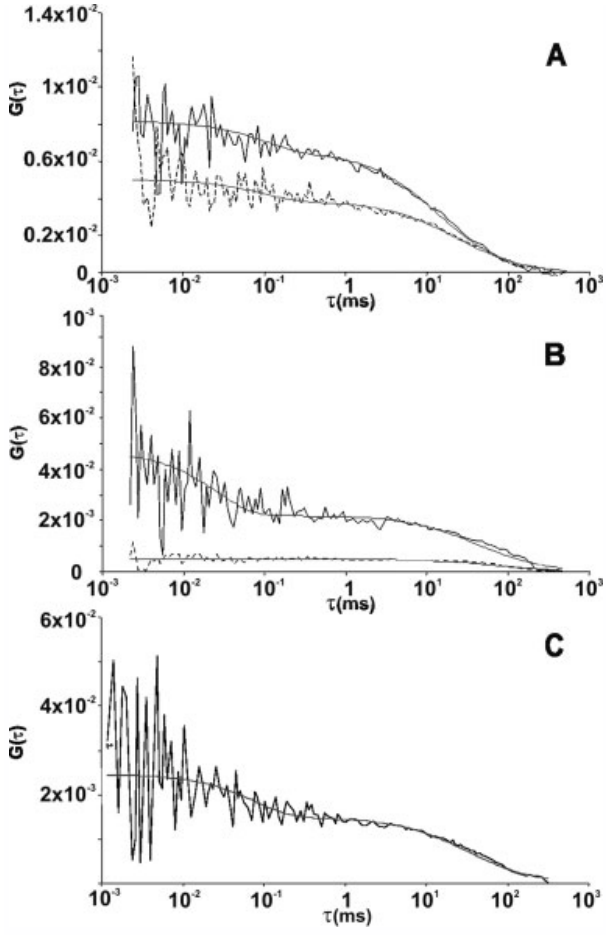

Figure 4. Fluorescence autocorrelation curves of diIC18(3) measured on Kit 225 K6 cells. For each sample $n \geq 10$ cells were measured; 10 runs lasting for 6 s each were carried out in every selected point. Presented curves are the averages of 10 runs. Representative curves from measurements on two control cells (**A**), two MBCD-treated cells (**B**), and one CD48 crosslinked cell (**C**) are shown. Autocorrelation curves were fitted to a model assuming a single free diffusion component and triplet correction (smooth curves). The average diffusion times for the control, MBCD-treated, and CD48-crosslinked samples were 24.1 $\pm$ 13.4, 62.9 $\pm$ 42, and 33.7 $\pm$ 7.8 ms, respectively.

CD90) may result in coexistence of phase separated Ld and Lo domains, at least in such models. Our DP-CLSM imaging data on diIC18 probe in live lymphocytes confirm that this might be an operating mechanism, when raft proteins, e.g. CD48 are crosslinked. The membrane reorganization induced by CD48 or CD71 crosslinking can also influence local diffusion properties of the investigated diIC18 probes either through the increased size of obstacles against their free diffusion or through an increase in the affinity of lipid–protein interaction upon protein aggregation, consistently with our present FCS microscopic data.

In conclusion, our data provided several pieces of evidence for protein compositional diversity of lipid rafts in live lymphoid cells. It was also shown that Lo (liquid ordered) domains defined by the diIC18 probe weakly overlap with the raft microdomains defined by $G_{M1,3}$ gangliosides and the new anti-cholesterol antibody reactive with clustered cholesterol. Finally, we demonstrated usefulness of the DP imaging in live human lymphoma cells. Using diIC18 probe, the *P*-images, in accordance with FCS microscopic data revealed a dynamic coupling between raft modulations and the neighboring lipid regions. To elucidate the mechanistic details of the latter, however, requires further analysis.

Acknowledgments

The skillful technical assistance of E. Veress and the helpful discussions with O. Zsiros is gratefully acknowledged. We also acknowledge the financial and technical supports by Carl Zeiss Jena GmbH, in particular we wish to thank Dr. Reinhard Jörgens and Dr. Georg Weiss for their help in configuring our DP-LSM. We are grateful to Dr. Zsolt Tóth (Szeged University, Hungary) for his help in the Mueller matrix measurements on the dichroic beam splitters.

Literature Cited

1. Simons K, Ikonen E. Functional rafts in cell membranes. Nature 1997;387:569–572.
2. Edidin M. Shrinking patches and slippery rafts: Scales of domains in the plasma membrane. Trends Cell Biol 2001;11:492–496.
3. Matko J, Szöllősi J. Landing of immune receptors and signal proteins on lipid rafts: A safe way to be spatio-temporally coordinated? Immunol Lett 2002;82:3–15.
4. Horejsi V, Drbal K, Cebecauer M, Cerny J, Brdicka T, Angelisova P, Stockinger H. GPI microdomains: A role in signalling via immune receptors. Immunol Today 1999;20:356–361.
5. Alonso MA, Millán J. The role of lipid rafts in signaling and membrane trafficking in T lymphocytes. J Cell Sci 2001;114:3957–3965.
6. Matkó J, Szöllősi J. Regulatory apects of membrane microdomain (raft) dynamics in live cells: A biophysical approach. In: Mattson M, editor. Membrane Microdomain Signaling: Lipid Rafts in Biology and Medicine. Totowa, NJ: Humana Press; 2004. pp 15–46.
7. Rosenberger CM, Brumell JH, Finlay BB. Microbial pathogenesis: Lipid rafts as pathogen portals. Curr Biol 2000;10:R823–825.
8. Maekawa S, Iino S, Miyata S. Molecular characterization of detergent-insoluble cholesterol-rich membrane microdomain (raft) of the central nervous system. Biochim Biophys Acta 2003;1610:261–270.
9. Wolf Z, Orso E, Werner T, Klunemann HH, Schmitz G. Monocyte cholesterol homeostasis correlates with the presence of detergent resistant membrane microdomains. Cytometry A 2007;71A:486–494.
10. Grandl M, Bared SM, Liebisch G, Werner T, Barlage S, Schmitz G. E-LDL and Ox-LDL differentially regulate ceramide and cholesterol raft microdomains in human macrophages. Cytometry A 2006;69A:189–191.
11. Wu M, Holowka D, Craighead HD. Baird B. Visualization of plasma membrane compartmentalization with patterned lipid bilayers. Proc Natl Acad Sci USA 2004;101:13798–13803.
12. Edel JB, Wu M, Baird B, Craighead HG. High spatial resolution observation of single-molecule dynamics in living cell membranes. Biophys J 2005;88:L43–L45.
13. Kusumi A, Nakada C, Ritchie K, Murase K, Suzuki K, Murakoshi H, Kasai RS, Kondo J, Fujiwara T. Paradigm shift of the plasma membrane concept from the two-dimensional continuum fluid to the partitioned fluid: High-speed single-molecule tracking of membrane molecules. Annu Rev Biophys Biomol Struct 2005;34:351–378.
14. Kahya N, Schwille P. Fluorescence correlation studies of lipid domains in model membranes. Mol Membr Biol 2006;23:29–39.
15. Brock R, Vámosi G, Vereb G, Jovin TM. Rapid characterization of green fluorescent protein fusion proteins on the molecular and cellular level by fluorescence correlation microscopy. Proc Natl Acad Sci USA 1999;96:10123–10128.
16. Parasassi T, Gratton E, Yu WM, Wilson P, Levi M. Two-photon fluorescence microscopy of laurdan generalized polarization domains in model and natural membranes. Biophys J 1997;72:2413–2429.
17. Lawrence JC, Saslowsky DE, Edwardson JM, Henderson RM. Real-time analysis of the effects of cholesterol on lipid rafts behavior using atomic force microscopy. Biophys J 2003;84:1827–1832.
18. Giocondi M-C, Milhiet PE, Dosset P, Grimellec CL. Use of cyclodextrin for AFM monitoring of model raft formation. Biophys J 2004;86:861–869.
19. Biro A, Cervenak L, Balogh A, Lorincz A, Uray K, Horvath A, Romics L, Matko J, Fust G, Laszlo G. Novel anti-cholesterol monoclonal IgG antibodies as probes and potential modulators of membrane raft-dependent immune functions. J Lipid Res 2007;48:19–29.
20. Korlach J, Schwille P, Webb WW, Feigenson GW. Characterization of lipid bilayer phases by confocal microscopy and fluorescence correlation spectroscopy. Proc Natl Acad Sci USA 1999;96:8461–8466.

21. Feigenson GW, Buboltz JT. Ternary phase diagram of dipalmitoyl-PC/dilauroyl-PC/cholesterol: Nanoscopic domain formation driven by cholesterol. Biophys J 2001;80:2775–2788.
22. Bacia K, Schwille P, Kurzchalia T. Sterol structure determines the separation of phases and the curvature of the liquid-ordered phase in model membranes. Proc Natl Acad Sci USA 2005;102:3272–3277.
23. Kahya N, Scherfeld D, Bacia K, Poolman B, Schwille P. Probing lipid mobility of raft-exhibiting model membranes by fluorescence correlation spectroscopy. J Biol Chem 2003;278:28109–28115.
24. Bacia K, Scherfeld D, Kahya N, Schwille P. Fluorescence correlation spectroscopy relates rafts in model and native membranes. Biophys J 2004;87:1034–1043.
25. Garab G, Pomozi I, Jörgens R, Weiss G. Method and apparatus for determining the polarization properties of light emitted, reflected or transmitted by a material using a laser scanning microscope. U.S. Pat. 6,856,391 (2005).
26. Steinbach G, Pomozi I, Zsiros O, Garab G. Imaging fluorescence detected linear dichroism and emission anisotropy of plant cell walls in laser scanning confocal microscope. Cytometry A 2008; in press (this issue).
27. Axelrod D. Carbocyanine dye orientation in red cell membrane studied by microscopic fluorescence polarization. Biophys J 1979;26:557–573.
28. Matko J, Bodnár A, Vereb G, Bene L, Vámosi G, Szentesi G, Szöllősi J, Horejsi V, Waldmann TA, Damjanovich S. GPI-microdomains (membrane rafts) and signaling of the multichain interleukin-2 receptor in human lymphoma/leukemia T cell lines. Eur J Biochem 2002;269:1199–1208.
29. Spits H, de Vries JE, Terhorst C. A permanent human cytotoxic T-cell line with high killing capacity against a lymphoblastoid B-cell line shows preference for HLA A. B target antigens and lacks spontaneous cytotoxic activity. Cell Immunol 1981;59:435–447.
30. Gombos I, Detre C, Vamosi G, Matko J. Rafting MHC-II domains in the APC (presynaptic) plasma membrane and the thresholds for T-cell activation and immunological synapse formation. Immunol Lett 2004;92:117–124.
31. Szöllősi J, Matko J, Vereb G. Cytometry of fluorescence resonance energy transfer (FRET). In: Darzynkiewicz Z, Roederer M, Tanke H, editors. Methods in Cell Biology 2004;75:105–152.
32. Nagy P, Vámosi G, Bodnár A, Lockett SJ, Szöllösi J. Intensity-based energy transfer measurements in digital imaging microscopy. Eur Biophys J 1998;27:377–389.
33. Vámosi G, Bodnár A, Vereb G, Jenei A, Goldman CK, Langowski J, Tóth K, Mátyus L, Szöllősi J, Waldmann TA, Damjanovich S. IL-2 and IL-15 receptor alpha-subunits are coexpressed in a supramolecular receptor cluster in lipid rafts of T cells. Proc Natl Acad Sci USA 2004;101:11082–11087.
34. Wachsmuth M, Waldeck W, Langowski J. Anomalous diffusion of fluorescent probes inside living cell nuclei investigated by spatially-resolved fluorescence correlation spectroscopy. J Mol Biol 2000;298:677–689.
35. Gombos I, Bacsó Zs, Detre C, Nagy H, Goda K, Andrásfalvy M, Szabó G, Matkó J. Cholesterol-sensitivity of detergent resistance: A rapid flow cytometric test for detecting constitutive or induced raft association of membrane proteins. Cytometry A 2004;61A:117–126.
36. Poloso NJ, Roche PA. Association of MHC class II-peptide complexes with plasma membrane lipid microdomains. Curr Opin Immunol 2004;16:103–107.
37. Bodnár A, Bacsó Z, Jenei A, Jovin TM, Damjanovich S, Edidin M, Matkó J. Class I HLA oligomerization at the surface of B cells is controlled by exogenous β2-microglobulin: implications in activation of cytotoxic T lymphocytes. Int Immunol 2003;15:331–339.
38. Garab G. Linear and circular dichroism. In: Amesz J, Hoff A, editors. Biophysical Techniques in Photosynthesis. Dordrecht: Kluwer; 1996. pp. 11–40.
39. Bouillon M, El-Fakhry Y, Girouard J, Khalil H, Thibodeau J, Mourad W. Lipid raft-dependent and -independent signaling through HLA-DR molecules. J Biol Chem 2003;278:7099–7107.
40. Legembre P, Daburon S, Moreau P, Moreau JF, Taupin JL. Modulation of Fas mediated apoptosis by lipid rafts in T-lymphocytes. J Immunol 2006;176:716–720.
41. Drobnik W, Borsukova H, Böttcher A, Pfeiffer A, Liebisch G, Schütz GJ, Schindler H, Schmitz G. Apo AI/ABCA-1-dependent and HDL-3 mediated lipid efflux from compositionally distinct cholesterol-based microdomains. Traffic 2002;3:268–278.
42. Mendez AJ, Lin G, Wade DP, Lawn RM, Oram JF. Membrane lipid domains distinct from cholesterol/sphingomyelin-rich rafts are involved in the ABCA1-mediated lipid secretory pathway. J Biol Chem 2001;276:3158–3166.
43. Thomas JL, Holowka D, Baird B, Webb WW. Large-scale co-aggregation of fluorescent lipid probes with cell surface proteins. J Cell Biol 1994;125:795–802.
44. Dietrich C, Volovyk ZN, Levi M, Thompson NL, Jacobson K. Partitioning of Thy-1. GM1 and crosslinked phospholipid analogs into lipid rafts reconstituted in supported model membrane monolayers. Proc Natl Acad Sci USA 2001;98:10642–10647.

Chapter 6

Endre Kiss, Péter Nagy, Andrea Balogh, János Szöllősi, János Matkó

Cytometry of raft and caveola membrane microdomains: from flow and imaging techniques to high throughput screening assays

Cytometry A 2008. 73(7):599-614.

Cytometry
PART A
Journal of the International Society for Advancement of Cytometry

Cytometry of Raft and Caveola Membrane Microdomains: From Flow and Imaging Techniques to High Throughput Screening Assays

Endre Kiss,[4] Péter Nagy,[2] Andrea Balogh,[1] János Szöllősi,[2,3] János Matkó[1,4]*

[1]Department of Immunology, Institute of Biology, Eötvös Loránd University, Budapest, Hungary

[2]Department of Biophysics and Cell Biology, Health Science Center, University of Debrecen, Debrecen, Hungary

[3]Cell Biology and Signaling Research Group of the Hungarian Academy of Sciences, Health Science Center, University of Debrecen, Debrecen, Hungary

[4]Immunology Research Group of the Hungarian Academy of Sciences at Eötvös Loránd University, Budapest, Hungary

Received 7 February 2008; Accepted 25 March 2008

Grant sponsor: Hungarian National Science Fund (OTKA); Grant numbers: T049696, T043061, F49025; Grant sponsor: European Community; Grant numbers: EU FP6 LSHB-CT-2004-503467, EU FP6 LSHC-CT-2005-018914; Grant sponsor: Marie Curie grant; Grant numbers: EU FP6 MRTN-CT-2006-035946; Grant sponsor: Hungarian Academy of Sciences.

*Correspondence to: János Matkó, Department of Immunology, Institute of Biology, Eötvös Loránd University, Budapest, Hungary

Email: matko@elte.hu

Published online 12 May 2008 in Wiley InterScience (www.interscience.wiley.com)

DOI: 10.1002/cyto.a.20572

ISAC
International Society for Advancement of Cytometry

• Abstract

The evolutionarily developed microdomain structure of biological membranes has gained more and more attention in the past decade. The caveolin-free "membrane rafts," the caveolin-expressing rafts (caveolae), as well as other membrane microdomains seem to play an essential role in controlling and coordinating cell-surface molecular recognition, internalization/endocytosis of the bound molecules or pathogenic organisms and in regulation of transmembrane signal transduction processes. Therefore, in many research fields (e.g. neurobiology and immunology), there is an ongoing need to understand the nature of these microdomains and to quantitatively characterize their lipid and protein composition under various physiological and pathological conditions. Flow and image cytometry offer many sophisticated and routine tools to study these questions. In this review, we give an overview of the past efforts to detect and characterize these membrane microdomains by the use of classical cytometric technologies, and finally we will discuss the results and perspectives of a new line of raft cytometry, the "high throughput screening assays of membrane microdomains," based on "lipidomic" and "proteomic" approaches. © 2008 International Society for Advancement of Cytometry

• Key terms

rafts and caveolae; membrane microdomains; structure and composition; imaging rafts; flow cytometry of membrane microdomains; lipidomics and proteomics of rafts

Brief history of Raft and Caveola Microdomains

Since the term "lipid raft" has been introduced by Simons and Ikonen (1), the "raft concept" proposing coexisting microdomains in the continuous fluid lipid membrane has become widely accepted and revolutionized our view on biological membranes. The origin of the raft hypothesis was the observed resistance of certain membrane fractions to cold, nonionic detergents (2). Later on, flow and imaging cytometric investigations, such as transmission electron microscopy (TEM), fluorescence confocal (CLSM), and near-field (SNOM) microscopies identified and characterized the caveolae (3) and different forms of caveolin-free lipid rafts (4) by applying a variety of molecular labeling.

Considering the major properties of lipid rafts, still a lot of controversy and uncertainty remained, as demonstrated recently (5–8). According to the most recent definition (9), lipid rafts are small, highly dynamic microdomain structures of eukaryotic cells' plasma membrane, which are implicated mainly in molecular compartmentation of several membrane-associated cellular processes (1,10). In general, these microdomains are enriched in glycosphingolipids, sphingomyelin, cholesterol, and are preferentially associated with GPI-anchored and acylated proteins. Because of their unique lipid and protein composition, they can be characterized by their special

physicochemical properties and lateral segregation in the lipid bilayer of biological membranes.

Caveolae, which are expressed in highly cell type-restricted fashion, are small (50-80 nm diameter), flask-shaped plasma membrane invaginations, occurring generally in cell types with high capacity for endocytotic/transcytotic transport, such as endothel, epithel cells, or phagocytes. Caveolae have unique protein components, caveolins and flotillins, that show high affinity for cholesterol and required for formation and stabilization of these specialized membrane domains (11). Caveolae are also implicated in signal transduction, endocytosis, or uptake of certain pathogens (11,12).

Biological significance of membrane raft microdomains in a number of essential processes have been demonstrated, such as signal transduction (13–15), antigen presentation to lymphocytes (16,17), recognition and internalization of various pathogens (18), signaling to cell death (17,19), or neuronal communication/signal transduction (20). Thus, altered lipid composition of membrane rafts may lead to changes in their functional properties through differential clustering of signaling molecules within the domains, which might have relevance in several pathological disorders. For instance, modulatory effects of lipoproteins on cholesterol and ceramide content of plasma membrane highlighted the role of these raft components in regulation of the activation status and function of platelets and macrophages presumably involved in the pathogenesis of atherosclerosis (21,22). Such observations also raise the possibility of novel therapeutic applications exploiting the pharmacological inhibition of lipid rafts' functions through modulating their protein content (23). Therefore, there is a continuously increasing interest in detection of the compositional heterogeneity of rafts and its changes, for example, under pathological conditions. It is suggested that caveolae/lipid rafts are critical for the activation of many signaling pathways associated with cardiovascular changes that occur in hypertension (24), with certain types of diabetes (25) or with autoimmune diseases (e.g., systemic lupus erythematosus) (26). Defects in lipid raft formation, as in the case of glycosphingolipid (GSL) or cholesterol storage diseases (e.g. Niemann-Pick syndromes) (27), or when microdomains yield the site of abnormal protein processing like in prion disorders or Alzheimer disease (28,29), are adequate examples to show how crucial is the appropriate function of these microdomains in normal cellular functions.

Cytometry, as shown by the forthcoming examples, may provide several reasonably good tools to investigate lipid rafts. Because rafts are considered as highly dynamic microstructures (10), the large diversity of approaches and labels as well as of cellular models makes exploration of their general properties difficult. Therefore, besides the specific analysis methods developed for studies of their composition and dynamics, the high throughput screening (HTS) assay methods are badly needed for this purpose.

In the forthcoming chapters, we will briefly summarize the major cell analytical efforts directed to analyze membrane microdomains (rafts) in various cell types using flow and image cytometric methods and also describe the future directions in HTS assays of the "raft's proteome and lipidome."

Chemical definition of Membrane Microdomains

The classical biochemical approach to isolate and characterize membrane microdomains is based on the resistance of these structures to solubilization with nonionic detergents, such as Triton X-100, Brij, CHAPS, or Nonidet P40 (2,10,30–32). During this typical procedure, the low density, detergent-resistant membrane fraction (DRM) of the cell lysate is extracted using 1% neutral detergent at + 4 °C (or Brij at 37°C), followed by a subsequent separation step with sucrose-gradient ultracentrifugation. The protein and lipid composition of the obtained floating (light buoyant density), detergent-resistant (DRM), or detergent-soluble (DSM) membrane fractions can then be analyzed using sodium dodecyl-sulphate (SDS)-polyacrylamide gel electrophoresis (PAGE), immunoblotting or thin-layer chromatography, respectively. Although this approach is still widely applied to identify molecular associations to lipid microdomains, it should be emphasized that the information obtained from this assay should be handled with care (5,10,33). Several concerns have emerged in the literature about the capability of this method to identify *in situ* composition of lipid microdomains existing in intact cells. The concentration and chemical composition of the applied detergent seems to be a key factor, because the protein content of DRMs may be influenced by these parameters (33,34). One of the central questions is whether the DRMs recovered during the procedure are representing the real state of plasma membrane microdomains or are partially artificial due to the detergent extraction, itself. The obvious perturbing effects of detergents on the lipid membranes were demonstrated in case of Triton X-100, reported to induce reorganization of lipids, to enhance formation of liquid-ordered (Lo) domains, or occasionally to induce fusion of existing rafts to large confluent membrane aggregates (33). Because protein-lipid interactions may not be strong enough to resist detergent extraction, detergent solubility does not exclude the possibility of weak associations with microdomains (34). On the other hand, several studies on model membranes suggest that detergent extraction does not perturb significantly the domain composition and the DRM fractions obtained only from Lo domain-containing membranes (32,35).

Based on these uncertainties, several groups attempted to introduce modifications in the basic protocol to avoid using a detergent (7,33). Song et al. (36), for example, sonicated the cell lysate in pH 11 carbonate buffer and used a subsequent density gradient centrifugation to isolate caveolae. However, the selectivity of this method is still questioned, because the resulted raft/caveolae fractions are highly contaminated with non-raft membranes (7,37). A more selective, but still extremely time-consuming method by Smart et al. (38) is based on plasma membrane fractionation, sonication to release lipid rafts, and several density gradient ultracentrifugation steps. The method provides relatively pure lipid raft preparation, but with low yield. Moreover, the efficiency of separation of raft membranes from plasma membrane appears to be strongly influenced by the time of sonication. A procedure improved by Macdonald et al. (39) requires just one short (90 min) centrifugation step and omits the initial plasma membrane

purification, omits EDTA from lysis buffer, but adds divalent cations (Ca^{2+} and Mg^{2+}) to the lysis buffer, which presumably helps to maintain the integrity of lipid rafts. This protocol leads to higher yields and more consistent results without the discrepancies observed in Smart's method during the comparative analysis of different cell types, growth, and treatment conditions. Although the method appears to yield a fairly clean fraction of membranes that has all the characteristics of lipid rafts, interestingly, caveolin was recovered from fractions of significantly higher density than other raft marker proteins. The reason of this is not known yet, but might be explained by an association between caveolae and the actin cytoskeleton resistant to cell-lysing conditions.

In conclusion, detergent insolubility assays can still provide a substantial tool for investigating biological membranes. To define membrane microdomains, including cholesterol-sphingolipid rafts, DRMs are undoubtedly the most useful starting point (34).

Labeling of Lipid Rafts

In situ observation of lipid rafts by either flow or image cytometry requires specific labeling with different fluorophore-conjugated antibodies, lipid probes, or other reporter molecules. One of the earliest probes used to label rafts is the pentameric B-subunit of cholera toxin (CTX-B) derived from the heat-labile enterotoxin of *Vibrio cholerae* and showing high affinity to GM1 ganglioside (16,30,40,41). Because of the pentavalent binding of cholera toxin, it generates patches of GM1, therefore aggregates of rafts can be visualized by fluorescently labeled cholera toxin (30,42). Cholera toxin induces small aggregates when labeling is performed on ice, but extensive crosslinking and mobility are induced, if the labeling is at 37 ^{o}C. Flow and image cytometric analysis of the expression level of total gangliosides (as a measure of raft content), using fluorescently labeled CTX-B, should also be a matter of consideration, because the toxin has some crossreactivity with other type of gangliosides (43). These are pitfalls of cholera toxin labeling, but in certain cases it can be valuable. However, it was reported that CTX-B can be efficiently used in the classical biochemical DRM-isolation method (44) and for immunophenotyping purposes, as well. Recently, it was shown that GM1 positivity of freshly isolated and late apoptotic neutrophil granulocytes provides a new complementary marker of this cell type besides the traditionally applied but easily misinterpretable protein markers (e.g., CD16 versus CD49d) used to distinguish them from eosinophils (45). Monoclonal antibodies raised against GM1 ganglioside (46) are also applied to detect lipid rafts in intact cells.

Several fluorescent lipid derivatives have been used in microscopic studies with various degree of success to specifically label lipid rafts (liquid-ordered phase) or the liquid-disordered phase. Although Texas red-labeled dihexadecanoyl phosphatidylethanolamine (TR-DHPE) (47), rhodamine- or fluorescein-labeled dipalmitoyl phosphatidylethanolamine (Rho-DPPE and Fl-DPPE) (48,49) or fluorophore-conjugated dioleoyl-phosphatidylethanolamine (DOPE) (50) partition very effectively into the liquid-disordered phase, NBD-DPPE (49), Cy5-dimyristoyl-phosphatidylethanolamine (DMPE) (50), and the aromatic hydrocarbon dye perylene (48) show preferential accumulation in the liquid-ordered phase. It can be seen that both the fluorescent label (NBD *vs.* fluorescein) and the composition of the membrane (SM *vs.* DSPC) strongly influence partitioning of the fluorescent probes.

The widely used indocarbocyanine dye diIC_{18} (3) preferentially partitions in the liquid-disordered phase in dioleoyl phosphatidylcholine (DOPC)/sphingomyelin (SM)/cholesterol mixtures (48,51), but it favors the liquid-ordered phase in DOPC/distearoyl phosphatidylcholine (DSPC)/cholesterol membranes (52). Because its partitioning is never exclusive, it can be used to probe the lipid environment in the liquid-ordered phase even in DOPC/SM/cholesterol mixtures (51,53). Although its tendency to partition into liquid-ordered (Lo) lipid phases (54) predestined it as an ideal probe for lipid raft detection, its weak miscibility with sphingomyelin-enriched membrane regions does not permit it; moreover, now it is assumed as a nonraft lipid probe (51,55,56). Interestingly, in a cell-based study (56), a small, but nonnegligible colocalization have been observed between the membrane domains labeled with diIC_{18} (3) and with CTX-B or by specific antibodies for GPI-anchored proteins, suggesting that the boundaries between the domains of ordered and fluid phases in cell membranes are not as definite as we would expect from model membrane-based experimental data. Supporting this, fluorescence anisotropy of diIC_{18} (3) probe has been shown to increase in cholesterol-rich domains after crosslinking of FcεRI in mast cells (53).

Another old, but less known probe of lipid rafts is Laurdan (57), which has two properties sensitive to membrane phase:

1. It exhibits a blue-shift upon going from the liquid-disordered to the gel phase, because water penetrates less to the gel phase, and, in less polar environments, a higher energy locally excited state is the source of fluorescence. To quantify the spectral shift of Laurdan, the excitation generalized polarization (GP_{ex}) function was defined as

$$GP_{ex} = \frac{I_B - I_R}{I_B + I_R}$$

where I_B and I_R are the intensities measured at the blue and red edge of the emission spectrum, respectively, using a given excitation wavelength. The GP_{ex} function can be used to discriminate between liquid-disordered and liquid-ordered, that is, raft domains (58).

2. Laurdan is oriented strictly normal to the plane of the membrane in the gel phase, whereas it is more randomly oriented in the liquid crystalline phase, therefore polarized excitation of Laurdan can be used to discriminate between the two phases (57).

Laurdan has been used to visualize lipid rafts both in model membranes (49) and living cells (59) using two-photon microscopy. A novel derivative, C-Laurdan, exhibiting greater sensitivity to membrane polarity and brighter two-photon fluorescence reports on the membrane environment more

accurately (60). Concerning the selectivity of probes, Laurdan derivatives are in good position, because they are insensitive of lipid composition, but they rather sensitive to lipid-packing density.

For the same application, GPI-anchored membrane proteins, such as CD48, CD59, Thy-1 (CD90), alkaline phosphatases (AP), or anticaveolin antibody for the detection of caveolae (61) represent another major group of raft markers (40,42,62–66). These proteins are usually visualized through their immunocytochemical labeling with fluorophore-conjugated antibodies or their Fab fragments. It is noteworthy that a remarkable heterogeneity may exist in cellular lipid rafts regarding their protein composition and function (67,68).

The transmembrane protein influenza virus hemagglutinin (HA) has an intrinsic ability to associate with lipid rafts (69). Exploiting this molecular feature, expressing HA (e.g., genetically fused to GFP) in certain cell types can also be used in studying lipid raft organization (40).

Previously, it was shown that lysenin, a toxin isolated from the earthworm *Eisenia foetida*, specifically recognizes sphingomyelin-rich membrane domains (70,71). Because binding of lysenin to sphingomyelin is accompanied by the oligomerization of the toxin, which leads to pore-formation in the target membrane and a subsequent cytolysis, its suitability for cellular analysis of lipid rafts is limited (72–75). Recently, Kiyokawa et al. (76) have generated a genetically truncated form of the toxin, eliminating its undesirable properties, even toxicity, which makes it suitable for studying organization and location of sphingomyelin-rich microdomains.

Because the main stabilizing constituent of lipid rafts is cholesterol, antibodies against cholesterol may also be an efficient tool to detect/study raft microdomains. Previously, only IgM isotype antibodies were reported to react with plasma membrane cholesterol domains of macrophages responsive to changes in cholesterol trafficking. These IgMs bound to the cells only after artificial cholesterol enrichment by various treatments, suggesting that they define cholesterol arrays that are presumably not identical to native lipid rafts (77).

However, Biro et al. reported on two new IgG isotype monoclonal antibodies (ACHA) against cholesterol, AC1 and AC8 (61). These ACHAs specifically detect cholesterol and several structurally closely related sterols in ELISA assays, as well as bind to human lipoprotein fractions. They bound weakly to the surface of various murine and human lymphocyte and monocyte/macrophage cell lines. The binding was substantially enhanced by limited papain digestion of long, protruding extracellular protein domains (e.g., CD44 and CD45), indicating that the small epitope of cholesterol is likely masked by them at the cell surface. The membrane-bound ACHA displays a strongly patchy staining (domains with 2-400 nm diameter) and highly colocalized with both lipid (cholera toxin B) and protein (Thy1, caveolin-1) markers of noncaveolar and caveolar lipid rafts, as assessed by confocal microscopy. All these properties suggest that AC8 preferentially recognizes locally clustered membrane cholesterol, also consistent with its intracellular colocalization with markers of ER and Golgi complex (61). These properties of the new IgG

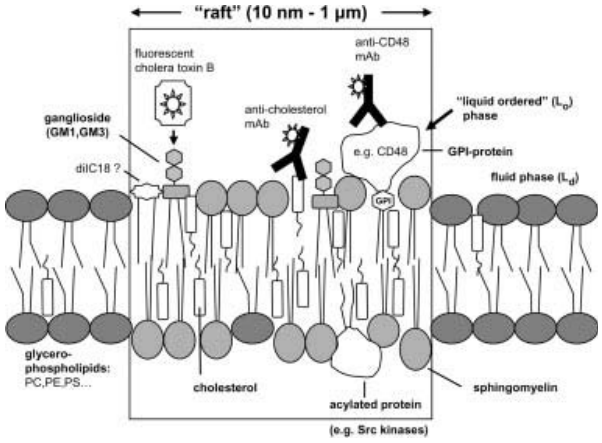

Figure 1. Some widely used fluorescent cytochemical labeling strategies of plasma membrane lipid rafts. Rafts can be visualized, among others, by using lipid probes incorporating into the bilayer or reacting with glycosphingolipids (e.g., cholera toxin B). Fluorescent conjugates of antibodies against GPI-anchored proteins (e.g., CD48, CD59, and PLAP) or with clustered membrane cholesterol (ACHA) are also often employed. Characteristic lipid constituents of fluid (Ld) and ''liquid-ordered'' (Lo) phase of the plasma membrane are also shown. Abbrevations: PC, phosphatidylcholine; PE, phosphatidylethanolamine; PS, phosphatidyl serine; GPI, glycosyl phosphatidylinositol.

ACHAs allow their applications in studying lipid raft functions, as well as in raft-ELISA or protein-chip HTS assay systems. Some selected widely used labeling strategies are shown in Figure 1.

Different research groups have used non-pore-forming derivatives of a cholesterol binding cytolysin perfringolysin O (also known as θ-toxin) from *Clostridium perfringens* to detect cholesterol-rich membrane microdomains in intact cells (78,79). An extensive review focusing on imaging approaches of different cholesterol-binding molecules (e.g., cholesterol oxidases and filipin III) along with θ-toxin, and photoreactive, spin-labeled or fluorescent cholesterol analogues has recently been published elsewhere (80).

Rafts appear to exist in both the outer and inner leaflets of the membrane, with outer leaflet rafts harboring GPI-anchored proteins and inner leaflet rafts containing acylated proteins. The coupling of raft domains at the outer and inner leaflets is thought to be important for signal transduction via lipid rafts (81), but still remained controversial and poorly known. It is commonly accepted that outer leaflet rafts are enriched in cholesterol and sphingolipids, however, such microdomains cannot be mirrored in the inner leaflet, because sphingolipids are mainly concentrated in the outer leaflet. Hayashi et al. constructed a fusion protein of Domain 4 (D4) of the above-mentioned θ-toxin and EGFP to visualize the inner leaflet of lipid rafts (82). D4 is the smallest functional unit that has the same cholesterol-binding activity as the full-size toxin. They expressed EGFP-D4 inside MEF fibroblast cells (a Tet-Off cell line) and showed that cholesterol-rich microdomains also exist in the inner leaflet of the plasma membrane. Pike's group studied lipid raft heterogeneity in

terms of epidermal growth factor receptors (83). They analyzed the distribution of EGFR, other proteins, as well as lipids in plasma membrane using different detergents and also compared the fatty acyl chain length in the inner and outer leaflet lipids. Outer leaflet rafts are stabilized by the interaction of sphingomyelin (SPM) and cholesterol. By comparison, inner leaflet rafts are significantly less stable because of the lack of SPM in these leaflets and hence the absence of its stabilizing interaction with cholesterol. Their data also suggest that inner leaflet rafts are preferentially destabilized by treatment with Triton X-100, giving rise to membrane preparations with a preponderance of outer leaflet lipids. By contrast, inner leaflet rafts were retained in both the detergent-free and Brij 98-resistant raft preparations. In summary, composition analysis of inner leaflet derived DRMs is an interesting and still poorly investigated area of lipid raft research.

Flow Cytometric Approaches for Detecting Detergent Resistance

Although biochemical techniques are still valuable in studying membrane microdomains, there is an increasing demand to substitute them with a rapid, less time- and cell-consuming, reliable, and reproducible assay of detergent resistance, with less possible risks of artifacts mentioned before.

Earlier several works reported on adapting flow cytometry to analyze detergent resistance of cell surface proteins, such as membrane immunoglobulin (84) lymphocyte membrane proteins (85,86), major histocompatibility class II (MHC-II) proteins (87), and integrins (88). The basic similarity among these studies is the application of medium-strength nonionic detergents (Nonidet-P40 or Triton X-100) in a relatively high (0.5-1%) concentration. Although these attempts yielded useful data about the detergent insolubility of the investigated proteins, the mechanisms underlying the detergent resistance were not revealed unequivocally.

As a novel alternative, Gombos et al. (16,89,90) developed a flow cytometric assay of differential detergent resistance (termed FCDR assay). The basic strategy of this approach and data evaluation are summarized in Figure 2. Briefly, the cell sample labeled with fluorescent antibodies specific for the investigated plasma membrane proteins is treated with cold nonionic detergent at low concentration (typically 0.05-0.1%) for a short period of time (5 min). Confocal microscopy revealed that this moderate, short-duration detergent treatment did not result in loss of cellular integrity, the cells remained intact particles, enabling them for flow cytometric analysis. Comparing the fluorescence signals obtained before and after detergent treatment provides information about the detergent sensitivity of the given protein. Moreover, if a protein appears to be detergent resistant (the fluorescence signal is unchanged), suggesting its possible association with DRMs or with actin cytoskeleton, the background mechanism can be easily resolved by selective cholesterol depletion with methyl-β-cyclodextrin (MBCD) (91) or cholesterol deprivation (with cholesterol oxidase), or as an alternative by pretreatment with actin cytoskeleton-destabilizing agents (lantrunculin A, cytochalasin-D) before applying the detergent (Fig. 2).

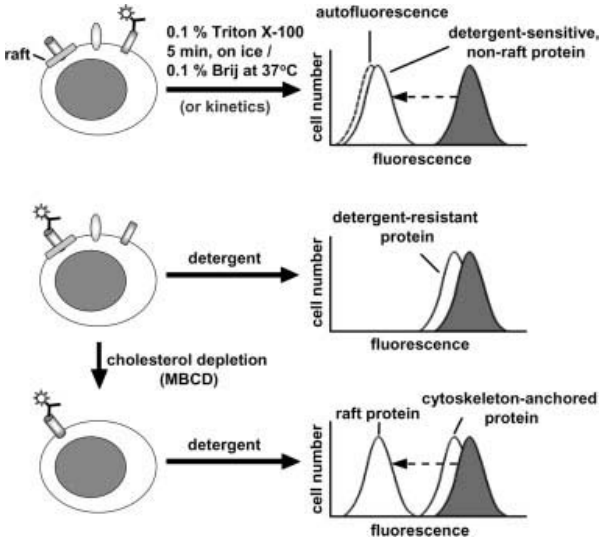

Figure 2. Basic principles of flow cytometric assay of detergent resistance. Top: nonionic detergents, even at low ($\leq$0.1%) concentrations, can rapidly dissolve detergent-sensitive membrane proteins. This becomes detectable from the decreased mean fluorescence intensity of the immunocytochemically labeled sample, upon the addition of the detergent. The kinetics of the dissolution process can also be followed by flow cytometry in time-resolved mode. Middle: proteins residing in raft microdomains or anchored by the cytoskeleton show remarkable detergent resistance. Bottom: to reveal the underlying mechanism of detergent resistance, selective disruption of lipid rafts (by cholesterol depletion or deprivation) or the cytoskeleton (by cytochalasin D or latrunculin) can be applied before detergent treatment. A subsequent increase in detergent solubility of the protein is indicative of its raft or cytoskeleton-association, respectively.

Among the major advantages of this method, it should be highlighted that using flow cytometry of intact cells minimizes artifacts concerning detergent-induced perturbation/rearrangement of *in situ* protein assemblies, which is likely to occur when the cells are fully lysed with high (typically 1%) detergent concentrations, at low temperature. The method requires low amount of cells ($\sim 10^4$/sample) is marked with high reproducibility, and according to kinetic measurements, 5-min detergent treatment is typically enough to resolve sensitive and resistant proteins into two resolvable peaks, although minor differences may appear among different cell types, as it has been demonstrated for CD4, CD5, CD14, CD225, and ND5 (92). This publication also points out that in certain cases the intracellular pool of the investigated protein should be also a matter of consideration, because treatment with nonionic detergents results in permeabilization of the cells and thus makes the antigen accessible for the detecting antibody. In contrast to the classical biochemical approach, results obtained from FCDR assay are weakly influenced by the type of nonionic detergent (90). Because the method can be performed on all types of conventional bench-top flow cytometers, the only parameter limiting the number of acquired proteins is the number of the available optical channels. As for the technical details of immunofluorescent labeling, it should be taken into account that using Fab is preferred to whole

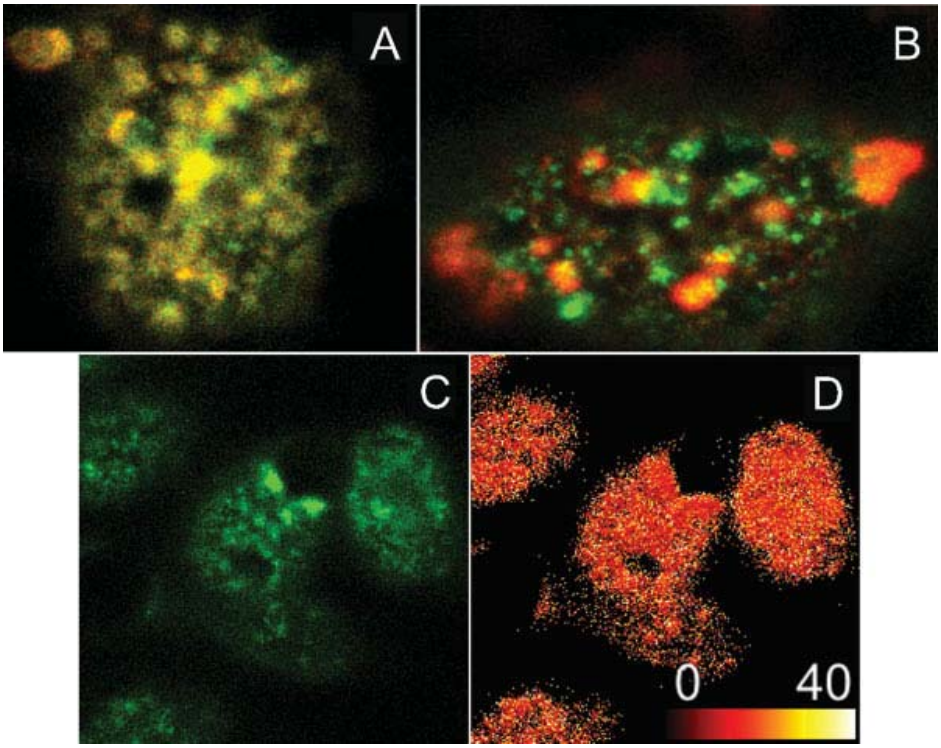

Figure 3. Demonstration of confocal microscopic colocalization and FRET analysis of ErbB2 protein clusters on tumor cells. **A**–**B**: SKBR-3 breast tumor cells were labeled with Cy3-tagged anti-ErbB2 Mab (trastuzumab, red channel) and FITC-labeled CTX-B (green channel) on ice (**A**) or at 37 °C followed by imaging the top or bottom layer of cells by confocal microscopy. Image **A** shows strong correlation between the two signals indicated by the presence of the yellow color, whereas image **B** implies that crosslinking of lipid rafts by CTX-B induced a separation between ErbB2 clusters and lipid rafts. **C**–**D**: SKBR-3 breast tumor cells were labeled by a 1:1 mixture of FITC-tagged and Cy3-tagged anti-ErbB2 Mab (trastuzumab), and ErbB2 homoassociation was measured by the donor photobleaching FRET technique. The fluorescence image taken in the FITC channel and the FRET image are shown in **C** and **D**, respectively. The scale in **D** represents the color-coded FRET efficiencies between 0 and 40%. The colocalization between ErbB2 and CTX was analyzed by ImageJ using the JaCoP plugin. Pearson's correlation coefficients for images of the control and CTX-treated samples are 0.933 and 0.472, respectively, corroborating the previous conclusions.

immunoglobulin to avoid crosslinking-induced detergent resistance effects (85). The major limitation of this approach is the heterogenous sensitivity of membrane proteins to the applied mild detergent treatment that may influence the resolution of detergent-sensitive and detergent-resistant proteins quantitatively.

The FCDR technique served as a basis of several experimental works published recently. Among others, its usefulness was demonstrated in investigating raft association of an ABC transporter protein in human colon carcinoma cells (89), proving raft-localization of transferrin receptor type 2 in hepatoblastoma and erythroleukemic cells (93) and in studying detergent resistance of surface antigens in human peripheral blood monocytes (94,95). Its suitability to follow signal-induced association of membrane proteins with lipid rafts was also demonstrated (90).

Image Cytometry of Rafts in Intact Cells: Results and Limitations

The classical definition of rafts is based on the density and detergent insolubility of these domains. To investigate these properties, the cell membrane has to be solubilized excluding the *in situ* investigation of raft domains. Therefore, alternative approaches abound including those based on microscopic investigation of cell or model membranes. These imaging approaches are usually, but not exclusively based on probes selectively partitioning into or excluded out of rafts. Therefore, the success of these approaches hinges on the validity of the assumption that the probe specifically identifies raft domains.

As an example, Harder et al. used cholera toxin-mediated crosslinking of GM1 to show that GPI-anchored proteins and GM1-rich domains copatch with each other. On the contrary, a transmembrane protein, ErbB2, was found not to copatch with cholera toxin, although it is colocalized with cholera toxin-labeled domains in cells labeled on ice (Fig. 3). These findings point to fundamental differences in the dynamics with which peripheral and transmembrane proteins are associated with rafts (42). Cholera toxin-mediated crosslinking of GM1 implied that aggregation of lipid rafts accompanies T cell receptor signaling. However, controversy exists over the role of lipid rafts in T cell receptor (TCR) mediated signaling,

since others showed that GPI-anchored GFP is excluded from the immunological synapse. Despite the controversy, the widespread assumption is that lipid rafts are indeed recruited to the immunological synapse and not only serve as platforms in which signaling proteins are concentrated, but these microdomains provide the means for regulating key elements in TCR activation, for example, by segregating lck and fyn kinases from each other in unstimulated cells.

One also has to bear in mind that rafts are also heterogeneous with respect to lipid composition, and GM1-free lipid rafts will not be visualized by cholera toxin labeling (96). Despite the limitations and disadvantages of cholera toxin as a raft marker, it has been shown that it highly colocalizes with other lipid raft markers such as GPI-anchored proteins and anticholesterol antibody (56,61).

Scanning near-field optical microscopy (SNOM) offers superior resolution of fluorescent samples compared to conventional microscopy (97). Hwang et al. reported on the patchy distribution of Bodipy-labeled phosphatidylcholine in the cell membrane, but they did not attempt to relate this phenomenon to lipid rafts (98). Model membranes lend themselves easily to SNOM investigations for which a flat surface is advantageous. Uneven distribution of TR-DPPE (99) and TR-DHPE (47) has been observed in binary and ternary model membranes implying phase separation. Electron microscopy of immunogold-labeled cell membranes also implied the clustered distribution of raft-associated membrane proteins (100,101). Even the 3-dimensional distribution of caveolin labeled with ammonium nickel sulfate hexahydrate-intensified diaminobenzidine-horseradish peroxidase staining was constructed by high-voltage electron microscopic tomography (102). A slight drawback of both SNOM and electron microscopy is the need for expensive instrumentation and harsh sample treatment, although relatively recent developments in both imaging modalities make imaging under more physiological conditions possible.

Imaging approaches can also be used to investigate the dynamic aspects of lipid rafts, that is, the mobility of raft-associated proteins and lipids. Fluorescence correlation spectroscopy (FCS) is suitable for the determination of the diffusion constant of fluorescently labeled molecules (103). Being a diffraction-limited technique, FCS cannot measure the diffusion coefficient of molecules in domains smaller than its resolution limit (103). FCS data from ternary lipid mixtures have been used to create a phase diagram showing areas of coexisting liquid-ordered and liquid-disordered phases characteristic of lipid rafts floating in the membrane of living cells (51). The measurement of the diffusion constant of fluorescent or gold-labeled molecules is also possible with single particle tracking (SPT). The diffusion constant of lipids was shown to be reduced by a factor of $\sim$2 when entering the liquid-ordered phase from the liquid-disordered phase (49). These results indicate that diffusion is hindered by the more compact packing of lipids in raft domains. Lipid rafts not only reduce the diffusion rate, but also confine the movement of molecules, that is, both raft-associated lipids and proteins are locked into transient confinement zones (TCZ) corresponding to lipid rafts for several seconds, because the activation energy required to cross the boundary of rafts is high (104). This conclusion was reached by Schütz et al. in a seminal paper in which the trajectories of Cy5-DOPE (dioleoyl-phosphatidylethanolamine) and Cy5-DMPE (dimyristoyl-phosphatidylethanolamine) were compared. Cy5-DOPE, preferentially labeling liquid-disordered domains, showed unhindered diffusion, whereas Cy5-DMPE partitioning into liquid-ordered domains showed hindered diffusion. The size of transient confinement zones was $\sim$700 nm, and the average residence time of Cy5-DMPE in these domains was $\sim$13 sec (50). Tracking of colloidal gold-labeled membrane proteins confirmed that GPI-anchored proteins are transiently confined in areas with a diameter of $\sim$100 nm (104). It is usually accepted that tracking fluorescent and colloidal gold-labeled proteins yields similar data, although gold is believed to slow the long-term diffusion of the molecule it labels (105). These findings imply that the lipid environment plays a pivotal role in determining the mobility of membrane components. In contrast, several studies point to the fundamental role of protein–protein interactions in restricting lateral diffusion. Douglass et al. observed the diffusional trapping of T-cell signaling proteins (e.g., Lck and LAT) by CD2 protein complexes and show that this confinement is maintained by protein–protein interactions and do not require interactions with the actin skeleton or lipid rafts (106). Another twist to the story is the observation that membrane proteins anchored to the cytoskeleton act as "rows of pickets" creating a barrier hindering the diffusion of both lipids and proteins (41,107). Trapping beads bound to GPI-anchored or transmembrane proteins by a laser beam the viscous drag experienced by these proteins was measured and it was concluded that rafts are long-lasting entities with a mean diameter of $\sim$25 nm (108).

The morphology of lipid rafts can be studied by atomic force microscopy (AFM), which is exquisitely suited for the investigation of the surface topography of objects. Membrane pits with a mean diameter of $\sim$100 nm were identified, and these indentations coincided with caveolin-1-GFP fluorescence indicating that they corresponded to caveolae (109). AFM can also detect that the gel phase of the membrane is usually 1-2 nm higher than the coexistent fluid phase (110). In an interesting study, secondary ion mass spectroscopy was combined with AFM imaging of model membranes. The authors claim that quantitative information about the chemical composition of lipid domains can be obtained (110).

Imaging approaches provide a valuable alternative for classical biochemical approaches to study lipid rafts. However, one has to be aware of certain limitations of these techniques. Imaging studies often aim to measure the size of lipid raft microdomains. Because the reported size cannot be smaller than that permitted by the resolving power of the microscope, the resolution of the technique must not be forgotten. There is a nagging discrepancy between domain sizes observed in model and cell membranes, because the former are usually in the several hundred nanometer to micrometer range (49), while the latter are much smaller (108). Model membranes are much simpler, protein-free mixtures of 2–3 lipid species in

thermodynamic equilibrium. Cell membranes, on the other hand, are complex and dynamic structures of several types of lipids and proteins, which never reach thermodynamic equilibrium due to continuous transport of material to and from the membrane. The presence of proteins (111,112), the cytoskeleton (41), active vesicular transport, and the lack of equilibrium (113,114) have significant impact on the properties of microdomains explaining at least some of the conflicting results. Indeed, preliminary studies on proteins incorporated into model membranes suggest that raft-associated proteins show relatively weak preference for the liquid-ordered phase, which can be increased by crosslinking, showing that model membranes do not fully reproduce the selectivity of protein distribution (62,103). The complex protein and lipid mixture in cell membranes probably generates an environment, which is on the boundary favoring the formation of lipid rafts, and subtle changes in the local composition of the membrane caused by active cellular processes create transient nucleation centers for raft formation.

Fretting Rafts

As described in the previous sections, methods, including detergent extraction and cholesterol depletion, rely on harsh interference with the composition of the membrane. This circumstance casts some doubt on the correspondence between rafts in living cells and the detergent-resistant domains defined by these methods. This uncertainty calls for alternative, less destructive approaches in raft research. One such family of methods relies on the measurement of fluorescence resonance energy transfer (FRET), which is a radiation-less interaction between a fluorescent molecule (donor) and an acceptor. FRET is an inexpensive method, which can be used in fluorometry, flow cytometry, and fluorescence microscopy (115–118). Its utility in biological applications stems from the fact that the rate of the process changes as the inverse sixth power of the separation between the donor and the acceptor dyes. Because FRET takes place when the interacting molecules are 1-10 nm apart, its application essentially extends the resolution limit of diffraction-limited approaches from 200-300 nm to the nanometer range. Extensive literature is available for a general introduction to FRET and to aid in the selection of suitable experimental conditions (115–124); therefore, we resort to a brief summary of the principles only.

In a conventional, hetero-FRET interaction, an excited fluorophore (donor) transfers energy to a nearby, spectroscopically different acceptor molecule, which is usually, but not necessarily fluorescent too. In mathematical terms, the probability of FRET, defined as FRET efficiency, is the fraction of the energy of excited donor fluorophores tunneled to acceptors in FRET interaction. FRET efficiency is the function of the donor–acceptor separation distance, the orientation factor (the relative orientation of the donor and the acceptor), the donor quantum yield in the absence of the acceptor, the index of refraction of the medium and the overlap integral between the donor emission and acceptor absorption spectra. In most cases, all of these parameters except for the distance can be expressed as a single parameter (R_o), which is constant for a specific donor–acceptor pair under given experimental conditions. Using this simplification, the FRET efficiency can be expressed by the following equation:

$$E = \frac{R_o^6}{R_o^6 + R^6}$$

where R_o is the distance at which FRET efficiency is 50% and R is the separation distance between the donor and the acceptor. R_o can be expressed as

$$R_o = \left[const\ n^{-4}\ Q\ \kappa^2\ J \right]^{1/6}$$

where n is the index of refraction of the medium, Q is the quantum efficiency of the donor in the absence of the acceptor, κ^2 is the orientation factor, and J is the overlap integral. The most important assumption in this simplification is that the donor and the acceptor molecules are randomly oriented relative to each other and that they rotate fast during the excited state lifetime, which turns κ^2 to a constant equal to two-third. The validity of this assumption has to be verified. For most donor–acceptor pairs R_o is ~3–8 nm setting the distance range amenable for FRET investigations to 1–10 nm (125).

The excited donor can also interact with another donor molecule, if the absorption and emission spectra of the donor overlap. Because this is the case for most fluorophores, such an interaction, termed homo-FRET, is very common (126,127). In this interaction, the donor and acceptor fluorophores are spectroscopically identical. The only manifestation of homo-FRET is the decreased fluorescence anisotropy of the fluorophore, a phenomenon observed as early as the 1930s by Perrin. Anisotropy is defined according to the following equation:

$$r = \frac{I_{VV} - I_{VH}}{I_{VV} + 2I_{VH}}$$

where I_{VV} and I_{VH} are the vertical and horizontal, respectively, components of fluorescence emission excited by vertically polarized light. In order for homo-FRET to achieve a measurable decrease in anisotropy, the fluorophore ("donor") needs to have sufficiently high anisotropy to begin with, and the fluorophores ("acceptors") have to be randomly oriented relative to the donor, so that their fluorescence emission loses the preferential orientation of the donor.

Both homo- and hetero-FRET measurements have been used extensively to study the structure and dynamism of rafts. The question asked in most of these studies was whether GPI-anchored proteins are concentrated in clusters or are randomly distributed in the membrane. By examining the dependence of FRET efficiency on acceptor density (fluorophore density in the case of homo-FRET), clustered and random distribution can be detected. Because FRET efficiency (anisotropy in the case of homo-FRET) is independent of acceptor density, the fluorophores are concentrated in clusters, whereas these parameters change as a function of fluorophore density, if the distribution is random. We stress again that by examining the

concentration dependence of FRET efficiency, it is possible to detect subpixel clusters, that is, clusters with a diameter below the resolution limit of conventional fluorescence microscopes. Using such an approach, Varma et al. concluded that GPI-anchored proteins are clustered in domains likely to be smaller than 70 nm in diameter (128). Although the existence of such clusters was further supported by an independent study using chemical crosslinking (129), two consecutive papers from the Edidin laboratory questioned the existence of GPI-anchored microdomains (63,130). Although the homo-FRET approach used by Varma et al. is somewhat more sensitive for the detection of small clusters compared to hetero-FRET applied in the later publications, a common denominator was reached by assuming that only a small fraction of GPI-anchored proteins are enriched in clusters, with the majority of molecules being randomly distributed at low densities outside these domains (63).

Using hetero-FRET measurements, GPI-anchored proteins were shown to be unclustered both in resting T cells, and they were not concentrated into clusters even in the immunological synapse after antigen challenge (131,132). Depending on the context the term "clustering" refers to several distinct phenomena: a) increase in the fluorescence intensity of a raft marker due to membrane convolution resulting in a higher membrane surface area/pixel, that is, higher fluorescence intensity/pixel even without a higher density of the raft marker in the membrane; b) increased concentration of the raft marker in the membrane without increased FRET. This can happen if microdomains harbor only few proteins, and their size is well below the resolution limit of confocal microscopy. If such microdomains are recruited, but they do not fuse with each other, the FRET efficiency reporting molecular proximities will not change. c) Increased molecular association of raft markers indicated by increased FRET. Although currently it is not possible to conclude what happens in the immunological synapse in terms of raft recruitment, one can envisage that diminishingly small rafts are recruited into the immunological synapse. Depending on how close the microdomains get to each other and whether they fuse with each other, FRET between raft markers will either increase or not.

By following the time-dependent decay of anisotropy, even more sensitive detection of clustering is possible (133). Combining steady-state and time-dependent homo- and hetero-FRET experiments, Sharma et al. provide conclusive evidence that GPI-anchored proteins, albeit a small fraction thereof, are indeed concentrated in clusters composed of at most four proteins with the rest of the GPI-anchored molecules being randomly dispersed in the membrane. They showed that different types of GPI-anchored proteins float in the same rafts and crosslinking induces raft reorganization by segregating the crosslinked species from preexisting clusters (134). This latter observation is in apparent contradiction with the results of Harder et al., who reported comigration of noncrosslinked raft markers with the crosslinked raft-associated protein (40). However, one has to make note of the different scales of the two measurements: segregation of the crosslinked species was observed with FRET measurements, whereas comigration was seen in confocal microscopic experiments.

FRET measurements have proved valuable in bridging the gap between the submicron resolution of conventional microscopy and the world of single molecular interactions driving signal transduction in living cells and provided evidence for the existence of diminishingly small raft microdomains floating among the majority of unclustered molecules, randomly distributed in the membrane. Such preexisting rafts are recruited to larger associations upon crosslinking to form the signaling platforms corresponding to clusters seen in confocal microscopy. However, both the small and the large rafts are detergent-resistant indicating the indispensible nature of FRET measurements to elucidate the dynamic processes taking place in lipid rafts (134–136).

Besides the distribution of GPI-anchored proteins, the target of the investigations described earlier, FRET has been used to study the size of lipid microdomains in binary (phosphatidylcholine/cholesterol) and ternary (phosphatidylcholine/sphingomyelin/cholesterol) protein-free large unilamellar vesicles (LUV) (137). Model calculations were performed to find the size of lipid rafts, with which the theoretical curves fit the time-resolved FRET measurements. It is worth noting that lipid rafts exist in the phase coexistence region, where liquid-ordered and -disordered phases are mixed. It has been shown that by increasing the fraction of the liquid-ordered phase in the phase coexistence region by increasing the molar fraction of cholesterol or sphingomyelin, the size of rafts increased. GM1 ganglioside and CTX-B increased the size of lipid rafts in accordance with confocal microscopic results (40,42).

The acceptor concentration dependence of hetero-FRET has been used to demonstrate that acyl chain-modified GFP derivatives are concentrated in clusters probably corresponding to inner leaflet rafts, but prenyl modification was insufficient to induce clustering (138). Inner leaflet rafts serve as signaling platforms for Ras proteins. Single-molecule FRET imaging was used to follow the binding of Bodipy-TR-GTP (acceptor) to YFP-Ras (donor). Binding coincided with an increase in the immobile fraction of Ras corresponding to the formation of large aggregates serving as signaling platforms (139).

FRET can be used for the detection of alterations in transmembrane-signaling complexes in diseases. CD14, the GPI-anchored membrane receptor of lipopolysaccharide and other lipids, has been shown to recruit a signaling complex with distinct composition depending on the stimulating lipid molecule (140). It was concluded that clustering of CD14 may reflect the condition of monocytes, and it has a potential as a diagnostic marker in sepsis and atherosclerosis (22).

Rafts not only harbor peripheral, but also transmembrane proteins. A representative of raft-associated transmembrane proteins is ErbB2, a member of the epidermal growth factor receptor family (141). We have shown using microscopic hetero-FRET measurements that the homoassociation of ErbB2 is proportional to the local density of ErbB2, inversely correlated with the local density of ErbB3 and of the raft-specific lipid, GM1 (42). These results implied that local densities of ErbB2

and ErbB3, as well as the lipid environment profoundly influence the association properties and biological function of ErbB2. We have also studied the dynamics of raft-associated membrane protein clusters by measuring the kinetics of protein exchange between clusters (142). We labeled one-cell sample with donor-tagged antibody, the other with acceptor-tagged antibody against the same protein and recorded the appearance of FRET after fusing the donor- and acceptor-labeled cells. FRET reappeared in the case of several raft-associated peripheral (CD48) and transmembrane proteins (IL2Rα, MHC-I) after cell fusion indicating that these protein clusters are dynamic and exchange partners with each other. We found a notable exception to the rule, MHC-II, which did not allow the development of FRET after cell fusion implying that MHC-II molecular associations are static. We also followed the intermingling of donor- and acceptor-tagged clusters with confocal microscopy. These experiments showed that large-scale protein clusters visualized by confocal microscopy exchange components with the same type of clusters.

High throughput Screening (HTS) Assays of Rafts: Towards Systems Biology

For isolation of lipid rafts, widely accepted methods are available based on cold nonionic detergent- (or high pH-) extraction of DRMs combined with sucrose gradient ultracentrifugation (SGUC). After separation of these microdomains, the protein and lipid composition can be analyzed by different methods. Traditionally, proteins have been studied with conventional protein analysis techniques (e.g., SDS-PAGE and immunoblot analysis), where qualitative evaluation is limited for only a few proteins at a time. For lipids, the classical extraction is possible by using organic solvents, such as methanol-chloroform or hexane-isopropanol (143–145). Lots of modified versions of this method were reported in the literature. Nevertheless, no standard method for lipid extraction from biological samples has been established. Therefore, results between research groups may vary, and this should be taken into consideration.

The next step is lipid class separation, generally relying on analysis by thin-layer chromatography (TLC), which is however, not as sensitive as other methods. It offers a rapid and comprehensive screening tool before more sensitive and sophisticated techniques. High-performance liquid chromatography (HPLC) and gas chromatography are also well-assumed techniques, requiring optional prior derivatization and availability of known standards. These conventional approaches are, however, time-consuming and require relatively large sample volumes for accurate separation (146–148).

By visualization, analysis, and identification of lipid raft components by flow and image cytometry (i.e., fluorescence and electron microscopies), Western-blot analysis, etc., the conception emerged that cholesterol-rich microdomains are dynamic and heterogeneous structures in the membrane of eukaryotic cells (96,149–151). This heterogeneity in the protein and lipid content as well depends on the type and developmental stage of a cell and also on the different stimuli it is exposed to. Systems biology, an iterative application of biological knowledge with mathematical and computational techniques, seems to be a new field to study complexity of biological systems, including physiological role of heterogeneous lipid rafts in cell communication and signaling networks. It is well accepted that two main criteria can be defined for systems biology: (i) quantitative measures, multiple components of a cell simultaneously and (ii) rigorous data integration with mathematical models. The models, once developed and validated, can be used to study a vastly greater range of situations and interventions than would be possible by applying classical reductionist experimental methods that usually involve changes only in a small number of variables.

Here, we focus on two main subsets of analysis of lipid raft composition and its changes, namely proteomics and lipidomics. Using 2D-gel electrophoresis, a large number of proteins could be separated and visualized by staining with Coomassie blue, silver, or fluorescent stains, as well as autoradiography, if the proteins have been labeled before sample collection. Identification of proteins is possible by excision of spots and digestion with trypsin followed by mass spectrometry (MS). However, the problem with this approach is that many proteins are excluded by their size (too small or too large) or by their solubility/hydrophobicity, such as lot of membrane proteins. To avoid gel-electrophoretic separation, HPLC seems to be a sufficient tool to purify protein fragments following in-solution digestion approach (152).

To improve precision of the quantitative proteome analysis by liquid chromatography tandem spectrometry (LC-MS/MS), the proven technique of stable-isotope dilution has been applied. This method makes use of the facts that pairs of chemically identical analytes of different stable-isotope composition can be differentiated in a mass spectrometer owing to their mass difference and that the ratio of signal intensities for such analyte pairs accurately indicates the abundance ratio for the two analytes. To this end, stable-isotope tags have been introduced to proteins via transfer of ^{18}O by enzymes from water to peptides (153,154), via chemical reactions using isotope-coded affinity tags (ICAT) (155), or via metabolic labeling using heavy salts or amino acids (156). The recently developed ICAT technology is a quantitative proteomic approach to evaluate changes occurring in lipid rafts (157–159). ICAT reagents consist of three functional elements: a thiol-reactive group for the selective labeling of reduced Cys residues, a biotin affinity tag to allow for selective isolation of labeled peptides, and a linker synthesized either in an isotopically normal ("light") or a "heavy" form (utilizing 2H or 13C) that allows for the incorporation of the stable isotope tags. In a typical experiment, protein disulfide bridges are reduced under denaturing conditions, and the free sulfydryl groups of the proteins from the two related samples to be compared are labeled respectively with the isotopically "light" or "heavy" forms of the reagent. However, ICAT allows the use of protein material from nonliving sources but requires chemical modification and affinity steps (ion exchange and affinity chromatography). For the complex lipid raft proteomic analysis by liquid chromatography electrospray ionization tandem mass spectrometry (LC-ESI-MS/MS) of anti-IgM stimulated and control

human Ramos cell line or splenic cells of Balb/c mice, Gupta et al. has adopted this procedure (157). They compiled a list of some of the proteins that were identified in lipid rafts and grouped these into functional categories. The list includes cytoskeletal proteins, transmembrane receptors, cell surface glycoproteins, Src family kinases, small G proteins, heterotrimeric G proteins, motor proteins, and trafficking proteins. Besides the B-cell receptor (BCR), the other proteins that showed altered localization to lipid rafts upon stimuli were all related to the cytoskeleton, including the nonmuscle myosin type 2A and myosin regulatory light chain, enriched in rafts. In contrast, ezrin, a linker protein between membrane proteins and actin filaments was dissociated from rafts after BCR engagement. As it has been suggested earlier that aggregation of lipid rafts may be controlled by cytoskeletal remodeling, all of these proteins are likely candidates to be involved in this process.

Another isotope-labeling, convenient, and inexpensive method is SILAC (stable isotope labeling by amino acids in cell culture). Labeled, essential amino acids are added to amino acid deficient cell-culture media and are therefore incorporated into all proteins as they are synthesized, "encoded into the proteome." No chemical labeling or affinity purification steps are performed, and the method is compatible with virtually all cell culture conditions, including primary cells (37,160,161). Foster et al. has applied this method to study the lipid raft proteome of HeLa cells. They used two raft isolation schemes (based on detergent and pH/carbonate resistance, respectively) and three cholesterol-disrupting drugs (nystatin, filipin and MBCD) followed by LS-MS/MS, for quantitative proteomic analysis, and found that nystatin and filipin were less efficient in depleting proteins in detergent-resistant fractions than MBCD. In the MBCD experiments, 241 proteins were identified as raft proteins, the majority of which were signaling proteins, but a number of structural proteins were found as well (37).

For high-throughput screening of lipids from any biological source with high sensitivity, ESI-MS and matrix-assisted laser desorption/ionization-time of flight (MALDI-TOF) mass spectrometry methods have been developed (162). A novel approach to the computational analysis of global pattern changes in membrane lipid composition is the lipid array technology, when MS outputs are in an arrayed organization. The goal of this analysis is the rapid, objective identification of statistically significant differences in mass spectra between two biological conditions (163). The strategic scheme of different HTS methods based on chromatographic separation and MS analysis are summarized on Figure 4.

Microarray techniques are widely used in genomics (DNA-chips and -arrays) and proteomics; however, lipid microarrays are still under ongoing development and awaiting for reaching a reasonable level of sensitivity and reproducibility. Lipid microarrays fall into the category of protein detecting microarrays (PMDs). Current PMD technologies, including proteomic arrays, microspot ELISA and antibody arrays, reverse arrays, and single capture antibody arrays, were currently reviewed (164). However, probing the interaction of

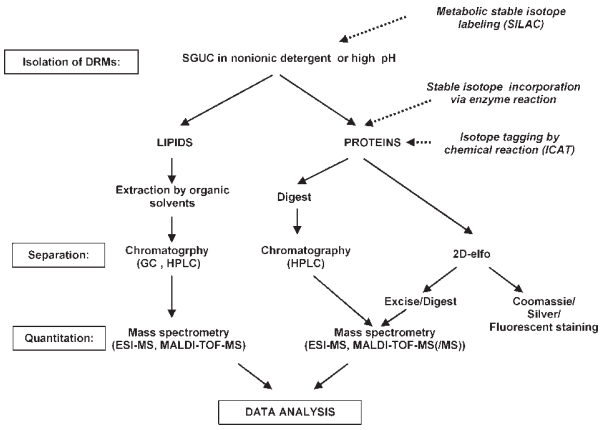

Figure 4. Strategic scheme of high-throughput assay of lipid raft composition. Widely used proteome and lipidome analysis methodologies are based on high-performance chromatographic separation of the molecular components of membrane microdomain fractions followed by mass spectrometric (MS) analysis. From the ionized molecular fragment spectra detected by MS, the protein or lipid molecules can be identified using software data bases. For proteins, 2D-gelelectrophoretic separation (2DIGE) with differential fluorescent staining is also widely used. To improve the precision of the quantitative proteome analysis, stable-isotope protein-labeling methods (broken line) can be inserted into the protocol.

a lipid aggregate structure with their protein targets in a high-throughput fashion would not be addressed by the current generation of lipid microarrays. Lipids complexed with protein and sugars and other lipid structures, such as lipid vesicles and lipid rafts, are beyond the capacity of current microarray technologies (165).

For study, the compositional heterogeneity of rafts, a novel approach, raft-ELISA, has also been developed (166). George et al. have designed a cell-free assay (sandwich ELISA) that provides a simple and quick way to examine the simultaneous presence of two proteins in the lipid rafts and has the potential to estimate trafficking of molecules in and out of the lipid microdomains during cell signaling on a single detergent-resistant lipid raft basis. Extrapolating from these limited studies, we expect that combining different proteomic and lipidomic results obtained from the same biological system will substantially increase our understanding of complex biological processes, including the complexity and heterogeneity of lipid raft microdomains. More specifically, the systems biology studies based on diverse and high-quality proteomic data will define functional biological modules reveal previously unrecognized connections between biochemical processes and modules and may also help in modeling the interacting protein networks (i.e., to identify the cellular protein "interactomes").

Developments in this area may lead to new hypotheses that can be tested either by traditional methods or by the new generations of proteomic and lipidomic technologies.

There are several attempts to combine classical cytometric methods (e.g., flow cytometry, slide-based cytometry, and

Table 1. Methods for analysis of properties and composition of lipid rafts

METHOD	ADVANTAGES	LIMITATIONS	APPLICATIONS	REFS.
Flow cytometry (FCDR)	Rapid, low cell consumption (10^5/sample), intact cells, low ($\leq$0.1%) detergent concentration, artifacts minimized, cause of detergent resistance can be revealed, good statistics	Small scale (limited by optical channel number in the flow cytometer), assay conditions may vary with cell type	T and B lymphocytes, various tumor cells, monocytes, hepatoblastoma, erythroleukemic cells	16, 85–87, 89, 90, 92–95
– HyperCyt (high-throughput flow cytometry)	Combination of cell sorting with HTS of multiparameter cell analysis, automatized sample handling, rapid	Perspectivic, but needs adaptation/ development to lipid raft analysis		167–169
Image cytometry (2 photon, confocal fluorescence microscopy)	Nearly physiological conditions, location visualized, colocalization by FRET is possible	Small scale (max. 4 molecules at a time), weak statistics, labeling may occasionally cause microaggregation	T and B lymphocytes, monocytes, macrophages, tumor cells, mast cells, muscle cells	66–68, 98–106, 108, 109, 117, 118, 128, 130,133–137, 139, 140, 142
– Hyperchromatic slide based cytometry (LSC)	Iterative restaining, multiplication of the investigated parameters, high content cell analysis, single cell level also available	Perspectivic, but needs adaptation/ development to lipid raft analysis		170–172
Classical immuno-biochemical detection	Direct immunocytochemical detection from isolated membrane microdomain fractions	Small scale, highly cell consuming ($\sim10^8$ cells for raft isolation), possible artifacts: low temperature, high detergent concentration; time consuming	T and B lymphocytes, epithel cells, MDCK cells, vascular system, neurons	2, 16, 22, 24, 25, 26–29, 31, 32, 34, 46, 68
HTS assays – Classical raft proteomics: membrane fractionation, protein separation, protein identification – Microchip array of raft proteome	Large scale (thousands of proteins or lipids at a time), good statistics, altered protein composition rapidly detectable (in diseases), proteins with altered raft localization can be identified (with MS): "protein interactome" building	Usually needs isolated membrane raft fractions, highly cell-consuming	T cells, B cells, muscle cells, neurons, synaptosomes, neutrophil granulocytes	152–160, 162–165, 166

fluorescence microscopy) with proteomics or genomics. One is combination of cell sorting with rapid protein-profiling platforms (mass spectrometric analysis) that can offer an automated and rapid technique for greater clarity, accuracy, and efficiency in identification of protein expression differences in mixed cell populations (167). Another concept is to increase throughput and content of the above-mentioned fluorescence-based multiparametric methods. This can be executed by automatization of sample loading, handling acquisition, and analysis. HyperCyt® interfaces a flow cytometer and autosampler (168) and with this, up to 14 optical parameters can be collected simultaneously from billions of cells in less than 3 min. For example, in a multiparameter lymphocyte immunophenotyping microassay at analysis rates of 1.5 s/sample was reached in a 96-well plate, and results were comparable to manual analysis (169). Another way to combine cytomics and systemic approach is hyperchromatic slide-based cytometry (170). Mittag et al. traversed how hyperchromatic cytometry can increase the amount of analyzed antigens, and this way making possible a high content and high-throughput single-cell analysis of slide-touched samples. Mixing of iterative restaining and differential photobleaching, photoactivation, photodestruction, photoconversion, or photocaging using respective fluoprophores provides facilities to measure up to 100 antigens. High-throughput screening with fluorescence microscopy is an enormous challenge for engineers and researchers (171,172). To get more and more data from cells in a very short time, by decreasing the screening time with multibeam imaging, automatized sample handling using multiwell plates and autofocusing and autoscreening mode are required. The time limitation of microscopy is, however, moving from one cell to another that requires the movement of the stage relative to optical axis, either by stage or beam scanning. Flow cytometry, with its other advantage of the ease of sample handling, is about 100 times faster than imaging cytometry, so incorporating special optical/electrical capturing devices (e.g., optofluidic microscopy or a cell rotator) into the flow cytometer seems to be a good solution for increasing the throughput of imaging. Such novel strategies provide possibility to immobilize cells in flow and this way taking snapshot images (171). Nevertheless, the synthesis of these techniques are not yet adopted to investigate the nature of lipid rafts, so as a great goal in the future it can open up a new area for proteomic or even lipidomic analysis of rafts.

Conclusions and Perspectives

As discussed throughout this review, the classical cytoanalytical methods, such as flow cytometry and the different forms of image cytometry, lead to a continuous and significant clarification of our view on the complex structure of biological membranes, particularly, the structure and function of raft and caveola microdomains (Table 1). We learned that these microdomains are small (several tens of nanometers diameter) and highly dynamic molecular assemblies in the plasma membranes, where signaling processes often lead to their aggregation forming larger (sometimes 0.5-1 micrometer diameter) and more stable signal platforms. Many questions about their compositional heterogeneity, lifetime, etc., however, still remained controversial. Introduction of new probes and techniques, such as Laurdan derivatives for 2-photon microscopic imaging, anticholesterol and antiphosphatidylinositol bisphosphate (PIP2) antibody probes (conjugated with fluorescent dyes or quantum dots) may reveal new faces of these microdomains. The novel fluorescence imaging technique with highly improved resolution, stimulated emission depletion (STED) microscopy, resulting in 20-30-nm lateral resolution, may also contribute to such progress. The future trend is, however, clearly the system biology approach, including high-throughput screening assays of raft composition. Here, automatization and optical developments on classical cell analytical techniques (e.g., flow cytometry or slide-based laser scanning microscopy) may also result in a new milestone. In addition, such analyses may be coupled to system biology modeling approaches and can reveal altered raft composition and "protein interactome" in diseases.

Literature Cited

1. Simons K, Ikonen E. Functional rafts in cell membranes. Nature 1997;387:569–572.
2. Brown DA, Rose JK. Sorting of GPI-anchored proteins to glycolipid-enriched membrane subdomains during transport to the apical cell surface. Cell 1992;68:533–544.
3. Parton RG. Caveolae and caveolins. Curr Opin Cell Biol 1996;8:542–548.
4. Luna EJ, Nebl T, Takizawa N, Crowley JL. Lipid raft membrane skeletons. In: Mattson MP, editor. Membrane Microdomain Signaling. Lipid Rafts in Biology and Medicine. Totowa, NJ: Humana Press; 2005. pp 47–71.
5. Edidin M. The state of lipid rafts: From model membranes to cells. Annu Rev Biophys Biomol Struct 2003;32:257–283.
6. Kusumi A, Ike H, Nakada C, Murase K, Fujiwara T. Single-molecule tracking of membrane molecules: Plasma membrane compartmentalization and dynamic assembly of raft-philic signaling molecules. Semin Immunol 2005;17:3–21.
7. Pike LJ. Lipid rafts: Bringing order to chaos. J Lipid Res 2003;44:655–667.
8. Matko J, Szollosi J. Regulatory aspects of membrane microdomain (raft) dynamics in live cells. In: Mattson MP, editor. Membrane Microdomain Signaling. Lipid Rafts in Biology and Medicine. Totowa, NJ: Humana Press; 2005. pp 15–46.
9. Pike LJ. Rafts defined: A report on the keystone symposium on lipid rafts and cell function. J Lipid Res 2006;47:1597–1598.
10. Mattson M, editor. Membrane microdomain signaling: Lipid rafts in biology and medicine. Totowa, NJ: Humana Press; 2005.
11. Parton RG, Simons K. The multiple faces of caveolae. Nat Rev Mol Cell Biol 2007;8:185–194.
12. Harris J, Werling D, Hope JC, Taylor G, Howard CJ. Caveolae and caveolin in immune cells: Distribution and functions. Trends Immunol 2002;23:158–164.
13. Matko J, Szollosi J. Landing of immune receptors and signal proteins on lipid rafts: A safe way to be spatio-temporally coordinated? Immunol Lett 2002;82:3–15.
14. Pierce SK. Lipid rafts and B-cell activation. Nat Rev Immunol 2002;2:96–105.
15. Simons K, Toomre D. Lipid rafts and signal transduction. Nat Rev Mol Cell Biol 2000;1:31–39.
16. Gombos I, Detre C, Vamosi G, Matko J. Rafting MHC-II domains in the APC (presynaptic) plasma membrane and the thresholds for T-cell activation and immunological synapse formation. Immunol Lett 2004;92:117–124.
17. Gombos I, Kiss E, Detre C, Laszlo G, Matko J. Cholesterol and sphingolipids as lipid organizers of the immune cells' plasma membrane: Their impact on the functions of MHC molecules, effector T-lymphocytes and T-cell death. Immunol Lett 2006;104:59–69.
18. Rosenberger CM, Brumell JH, Finlay BB. Microbial pathogenesis: Lipid rafts as pathogen portals. Curr Biol 2000;10:R823–R825.
19. Grassme H, Jekle A, Riehle A, Schwarz H, Berger J, Sandhoff K, Kolesnick R, Gulbins E. CD95 signaling via ceramide-rich membrane rafts. J Biol Chem 2001;276:20589–20596.
20. Tansey MG, Baloh RH, Milbrandt J, Johnson EM Jr. GFRalpha-mediated localization of RET to lipid rafts is required for effective downstream signaling, differentiation, and neuronal survival. Neuron 2000;25:611–623.
21. Barlage S, Boettcher D, Boettcher A, Dada A, Schmitz G. High density lipoprotein modulates platelet function. Cytometry Part A 2006;69A:196–199.
22. Grandl M, Bared SM, Liebisch G, Werner T, Barlage S, Schmitz G. E-LDL and Ox-LDL differentially regulate ceramide and cholesterol raft microdomains in human macrophages. Cytometry Part A 2006;69A:189–191.
23. Orso E, Werner T, Wolf Z, Bandulik S, Kramer W, Schmitz G. Ezetimib influences the expression of raft-associated antigens in human monocytes. Cytometry Part A 2006;69A:206–208.

24. Callera GE, Montezano AC, Yogi A, Tostes RC, Touyz RM. Vascular signaling through cholesterol-rich domains: Implications in hypertension. Curr Opin Nephrol Hypertens 2007;16:90–104.
25. Ma DW. Lipid mediators in membrane rafts are important determinants of human health and disease. Appl Physiol Nutr Metab 2007;32:341–350.
26. Jury EC, Flores-Borja F, Kabouridis PS. Lipid rafts in T cell signalling and disease. Semin Cell Dev Biol 2007;18:608–615.
27. Sillence DJ. New insights into glycosphingolipid functions–storage, lipid rafts, and translocators. Int Rev Cytol 2007;262:151–189.
28. Benarroch EE. Lipid rafts, protein scaffolds, and neurologic disease. Neurology 2007;69:1635–1639.
29. Taylor DR, Hooper NM. Role of lipid rafts in the processing of the pathogenic prion and Alzheimer's amyloid-beta proteins. Semin Cell Dev Biol 2007;18:638–648.
30. Brown DA, London E. Structure and function of sphingolipid- and cholesterol-rich membrane rafts. J Biol Chem 2000;275:17221–17224.
31. Ilangumaran S, Arni S, van Echten-Deckert G, Borisch B, Hoessli DC. Microdomain-dependent regulation of Lck and Fyn protein-tyrosine kinases in T lymphocyte plasma membranes. Mol Biol Cell 1999;10:891–905.
32. London E, Brown DA. Insolubility of lipids in triton X-100: Physical origin and relationship to sphingolipid/cholesterol membrane domains (rafts). Biochim Biophys Acta 2000;1508:182–195.
33. Simons K, Vaz WL. Model systems, lipid rafts, and cell membranes. Annu Rev Biophys Biomol Struct 2004;33:269–295.
34. Schuck S, Honsho M, Ekroos K, Shevchenko A, Simons K. Resistance of cell membranes to different detergents. Proc Natl Acad Sci USA 2003;100:5795–5800.
35. Ahmed SN, Brown DA, London E. On the origin of sphingolipid/cholesterol-rich detergent-insoluble cell membranes: Physiological concentrations of cholesterol and sphingolipid induce formation of a detergent-insoluble, liquid-ordered lipid phase in model membranes. Biochemistry 1997;36:10944–10953.
36. Song KS, Li S, Okamoto T, Quilliam LA, Sargiacomo M, Lisanti MP. Co-purification and direct interaction of Ras with caveolin, an integral membrane protein of caveolae microdomains. Detergent-free purification of caveolae microdomains. J Biol Chem 1996;271:9690–9697.
37. Foster LJ, De Hoog CL, Mann M. Unbiased quantitative proteomics of lipid rafts reveals high specificity for signaling factors. Proc Natl Acad Sci USA 2003;100:5813–5818.
38. Smart EJ, Ying YS, Mineo C, Anderson RG. A detergent-free method for purifying caveolae membrane from tissue culture cells. Proc Natl Acad Sci USA 1995;92:10104–10108.
39. Macdonald JL, Pike LJ. A simplified method for the preparation of detergent-free lipid rafts. J Lipid Res 2005;46:1061–1067.
40. Harder T, Scheiffele P, Verkade P, Simons K. Lipid domain structure of the plasma membrane revealed by patching of membrane components. J Cell Biol 1998;141:929–942.
41. Kusumi A, Suzuki K. Toward understanding the dynamics of membrane-raft-based molecular interactions. Biochim Biophys Acta 2005;1746:234–251.
42. Nagy P, Vereb G, Sebestyén Z, Horváth G, Lockett SJ, Damjanovich S, Park JW, Jovin TM, Szöllösi J Lipid rafts and the local density of ErbB proteins influence the biological role of homo- and heteroassociations of ErbB2. J Cell Sci 2002;115:4251–4262.
43. Yanagisawa M, Ariga T, Yu RK. Cholera toxin B subunit binding does not correlate with GM1 expression: A study using mouse embryonic neural precursor cells. Glycobiology 2006;16:19G–22G.
44. Blank N, Gabler C, Schiller M, Kriegel M, Kalden JR, Lorenz HM. A fast, simple and sensitive method for the detection and quantification of detergent-resistant membranes. J Immunol Methods 2002;271:25–35.
45. Sheriff A, Gaipl US, Franz S, Heyder P, Voll RE, Kalden JR, Herrmann M. Loss of GM1 surface expression precedes annexin V-phycoerythrin binding of neutrophils undergoing spontaneous apoptosis during in vitro aging. Cytometry Part A 2004;62A:75–80.
46. Janes PW, Ley SC, Magee AI. Aggregation of lipid rafts accompanies signaling via the T cell antigen receptor. J Cell Biol 1999;147:447–461.
47. Johnston LJ. Nanoscale imaging of domains in supported lipid membranes. Langmuir 2007;23:5886–5895.
48. Baumgart T, Hess ST, Webb WW. Imaging coexisting fluid domains in biomembrane models coupling curvature and line tension. Nature 2003;425:821–824.
49. Dietrich C, Bagatolli LA, Volovyk ZN, Thompson NL, Levi M, Jacobson K, Gratton E. Lipid rafts reconstituted in model membranes. Biophys J 2001;80:1417–1428.
50. Schutz GJ, Kada G, Pastushenko VP, Schindler H. Properties of lipid microdomains in a muscle cell membrane visualized by single molecule microscopy. EMBO J 2000;19:892–901.
51. Kahya N, Scherfeld D, Bacia K, Poolman B, Schwille P. Probing lipid mobility of raft-exhibiting model membranes by fluorescence correlation spectroscopy. J Biol Chem 2003;278:28109–28115.
52. Scherfeld D, Kahya N, Schwille P. Lipid dynamics and domain formation in model membranes composed of ternary mixtures of unsaturated and saturated phosphatidylcholines and cholesterol. Biophys J 2003;85:3758–3768.
53. Davey AM, Walvick RP, Liu Y, Heikal AA, Sheets ED. Membrane order and molecular dynamics associated with IgE receptor cross-linking in mast cells. Biophys J 2007;92:343–355.
54. Korlach J, Schwille P, Webb WW, Feigenson GW. Characterization of lipid bilayer phases by confocal microscopy and fluorescence correlation spectroscopy. Proc Natl Acad Sci USA 1999;96:8461–8466.
55. Bacia K, Scherfeld D, Kahya N, Schwille P. Fluorescence correlation spectroscopy relates rafts in model and native membranes. Biophys J 2004;87:1034–1043.
56. Gombos I, Steinbach G, Pomozi I, Balogh A, Vamosi G, Gansen A, Laszlo G, Garab G, Matko J. Some new faces of membrane microdomains: A complex confocal fluorescence, differential polarization, and FCS imaging study on live immune cells. Cytometry Part A 2008;73A:220–229.
57. Bagatolli LA, Gratton E. Two-photon fluorescence microscopy observation of shape changes at the phase transition in phospholipid giant unilamellar vesicles. Biophys J 1999;77:2090–2101.
58. Gaus K, Zech T, Harder T. Visualizing membrane microdomains by Laurdan 2-photon microscopy. Mol Membr Biol 2006;23:41–48.
59. Gaus K, Gratton E, Kable EP, Jones AS, Gelissen I, Kritharides L, Jessup W. Visualizing lipid structure and raft domains in living cells with two-photon microscopy. Proc Natl Acad Sci USA 2003;100:15554–15559.
60. Kim HM, Choo HJ, Jung SY, Ko YG, Park WH, Jeon SJ, Kim CH, Joo T, Cho BR. A two-photon fluorescent probe for lipid raft imaging: C-laurdan. Chembiochem 2007;8:553–559.
61. Bíró A, Cervenak L, Balogh A, Lőrincz A, Uray K, Horváth A, Romics L, Matkó J, Füst G, László G. Novel anti-cholesterol monoclonal immunoglobulin G antibodies as probes and potential modulators of membrane raft-dependent immune functions. J Lipid Res 2007;48:19–29.
62. Kahya N, Brown DA, Schwille P. Raft partitioning and dynamic behavior of human placental alkaline phosphatase in giant unilamellar vesicles. Biochem 2005;44:7479–74789.
63. Kenworthy AK, Petranova N, Edidin M. High-resolution FRET microscopy of cholera toxin B-subunit and GPI-anchored proteins in cell plasma membranes. Mol Biol Cell 2000;11:1645–1655.
64. Matko J, Bodnar A, Vereb G, Bene L, Vamosi G, Szentesi G, Szollosi J, Gaspar R, Horejsi V, Waldmann TA, Damjanovich S. GPI-microdomains (membrane rafts) and signaling of the multi-chain interleukin-2 receptor in human lymphoma/leukemia T cell lines. Eur J Biochem 2002;269:1199–1208.
65. Saslowsky DE, Lawrence J, Ren X, Brown DA, Henderson RM, Edwardson JM. Placental alkaline phosphatase is efficiently targeted to rafts in supported lipid bilayers. J Biol Chem 2002;277:26966–26970.
66. Vereb G, Matko J, Vamosi G, Ibrahim SM, Magyar E, Varga S, Szollosi J, Jenei A, Gaspar R Jr, Waldmann TA, Damjanovich S. Cholesterol-dependent clustering of IL-2Ralpha and its colocalization with HLA and CD48 on T lymphoma cells suggest their functional association with lipid rafts. Proc Natl Acad Sci USA 2000;97:6013–6018.
67. Drbal K, Moertelmaier M, Holzhauser C, Muhammad A, Fuertbauer E, Howorka S, Hinterberger M, Stockinger H, Schutz GJ. Single-molecule microscopy reveals heterogeneous dynamics of lipid raft components upon TCR engagement. Int Immunol 2007;19:675–684.
68. Legembre P, Daburon S, Moreau P, Moreau JF, Taupin JL. Modulation of Fas-mediated apoptosis by lipid rafts in T lymphocytes. J Immunol 2006;176:716–720.
69. Scheiffele P, Roth MG, Simons K. Interaction of influenza virus haemagglutinin with sphingolipid-cholesterol membrane domains via its transmembrane domain. EMBO J 1997;16:5501–5508.
70. Shakor AB, Czurylo EA, Sobota A. Lysenin, a unique sphingomyelin-binding protein. FEBS Lett 2003;542:1–6.
71. Yamaji A, Sekizawa Y, Emoto K, Sakuraba H, Inoue K, Kobayashi H, Umeda M. Lysenin, a novel sphingomyelin-specific binding protein. J Biol Chem 1998;273:5300–5306.
72. Ishitsuka R, Sato SB, Kobayashi T. Imaging lipid rafts. J Biochem 2005;137:249–254.
73. Ishitsuka R, Yamaji-Hasegawa A, Makino A, Hirabayashi Y, Kobayashi T. A lipid-specific toxin reveals heterogeneity of sphingomyelin-containing membranes. Biophys J 2004;86:296–307.
74. Kiyokawa E, Makino A, Ishii K, Otsuka N, Yamaji-Hasegawa A, Kobayashi T. Recognition of sphingomyelin by lysenin and lysenin-related proteins. Biochem 2004;43:9766–9773.
75. Yamaji-Hasegawa A, Makino A, Baba T, Senoh Y, Kimura-Suda H, Sato SB, Terada N, Ohno S, Kiyokawa E, Umeda M, Kobayashi T. Oligomerization and pore formation of a sphingomyelin-specific toxin, lysenin. J Biol Chem 2003;278:22762–22770.
76. Kiyokawa E, Baba T, Otsuka N, Makino A, Ohno S, Kobayashi T. Spatial and functional heterogeneity of sphingolipid-rich membrane domains. J Biol Chem 2005;280:24072–24084.
77. Kruth HS, Ifrim I, Chang J, Addadi L, Perl-Treves D, Zhang WY. Monoclonal antibody detection of plasma membrane cholesterol microdomains responsive to cholesterol trafficking. J Lipid Res 2001;42:1492–1500.
78. Ohno-Iwashita Y, Shimada Y, Waheed AA, Hayashi M, Inomata M, Nakamura M, Maruya M, Iwashita S. Perfringolysin O, a cholesterol-binding cytolysin, as a probe for lipid rafts. Anaerobe 2004;10:125–134.
79. Waheed AA, Shimada Y, Heijnen HF, Nakamura M, Inomata M, Hayashi M, Iwashita S, Slot JW, Ohno-Iwashita Y. Selective binding of perfringolysin O derivative to cholesterol-rich membrane microdomains (rafts). Proc Natl Acad Sci USA 2001;98:4926–4931.
80. Gimpl G, Gehrig-Burger K. Cholesterol reporter molecules. Biosci Rep 2007;27:335–358.
81. Gri G, Molon B, Manes S, Pozzan T, Viola A. The inner side of T cell lipid rafts. Immunol Lett 2004;94:247–252.
82. Hayashi M, Shimada Y, Inomata M, Ohno-Iwashita Y. Detection of cholesterol-rich microdomains in the inner leaflet of the plasma membrane. Biochem Biophys Res Commun 2006;351:713–718.
83. Pike LJ, Han X, Gross RW. Epidermal growth factor receptors are localized to lipid rafts that contain a balance of inner and outer leaflet lipids: A shotgun lipidomics study. J Biol Chem 2005;280:26796–26804.

84. Albrecht DL, Noelle RJ. Membrane Ig-cytoskeletal interactions. I. Flow cytofluorometric and biochemical analysis of membrane IgM-cytoskeletal interactions. J Immunol 1988;141:3915–3922.
85. Filatov AV, Shmigol IB, Sharonov GV, Feofanov AV, Volkov Y. Direct and indirect antibody-induced TX-100 resistance of cell surface antigens. Immunol Lett 2003;85:287–295.
86. Geppert TD, Lipsky PE. Association of various T cell-surface molecules with the cytoskeleton. Effect of cross-linking and activation. J Immunol 1991;146:3298–3305.
87. Chia CP, Khrebtukova I, McCluskey J, Wade WF. MHC class II molecules that lack cytoplasmic domains are associated with the cytoskeleton. J Immunol 1994;153:3398–3407.
88. Nebe B, Bohn W, Pommerenke H, Rychly J. Flow cytometric detection of the association between cell surface receptors and the cytoskeleton. Cytometry 1997;28:66–73.
89. Bacso Z, Nagy H, Goda K, Bene L, Fenyvesi F, Matko J, Szabo G. Raft and cytoskeleton associations of an ABC transporter: P-glycoprotein. Cytometry Part A 2004;61A:105–116.
90. Gombos I, Bacso Z, Detre C, Nagy H, Goda K, Andrasfalvy M, Szabo G, Matko J. Cholesterol sensitivity of detergent resistance: A rapid flow cytometric test for detecting constitutive or induced raft association of membrane proteins. Cytometry Part A 2004;61A:117–126.
91. Ilangumaran S, Hoessli DC. Effects of cholesterol depletion by cyclodextrin on the sphingolipid microdomains of the plasma membrane. Biochem J 1998;335:433–440.
92. Filatov AV, Shmigol IB, Kuzin II, Sharonov GV, Feofanov AV. Resistance of cellular membrane antigens to solubilization with Triton X-100 as a marker of their association with lipid rafts–analysis by flow cytometry. J Immunol Methods 2003;278:211–219.
93. Calzolari A, Raggi C, Deaglio S, Sposi NM, Stafsnes M, Fecchi K, Parolini I, Malavasi F, Peschle C, Sargiacomo M, Testa U. TfR2 localizes in lipid raft domains and is released in exosomes to activate signal transduction along the MAPK pathway. J Cell Sci 2006;119:4486–4498.
94. Wolf Z, Orso E, Werner T, Boettcher A, Schmitz G. A flow cytometric screening test for detergent-resistant surface antigens in monocytes. Cytometry Part A 2006;69A:192–195.
95. Wolf Z, Orso E, Werner T, Klunemann HH, Schmitz G. Monocyte cholesterol homeostasis correlates with the presence of detergent resistant membrane microdomains. Cytometry Part A 2007;71A:486–494.
96. Pike LJ. Lipid rafts: Heterogeneity on the high seas. Biochem J 2004;378 (Part 2):281–292.
97. Lewis A, Taha H, Strinkovski A, Manevitch A, Khatchatouriants A, Dekhter R, Ammann E. Near-field optics: From subwavelength illumination to nanometric shadowing. Nat Biotechnol 2003;21:1378–1386.
98. Hwang J, Gheber LA, Margolis L, Edidin M. Domains in cell plasma membranes investigated by near-field scanning optical microscopy. Biophys J 1998;74:2184–2190.
99. Ianoul A, Johnston LJ. Near-field scanning optical microscopy to identify membrane microdomains. Methods Mol Biol 2007;400:469–480.
100. Damjanovich S, Vereb G, Schaper A, Jenei A, Matko J, Starink JP, Fox GQ, Arndt-Jovin DJ, Jovin TM. Structural hierarchy in the clustering of HLA class I molecules in the plasma membrane of human lymphoblastoid cells. Proc Natl Acad Sci USA 1995;92:1122–1126.
101. Wilson BS, Pfeiffer JR, Oliver JM. Observing FcεRI signaling from the inside of the mast cell membrane. J Cell Biol 2000;149:1131–11342.
102. Nishida T, Arii T, Takaoka A, Yoshimura R, Endo Y. Three-dimensional, computer-tomographic analysis of membrane proteins (TrkA, caveolin, clathrin) in PC12 cells. Acta Histochem Cytochem 2007;40:93–99.
103. Kahya N, Schwille P. Fluorescence correlation studies of lipid domains in model membranes. Mol Membr Biol 2006;23:29–39.
104. Dietrich C, Yang B, Fujiwara T, Kusumi A, Jacobson K. Relationship of lipid rafts to transient confinement zones detected by single particle tracking. Biophys J 2002;82 (1 Part 1):274–284.
105. Suzuki K, Ritchie K, Kajikawa E, Fujiwara T, Kusumi A. Rapid hop diffusion of a G-protein-coupled receptor in the plasma membrane as revealed by single-molecule techniques. Biophys J 2005;88:3659–3680.
106. Douglass AD, Vale RD. Single-molecule microscopy reveals plasma membrane microdomains created by protein-protein networks that exclude or trap signaling molecules in T cells. Cell 2005;121:937–950.
107. Nakada C, Ritchie K, Oba Y, Nakamura M, Hotta Y, Iino R, Kasai RS, Yamaguchi K, Fujiwara T, Kusumi A. Accumulation of anchored proteins forms membrane diffusion barriers during neuronal polarization. Nat Cell Biol 2003;5:626–632.
108. Pralle A, Keller P, Florin EL, Simons K, Horber JK. Sphingolipid-cholesterol rafts diffuse as small entities in the plasma membrane of mammalian cells. J Cell Biol 2000;148:997–1008.
109. Lucius H, Friedrichson T, Kurzchalia TV, Lewin GR. Identification of caveolae-like structures on the surface of intact cells using scanning force microscopy. J Membr Biol 2003;194:97–108.
110. Kraft ML, Weber PK, Longo ML, Hutcheon ID, Boxer SG. Phase separation of lipid membranes analyzed with high-resolution secondary ion mass spectrometry. Science 2006;313:1948–1951.
111. London E. How principles of domain formation in model membranes may explain ambiguities concerning lipid raft formation in cells. Biochim Biophys Acta 2005;1746:203–220.
112. Vereb G, Szollosi J, Matko J, Nagy P, Farkas T, Vigh L, Matyus L, Waldmann TA, Damjanovich S. Dynamic, yet structured: The cell membrane three decades after the Singer-Nicolson model. Proc Natl Acad Sci USA 2003;100:8053–8058.
113. Tang Q, Edidin M. Vesicle trafficking and cell surface membrane patchiness. Biophys J 2001;81:196–203.
114. Gheber LA, Edidin M. A model for membrane patchiness: Lateral diffusion in the presence of barriers and vesicle traffic. Biophys J 1999;77:3163–75.
115. Mátyus L, Szöllősi J, Jenei A. Steady-state fluorescence quenching applications for studying protein structure and dynamics. J Photochem Photobiol B 2006;83:223–236.
116. Szöllősi J, Damjanovich S, Mátyus L. Application of fluorescence resonance energy transfer in the clinical laboratory: Routine and research. Cytometry 1998;34:159–179.
117. Jares-Erijman EA, Jovin TM. Imaging molecular interactions in living cells by FRET microscopy. Curr Opin Chem Biol 2006;10:409–416.
118. Jares-Erijman EA, Jovin TM. FRET imaging. Nat Biotechnol 2003;21:1387–1395.
119. Nagy P, Bene L, Hyun WC, Vereb G, Braun M, Antz C, Paysan J, Damjanovich S, Park JW, Szöllősi J. Novel calibration method for flow cytometric fluorescence resonance energy transfer measurements between visible fluorescent proteins. Cytometry Part A 2005;67A:86–96.
120. Nagy P, Vámosi G, Bodnár A, Lockett SJ, Szöllősi J. Intensity-based energy transfer measurements in digital imaging microscopy. Eur Biophys J 1998;27:377–389.
121. Horváth G, Petrás M, Szentesi G, Fabián A, Park JW, Vereb G, Szöllősi J Selecting the right fluorophores and flow cytometer for fluorescence resonance energy transfer measurements. Cytometry Part A 2005;65A:148-57.
122. Sebestyén Z, Nagy P, Horváth G, Vámosi G, Debets R, Gratama JW, Alexander DR, Szöllősi J. Long wavelength fluorophores and cell-by-cell correction for autofluorescence significantly improves the accuracy of flow cytometric energy transfer measurements on a dual-laser benchtop flow cytometer. Cytometry 2002;48:124–135.
123. Nagy P, Vereb G, Damjanovich S, Mátyus L, Szöllősi J. Measuring FRET in flow cytometry and microscopy. In: Robinson JP, editor. Current Protocols in Cytometry. Wiley; 2006. pp 12.8.1–12.8.13.
124. Szöllősi J, Damjanovich S, Nagy P, Vereb G, Mátyus L. Principles of resonance energy transfer. In: Robinson JP, editor. Current Protocols in Cytometry. Vol. 1.12: Wiley; 2006. pp 1.12.1–1.12.16.
125. Patterson GH, Piston DW, Barisas BG. Förster distances between green fluorescent protein pairs. Anal Biochem 2000;284:438–440.
126. Lidke DS, Nagy P, Barisas BG, Heintzmann R, Post JN, Lidke KA, Clayton AH, Arndt-Jovin DJ, Jovin TM. Imaging molecular interactions in cells by dynamic and static fluorescence anisotropy (rFLIM and emFRET). Biochem Soc Trans 2003;31 (Part 5):1020–1027.
127. Rocheleau JV, Edidin M, Piston DW. Intrasequence GFP in class I MHC molecules, a rigid probe for fluorescence anisotropy measurements of the membrane environment. Biophys J 2003;84:4078–4086.
128. Varma R, Mayor S. GPI-anchored proteins are organized in submicron domains at the cell surface. Nature 1998;394:798–801.
129. Friedrichson T, Kurzchalia TV. Microdomains of GPI-anchored proteins in living cells revealed by crosslinking. Nature 1998;394:802–805.
130. Kenworthy AK, Edidin M. Distribution of a glycosylphosphatidylinositol-anchored protein at the apical surface of MDCK cells examined at a resolution of <100 A using imaging fluorescence resonance energy transfer. J Cell Biol 1998;142:69–84.
131. Glebov OO, Nichols BJ. Distribution of lipid raft markers in live cells. Biochem Soc Trans 2004;32 (Part 5):673–675.
132. Glebov OO, Nichols BJ. Lipid raft proteins have a random distribution during localized activation of the T-cell receptor. Nat Cell Biol 2004;6:238–243.
133. Gautier I, Tramier M, Durieux C, Coppey J, Pansu RB, Nicolas JC, Kemnitz K, Coppey-Moisan M. Homo-FRET microscopy in living cells to measure monomer-dimer transition of GFP-tagged proteins. Biophys J 2001;80:3000–3008.
134. Sharma P, Varma R, Sarasij RC, Ira, Gousset K, Krishnamoorthy G, Rao M, Mayor S. Nanoscale organization of multiple GPI-anchored proteins in living cell membranes. Cell 2004;116:577–589.
135. Rao M, Mayor S. Use of Forster's resonance energy transfer microscopy to study lipid rafts. Biochim Biophys Acta 2005;1746:221–233.
136. Mayor S, Rao M. Rafts: Scale-dependent, active lipid organization at the cell surface. Traffic 2004;5:231–240.
137. de Almeida RF, Loura LM, Fedorov A, Prieto M. Lipid rafts have different sizes depending on membrane composition: A time-resolved fluorescence resonance energy transfer study. J Mol Biol 2005;346:1109–1120.
138. Zacharias DA, Violin JD, Newton AC, Tsien RY. Partitioning of lipid-modified monomeric GFPs into membrane microdomains of live cells. Science 2002;296:913–916.
139. Murakoshi H, Iino R, Kobayashi T, Fujiwara T, Ohshima C, Yoshimura A, Kusumi A. Single-molecule imaging analysis of Ras activation in living cells. Proc Natl Acad Sci USA 2004;101:7317–7322.
140. Pfeiffer A, Bottcher A, Orso E, Kapinsky M, Nagy P, Bodnar A, Spreitzer I, Liebisch G, Drobnik W, Gempel K, Horn M, Holmer S, Hartung T, Multhoff G, Schütz G, Schindler H, Ulmer AJ, Heine H, Stelter F, Schütt C, Rothe G, Szöllôsi J, Damjanovich S, Schmitz G. Lipopolysaccharide and ceramide docking to CD14 provokes ligand-specific receptor clustering in rafts. Eur J Immunol 2001;31:3153–3164.
141. Zhou W, Carpenter G. Heregulin-dependent translocation and hyperphosphorylation of ErbB-2. Oncogene 2001;20:3918–3920.
142. Nagy P, Mátyus L, Jenei A, Panyi G, Varga S, Matkó J, Szöllősi J, Gáspár R, Jovin TM, Damjanovich S. Cell fusion experiments reveal distinctly different association characteristics of cell-surface receptors. J Cell Sci 2001;114 (Part 22):4063–4071.
143. Bligh EG, Dyer WJ. A rapid method of total lipid extraction and purification. Can J Biochem Physiol 1959;37:911–917.
144. Folch J, Lees M, Sloane Stanley GH. A simple method for the isolation and purification of total lipides from animal tissues. J Biol Chem 1957;226:497–509.

145. Saunders RD, Horrocks LA. Simultaneous extraction and preparation for high-performance liquid chromatography of prostaglandins and phospholipids. Anal Biochem 1984;143:71–75.
146. Homan R, Anderson MK. Rapid separation and quantitation of combined neutral and polar lipid classes by high-performance liquid chromatography and evaporative light-scattering mass detection. J Chromatogr B Biomed Sci Appl 1998;708:21–6.
147. Lesnefsky EJ, Stoll MS, Minkler PE, Hoppel CL. Separation and quantitation of phospholipids and lysophospholipids by high-performance liquid chromatography. Anal Biochem 2000;285:246–254.
148. Wang WQ, Gustafson A. One-dimensional thin-layer chromatographic separation of phospholipids and lysophospholipids from tissue lipid extracts. J Chromatogr 1992;581:139–142.
149. Marwali MR, Rey-Ladino J, Dreolini L, Shaw D, Takei F. Membrane cholesterol regulates LFA-1 function and lipid raft heterogeneity. Blood 2003;102:215–222.
150. Razzaq TM, Ozegbe P, Jury EC, Sembi P, Blackwell NM, Kabouridis PS. Regulation of T-cell receptor signalling by membrane microdomains. Immunol 2004;113:413–426.
151. Schade AE, Levine AD. Lipid raft heterogeneity in human peripheral blood T lymphoblasts: A mechanism for regulating the initiation of TCR signal transduction. J Immunol 2002;168:2233–2239.
152. Li N, Shaw AR, Zhang N, Mak A, Li L. Lipid raft proteomics: Analysis of in-solution digest of sodium dodecyl sulfate-solubilized lipid raft proteins by liquid chromatography-matrix-assisted laser desorption/ionization tandem mass spectrometry. Proteomics 2004;4:3156–3166.
153. Miyagi M, Rao KC. Proteolytic 18O-labeling strategies for quantitative proteomics. Mass Spectrom Rev 2007;26:121–136.
154. Yao X, Freas A, Ramirez J, Demirev PA, Fenselau C. Proteolytic 18O labeling for comparative proteomics: Model studies with two serotypes of adenovirus. Anal Chem 2001;73:2836–2842.
155. Zhou H, Ranish JA, Watts JD, Aebersold R. Quantitative proteome analysis by solid-phase isotope tagging and mass spectrometry. Nat Biotechnol 2002;20:512–515.
156. Conrads TP, Issaq HJ, Veenstra TD. New tools for quantitative phosphoproteome analysis. Biochem Biophys Res Commun 2002;290:885–890.
157. Gupta N, Wollscheid B, Watts JD, Scheer B, Aebersold R, DeFranco AL. Quantitative proteomic analysis of B cell lipid rafts reveals that ezrin regulates antigen receptor-mediated lipid raft dynamics. Nat Immunol 2006;7:625–633.
158. MacLellan DL, Steen H, Adam RM, Garlick M, Zurakowski D, Gygi SP, Freeman MR, Solomon KR. A quantitative proteomic analysis of growth factor-induced compositional changes in lipid rafts of human smooth muscle cells. Proteomics 2005;5:4733–4742.
159. von Haller PD, Yi E, Donohoe S, Vaughn K, Keller A, Nesvizhskii AI, Eng J, Li XJ, Goodlett DR, Aebersold R Watts JD. The application of new software tools to quantitative protein profiling via isotope-coded affinity tag (ICAT) and tandem mass spectrometry: II. Evaluation of tandem mass spectrometry methodologies for large-scale protein analysis, and the application of statistical tools for data analysis and interpretation. Mol Cell Proteomics 2003;2:428–442.
160. Bunnell SC, Hong DI, Kardon JR, Yamazaki T, McGlade CJ, Barr VA, Samelson LE. T cell receptor ligation induces the formation of dynamically regulated signaling assemblies. J Cell Biol 2002;158:1263–1275.
161. Romijn EP, Christis C, Wieffer M, Gouw JW, Fullaondo A, van der Sluijs P, Braakman I, Heck AJ. Expression clustering reveals detailed co-expression patterns of functionally related proteins during B cell differentiation: A proteomic study using a combination of one-dimensional gel electrophoresis, LC-MS/MS, and stable isotope labeling by amino acids in cell culture (SILAC). Mol Cell Proteomics 2005;4:1297–1310.
162. Watson AD. Thematic review series: Systems biology approaches to metabolic and cardiovascular disorders. Lipidomics: A global approach to lipid analysis in biological systems. J Lipid Res 2006;47:2101–2111.
163. Ivanova PT, Milne SB, Forrester JS, Brown HA. LIPID arrays: New tools in the understanding of membrane dynamics and lipid signaling. Mol Interv 2004;4:86–96.
164. Khandurina J, Guttman A. Microchip-based high-throughput screening analysis of combinatorial libraries. Curr Opin Chem Biol 2002;6:359–366.
165. Feng L. Probing lipid-protein interactions using lipid microarrays. Prostaglandins Other Lipid Mediat 2005;77:158–167.
166. George S, Nelson MD, Dollahon N, Bamezai A. A novel approach to examining compositional heterogeneity of detergent-resistant lipid rafts. Immunol Cell Biol 2006;84:192–202.
167. Bernas T, Gregori G, Asem EK, Robinson JP. Integrating cytomics and proteomics. Mol Cell Proteomics 2006;5:2–13.
168. Edwards BS, Oprea T, Prossnitz ER, Sklar LA. Flow cytometry for high-throughput, high-content screening. Curr Opin Chem Biol 2004;8:392–398.
169. Ramirez S, Aiken CT, Andrzejewski B, Sklar LA, Edwards BS. High-throughput flow cytometry: Validation in microvolume bioassays. Cytometry Part A 2003;53A:55–65.
170. Mittag A, Lenz D, Gerstner AO, Tarnok A. Hyperchromatic cytometry principles for cytomics using slide based cytometry. Cytometry Part A 2006;69A:691–703.
171. Oheim M. High-throughput microscopy must re-invent the microscope rather than speed up its functions. Br J Pharmacol 2007;152:1–4.
172. Herrera G, Diaz L, Martinez-Romero A, Gomes A, Villamon E, Callaghan RC, O'Connor JE. Cytomics: A multiparametric, dynamic approach to cell research. Toxicol In Vitro 2007;21:176–182.

Chapter 7

Zoltán Beck, Andrea Balogh, Andrea Kis, Emese Izsépi, Adrienn Bíró, Glória László, László Cervenak, Károly Liliom, Gábor Mocsár, György Vámosi, George Füst, Janos Matko

New cholesterol-specific antibodies remodel HIV-1 target cells' surface and inhibit their *in vitro* virus production

Journal of Lipid Research 2010. 51(2):286-296.

New cholesterol-specific antibodies remodel HIV-1 target cells' surface and inhibit their in vitro virus production

Zoltán Beck,[1,*] Andrea Balogh,[1,†] Andrea Kis,[*] Emese Izsépi,[†] László Cervenak,[§] Glória László,[†] Adrienn Bíró,[**] Károly Liliom,[††] Gábor Mocsár,[§§] György Vámosi,[§§] George Füst,[§] and Janos Matko[3,†,*]**

Institute of Medical Microbiology,* University of Debrecen, H-4012, Debrecen, Hungary; Department of Immunology† and Immunology Research Group of Hungarian Academy of Sciences,*** Eötvös Loránd University, H-1117, Budapest, Hungary; Research Group of Immunogenomics,§ Hungarian Academy of Sciences at Semmelweis University, H-1089, Budapest, Hungary; Research Laboratory,** 3rd Department of Internal Medicine, Semmelweis University, H-1125, Budapest Hungary; Institute of Enzymology,†† Biological Research Center, Hungarian Academy of Sciences, H-1518, Budapest, Hungary; and Cell Biology and Signaling Research Group of the Hungarian Academy of Sciences,§§ Department of Biophysics and Cell Biology, Research Center for Molecular Biology, University of Debrecen, H-4012, Debrecen, Hungary

Abstract The importance of membrane rafts in HIV-1 infection is still in the focus of interest. Here, we report that new monoclonal anticholesterol IgG antibodies (ACHAs), recognizing clustered membrane cholesterol (e.g., in lipid rafts), rearrange the lateral molecular organization of HIV-1 receptors and coreceptors in the plasma membrane of HIV-1 permissive human T-cells and macrophages. This remodeling is accompanied with a substantial inhibition of their infection and HIV-1 production in vitro. ACHAs promote the association of CXCR4 with both CD4 and lipid rafts, consistent with the decreased lateral mobility of CXCR4, while Fab fragments of ACHAs do not show these effects. ACHAs do not directly mask the extracellular domains of either CD4 or CXCR4 nor do they affect CXCR4 internalization. No significant inhibition of HIV production is seen when the virus is preincubated with the antibodies prior to infection. Thus, we propose that the observed inhibition is mainly due to the membrane remodeling induced by cholesterol-specific antibodies on the target cells. This, in turn, may prevent the proper spatio-temporal juxtaposition of HIV-1 glycoproteins with CD4 and chemokine receptors, thus negatively interfering with virus attachment/entry.—Beck, Z., A. Balogh, A. Kis, E. Izsépi, L. Cervenak, G. László, A. Bíró, K. Liliom, G. Mocsár, G. Vámosi, G. Füst, and J. Matko. **New cholesterol-specific antibodies remodel HIV-1 target cells' surface and inhibit their in vitro virus production.** ***J. Lipid Res.*** **2010.** 51: **286–296.**

Supplementary key words membrane cholesterol • cholesterol-specific IgG • monocyte-macrophage cells • T-cells • lipid rafts • HIV-1 receptors • HIV-1 production

Anticholesterol antibodies (ACHAs) naturally occur in the sera of most healthy individuals with yet unknown functions (1). Recently, we reported on new IgG-type monoclonal antibodies, AC1 and AC8, which are highly specific to clustered cholesterol and some 3β-OH-containing sterols and do not cross-react with other lipids (2). These antibodies, in contrast to the IgM-type ACHAs reported earlier, have a unique property of spontaneous binding to live phagocytes and T-cells. Furthermore, their binding to the cell surface was substantially sensitive to the epitope accessibility, e.g., it was greatly enhanced by limited papain digestion of membrane proteins with long extracellular domains. Their spontaneous binding to intact cells also showed cell-type dependence. The preferential binding sites for these new cholesterol-specific mAbs were identified as cell surface or intracellular membrane compartments enriched in clustered cholesterol, such as lipid rafts, caveolas, or Golgi complexes (2).

Lipid rafts are dynamic, glycosphingolipid-, and cholesterol-rich membrane microdomains considered to make "some order into the chaos" of biological membranes (3, 4). Many pieces of experimental evidence indicate that the human immunodeficiency virus type 1, HIV-1, enters target cells through these lipid rafts (5–7). The last stage of

The financial support from the Hungarian Academy of Sciences, the Hungarian Ministry of Health (ETT grants 2003/102 to Z.B. and 2006/070 and 2006/065 to G.V.), the Hungarian National Science Fund (OTKA grants T49696 to J.M., F49164 to L.C., and T48745 and NK61412 to G.V.), the National Office of Research and Development (Pázmány Grant RET-06/2006 to J.M.), and the support from the Hungarian Academy of Sciences are gratefully acknowledged.

Manuscript received 28 July 2009 and in revised form 3 August 2009.

Published, JLR Papers in Press, August 3, 2009
DOI 10.1194/jlr.M000372

[1] Z. Beck and A. Balogh contributed equally to this work.

[2] Present address of Z. Beck: U.S. Military HIV Research Program, Henry M. Jackson Foundation for the Advancement of Military Medicine, Walter Reed Army Institute of Research, Rockville, MD 20850

[3] To whom correspondence should be addressed.
e-mail: matko@elte.hu

the multistep process of HIV-1 entry, the fusion of the virus with the target cell membrane, entails multifocal interactions between virus shell glycoproteins and lipids and their receptor/coreceptor and lipid raft counterparts on target cells (8). Lipid rafts were also implicated in the budding of the progeny virus (9, 10).

HIV-1 was shown to use the CD4 receptor and CCR5 or CXCR4 chemokine receptors for productive entry into $CD4^+$ cells. CD4 and CCR5 are constitutively raft associated, while CXCR4 molecules are mostly recruited to lipid rafts after the initial binding of the virus (11). However, the exact molecular mechanism of this entry is still under debate (9, 12). Since the new cholesterol-specific mAbs selectively bind to cholesterol-enriched lipid raft or caveola microdomains of intact HIV-1 permissive cells, it is plausible to assume that they may interfere somehow with the mechanisms leading to membrane attachment or internalization of the virus.

Therefore, this study aimed to investigate whether the new ACHAs can modulate the receptor or microdomain architecture at the surface of target cells, such as human macrophages and T-cells: namely, the distribution/interaction pattern, accessibility, internalization, mobility, or raft association of CD4 and chemokine receptors. These properties are all critical for membrane attachment and internalization of the virus.

Since in a recent work (13) another antilipid antibody, a mAb against phosphatidylinositol-4-phosphate, was reported to inhibit infection of peripheral blood mononuclear cells (PBMCs) with two HIV-1 primary isolates, we also investigated whether the new cholesterol-specific antibodies can affect in vitro HIV-1 infection/production of primary monocyte-derived macrophages (MDMs) and T-cells in cultures.

The new IgG-type cholesterol-specific antibodies caused a remarkable lateral clustering of membrane rafts upon binding to both cell types and remodeled the interaction pattern of CXCR4 chemokine receptors with both CD4 and lipid rafts. The membrane-bound antibodies substantially inhibited production of two different HIV strains in MDM and T-cells in vitro. In contrast, no significant inhibition was achieved when the virus strains themselves were preincubated with the antibodies before infection. Thus, these data demonstrate a novel type of inhibition of HIV-1 infection by lipid (cholesterol)-specific mAbs, which is linked to their primary membrane remodeling effect on target cells. This, in turn, can prevent the efficient multistep virus anchorage.

MATERIALS AND METHODS

Cells, immunofluorescence labeling, and flow cytometry

The monoclonal IgG_3 Abs to cholesterol, AC1 and AC8, were generated, characterized, and applied for cell labeling as described previously (2). Cell surface binding of Alexa488-ACHA, PE/Cy5-anti-CD4 (ImmunoTools, Friesoythe, Germany), or APC-anti-CXCR4 (R and D Systems, Minneapolis, MN) was assayed by flow cytometry. After FcR blocking with affinity-purified human IgG_1, cells were washed with FACS (fluorescence activated cell analysis and sorting) buffer containing 0.1% BSA and then stained as described elsewhere (2). Occasionally, prior to receptor staining, U937 human macrophages (ATTC, maintained in RPMI 1640 medium + 10% FBS) and MT-4 T-cells were preincubated with ACHA or the Ka40 isotype control Ab (specific to tobacco mosaic virus) at 37°C for 60 min.

In the CXCR4 receptor internalization assay, U937 cells were incubated (or not) with ACHA as described above. After washing, cells were treated with 300 nM SDF-1α chemokine ligand or, alternatively, with 100 ng/ml of the phorbol ester PMA, at 37°C, for 0–60 min. Cells were then washed, FcR-blocked, and labeled with APC-anti-CXCR4 as described above. Before measurement, cells were fixed with 3% paraformaldehyde. CXCR4 expression on the cell surface was measured and evaluated by flow cytometry.

Data from 10,000 stained cells/sample were acquired in a Becton-Dickinson FACSCalibur flow cytometer using CellQuest Pro software (Becton-Dickinson, San Jose, CA) and then analyzed with FCS3 Express software (De Novo Software, Los Angeles, CA).

Surface plasmon resonance

Surface plasmon resonance measurements were performed using a BIACORE X instrument (Biacore, Uppsala, Sweden) at 25°C. AC8 ACHA and anti-CD8 control IgG (30 μg/ml) were immobilized onto the surface of a carboxymethylated dextran chip (CM5) using standard amine-coupling chemistry in 10 mM sodium acetate, pH 5.0, according to the manufacturer's instructions. The mean amount of immobilized protein was ~7000 resonance units. Cholesterol-rich (1,2-dimiristoyl-*sn*-glycero-3-phosphocholine, 1,2 dimiristoyl-*sn*-3-phosphoglyerol and cholesterol, in a 9:1:25 molar ratio) and cholesterol-free control liposomes were prepared as described earlier (2), reconstituted in 10 mM HEPES, pH 7.2, 150 mM NaCl solution (running buffer) at a concentration of 1 mM total lipid, and were passed over the chip surface at a flow rate of 10 μl/min. The results were analyzed by BIAevaluation 4.1 software (Biacore). The corresponding association and dissociation regimes of sensorgrams were fitted to a builtin Langmuir binding model, and the equilibrium dissociation constant, K_D, was calculated as the ratio of dissociation to association rate constants.

Confocal microscopy

U937 human macrophages were treated with AC8 (or Ka40 isotype control) antibodies as described above and, as a negative control to raft-associated proteins, with anti-CD71 (transferrin receptor) mAb (MEM-75; a kind gift from Vaclav Horejsi, Prague, CZ). Alternatively, cells were treated with monovalent Fab fragment of AC8 IgG, generated by the method of Adamczyk (14). The enzyme reaction was stopped by adding iodoacetamide, the digested protein was separated on Sephadex G-100 column (Pharmacia Fine Chemicals, Uppsala, Sweden), and the homogeneity of the Fab-containing fractions was analyzed by SDS gel electrophoresis.

Cells were then washed, FcR blocked, and stained with fluorophore-conjugated anti-CD4, anti-CXCR4, and Alexa488- or Alexa647-CTX (Invitrogen-Molecular Probes, Eugene, OR) in different combinations. After washing and fixing in 3% paraformaldehyde, labeled cells were mounted on quartz-glass bottomed microplates (Lab-Tek, Nalge Nunc, Rochester, NY) and assayed with an Olympus Fluoview 500 confocal microscope (Hamburg, Germany) equipped with four optical channels, using a 60× (numerical aperture of 1.45) oil immersion objective.

Colocalization indices were determined from ⩾100 cells (~200 regions of interest/sample, in four independent experi-

ments) by ImageJ software (http://rsbweb.nih.gov/ij) using the appropriate colocalization plug-in. The Pearson's colocalization index (CI) provides a reliable estimate on the extent of protein colocalization: CI values close to zero indicate no or a very low degree, while CI ≥0.5 reflects a high degree of colocalization, whereas the CI = 1 value would correspond to a full overlap between the two colors in each pixel of the image (15).

Fluorescence resonance energy transfer

For ratiometric intensity-based fluorescence resonance energy transfer (RiFRET) measurements, U937 macrophages were treated with AC8 or Ka40 isotype control antibodies and stained with Alexa546-conjugated anti-CD4 (donor only sample), with APC-conjugated anti-CXCR4 (acceptor only sample), or with both antibodies as described above. After washing, labeled cells were mounted on quartz-glass bottomed microplates treated with BD Cell-Tak cell and tissue adhesive (Becton-Dickinson), according to the manufacturer's protocol. RiFRET measurements on a pixel-by-pixel basis were performed at room temperature on an Olympus Fluoview 500 confocal microscope using a 60× (numerical aperture of 1.45) oil immersion objective. The Alexa546-conjugated antibody was excited with a 532 nm HeNe laser and detected through a 560–600 nm emission filter, and the Alexa647-labeled protein was excited with a 633 nm HeNe laser and detected through a 660 nm long-pass filter. FRET efficiency was calculated from ≥30 cells by the ImageJ RiFRET plugin (16).

Fluorescence correlation spectroscopy

For fluorescence correlation spectroscopy (FCS) measurements, U937 human macrophage cells were treated with AC8 or Ka40 isotype control antibodies and stained with Alexa488-conjugated anti-CD4 or APC-conjugated anti-CXCR4 as described above. As control, cells were labeled with Alexa647-anti-CD2 (Exbio, Praha, CZ) or Alexa488-AC8 antibodies for 30 min on ice. After washing, labeled cells were mounted on quartz-glass bottomed microplates.

FCS (17) measurements were carried out at room temperature, in a fluorescence fluctuation microscope set on an Olympus FluoView 1000 confocal microscope base, with a two-channel FCS extension. Desired points were selected for FCS analysis from confocal sections of the sample. Fluorescence fluctuations were detected by avalanche photodiodes (Perkin-Elmer, Wellesley, MA), and the autocorrelation function was calculated by an ALV-5000E hardware correlator card (ALV Laser, Langen, Germany) in real time. From each sample n > 22 cells were measured, and 10 × 5 s runs were recorded per cell. Data were fitted to a single-component two-dimensional diffusion model with a triplet term using the program QuickFit (written in the laboratory of J. Langowski, DKFZ, Heidelberg, Germany):

$$G(\tau)=\frac{1}{N}\frac{\left(1-T+Te^{-\tau/\tau_{tr}}\right)}{1-T}\left[\left(1+\frac{\tau}{\tau_d}\right)^{-1}\right]$$

where N is the average number of molecules in the detection volume, T is the fraction of dyes being in the triplet state within the detection volume, τ_{tr} is the phosphorescence lifetime, and τ_d is the diffusion time, which is the average time spent by the dye in the detection volume. The half-decay time $\tau_{1/2}$ was used to determine the average diffusion coefficients as described earlier (18).

Target cells and HIV-1 strains

$HIV\text{-}1_{IIIB}$ permissive H9 cell line (for virus propagation) and MT-4 T cells (ATCC) were maintained in complete RPMI 1640 medium (cRPMI; 10% FBS, 100 U/ml penicillin, 100 μg/ml streptomycin, and 1 mM L-glutamine; Gibco BRL, Gaithersburg, MD). The primary MDM cells were separated from peripheral blood mononuclear cells of healthy, HIV-1 seronegative donors using PHA stimulation as described earlier (19). The MDM cultures were used for HIV-1 infection in all experiments on day 7 after separation.

The ×4 phenotype IIIB strain of HIV-1 (20) was grown in H9 cell line, while the R5 characteristic Ada-M strain of HIV-1 (19) was propagated in primary MDM cultures, then harvested and stored in liquid nitrogen.

Infection and measurement of HIV-1 production

Different protocols for antibody treatment, infection, and washing prior to virus production measurement were used for assaying with which stage of the HIV-1 infection and virus cycle (attachment, fusion, entry, or budding) the ACHAs interfere. Protocol 1: Prior to infection with the appropriate virus strains, either the target cells or the viruses were pretreated with ACHAs for 60 min at 37°C. Then, the untreated or ACHA-pretreated cells in culture were infected with untreated or ACHA-pretreated virus for 1 h at 37°C. Infection was followed by culturing T-cells or MDM cells for 4 or 14 days, respectively, before measurement of virus production.

Protocol 2: Target cells were treated with the appropriate ACHAs for 1 h at 37°C, infected with HIV-1 strains for 1 h at 37°C, and then washed out carefully (or not). The samples were then left in culture for 4 or 14 days, respectively, before measurement of virus production.

Protocol 3: Since during the assay period a continuous decline of ACHA concentration in the supernatant was observed, a third strategy was applied to investigate ACHA's effects on virus production. Cells were preincubated with ACHAs according to protocol 1, washed, and infected, and a continuous supplementation of ACHA was applied during the 4 or 14 day assay periods to maintain a constant level of ACHAs in the extracellular fluid. This strategy aimed to reveal any effect of the antibodies on the budding phase.

Untreated and Newcastle Disease Virus-specific isotype control antibody treated cells were also used as controls in all infection experiments.

HIV-1 infection was carried out with 100 μl of IIIB or Ada-M strains of HIV-1 with 15,000 cpm reverse transcriptase activity in all protocols. Target cells (in 300 μl cRPMI) were incubated with the virus at 37°C for 60 min, washed (or not) with medium, and then completed up to 1 ml with fresh cRPMI medium.

HIV-1 production was measured by reverse transcriptase assay (21) with a Packard 2200CA TRI-CARB Liquid Scintillation Analyzer (Packard Instrument, Meriden, CT) and corrected to dpm values.

Cellular cytotoxicity assay

MT-4 and MDM cells were treated with different concentrations of ACHA and incubated in the appropriate medium for 4 or 14 days, respectively. Cells were assayed periodically for in vitro cytotoxicity of the ACHAs. Viability of cells was determined by the CellTiter 96® AQ_{ueous} nonradioactive Cell Proliferation Assay (Promega, Madison, WI) (22) according to the manufacturer's protocol. The assay is based on MTT-formazan reaction of metabolically active cells. In each experiment, the survival rate and the standard deviation were calculated from triplicates of samples.

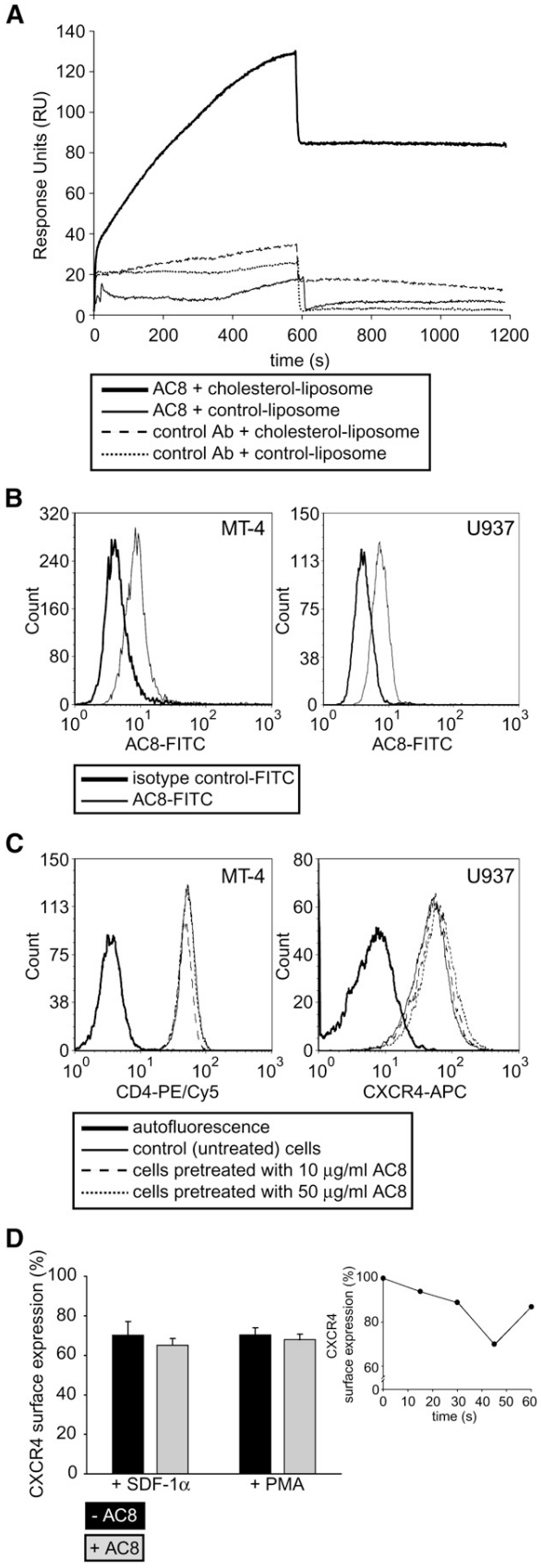

Fig. 1. AC8 mAb bound to HIV-permissive T-cells and macrophages neither masks the accessibility of CD4 and CXCR4 receptors nor affects internalization of CXCR4. A: Surface plasmon resonance measurement of the interaction between ACHA and cholesterol-rich liposomes. Liposomal presentation of cholesterol resulted in binding to immobilized AC8 ACHA but not to anti-CD8. Cholesterol-free liposomes exhibited no binding to the IgGs. Fitting of a Langmuir binding model to AC8 data yielded an equilibrium dissociation constant $K_d = k_{off}/k_{on} = 78 \pm 27$ nM. Typical traces of three to four experiments are shown. B: The AC8 antibody spontaneously binds to the surface of MT-4 T and U937 macrophage cells, respectively. C: Flow cytometric histograms of untreated or AC8-treated MT-4 or U937 cells stained with PE/Cy5-anti-CD4 or APC-anti-CXCR4, respectively, are shown. D: SDF-1α or PMA-induced internalization of CXCR4 is shown for untreated or AC8-pretreated U937 cells. Cell surface expression of CXCR4, measured by flow cytometry 45 min after stimulation, is displayed as mean ± SD from three independent experiments. The time course of internalization is also shown in the insert. The expression level of untreated cells was taken as 100%.

Measurement of anticholesterol antibodies in cell culture supernatants by ELISA

Concentration of anticholesterol antibodies in cell culture supernatants was measured by the ELISA method as described previously (2).

Statistical analysis

Diffusion coefficients in control and ACHA-treated cells were compared using Student's *t*-test (the number of individual cells for each sample is given in Table 1).

RESULTS

Binding properties of ACHAs to cholesterol-rich surfaces assessed by surface plasmon resonance

To quantitate binding of ACHA to highly homogenous cholesterol-rich liposomes used in generating these antibodies (2), as an optimal epitope, we used surface plasmon resonance experiments. AC8 ACHA and anti-CD8 control IgGs were immobilized in different flow channels on the surface of the same CM5 sensor chip. As depicted on the representative binding curves of **Fig. 1A**, liposomal presentation of cholesterol resulted in a significant binding to the AC8 ACHA but not to the anti-CD8 control antibody. Cholesterol-free liposomes exhibited no binding to the IgGs, as expected. The dissociation phase of the binding reaction can be fitted to a single exponential, yielding a dissociation rate, $k_{off} = 1.6 \pm 0.5 \times 10^{-5}\ s^{-1}$ (n = 3). The association phase can be estimated kinetically only if the concentration of the analyte (binding partner in solution) is known. ACHA is expected to interact with the cholesterol-rich liposome as a whole rather than with individual cholesterol molecules. Since the lipid was presented as a 1 mM solution (regarding total lipid concentration), a rough estimate of analyte concentration is 10 µM, assuming ~100 lipids/liposome (based on average liposome size). Using this analyte concentration, the fit yielded an association rate, $k_{on} = 205 \pm 8\ M^{-1}\ s^{-1}$ (n = 3). The equilibrium dissociation constant estimated from these rate constants is $K_d = k_{off}/k_{on} = 78 \pm 27$ nM.

These data, completing recent semiquantitative results showing low/medium affinity ACHA binding to isolated

membrane raft fractions of T-cells (2), suggest that the optimal affinity of ACHAs to clustered cholesterol is medium, meanwhile the binding is highly selective.

Binding of AC8 does not alter the accessibility or internalization of HIV-1 receptors on target cells

Earlier, we demonstrated the spontaneous binding of the new cholesterol-specific antibodies to several mouse and human lymphoid and myeloid cell types (2). Here, we show that AC8 can also bind to HIV-1 permissive human MT-4 T cells and U937 macrophages (Fig. 1B), the potential target cells of the IIIB and Ada-M HIV-1 strains, respectively. In addition, AC8 does not mask the extracellular domains of CD4 or CXCR4 receptors on these cells, since the binding of antibodies against these epitopes remained unchanged after AC8 binding (Fig. 1C).

The HIV-1 coreceptor CXCR4 was shown to rapidly internalize upon binding chemokine ligand SDF-1α or after PMA treatment, and a mechanism involving the cytoskeleton and motor proteins (myosin IIa) was also proposed for this process (23). It was supposed that internalization of the chemokine receptor may also influence HIV-1 interaction/entry to target cells. Therefore, the SDF-1 or PMA-induced internalization of CXCR4 was also followed in context with the possible effects of the AC8 antibody. Results with human U937 macrophage cells showed that the cholesterol-specific antibody AC8 does not significantly affect internalization of CXCR4 induced either by SDF-1 or PMA (Fig. 1D).

Binding of AC8 to the target cells' surface induces lateral lipid raft clustering

Interestingly, binding of AC8 to U937 macrophages induced several remarkable changes in their global plasma membrane organization. The cell surface ganglioside (GM1-rich raft) pattern was markedly altered as indicated by the increased fraction of highly patchy cells (from 10 to 67%) and the increased average GM1 raft size (from 200–300 nm to 0.5–1 μm in diameter) (**Fig. 2**). Similar changes were observed on T-cells as well (data not shown).

The AC8 antibody remodels the lateral plasma membrane interaction pattern of chemokine receptor CXCR4 with CD4 and lipid rafts on target cells

First, the interaction pattern of CD4 HIV-1 receptor and the CXCR4 coreceptor with each other and with the lipid rafts was investigated in human U937 monocyte-macrophage cells by means of confocal microscopy colocalization analysis. The chemokine receptor CXCR4 colocalized only weakly with CD4 (CI: ~0.2), in accordance with earlier reports on other cells (6, 24), and also moderately (CI: 0.2–0.3) with GM_1 ganglioside rafts marked with fluorescent cholera toxin B subunit. In contrast, the CD4-cholera toxin B subunit colocalization was high (CI: >0.6), similar to many other cell types (**Fig. 3**). This indicates the lack of significant association between CD4 and CXCR4 on these target cells and is also consistent with their localization in distinct membrane microdomains in the absence of the virus.

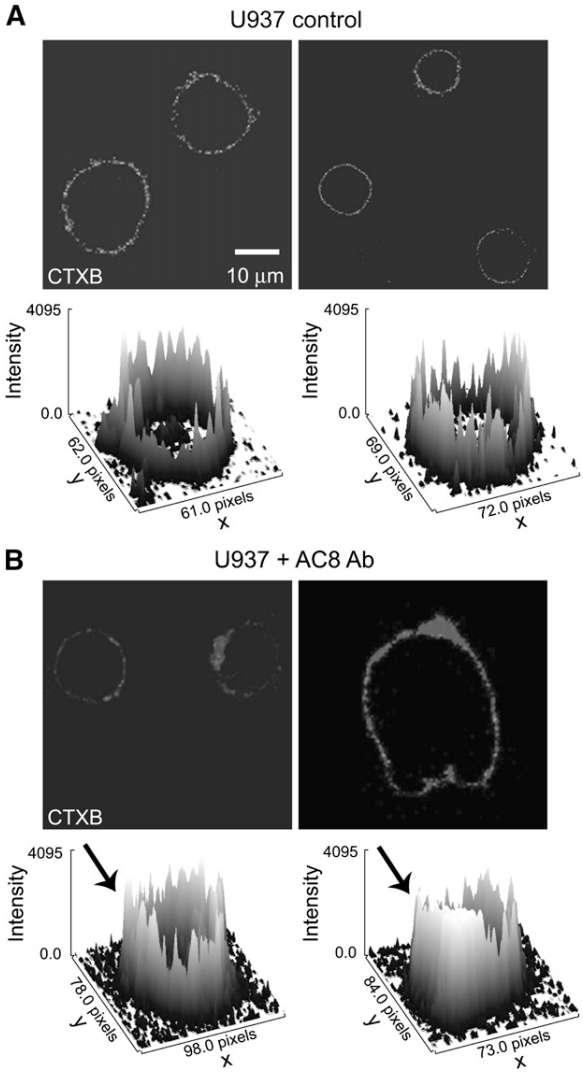

Fig. 2. Binding of monoclonal ACHA to human macrophages alters the size distribution of GM_1-rich rafts. Untreated (A) or ACHA-pretreated (B) U937 cells were stained with Alexa488-cholera toxin B and assayed by confocal microscopy. Representative images and surface intensity plots reflect an AC8-induced microaggregation/coalescence (see arrows) of lipid rafts. The average size of GM_1 rafts increased from 200–300 nm to 0.5–1 μm in diameter. Results were obtained evaluating >120 cells from three independent experiments.

Binding of AC8 antibody to these cells caused an ~2-fold increase of the colocalization between CXCR4 and CD4 as well as between CXCR4 and GM_1 rafts, while leaving CD4 raft colocalization unchanged. Neither the engagement/cross-linking of a nonraft protein, the transferrin receptor (CD71) with its specific mAb, nor the isotype control antibody affected these colocalization patterns. The monovalent Fab fragment of AC8 antibody, without cross-binding capacity, had no effect on the colocalization between HIV receptors (**Fig. 4A**).

The increased proximity/interaction between CXCR4 and CD4 was further confirmed by intensity-based FRET measurements. Mean FRET values (±SD) were 0.17 (±0.02)

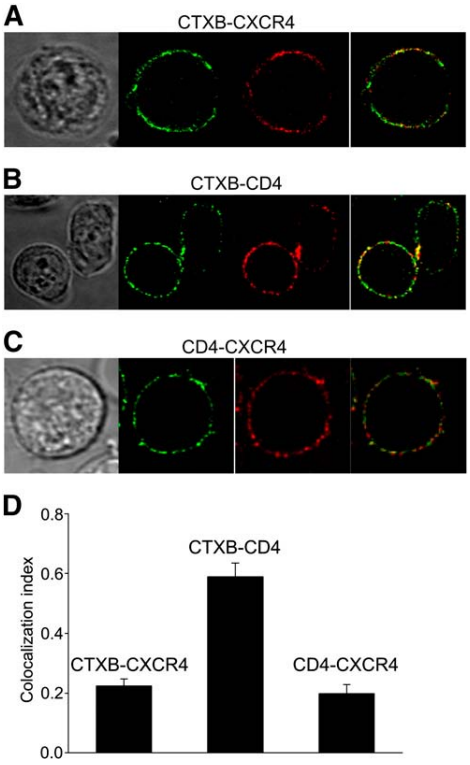

Fig. 3. Colocalization pattern of CD4, CXCR4, and GM_1-enriched lipid rafts in HIV-1 permissive human macrophage cells. Representative confocal images of U937 cells double labeled with Alexa488-cholera toxin B subunit (CTXB) (green) and APC-anti-CXCR4 (red) (A), RPE-anti-CD4 (green) and Alexa647-CTXB (red) (B), and RPE-anti-CD4 (green) and APC-anti-CXCR4 (red) (C) are shown. Colocalization indices for CD4, CXCR4, and CTXB in different combinations (D) were derived from ⩾100 cells (∼250 regions of interest) of three independent samples and displayed as mean ± SD.

in control cells, while it elevated to 0.28 (±0.06) upon AC8 binding of target cells (Fig. 4B).

The AC8 antibody selectively reduces the lateral mobility of CXCR4 but not that of CD4

In order to see whether AC8 has any influence on the molecular mobility of plasma membrane HIV-1 receptors, the diffusion properties of CXCR4 and CD4 were assessed by FCS imaging. AC8 binding to macrophages significantly reduced two-dimensional diffusion of CXCR4 but not that of CD4 (**Fig. 5A, B**). Diffusion of a nonraft protein, CD2, was not affected by ACHA treatment either in macrophages (Fig. 5C; **Table 1**) or in T-cells (data not shown). The average diffusion coefficient of CXCR4 decreased by ∼40% ($P < 0.01$). Fab fragment of AC8 did not show this effect (data not shown). The AC8 mAb bound to the cell membrane diffused remarkably slower (diffusion coefficient, D: 0.2 $\mu m^2/s$) than small fluorescent cholesterol probes (e.g., Bodipy cholesterol) do in model membranes with high cholesterol content (D: 0.5 $\mu m^2/s$) and almost 10-fold slower than cholesterol does in fluid membrane phases (25). This indicates that the cell-surface-bound ACHA diffuses in large molecular clusters (Table 1).

Cholesterol-specific AC1 and AC8 monoclonal antibodies inhibit in vitro HIV-1 production by T-cells and macrophages

Next we investigated whether these substantial changes in the membrane organization of HIV-1 permissive target cell types have any effect on their infection and virus production. First, it was observed that the presence of ACHAs in cell cultures of MT-4 or MDM cells, at the time of infection, resulted in significant inhibition of the virus production of these cells (data not shown). Analyzing the details of this inhibitory effect, cultured MT-4 T-cells and primary MDM cells were preincubated with ACHAs prior to infection with IIIB and Ada-M strains of HIV-1, respectively (see protocol 1 in Materials and Methods). Such preincubation resulted in a significant (up to 50–60%) dose-dependent inhibition of virus production by both mAbs in both cell types relative to the control (untreated) cells (**Fig. 6A, B**). The isotype control antibody left the infection unchanged (data not shown).

Importantly, much less if any inhibition was observed when the virus strains were preincubated, at the same conditions, with the ACHAs prior to infection (Fig. 6C, D).

ACHAs interfere mostly with the attachment phase of HIV-1 infection

To reveal with which stage of HIV-1 infection (attachment/entry/budding) the ACHAs interfere, we compared their inhibitory effects under different experimental conditions (concerning antibody treatment, infection, washing, and culturing).

When ACHA was washed out from the sample after virus infection (see protocol 2 in Materials and Methods), the extent of inhibition remained the same as in case if it was not washed out from the culture after infection (**Fig. 7A**). This indicates that the postinfection presence of ACHAs did not decrease the virus production further.

Since the level of ACHAs in the culture medium gradually declines during the relatively long assay period (Fig. 7B), we also tested if a continuous supplementation of ACHA after infection (see protocol 3 in Materials and Methods) can influence the observed inhibition. Such supplementation, however, did not result in any significant change in the final HIV-1 production (Fig.7B), suggesting that the inhibitory effect is not coupled to inhibition of the later, budding phase.

Monoclonal ACHAs are not cytotoxic to MT-4 T and MDM cells

Finally, it was tested if the observed inhibition is due to any significant cytotoxic effect of the anticholesterol mAbs exerted on the target cells. MT-4 cells and monocyte-derived macrophages were treated with serial dilutions of ACHAs and cultured for 4 and 14 days, respectively. ACHAs proved to be nontoxic to the investigated cell types, since their survival rate remained above 90% over the whole experimental period (the cells retained both their metabolic activity and proliferation capacity) at any ACHA concentrations examined (Fig. 7C).

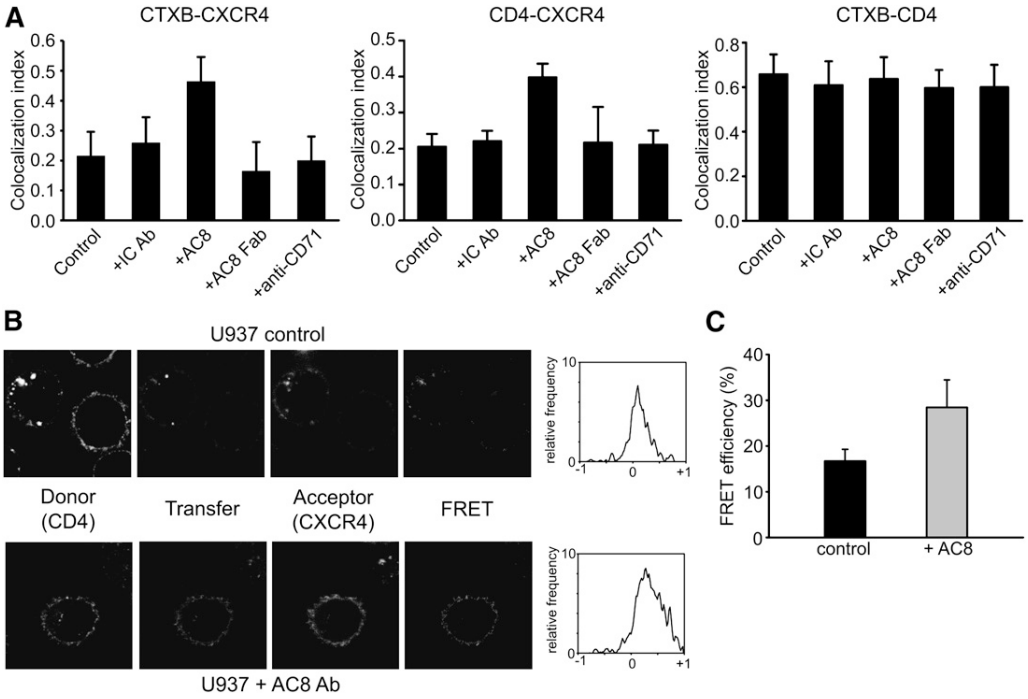

Fig. 4. AC8 substantially enhanced colocalization and FRET between CXCR4 and CD4 on human U937 macrophages. A: Colocalization indices (derived from ⩾100 cells/250 regions of interest of both untreated and AC8-treated cell samples) are shown as mean ± SD for CXCR4, CD4, and CTXB in different combinations. Cells untreated or treated with AC8, isotype control Ab, Fab fragment of AC8, or anti-CD71 are displayed for comparison. B: Cells were incubated with AC8 or left untreated prior to staining with antibodies specific to CD4 and/or CXCR4. FRET measurement was carried out by confocal microscopy. Correction factors (S1, S2, S3, and S4) and factor α were calculated from only donor and only acceptor labeled samples and determined by the ImageJ RiFRET plug-in. Representative images and FRET histograms of control and AC8-treated cells are shown, respectively. FRET efficiency between CD4 and CXCR4, derived from ⩾30 cells, are displayed as mean ± SD.

DISCUSSION

We report here the inhibition of HIV-1 infection/production of human monocyte-macrophage and T-cells by two new cholesterol-specific IgG antibodies, AC1 and AC8. As a novel aspect, this study points out that antilipid antibodies may act effectively not only on the virus but also on the target cell membrane, in contrast to the principle considered earlier in context of most neutralizing antibodies (26, 27).

The new cholesterol-specific monoclonal antibodies bind to cholesterol- and ganglioside-rich microdomains in the membrane of various immune cells, as reported recently (2, 18). They strongly colocalize with GM_1 gangliosides as well as with GPI-anchored raft proteins (e.g., CD48 and Thy-1). Moreover, as shown here, upon binding to lipid rafts (or caveolas), these antibodies, without masking the CD4 and CXCR4 HIV-1 receptors or affecting their internalization, can remarkably remodel the plasma membrane microdomains and the spatial proximity of the above two receptor proteins.

These effects were clearly initiated by a lateral clustering (coalescence) of lipid rafts induced by binding of the mAbs to the cell surface. Cross-linking of CD71 (a nonraft protein) with mAbs was also reported to induce cell surface patches, but with no overlap with GM_1 rafts (28). Since cross-linking of CD71 in our cells did not change the receptor distribution pattern, it seems that the AC8 antibody similarly to the viral gp120 (6) induces selective, cholesterol-rich raft-targeted effects on the membrane organization of HIV-1 receptors. The lack of such effect by the monovalent Fab fragment of AC8 on the target cells further confirms this notion.

Receptors and coreceptors in the cell membranes are usually not randomly distributed, and, among others, their lipid environment can also control their movement and interactions. As shown by a body of data, cholesterol is indeed required for the interaction between gp120/gp41 trimers on the surface of HIV-1 and their receptor/coreceptor counterparts on the target cells. It seems that cholesterol is a critical lipid for stabilization of raft microdomains and often of clusters of coreceptor proteins with multiple membrane-spanning helices (29), such as most, but not all chemokine receptors.

In the plasma membrane of the investigated cell types, CD4 is constitutively and highly localized, whereas CXCR4 is much more weakly raft localized. Their localization and clustering in distinct membrane microdomains on HIV-1 permissive target cells was proposed earlier (30, 31). Binding of the cholesterol-specific mAb (AC8), but not of its

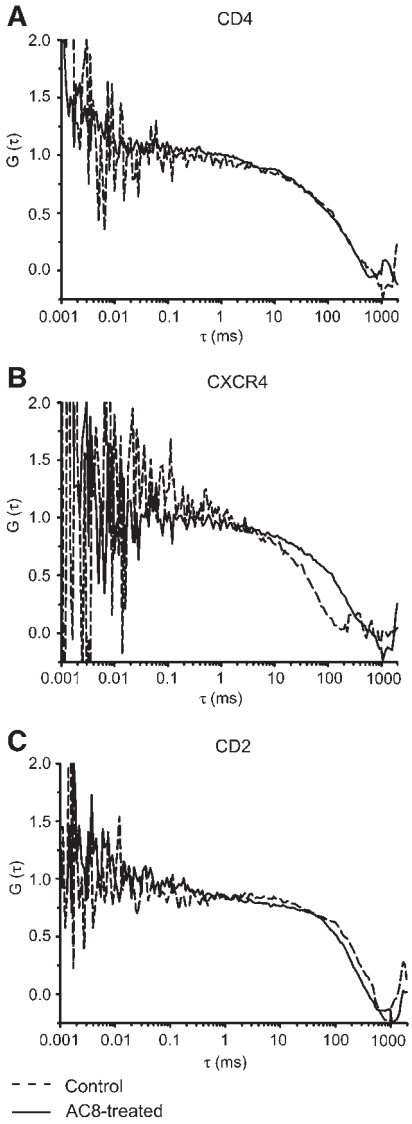

Fig. 5. Lateral mobility of CXCR4, but not of CD4 receptor, is markedly reduced upon AC8 mAb binding to macrophages. Cells were incubated with AC8 or left untreated prior to staining with antibodies specific to CD4 (A), CXCR4 (B), or a nonraft protein CD2 (C), and the lateral mobility of the molecules at 22°C was monitored by FCS imaging. Figures show representative fluorescence autocorrelation curves for CD4, CXCR4, and CD2 in control/untreated (dashed line) and AC8-treated cells (solid line), respectively.

Fab fragment, to the cells increased both CD4-CXCR4 colocalization and the raft association of CXCR4 by ~2-fold. These observations, confirmed by FRET data, together suggest a view that ACHAs may induce lateral clustering of cholesterol-rich lipid rafts (or caveolas) and thus modulate the interaction pattern between raft gangliosides, CD4 and CXCR4, which are all critical in membrane attachment/entry of the virus.

The cell surface targets of both the HIV-1 virus and the new ACHAs can be the caveolin$^-$ and caveolin$^+$ lipid rafts alike, depending on the type of HIV-1 permissive cell. A strong association of ACHA with these microdomains was

TABLE 1. Translational mobility of HIV receptors on target cells assessed by FCS imaging

	Diffusion CoefficientD ± SD ($\mu m^2/s$)	
Epitope/Marker	Control	+ AC8 ACHA
CXCR4/APC-anti-CXCR4 mAb	0.17 ± 0.05* (n:26)	0.10 ± 0.02* (n:32)
CD4/Alexa 488-anti-CD4 mAb	0.10 ± 0.01 (n:22)	0.12 ± 0.03 (n:34)
CD2/Alexa 647-anti-CD2 mAb	0.15 ± 0.02 (n:23)	0.16 ± 0.03 (n:18)
Membrane cholesterol/ Alexa488-AC8	NA	0.20 ± 0.04 (n:16)

*The difference is significant between control and ACHA-treated cells ($P < 0.01$). Numbers in parentheses denote the number of cells measured. NA, not applicable.

observed in macrophages and T-cells equally (2). Although cholesterol was shown to be essential to trigger events leading to membrane fusion between the target cell and the virus, it is not required for the Env-mediated membrane fusion itself (32). Interestingly, immunization with a peptide corresponding to the caveolin-1 binding domain of gp41 virus glycoprotein was able to elicit efficient neutralizing antibodies, which act predominantly on the virus to prevent HIV-1 infection (33).

So, our view is that, in contrast to such primarily neutralizing antibodies, the cholesterol-specific antibodies may interfere mostly with the cholesterol-dependent virus-target cell interaction by modifying the membrane organization of the latter. Similarly, reorganization of ErbB membrane proteins was reported upon cross-linking of gangliosides through cholera toxin B in breast tumor cells (34). Here, we conclude that the antibodies

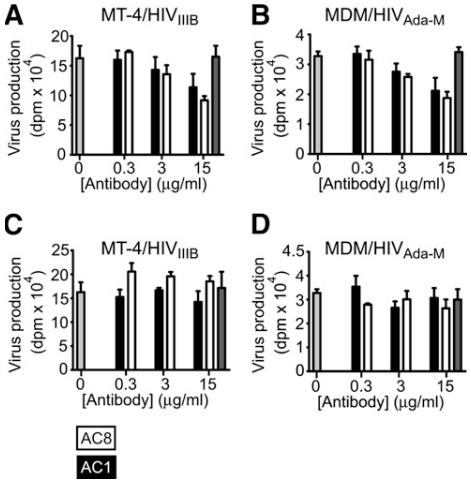

Fig. 6. Monoclonal ACHAs substantially inhibit in vitro HIV production of human T-cells and macrophages. MT-4 cells (A, C) and MDM cells (B, D) were infected with IIIB and Ada-M strains of HIV-1, respectively. Either the cells (A, B) or the viruses (C, D) were incubated with different concentrations of monoclonal ACHAs (black columns for AC1 and white columns for AC8) or left untreated (gray columns) for 1 h, prior to virus infection (see protocol 1 in Materials and Methods). Virus production, measured by RT assay, is displayed in dpm units as mean ± SD (from three independent measurements).

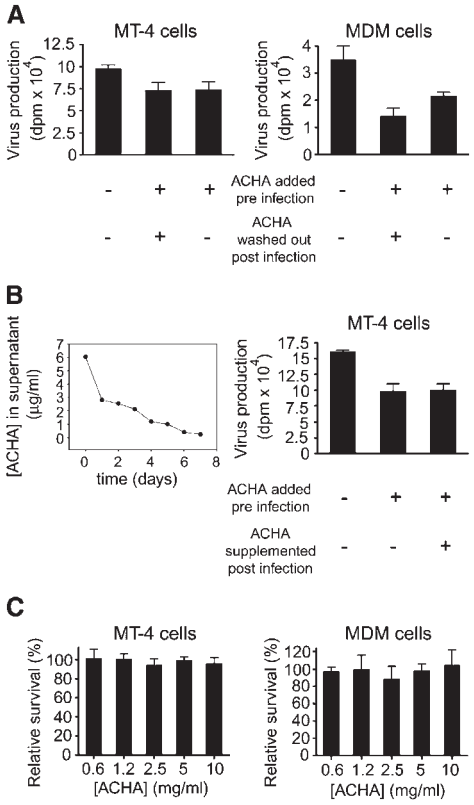

Fig. 7. The presence of ACHAs postinfection is not required for the inhibition and the antibodies are not cytotoxic. The virus production under different conditions (see protocols 2 and 3 in Materials and Methods) is shown in panels A and B. A: MT-4 cells and MDM cells were infected with IIIB and Ada-M strains of HIV-1, respectively. Monoclonal ACHAs were either not added to the cells (left columns), were preincubated with the cells and washed out (middle columns), or not washed out (right columns) after viral infection. B: ACHA level decreased in the culture supernatant of MT-4 cells postinfection as assessed by ELISA. MT-4 cells in the absence (left column) or presence (middle and right columns) of ACHA were infected with HIV-1. In order to maintain a constant level of ACHA (5 μg/ml) postinfection, the culture medium was continuously supplemented with the Ab (right column). Virus production, measured by RT assay, is displayed in dpm units as mean ± SD from three independent measurements. C: Viability of MT-4 cells and MDM cells treated with serially diluted concentrations of ACHA was determined after the whole assay period by Cell Titer assay and displayed as survival percentages (calculated from triplicates of cell samples). Viability of the untreated target cells was taken as 100%.

restrict somehow CXCR4 mobility and seemingly bring together the two critical HIV-1 receptor proteins into the same membrane microdomain, resulting in a crowding of these proteins. This may prevent attachment of the virus by "pulling together the carpet" necessary for multiple binding of viral glycoproteins to the surface of target cells.

The lateral diffusion properties of the molecules involved in HIV-1 entry, i.e., cholesterol, CD4, and CXCR4, gave further support to this view. The AC8 antibody bound to membrane cholesterol diffused moderately and strongly slower than small fluorescent cholesterol probes in model membranes with high cholesterol content or the same probes in fluid membrane phases, respectively (25). The size of the antibody label may partly be responsible for these differences. However, since the diffusion of membrane cholesterol is mostly controlled by the membrane environment rather than the extracellular aqeous phase (where the antibody is located), the slower diffusion also indicates that the AC8 cholesterol complexes diffuse in large, cholesterol-enriched microdomains.

In untreated control cells, the HIV-1 receptor CD4 diffused slower than the nonraft membrane protein CD2, and the diffusional rate of CXCR4 was significantly higher than that of CD4. The lateral mobility of CXCR4 but not of CD4 decreased substantially upon AC8 binding. The selectivity of AC8 effect on CXCR4 mobility is also demonstrated by the unaffected mobility of CD2 nonraft protein on the same cells. These data, and the similarity in diffusion coefficients of CD4 and CXCR4 after AC8 binding, are consistent with the picture that AC8 colocalizes the chemokine receptor and CD4 into the same compartment.

Based on these substantial changes in the dynamic membrane organization of HIV-1 receptors, it is postulated

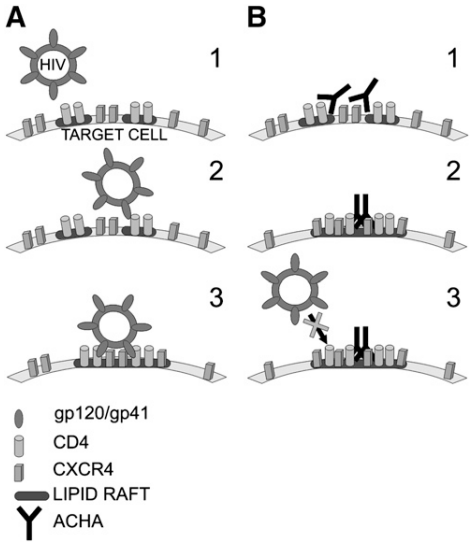

Fig. 8. A schematic model of the interference between ACHAs and HIV-1 attachment to T-cells and macrophages. A: HIV-1 enters the target cells through cholesterol-enriched membrane micorodomains (lipid rafts or caveolas). Interactions between viral glycoprotein, gp120, and raft-associated CD4 molecules result in conformational changes in gp120/gp41. Then, recruitment of CXCR4 chemokine receptors into the lipid rafts, near CD4-gp120 complexes, enables interactions of gp120 with coreceptors and formation of multimolecular complexes, resulting in attachment and internalization. B: Binding to HIV-1 permissive cells, the monoclonal cholesterol-specific IgG antibodies (ACHAs) cross-link smaller microdomains, and remodel the HIV-1 receptor-coreceptor interaction pattern. Molecular crowding of the receptors/coreceptors into the same larger microdomain may prevent a proper spatial juxtaposition of viral glycoproteins (gp120/gp41) to CD4 and chemokine receptors, necessary for formation of supramolecular complexes essential for HIV internalization. This may lead to inhibition of the viral attachment/entry.

that the AC8 mAb can mimic the action of viral glycoprotein gp120 in terms of coaggregating HIV-1 receptors and coreceptors, as proposed earlier (12). These data also concur with the findings that gp120-CD4 engagement leads to a cholesterol-sensitive lateral redistribution of membrane microdomains and a subsequent assembly of the virus internalization complex (6).

The novel cholesterol-specific antibodies preincubated with the target cells showed a significant and dose-dependent inhibitory effect on HIV-1 infection. This inhibition might be dependent on cell type, the nature of the virus strain, and the assay conditions. The inhibitory effects of AC1 and AC8 cholesterol-specific antibodies on MDM and T-cells were comparable to those previously reported for antiphosphatidylinositol-4-phosphate antibody exhibiting neutralizing activity and blocking infection of PBMC by two primary isolates of HIV-1 and to the well-known broadly neutralizing 4E10 on PBMC (13).

Considering that washing out of ACHAs prior to (or after) infection or their continuous supplementation throughout culturing did not significantly affect the final HIV-1 production, we concluded that their inhibitory effect is mostly due to modulation of the attachment/entry phase. Although it is difficult to distinguish between these two possibilities based on the present data, the unchanged inhibition observed after immediate washing out of ACHAs after infection suggests that the most likely phase that is inhibited is the attachment/anchorage of the virus to the target cell surface.

Thus, the presented data unequivocally show that the ACHAs act predominantly on the target cell membrane. Furthermore, the inhibition was found not to be due to either a direct, steric, masking effect of ACHAs or to their effects on chemokine receptor internalization. It still remains a question why the ACHAs did not act on the virus, although the viral membrane also contains cholesterol. This can be due, in part, to an insufficient extent of viral membrane-cholesterol clustering or a highly shielded epitope by surrounding viral glycoproteins.

The findings presented here may have an impact on the future development of HIV-1 specific vaccines as well (26). Recent data indicate that antibodies with membrane-pattern binding characteristics versus antibodies binding to one lipid or one protein may offer a better perspective to develop new, efficient vaccine candidates (35). The novel cholesterol-specific antibodies, recognizing "properly clustered membrane cholesterol only", seem useful to investigate the eventual role of cholesterol in the process of virus entry, which may be the Achilles' heel of the virion (36). Induction of broadly neutralizing antibodies is an essential prerequisite of an effective anti-HIV-1 vaccine. Although several different promising approaches have been applied in development of such vaccines against different viral proteins, this task seems to be extremely difficult. Therefore, alternative approaches for interfering with HIV-1 entry to target cells utilizing drugs or antibodies against cellular structures (CD4, CCR5, CXCR4, HLA class I and II, and ICAM-1) involved in the entry process (37) seem to be equally important. Since, as detailed above, cholesterol also has a major role in these processes, cholesterol-specific antibodies may also merit consideration.

In conclusion, the new cholesterol-specific mAbs, AC1 and AC8, inhibit HIV-1 production of human T-cells and macrophages by acting on the plasma membrane and HIV-1 receptors of target cells (**Fig. 8**), and not on the virus, as most known neutralizing antibodies do. They interfere most likely with the virus attachment. Although some mechanistic details of their action on target cells remain open, we believe that the inhibitory effect and the basic background mechanisms described herein may be helpful in further studies to clarify the cholesterol dependence of the attachment/entry mechanism, as well as may serve as a molecular basis for the development of new, combined lipid raft-oriented approaches in HIV-1 therapy (26).

The authors are grateful to Erzsebet T. Veress for the skillful technical assistance.

REFERENCES

1. Alving, C. R., and N. M. Wassef. 1999. Naturally occurring antibodies to cholesterol: a new theory of LDL cholesterol metabolism. *Immunol. Today.* **20:** 362–366.
2. Biro, A., L. Cervenak, A. Balogh, A. Lorincz, K. Uray, A. Horvath, L. Romics, J. Matko, G. Fust, and G. Laszlo. 2007. Novel anti-cholesterol monoclonal immunoglobulin G antibodies as probes and potential modulators of membrane raft-dependent immune functions. *J. Lipid Res.* **48:** 19–29.
3. Matko, J., and J. Szollosi. 2005. Regulatory aspects of membrane microdomain (raft) dynamics in live cells. *In* Membrane Microdomain Signaling: Lipid Rafts in Biology and Medicine. M. P. Mattson, editor. Humana Press, Totowa, NJ. 15–46.
4. Pike, L. J. 2003. Lipid rafts: bringing order to chaos. *J. Lipid Res.* **44:** 655–667.
5. Hug, P., H. M. Lin, T. Korte, X. Xiao, D. S. Dimitrov, J. M. Wang, A. Puri, and R. Blumenthal. 2000. Glycosphingolipids promote entry of a broad range of human immunodeficiency virus type 1 isolates into cell lines expressing CD4, CXCR4, and/or CCR5. *J. Virol.* **74:** 6377–6385.
6. Manes, S., G. del Real, R. A. Lacalle, P. Lucas, C. Gomez-Mouton, S. Sanchez-Palomino, R. Delgado, J. Alcami, E. Mira, and A. C. Martinez. 2000. Membrane raft microdomains mediate lateral assemblies required for HIV-1 infection. *EMBO Rep.* **1:** 190–196.
7. Nisole, S., B. Krust, and A. G. Hovanessian. 2002. Anchorage of HIV on permissive cells leads to coaggregation of viral particles with surface nucleolin at membrane raft microdomains. *Exp. Cell Res.* **276:** 155–173.
8. Fantini, J., N. Garmy, R. Mahfoud, and N. Yahi. 2002. Lipid rafts: structure, function and role in HIV, Alzheimer's and prion diseases. *Expert Rev. Mol. Med.* **4:** 1–22.
9. Jolly, C., and Q. J. Sattentau. 2005. Human immunodeficiency virus type 1 virological synapse formation in T cells requires lipid raft integrity. *J. Virol.* **79:** 12088–12094.
10. Nguyen, D. H., and J. E. Hildreth. 2000. Evidence for budding of human immunodeficiency virus type 1 selectively from glycolipid-enriched membrane lipid rafts. *J. Virol.* **74:** 3264–3272.
11. Popik, W., T. M. Alce, and W. C. Au. 2002. Human immunodeficiency virus type 1 uses lipid raft-colocalized CD4 and chemokine receptors for productive entry into CD4(+) T cells. *J. Virol.* **76:** 4709–4722.
12. Nguyen, D. H., B. Giri, G. Collins, and D. D. Taub. 2005. Dynamic reorganization of chemokine receptors, cholesterol, lipid rafts, and adhesion molecules to sites of CD4 engagement. *Exp. Cell Res.* **304:** 559–569.
13. Brown, B. K., N. Karasavvas, Z. Beck, G. R. Matyas, D. L. Birx, V. R. Polonis, and C. R. Alving. 2007. Monoclonal antibodies to

phosphatidylinositol phosphate neutralize human immunodeficiency virus type 1: role of phosphate-binding subsites. *J. Virol.* **81:** 2087–2091.
14. Adamczyk, M., J. C. Gebler, and J. Wu. 2000. Papain digestion of different mouse IgG subclasses as studied by electrospray mass spectrometry. *J. Immunol. Methods.* **237:** 95–104.
15. Costes, S. V., D. Daelemans, E. H. Cho, Z. Dobbin, G. Pavlakis, and S. Lockett. 2004. Automatic and quantitative measurement of protein-protein colocalization in live cells. *Biophys. J.* **86:** 3993–4003.
16. Roszik, J., D. Lisboa, J. Szollosi, and G. Vereb. 2009. Evaluation of intensity-based ratiometric FRET in image cytometry - approaches and a software solution. *Cytometry A.* **75:** 761–777.
17. Haustein, E., and P. Schwille. 2007. Fluorescence correlation spectroscopy: novel variations of an established technique. *Annu. Rev. Biophys. Biomol. Struct.* **36:** 151–169.
18. Gombos, I., G. Steinbach, I. Pomozi, A. Balogh, G. Vamosi, A. Gansen, G. Laszlo, G. Garab, and J. Matko. 2008. Some new faces of membrane microdomains: a complex confocal fluorescence, differential polarization, and FCS imaging study on live immune cells. *Cytometry A.* **73:** 220–229.
19. Gendelman, H. E., J. M. Orenstein, M. A. Martin, C. Ferrua, R. Mitra, T. Phipps, L. A. Wahl, H. C. Lane, A. S. Fauci, D. S. Burke, et al. 1988. Efficient isolation and propagation of human immunodeficiency virus on recombinant colony-stimulating factor 1-treated monocytes. *J. Exp. Med.* **167:** 1428–1441.
20. Wong-Staal, F., G. M. Shaw, B. H. Hahn, S. Z. Salahuddin, M. Popovic, P. Markham, R. Redfield, and R. C. Gallo. 1985. Genomic diversity of human T-lymphotropic virus type III (HTLV-III). *Science.* **229:** 759–762.
21. Hoffman, A. D., B. Banapour, and J. A. Levy. 1985. Characterization of the AIDS-associated retrovirus reverse transcriptase and optimal conditions for its detection in virions. *Virology.* **147:** 326–335.
22. Zhao, Q., J. T. Ernst, A. D. Hamilton, A. K. Debnath, and S. Jiang. 2002. XTT formazan widely used to detect cell viability inhibits HIV type 1 infection in vitro by targeting gp41. *AIDS Res. Hum. Retroviruses.* **18:** 989–997.
23. Rey, M., A. Valenzuela-Fernandez, A. Urzainqui, M. Yanez-Mo, M. Perez-Martinez, P. Penela, F. Mayor, Jr., and F. Sanchez-Madrid. 2007. Myosin IIA is involved in the endocytosis of CXCR4 induced by SDF-1alpha. *J. Cell Sci.* **120:** 1126–1133.
24. Xiao, X., L. Wu, T. S. Stantchev, Y. R. Feng, S. Ugolini, H. Chen, Z. Shen, J. L. Riley, C. C. Broder, Q. J. Sattentau, et al. 1999. Constitutive cell surface association between CD4 and CCR5. *Proc. Natl. Acad. Sci. USA.* **96:** 7496–7501.
25. Bacia, K., P. Schwille, and T. Kurzchalia. 2005. Sterol structure determines the separation of phases and the curvature of the liquid-ordered phase in model membranes. *Proc. Natl. Acad. Sci. USA.* **102:** 3272–3277.
26. Alving, C. R., Z. Beck, N. Karasavva, G. R. Matyas, and M. Rao. 2006. HIV-1, lipid rafts, and antibodies to liposomes: implications for anti-viral-neutralizing antibodies. *Mol. Membr. Biol.* **23:** 453–465.
27. Haynes, B. F., J. Fleming, E. W. St Clair, H. Katinger, G. Stiegler, R. Kunert, J. Robinson, R. M. Scearce, K. Plonk, H. F. Staats, et al. 2005. Cardiolipin polyspecific autoreactivity in two broadly neutralizing HIV-1 antibodies. *Science.* **308:** 1906–1908.
28. Harder, T., P. Scheiffele, P. Verkade, and K. Simons. 1998. Lipid domain structure of the plasma membrane revealed by patching of membrane components. *J. Cell Biol.* **141:** 929–942.
29. Charrin, S., S. Manie, C. Thiele, M. Billard, D. Gerlier, C. Boucheix, and E. Rubinstein. 2003. A physical and functional link between cholesterol and tetraspanins. *Eur. J. Immunol.* **33:** 2479–2489.
30. Kozak, S. L., J. M. Heard, and D. Kabat. 2002. Segregation of CD4 and CXCR4 into distinct lipid microdomains in T lymphocytes suggests a mechanism for membrane destabilization by human immunodeficiency virus. *J. Virol.* **76:** 1802–1815.
31. Singer, I. I., S. Scott, D. W. Kawka, J. Chin, B. L. Daugherty, J. A. DeMartino, J. DiSalvo, S. L. Gould, J. E. Lineberger, L. Malkowitz, et al. 2001. CCR5, CXCR4, and CD4 are clustered and closely apposed on microvilli of human macrophages and T cells. *J. Virol.* **75:** 3779–3790.
32. Viard, M., I. Parolini, M. Sargiacomo, K. Fecchi, C. Ramoni, S. Ablan, F. W. Ruscetti, J. M. Wang, and R. Blumenthal. 2002. Role of cholesterol in human immunodeficiency virus type 1 envelope protein-mediated fusion with host cells. *J. Virol.* **76:** 11584–11595.
33. Hovanessian, A. G., J. P. Briand, E. A. Said, J. Svab, S. Ferris, H. Dali, S. Muller, C. Desgranges, and B. Krust. 2004. The caveolin-1 binding domain of HIV-1 glycoprotein gp41 is an efficient B cell epitope vaccine candidate against virus infection. *Immunity.* **21:** 617–627.
34. Nagy, P., G. Vereb, Z. Sebestyen, G. Horvath, S. J. Lockett, S. Damjanovich, J. W. Park, T. M. Jovin, and J. Szollosi. 2002. Lipid rafts and the local density of ErbB proteins influence the biological role of homo- and heteroassociations of ErbB2. *J. Cell Sci.* **115:** 4251–4262.
35. Beck, Z., N. Karasavvas, G. R. Matyas, and C. R. Alving. 2008. Membrane-specific antibodies induced by liposomes can simultaneously bind to HIV-1 protein, peptide, and membrane lipid epitopes. *J. Drug Target.* **16:** 535–542.
36. Haynes, B. F., and S. M. Alam. 2008. HIV-1 hides an Achilles' heel in virion lipids. *Immunity.* **28:** 10–12.
37. Phogat, S., R. T. Wyatt, and G. B. Karlsson Hedestam. 2007. Inhibition of HIV-1 entry by antibodies: potential viral and cellular targets. *J. Intern. Med.* **262:** 26–43.

Chapter 8

Andrea Balogh, Mónika Ádori, Katalin Török, Janos Matko, Glória László

Closer look into the GL7 antigen: Its spatio-temporally selective differential expression and localization in lymphoid cells and organs in human

Immunology Letters 2009. doi:10.1016/j.imlet.2009.12.008

G Model
IMLET-4890; No. of Pages 8
ARTICLE IN PRESS

Immunology Letters xxx (2009) xxx–xxx

Contents lists available at ScienceDirect

Immunology Letters

journal homepage: www.elsevier.com/locate/

A closer look into the GL7 antigen: Its spatio-temporally selective differential expression and localization in lymphoid cells and organs in human

Andrea Balogh[b,1], Mónika Ádori[a,1], Katalin Török[a], Janos Matko[a,b], Glória László[a,*]

[a] Department of Immunology, Eotvos Lorand University, Pazmany Peter setany 1/C, H-1117 Budapest, Hungary
[b] Immunology Research Group of Hungarian Academy of Sciences at Eotvos Lorand University, Pazmany Peter setany 1/C, H-1117 Budapest, Hungary

ARTICLE INFO

Article history:
Received 16 November 2009
Received in revised form
26 November 2009
Accepted 2 December 2009
Available online xxx

Keywords:
GL7
Human lymphocytes
Rat lymphocytes
Lipid rafts
Lectins
Carbohydrate epitope

ABSTRACT

The GL7 epitope was originally described as part of a late lymphocyte activation antigen expressed in mouse and widely used since then as a marker of germinal center. Here we report on its differential expression by rat and human immune cells and lymphoid organs. Expression pattern of the GL7 epitope in rats is similar to that described earlier in mice, namely that GL7 antigen appears only on lymphocytes after 48 h activation. In humans lymphocytes, but not the differentiated cells of myeloid origin, express this epitope. The GL7 epitope is up-regulated upon *in vitro* activation of primary T cells, while a slightly decreased expression is found on B lymphocytes. Fluorescent immunohistochemistry shows discrete location of $GL7^{hi}$ cells in human tonsil. GL7 antibody intensely stains $CD19^{+}$, IgD^{+}, IgM^{low} B lymphocytes found at the margin of B cell follicles. The GL7 epitope is constitutively and highly raft-associated in human lymphoid cells. Strong neuraminidase- and partial papain-sensitivity of the GL7 epitope on human lymphocytes indicates a sialic acid-containing epitope linked either to one (or more) membrane protein(s) or to lipids. The lymphocyte-restricted GL7 epitope expression and the activation-dependent bi-directional change in the amount of the epitope suggest a functional role for GL7 epitope linked to carbohydrate-based immunoregulation.

1. Introduction

Glycosylation is an enzymatic process producing a diverse repertoire of glycans linked to proteins, lipids or other saccharides. An increasing number of studies show the importance of glycosylation in pathogen recognition, in controlling homeostasis and inflammation or in the maturation and activation of adaptive immune cells [1,2]. Sialic acid (Sia) is a general term for a diverse family of nine-carbon sugars that are all derived from neuraminic acid (Neu) or keto-deoxynonulosonic acid (KDN). They are typically found on the exposed termini of mammalian oligosaccharide chains attached to cell surface proteins or lipids [3]. Sias are transferred using α2–3, α2–6 or α2–8 linkages to subterminal sugars by a family of about twenty sialyltransferases [4,5]. Siglecs are a family of sialic acid binding proteins with immunoglobulin like domains, that are known to influence various functions of mammalian immune cells [6,7]. Most of them contains ITIM- and/or ITIM-like motifs, just as CD22, indicating a negative regulatory role. Although signaling and function of siglecs is still controversial, this question is an intensely examined field of nowadays immunology.

GL7, a rat monoclonal IgM antibody was produced against *in vitro* activated mouse B lymphoblasts and described to bind to a 35 kDa late activation antigen expressed by mouse B and T lymphocytes [8]. All tested DNA, RNA and protein synthesis inhibitors strongly prevented the expression of the GL7 epitope [8]. In lymph node and spleen the GL7 staining pattern was found very similar to that of peanut agglutinin (PNA) and so the GL7 epitope has become a frequently used marker of germinal centers [9–12]. The epitope has also been found on a small subpopulation of thymocytes [13]. In the mouse bone marrow the GL7 epitope is detectable as early as on the pro-B/early pre-B cell stages and its expression becomes very high on large pre-B cells but it is completely down-regulated on mature naive resting B cells, so it may define the cycling stage of B cell maturation [14,15]. In a study that compared functional capacities of sorted and activated spleen and lymph node B lymphocytes, only the $GL7^{+}$ cells proliferated and produced antibodies [8,14]. Later the antibody was shown to recognize the Neu5Acα2-6Galβ1-4GlcNAcβ1-3Galβ1-4Glc carbohydrate epitope [16]. Since no single protein could be identified clearly as a well defined antigen, the question arises whether the epitope is linked to a single protein or a mixture of various cell surface glycosylated proteins and/or lipids.

Maturation and activation of B cells are accompanied with an elevated β-galactoside α2,6-sialyltransferase (ST6Gal I) level. This enzyme is responsible for the attachment of α2,6-linked Sias to

* Corresponding author. Tel.: +36 1 381 2175; fax: +36 1 381 2176.
E-mail address: glorial@elte.hu (G. László).
[1] They contributed equally to this work.

0165-2478/$ – see front matter © 2009 Elsevier B.V. All rights reserved.
doi:10.1016/j.imlet.2009.12.008

Galβ1,4-GlcNAc-R termini in lymphoid cells [17,18]. CMP-Neu-5Ac hydroxylase (CMAH) was shown to convert N-actylneuraminic acid (Neu5Ac) to N-glycolylneuraminic acid (Neu5Gc). These two enzymes are considered as key players in regulation of GL7 level in mice. Due to a mutation that occurred after our segregation from the great apes, CMAH hydroxylase activity had been lost in humans and significant changes in binding preferences and expression profile of certain siglecs have also been resided [19,20].

The present study thus aimed at comparing GL7 epitope expression and membrane localization in rat and human immunocytes and lymphoid tissues, with the purpose to understand how the appearance of this epitope at discrete sites of the immune system may correlate with the major events of immune cells activation and function. Our results show that although human peripheral lymphocytes constitutively express the GL7 epitope due to the absence of CMAH activity, the expression level of GL7 epitope can further increase or decrease upon activation of T and B lymphocytes, respectively. The correlation pattern between GL7 epitope expression and binding of various lectins to the surface of human immunocytes further confirms that the α2,6-linked Neu5Ac is involved in the GL7 epitope in human as well. The expressed GL7 epitope (possibly attached to protein or lipid molecules) is highly raft-associated in lymphoid cells. This and the spatially and temporally selective expression pattern, which differs from that of rodents, suggest a possible regulatory or adhesion functions of the GL7 epitope-linked molecule(s) in human.

2. Materials and methods

2.1. Cells

Rat cell suspension was prepared from spleen after removing erythrocytes with ACK lysing buffer (155 mM ammonium chloride, 10 mM potassium bicarbonate, 102 μM disodium ethylenediamine tetraacetate, pH 7.2) then culturing in DMEM (Sigma–Aldrich, St. Louis, MO) supplemented with 2-mercapthoethanol and 10% FCS.

Ramos and Daudi human B lymphomas (American Type Cell Culture/ATTC), Jurkat human leukemic T cell line and THP-1 human leukemic monocyte cell line were cultured in RPMI 1640 medium supplemented with 10% FCS. Tonsils were obtained from St. Imre Hospital and the buffy coat, obtained from healthy donors, was provided by the Hungarian National Blood Transfusion Service. Human B cells were isolated from tonsils using Ficoll-Hypaque (Amersham, Uppsala, Sweden) and depletion of T cells with 2-aminoethylisothiouronium bromide (AET)-treated sheep erythrocytes. Human $CD4^+$ T lymphocytes were isolated from buffy coat with RosetteSep® Human $CD4^+$ T Cell Enrichment Coctail (StemCell Technologies, Vancouver, BC, Canada) according to the manufacturer's protocol. Isolated primary lymphocytes were maintained in RPMI 1640 medium supplemented with 10% FCS and gentamycin. Peripheral blood mononuclear cells (PBMCs) were isolated from buffy coat with Ficoll-Hypaque. DCs were differentiated from blood monocytes as described by Csomor et al. [21]. Human granulocytes were purified from buffy coat by combining the dextran sedimentation method with a Ficoll-Hypaque gradient procedure as described previously [22]. All experiments with human samples were in accordance with national regulations and were authorized by the ethical committee of the institute.

2.2. Activation of cells

To activate cells, rat splenocytes were cultured in the presence of 5 μg/ml ConA (Sigma–Aldrich), or of 10 μg/ml LPS (Sigma–Aldrich).

Primary B cells were activated with 10 μg/ml $F(ab')_2$ fragment of goat anti-human IgG + IgM (Jackson ImmunoResearch, Suffolk, UK). T lymphocytes were stimulated with 10 μg/ml of anti-human CD3 on coat (ImmunoTools, Friesoythe, Germany).

2.3. Immunofluorescence labeling of cells and flow cytometry

Activated or control rat spleen cells were also analyzed in terms of the GL7 epitope expression. To distinguish rat splenic cell populations, cells were stained with FITC-conjugated anti-rat CD3 (Invitrogen-Caltag, Eugen, OR) and mouse biotin-conjugated anti-rat IgM (MAR2/2 clone from Eotvos Lorand University, ELU, Budapest, Hungary) followed by incubation with avidin-FITC (Sigma–Aldrich).

Lymphocytes and myeloid cells were incubated with monoclonal GL7 antibody (GL7 clone from Gloria Laszlo, ELU), washed and incubated with FITC-conjugated mouse anti-rat IgM (MAR2/2 clone from ELU) or Alexa Fluor647-conjugated goat anti-rat IgM (Invitrogen-Molecular Probes, Eugene, OR). To distinguish blood cell populations, PBLs were stained with antibodies specific to different cell types: anti-human CD4-FITC (ImmunoTools) and anti-human CD8-PE (ImmunoTools) for T cell subpopulations, biotin-conjugated anti-human CD19 (BD Pharmingen, San Jose, CA) and avidin-FITC (Sigma–Aldrich) as secondary reagent for B cells, and anti-human CD14-PE (Santa Cruz Biotechnology, Santa Cruz, CA) for monocytes. The purity of granulocytes was determined by staining with anti-human CD66abce-FITC (Dako, Glostrup, Denmark), and the purity of DCs was monitored using anti-human CD11c-Alexa Fluor647 (AbD Serotec, Oxford, UK). In some experiments, cells were stained at first with biotinylated Sambucus Nigra Lectin (SNA), biotinylated Maackia Amurensis Lectin II (MAA) (Vector Laboratories, Burlingame, CA) or biotinylated Peanut Agglutinin (PNA) (Sigma–Aldrich) lectin, and washing was followed by incubation with avidin-FITC.

Activated lymphocytes were labeled with different activation marker-specific antibodies. Activated B cells were labeled with GL7 Ab in combination with the following antibodies: Alexa Fluor647-conjugated cholera toxin B-subunit (CTX-B) (Invitrogen-Molecular Probes), anti-human MHCII-FITC (BD Pharmingen) and anti-human CD86 (ImmunoTools)/Alexa Fluor488-conjugated goat anti-mouse IgG1 (Invitrogen-Molecular Probes). Activated T lymphocytes were stained with GL7 antibody and CTX-Alexa Fluor647, anti-human CD69-APC (BD Pharmingen), anti-human CD25-APC (BD Pharmingen). All incubation steps were performed at 4 °C for 20 min. The washing was carried out with ice-cold FACS buffer (PBS supplemented with 1% FCS). Isotype control antibodies were used as negative controls in all experiments: rIgM (ROX4, clone from ELU), mIgG1-FITC (PPV-06, ImmunoTools), mIgG1-PE (PPV-06, ImmunoTools), mIgG1-biotin (PPV-06, ImmunoTools), mIgG1-APC (MOPC-21, BD Pharmingen) and affinity purified mIgG1 (15H6, Southern Biotech, Birmingham, AL).

Twenty thousand cells were collected and analyzed in a FACSCalibur flow cytometer (Becton-Dickinson) using CellQuest Pro software, and then analyzed with FCS Express 3 software (De Novo Software, Los Angeles, CA).

2.4. Enzymatic treatment of cells

In some assays cells were exposed to a limited papain digestion (Sigma–Aldrich) (20 U/ml) for 20 min at 37 °C in Hank's balanced salt solution (HBSS, pH 6) (Sigma–Aldrich). This treatment served to remove long protruding extracellular domains of glycoproteins. Cells were then washed extensively with ice-cold FACS buffer and stained as described previously.

To remove sialic acid residues from cell surface, cells were incubated with 50 mU/ml neuraminidase form Vibrio cholerae (Sigma–Aldrich) for 30 min at 37 °C in HEPES buffered saline (HEBS) buffer (20 mM HEPES, 140 mM natrium chloride, 1 mM calcium

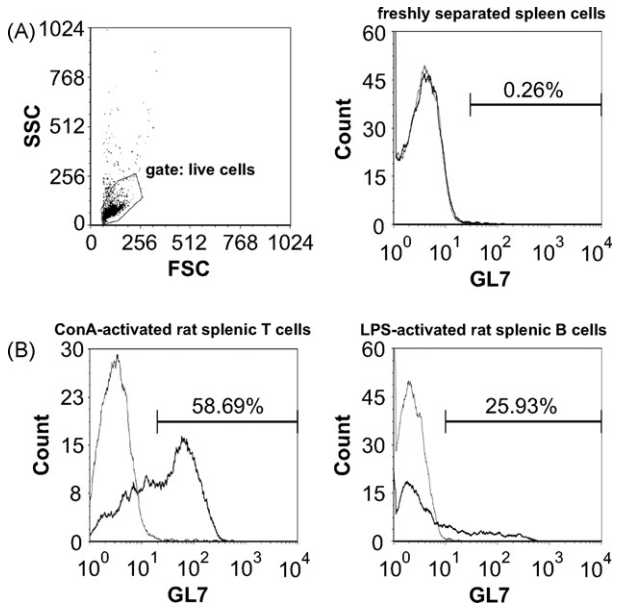

Fig. 1. Expression of GL7 is activation dependent in rat lymphocytes. GL7 epitope expression of freshly prepared rat spleen cells (A) or activated T and B lymphocytes (B) were analyzed by flow cytometry. Representative flow cytometric histograms of three independent measurements are displayed. Thick line shows GL7 Ab binding and thin line corresponds to the isotype control.

chloride, pH 7). Washed cells were then stained as described previously.

2.5. Flow cytometric detergent resistance measurements (FCDR)

Detergent resistance of some cell surface molecules were determined by the method of Gombos et al. [23]. Briefly, Ramos B cells (10^6 ml^{-1}) were treated or not with 10 mM methyl-beta-cyclodextrin (MBCD) (Cyclolab, Budapest, Hungary) for 15 min at 37 °C in phosphate buffered saline (PBS). After washing, cells were labeled with biotinylated GL7 antibody and Alexa Fluor647-conjugated streptavidin (Invitrogen-Molecular Probes), CTX-Alexa Fluor647 or anti-human CD71 and Alexa Fluor647-conjugated goat anti-mouse IgG2a (Invitrogen-Molecular Probes) as described previously. Labeled cells were measured on a FACSCalibur flow cytometer before and 10 min after mixing cells with 0.1% (final concentration) cold Triton X-100 (Sigma–Aldrich). The calculation of detergent resistance (FCDR) is detailed elsewhere [23].

2.6. Confocal microscopy

Activated rat lymphocytes or human cell lines and primary T or B cells were labeled with GL7 antibody in combination with CTX-Alexa Fluor647. Cells were also incubated with anti-human CD71-Alexa Fluor488 (Exbio, Prague, Czech Republic) as described previously. Stained cells were mounted on coverslips and assayed with an Olympus Fluoview 500 confocal microscope (Hamburg, Germany) equipped with four optical channels, using a 60× (N.A.: 1.45) objective.

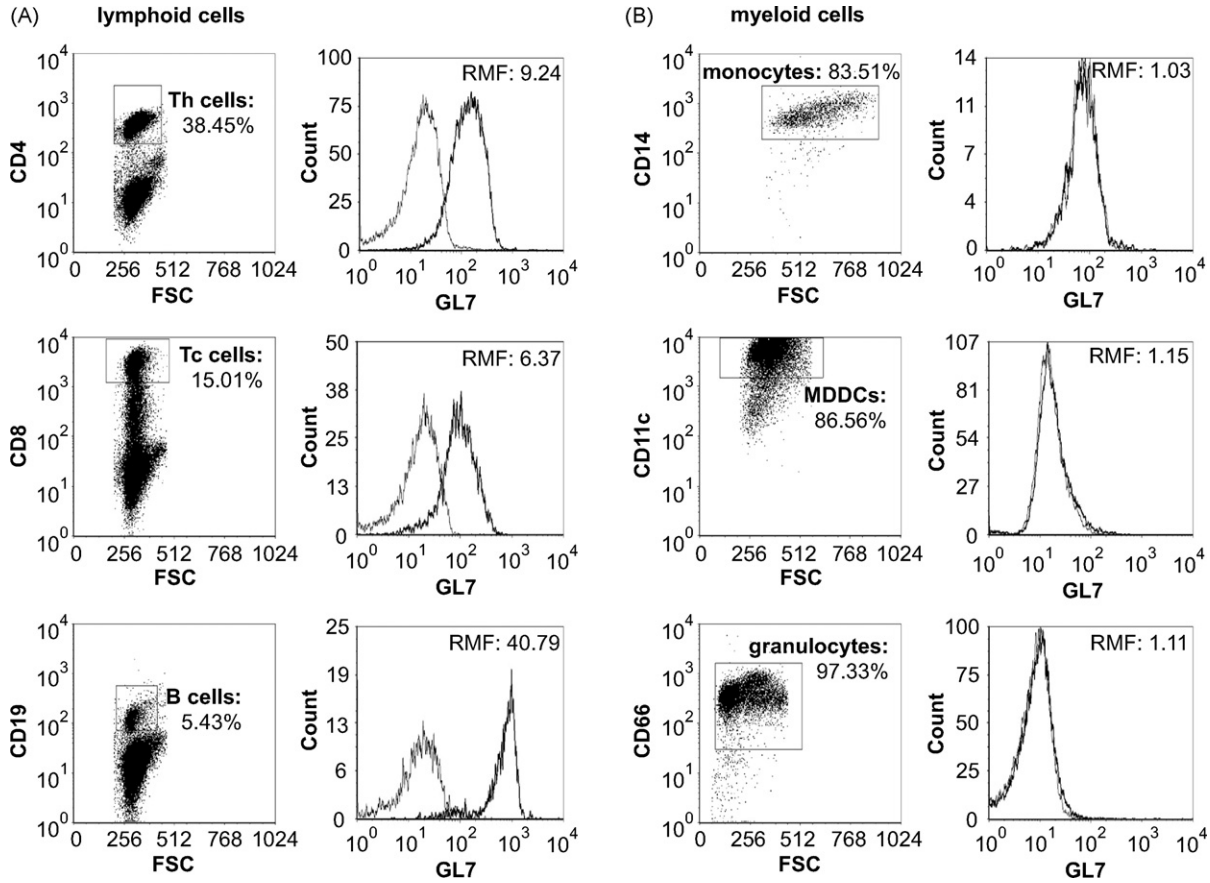

Fig. 2. GL7 is expressed only by lymphocytes among human blood cells. Different blood cell populations were stained for GL7 in combination with cell-type specific antibodies. Flow cytometric histograms of lymphoid (A) and myeloid (B) blood cells are shown. Relative mean of fluorescence (RMF) was calculated from mean fluorescence intensity (MFI) of GL7 Ab staining (thick line) divided by the MFI of isotype control binding (thin line). Plots are representatives of three independent measurements.

Colocalization indices were determined from ~100 ROIs (region of interest)/sample using the ImageJ software (http://rsbweb.nih.gov/ij), with the appropriate colocalization plugin. The Pearson's colocalization index (CI) provides a reliable estimate on the extent of protein colocalization: CI values close to zero indicate no or a very low degree, while CI ≥ 0.5 reflects a high degree of colocalization; CI = 1 corresponds to a full overlap between the two colors in each pixels of the image.

2.7. Fluorescence immunohistochemistry

Five μm thick cryosections of human tonsil samples were placed on Superfrost Ultra Plus slides (Thermo Scientific, Walthem, MA), fixed with 4% paraformaldehyde and kept at 4 °C in PBS until staining.

Unspecific antibody binding was blocked with 10% FCS in PBS (30 min at room temperature). Samples were incubated for 45 min at room temperature with the following antibodies and reagents in different combinations: affinity purified or biotinylated GL7 antibody (eBiosience, San Diego, CA), anti-human CD19 (BD Pharmingen), biotinylated anti-human IgD (Southern Biotech) antibodies, and SNA-biotin or MAA II-biotin in PBS containing 1% FCS. Washing was followed by incubation (45 min at room temperature) with secondary antibodies and reagents or directly labeled antibodies: FITC-conjugated anti-rat IgM for GL7 Ab, Alexa Fluor647-conjugated anti-mouse IgG1 (Invitrogen-Molecular Probes) for anti-CD19, streptavidin-Alexa Fluor488 or -Alexa Fluor647 (Invitrogen-Molecular Probes) for biotinylated antibodies/lectins, anti-human CD3-PE (ImmunoTools) and anti-human IgM-Cy5 (Jackson ImmunoResearch). Isotype control antibodies were used as negative controls: previously specified (see Section 2.3) antibodies and rIgM-biotin (R4-22, BD Pharmingen). Washed samples were assayed with an Olympus Fluoview 500 confocal microscope using a 10× objective.

3. Results

3.1. GL7 shows similar expression profile among rodents

Neu5Ac, part of a recently shown carbohydrate epitope recognized by GL7 Ab is commonly expressed in mammals. GL7 mAb was originally produced in rats so we were interested if the antibody binds to rat cells. Neither T nor B cells of freshly prepared rat spleen were GL7$^+$ (Fig. 1A). However 48–60 h after *in vitro* activa-

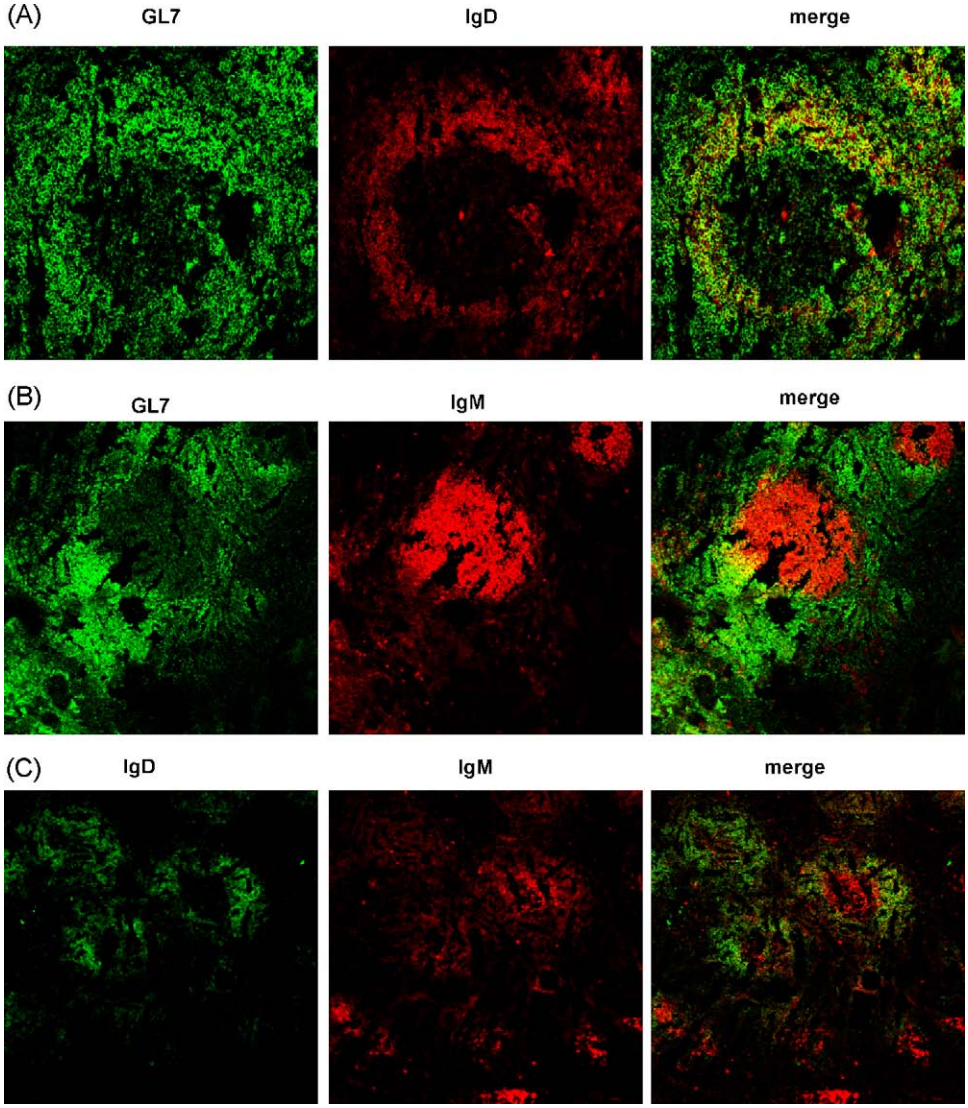

Fig. 3. High amount of GL7 expressing human tonsillar cells are IgD$^+$, IgM^{low} B cells. Cryosections of human tonsils were stained with GL7 Ab and anti-human IgD (A) or anti-human IgM (B), and assayed by confocal microscopy. Visualization of IgD$^+$ and IgM$^+$ cells is also shown (C). Images are representatives of three independent experiments.

tion a high GL7 epitope expression was observed on both B and T lymphocytes (Fig. 1B), similarly to the earlier finding in mice.

3.2. In human GL7 is expressed only on lymphocytes but not on cells of myeloid origin

Previously it was demonstrated that GL7 epitope is expressed by various human B cell lines [16]. In order to see which human immunocytes express the antigen, PBMCs and granulocytes were isolated from buffy coat and their GL7 expression was monitored by flow cytometry. In addition, DCs, differentiated from monocytes, were also analyzed. Among human blood cells, B and T lymphocytes are GL7$^+$ (Fig. 2A), while monocytes, granulocytes and DCs (Fig. 2B), even in mature stage, do not express the GL7 epitope on their surface. Furthermore, B cells express approximately fourfold more GL7 epitope than T cells (Fig. 2A). Thus, in human the GL7 epitope seems to be constitutively expressed, but exclusively on lymphocytes.

3.3. GL7 antibody firmly stains the border of germinal centers in human tonsil

Since the expression profile of GL7 epitope differs among human and rodent immune cells under normal conditions, as a next step, we analyzed the presence of GL7 epitope and other carbohydrate patterns in human lymphoid organs. Therefore, tonsil cryosections were incubated with GL7 antibody or various lectins in combination with antibodies specific to different cell types. The immunocytochemically stained samples were then assessed by confocal microscopy. The GL7 epitope is not homogenously expressed in the human tonsil. GL7^{hi} cells are located in the border of B cell follicles, as these cells are CD19$^+$, IgD$^+$ IgM^{med} B cells (Figs. 3 and 4A). Comparing the staining pattern of GL7 antibody and different lectins in the human tonsil, GL7 Ab and MAA II (α2–3 sialic acid specific) lectin showed disparate staining with a preferential binding of MAA II to CD3$^+$ T lymphocyte regions (Fig. 4B). In contrast, GL7 Ab and SNA (α2–6 sialic acid specific) lectin displayed an overlapping staining with their preferential binding to CD19$^+$ B cell regions over T lymphocytes (Fig. 4C). Nevertheless SNA has a broader binding spectrum by intensive staining of whole germinal centers. PNA lectin, dominantly recognizing the galactosyl-β1-3-N-acetylgalactosamine motif, intensely stained germinal centers and small capillary vessels (data not shown) showing a staining pattern distinct from that of GL7 Ab. These data together indicate that the GL7 epitope in human also contains the dominant α2,6-linked Neu5Ac residue.

3.4. Further insight into the nature of the GL7 epitope in human lymphoid cells

We also examined whether there is correlation between the binding of GL7 Ab and different lectins to cell surface. This is an interesting question, since the glycan expression profile is usually cell-type specific. Binding of GL7 Ab and SNA lectin to 6 different human T and B cell lines and primary lymphocytes showed strong positive correlation, whereas MAA II lectin and GL7 Ab displayed a strong negative correlation in staining of cells. The PNA lectin lacking sialic acid specificity showed no correlation at all with GL7 Ab staining (Fig. 5A).

In order to characterize the nature of the GL7 epitope, the digestion profile of neuraminidase and papain was compared for GL7 Ab and various lectins. Treatment of cells with neuraminidase from Vibrio cholerae completely abrogates binding of GL7 Ab and MAA II lectin, while only a partial decrease of SNA lectin binding was observed. The carbohydrate motif recognized by PNA lectin became more exposed upon neuraminidase digestion (Fig. 5B). Papain with a cleavage site of Phe-X–Y (X: non-specific, preferably Arg or Lys;

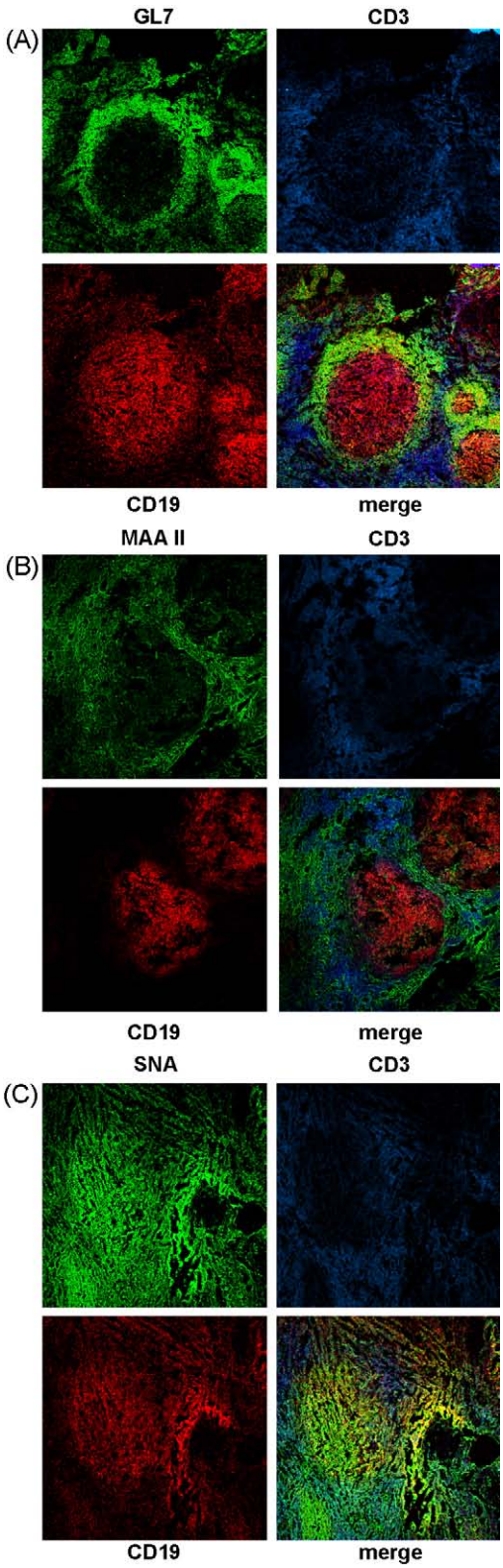

Fig. 4. GL7 Ab strongly stains the border of B cell follicles showing distinct staining pattern compared to plant lectins. Tonsillar cryosections were stained with GL7 Ab (A), simultaneously with anti-human CD3 and anti-human CD19 and visualized by confocal imaging. Binding of α2–3 specific MAA II lectin (B) and α2–6 specific SNA lectin (C) is also displayed. Images are representatives of three independent experiments.

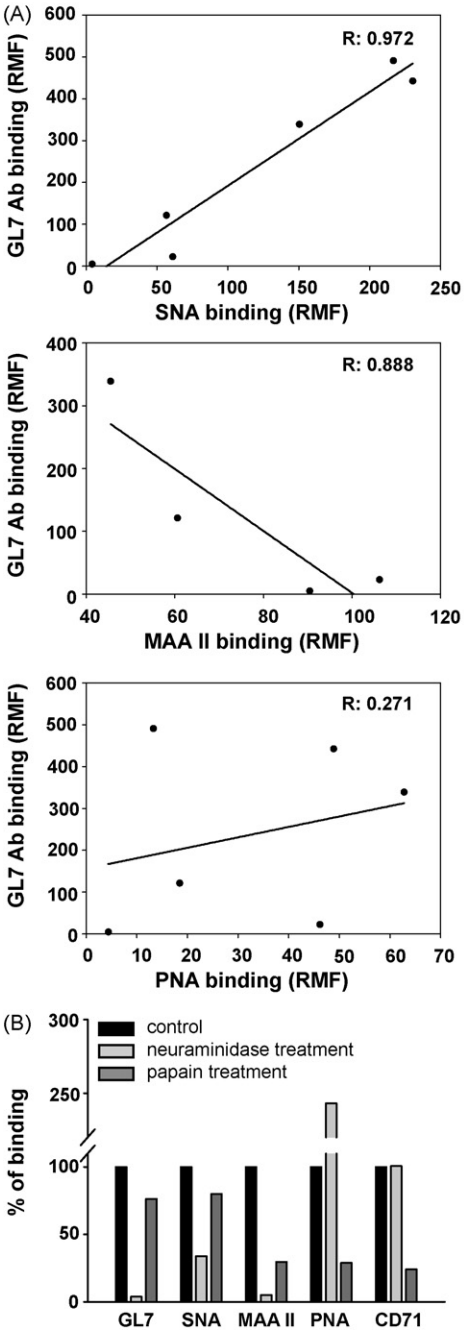

Fig. 5. Correlation of GL7 expression with lectin binding to the cells surface and enzyme sensitivity of the GL7 epitope. (A) Six different cell types (primary human T and B lymphocytes, Ramos and Daudi human B lymphomas, Jurkat T and THP-1 monocyte cell lines) were stained with GL7 Ab, SNA lectin, MAA II lectin and PNA lectin. GL7 expression shows strong positive correlation with SNA binding (upper diagram). There is a strong negative correlation between binding of GL7 Ab and MAA II (middle diagram), while no correlation is detected between GL7 Ab and PNA binding (lower diagram). The data were fitted to linear regression program (*R*: regression coefficient). (B) Human tonsillar B cells were treated with neuraminidase from Vibrio cholerae, with papain from Papaya latex or left untreated, and binding of GL7 Ab, SNA, MAA or PNA and anti-CD71 was analyzed. RMF values of controls were taken as 100%.

Y: non-specific amino acid residue) almost fully removed the cell surface CD71 from human B lymphocytes, while had only a partial (25–30%) effect on the level of bound GL7 Ab, similarly to SNA lectin. This suggests that the GL7 epitope cannot be linked to a single papain-sensitive protein.

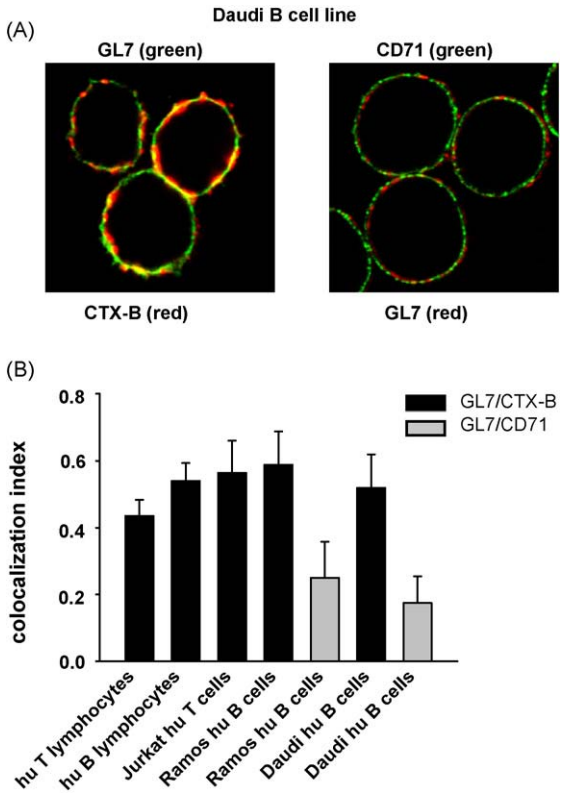

Fig. 6. GL7 is highly raft-associated in the membrane of human lymphocytes. Different human lymphocytes were stained with GL7 Ab and CTX-B or anti-CD71 and analyzed by confocal microscopy. Representative confocal images of stained Daudi cells are displayed (A). Colocalization indices (derived from ~100 ROIs/cell type) are also shown as mean ± SD for GL7 Ab and CTX-B or anti-CD71 (B).

3.5. GL7 is highly raft-associated on the lymphocyte surface

Since there are several sialoglycoproteins known to associate and function with lipid rafts (e.g. CD24, CD44), the membrane localization of the GL7 epitope was also analyzed by staining Ramos and Daudi B cell lines and Jurkat T cells as well as primary T and B lymphocytes with GL7 antibody and CTX-B bound to GM1 ganglioside, as a lipid raft marker. Anti-CD71 antibody was used to visualize non-raft membrane regions. The GL7 epitope displayed a constitutive and high extent of raft-association in the examined cells, as indicated by the high colocalization index, whereas CD71-GL7 colocalization was weak or moderate (Fig. 6A and B). Furthermore, activated rat and mouse lymphocytes also have high GL7-CTX-B colocalization (data not shown). Flow cytometric detergent resistance (FCDR) measurements were also carried out on Ramos B cells. The FCDR index of GL7 falls between those of GM_1 ganglioside and CD71 (Table 1). MBCD treatment of cells, removing approximately 40–50% of the plasma membrane cholesterol, made GL7 almost completely detergent soluble, which further confirms the raft-association of the epitope.

Table 1
FCDR values of GL7 epitope, GM_1 ganglioside and CD71 transferrin receptor measured on Ramos B cells.[a]

Cell surface molecule	FCDR	
	Control cells	MBCD-treated cells
GL7	0.503	0.064
GM_1 (raft resident)	1.000	0.449
CD71 (non-raft protein)	0.192	0.030

[a] Values are means of three independent measurements (S.E.M.: 0.3–8.5%).

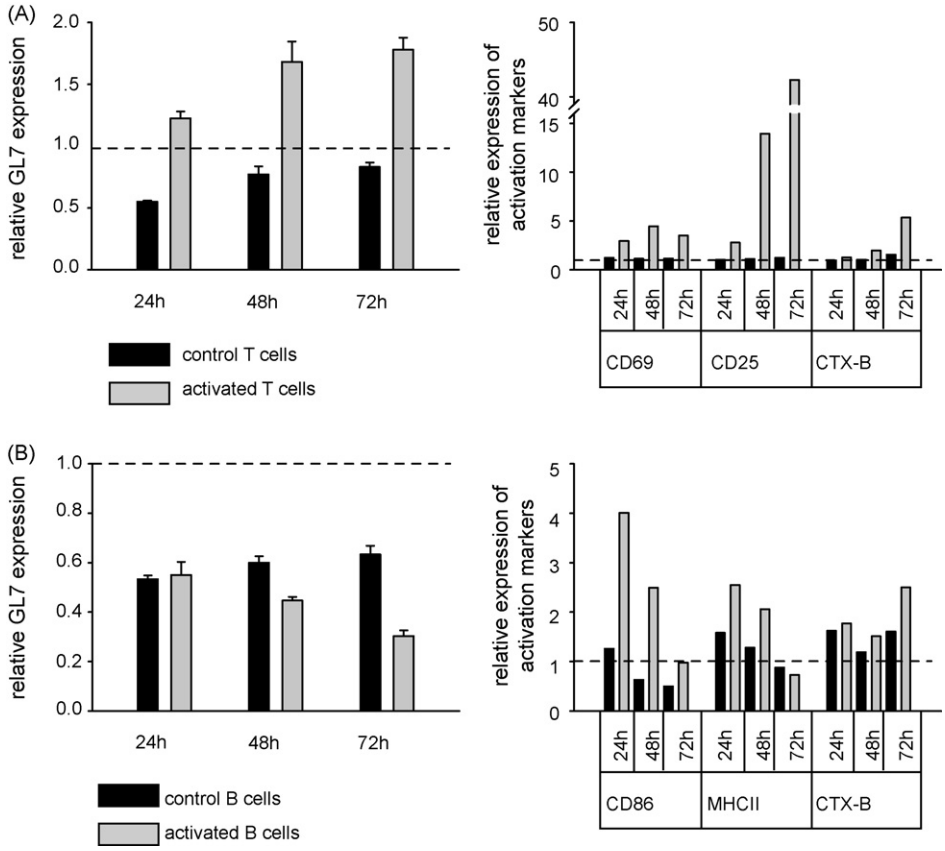

Fig. 7. Expression of the GL7 epitope is increased in human T lymphocytes and decreased in B cells upon activation. (A) Human periferal blood T cells were stimulated or not with anti-CD3 and expression of the GL7 epitope was monitored by flow cytometry (left diagram). Simultaneously changes in the expression of CD69 and CD25 activation markers and GM_1-gangliozide was also monitored (right diagram). (B) Human tonsillar B lymphocytes were activated or not with anti-IgM + G and expression of the GL7 epitope was analyzed by flow cytometry (left diagram). Simultaneously changes in the expression of CD86, MHCII and GM_1-gangliozide was also measured (right diagram). Relative RMF values, taking expression levels 1 at 0 h (dashed line), are shown.

3.6. Activation bi-directionally affects GL7 expression in lymphocytes

It was discussed by many papers [24,25], that glycosylation is determined by differentiation and activation stage of a given cell type. We were interested whether the expression of the GL7 epitope is altered upon activation of human lymphocytes. *In vitro* stimulation of human primary T and B lymphocytes was carried out with anti-CD3 and anti-IgM + G, respectively. Expression of GL7 and activation markers was assayed simultaneously, by flow cytometry. Interestingly, in activated T lymphocytes GL7 expression was elevated, while in B lymphocytes the expression of the GL7 epitope slightly decreased relative to the control/quiescent cells (Fig. 7). When naïve ($CD27^-$) B cells were activated and analyzed, we got the same result (data not shown). This result shows that although human lymphocytes constitutively express GL7, the epitope density is cell-type and activation dependent.

4. Discussion

Mammalian cells are covered by the so called glycocalyx, consisting of glycoproteins, glycolipids and proteoglycans. The biosynthesis of these glycan chains involves more than sixty glycan-modifying enzymes the expression of which is differentially regulated in various tissues and changing during ontogenesis and/or activation. Sias are typical monosaccharide units on the glycan chains of glycoproteins or glycolipids [1,3]. Siglecs are a growing family of lectins with selective binding to Sia-containing carbohydrate motifs and are thought to play an important role in immune regulation [7]. Most cells in the mouse and also in the human immune system express one or more siglecs. Each siglec has a unique specificity for sialylated ligands and most of them contain intracellular signaling motifs suggesting mediation of distinct or partially overlapping regulatory or adhesion function [6]. CD22, an α2,6-sialylated glycan binding siglec undoubtedly plays an important role in regulating B cell activation, however the exact mechanism of this regulation is still unclear [26].

GL7, a rat monoclonal IgM was also shown to recognize α2,6-sialylated glycans, but in contrast to CD22 it prefers Neu5Ac but not Neu5Gc in mice [16]. GL7 showed differential staining pattern in mice and recently, a negative correlation between GL7 and CD22 epitope expression in activated mouse B cells was demonstrated [14,16]. This is due to the inactivation of CMAH enzyme, converting Neu5Ac to Neu5Gc, in activated lymphocytes. Since a mutation occurred in the Cmah gene during evolution, Neu5Gc is not found in human [20]. As a result of this mutation, in contrast to rodents, human lymphocytes constitutively and exclusively express the Neu5Ac-containing GL7 epitope among peripheral immune cells and its level bi-directionally changes upon activation. Contrary to mouse CD22, human CD22 equally well binds either Neu5Ac or Neu5Gc but the binding capacity is also dependent on underlying sugar motifs. It was published that CD22 but not GL7 Ab binding prefers sulfated glycans [27]. This suggests that the preferential epitope in human is also different for GL7 Ab and for CD22. It was also demonstrated that B lymphocytes in germinal centers almost completely lack the sulfated determinants, but weakly expressed the non-sulfated ones [27]. This finding is in good correlation with

our results showing weak GL7 staining of germinal center B cells but strong staining in the surrounding IgD^{hi} area. Interestingly, in mice GL7 and IgD expression showed strong negative correlation in the spleen [17].

In humans not only the glycosylation pattern (caused by changes in enzyme levels and activities) but the expression profile and the specificity of certain carbohydrate binding receptors show significant changes compared to rodents [16]. Also, the structure of human secondary lymphoid organs show detectable histological alterations [14]. Expression of GL7 epitope cannot be regulated only by ST6Gal I and CMAH enzymes implicated in regulation of GL7 level. Since Cmah gene is inactive in human, and ST6Gal is also expressed by $GL7^-$ monocytes and DCs [20,28], further yet unidentified enzymes should also be assumed to modulate the amount of the epitope.

The characteristic signaling motifs in the intracellular part of siglecs strongly suggest their role in cell signaling however the ligands may also mediate inverse signals. CD22 was also shown to influence T cell activation upon binding not fully characterized ligands [29]. CD24 is a sialylated phosphatidyl-inositol anchored membrane protein that is able to provide co-stimulatory signals to T cells [26,30]. Moreover the newly identified siglec10 (siglec G in mice) was recently shown to bind CD24 [31], although their signaling function is completely unknown yet. The high and constitutive raft-association of GL7 epitope observed on mouse, rat (data not shown) and human lymphocytes suggest that GL7 epitope-containing proteins may receive and transmit signals through lipid raft.

Although previous precipitation results suggested a 35 kDa membrane glycoprotein on activated mouse B cells [8], the nature of the GL7 epitope bearing molecules is still unclear, consistent with the full neuraminidase- and partial papain-sensitivity shown by the present data. The GL7 carbohydrate epitope can be linked to either one or more glycoproteins or glycolipids as well, depending on the cell type.

In conclusion, the presented data clearly demonstrate that the expression profile of GL7 is different in human and rodents. The constitutively expressed GL7 epitope in human is lymphocyte-restricted and shows an activation dependent bi-directional regulation, up- and down-regulation in T and B cells, respectively. The regulated expression and the strong raft-association of GL7 epitope on either murine or human lymphocytes allow us to suggest a functional role for GL7 epitope and/or some supposed counterpart, however this function may be different in rodents and humans.

Acknowledgements

The financial support from the Hungarian National Science Fund (OTKA grants T49696 to J.M., K72026 to A.E.), the National Office of Research and Development (Pázmány grant RET-06/2006, to J.M.) and the support from the Hungarian Academy of Sciences are gratefully acknowledged. The authors are grateful to Judit Pozsgay for preparing all cryosections.

References

[1] Marth JD, Grewal PK. Mammalian glycosylation in immunity. Nat Rev Immunol 2008;8:874–87.
[2] van Kooyk Y, Rabinovich GA. Protein–glycan interactions in the control of innate and adaptive immune responses. Nat Immunol 2008;9:593–601.
[3] Taylor M, Drickamer K. Introduction to glycobiology. Oxford: Oxford University Press; 2003.
[4] Harduin-Lepers A, Vallejo-Ruiz V, Krzewinski-Recchi MA, Samyn-Petit B, Julien S, Delannoy P. The human sialyltransferase family. Biochimie 2001;83:727–37.
[5] Takashima S. Characterization of mouse sialyltransferase genes: their evolution and diversity. Biosci Biotechnol Biochem 2008;72:1155–67.
[6] Crocker PR, Paulson JC, Varki A. Siglecs and their roles in the immune system. Nat Rev Immunol 2007;7:255–66.
[7] Varki A, Angata T. Siglecs—the major subfamily of I-type lectins. Glycobiology 2006;16:1R–27R.
[8] Laszlo G, Hathcock KS, Dickler HB, Hodes RJ. Characterization of a novel cell-surface molecule expressed on subpopulations of activated T and B cells. J Immunol 1993;150:5252–62.
[9] Han S, Dillon SR, Zheng B, Shimoda M, Schlissel MS, Kelsoe G. V(D)J recombinase activity in a subset of germinal center B lymphocytes. Science 1997;278:301–5.
[10] Han S, Zheng B, Schatz DG, Spanopoulou E, Kelsoe G. Neoteny in lymphocytes: *Rag1* and *Rag2* expression in germinal center B cells. Science 1996;274:2094–7.
[11] Kendall PL, Yu G, Woodward EJ, Thomas JW. Tertiary lymphoid structures in the pancreas promote selection of B lymphocytes in autoimmune diabetes. J Immunol 2007;178:5643–51.
[12] Otero DC, Anzelon AN, Rickert RC. CD19 function in early and late B cell development: I. Maintenance of follicular and marginal zone B cells requires CD19-dependent survival signals. J Immunol 2003;170:73–83.
[13] Hathcock KS, Pucillo CE, Laszlo G, Lai L, Hodes RJ. Analysis of thymic subpopulations expressing the activation antigen GL7. Expression, genetics, and function. J Immunol 1995;155:4575–81.
[14] Cervenak L, Magyar A, Boja R, Laszlo G. Differential expression of GL7 activation antigen on bone marrow B cell subpopulations and peripheral B cells. Immunol Lett 2001;78:89–96.
[15] Murasawa M, Okada S, Obata S, Hatano M, Moriya H, Tokuhisa T. GL7 defines the cycling stage of pre-B cells in murine bone marrow. Eur J Immunol 2002;32:291–8.
[16] Naito Y, Takematsu H, Koyama S, Miyake S, Yamamoto H, Fujinawa R, et al. Germinal center marker GL7 probes activation-dependent repression of N-glycolylneuraminic acid, a sialic acid species involved in the negative modulation of B-cell activation. Mol Cell Biol 2007;27:3008–22.
[17] Hennet T, Chui D, Paulson JC, Marth JD. Immune regulation by the ST6Gal sialyltransferase. Proc Natl Acad Sci USA 1998;95:4504–9.
[18] Wuensch SA, Huang RY, Ewing J, Liang X, Lau JT. Murine B cell differentiation is accompanied by programmed expression of multiple novel β-galactoside α2,6-sialyltransferase mRNA forms. Glycobiology 2000;10:67–75.
[19] Brinkman-Van der Linden EC, Sjoberg ER, Juneja LR, Crocker PR, Varki N, Varki A. Loss of N-glycolylneuraminic acid in human evolution. Implications for sialic acid recognition by siglecs. J Biol Chem 2000;275:8633–40.
[20] Chou HH, Takematsu H, Diaz S, Iber J, Nickerson E, Wright KL, et al. A mutation in human CMP-sialic acid hydroxylase occurred after the Homo-Pan divergence. Proc Natl Acad Sci USA 1998;95:11751–6.
[21] Csomor E, Bajtay Z, Sandor N, Kristof K, Arlaud GJ, Thiel S, et al. Complement protein C1q induces maturation of human dendritic cells. Mol Immunol 2007;44:3389–97.
[22] Boyum A. Isolation of mononuclear cells and granulocytes from human blood. Isolation of mononuclear cells by one centrifugation, and of granulocytes by combining centrifugation and sedimentation at 1 g. Scand J Clin Lab Invest Suppl 1968;97:77–89.
[23] Gombos I, Bacso Z, Detre C, Nagy H, Goda K, Andrasfalvy M, et al. Cholesterol sensitivity of detergent resistance: a rapid flow cytometric test for detecting constitutive or induced raft association of membrane proteins. Cytometry A 2004;61:117–26.
[24] Varki A. Sialic acids as ligands in recognition phenomena. Faseb J 1997;11:248–55.
[25] Comelli EM, Sutton-Smith M, Yan Q, Amado M, Panico M, Gilmartin T, et al. Activation of murine $CD4^+$ and $CD8^+$ T lymphocytes leads to dramatic remodeling of N-linked glycans. J Immunol 2006;177:2431–40.
[26] Walker JA, Smith KG. CD22: an inhibitory enigma. Immunology 2008;123:314–25.
[27] Kimura N, Ohmori K, Miyazaki K, Izawa M, Matsuzaki Y, Yasuda Y, et al. Human B-lymphocytes express α2-6-sialylated 6-sulfo-N-acetyllactosamine serving as a preferred ligand for CD22/Siglec-2. J Biol Chem 2007;282:32200–7.
[28] Videira PA, Amado IF, Crespo HJ, Alguero MC, Dall'Olio F, Cabral MG, et al. Surface α2-3- and α2-6-sialylation of human monocytes and derived dendritic cells and its influence on endocytosis. Glycoconj J 2008;25:259–68.
[29] Bai XF, Li O, Zhou Q, Zhang H, Joshi PS, Zheng X, et al. CD24 controls expansion and persistence of autoreactive T cells in the central nervous system during experimental autoimmune encephalomyelitis. J Exp Med 2004;200:447–58.
[30] Hubbe M, Altevogt P. Heat-stable antigen/CD24 on mouse T lymphocytes: evidence for a costimulatory function. Eur J Immunol 1994;24:731–7.
[31] Chen GY, Tang J, Zheng P, Liu Y. CD24 and Siglec-10 selectively repress tissue damage-induced immune responses. Science 2009;323:1722–5.

Chapter 9

General discussion

The immunogenicity of cholesterol had been debated for long, because of its widespread distribution in mammalian cell membranes and lipoproteins and of its important and multifaceted biological role. Since 1977 several laboratories have reported on the complement system activation with involvement of cholesterol-specific antibodies in mice and rabbit (Alving et al., 1996; Swartz et al., 1988). Furthermore, an interesting and surprising discovery was made that naturally occurring antibodies against cholesterol, with yet unknown functions, are present in normal human sera (Alving et al., 1989). Therefore, many workgroups started to work on generating monoclonal cholesterol-specific antibodies for investigating the role of natural ACHAs in cholesterol-dependent cell functions and diseases. Swartz et al. found cholesterol to be surprisingly immunogenic when they immunized mice with cholesterol-rich liposome together with lipid A as an adjuvant. The generated cholesterol-specific 2C5-6 mAb bound to crystalline cholesterol and lipoproteins, and had complement-fixing capacity (Dijkstra et al., 1996; Swartz et al., 1988). This antibody was later applied to visualize cholesterol in the skeletal muscle of rats (Clarke et al., 2000). Perl-Treves and co-workers used another strategy to produce monoclonal ACHAs. They have implanted cholesterol monohydrate crystals in the spleen of mice (Perl-Treves et al., 1996). The produced 58B1 monoclonal antibody did not recognize the cholesterol molecule itself, but rather defined molecular motifs exposed on some of the crystal faces. Direct visualization of plasma membrane clustered cholesterol with the 58B1 mAb could also be obtained, but only when cells were artificially enriched with cholesterol (Kruth et al., 2001). However, these monoclonal antibodies were all IgM type and none of them were capable of binding to intact cell surface.

In contrast, our novel IgG monoclonal antibodies, AC1 and AC8, bound with low/intermediate avidity to the membrane of murine and human lymphocytes and macrophage cell lines *(Chapter 4, Figure 3)*. Their cell surface binding could be further enhanced by a limited papain digestion of long, protruding, extracellular protein domains *(Chapter 4, Figure 3)*, indicating that the accessibility of the supposedly small epitope is a critical factor for Ab binding. When surface plasmon resonance experiments were utilized, a medium affinity binding of AC8 Ab was measured to cholesterol-rich liposomes used in generating the antibody *(Chapter 7, Figure 1)*. These liposomes do not completely represent a cell membrane, but are suitable for estimation of the antibody's affinity. Exposure of cholesterol epitopes

may change during apoptosis or under pathological conditions (e.g. tumors, pathogen infections, cardio-vascular diseases) possibly due to the alteration of molecular composition, curvature or 'surface smoothness' of the involved membrane regions or other cholesterol-containing structures. In accordance with this, elevated ACHA level in human sera has been revealed in atherosclerosis, chronic viral infections (HIV-1 and HCV) and cancer (Biro et al., 2003; Egri and Orosz, 2006; Horvath et al., 2001a; Horvath et al., 2001b).

The high degree of colocalization between the IgG ACHA and CTX-B or anti-caveolin-1 antibodies indicates that rafts and caveolae can be considered as preferential binding sites for ACHAs in the plasma membrane *(Chapter 4, Figure 4; Chapter 5, Table 1)*. In lymphocytes and macrophages cholesterol is locally enriched in lipid rafts or, to a lesser extent, in clathrin-coated pits (Matko and Szollosi, 2005), consistent with our findings. The AC8 Ab intracellularly colocalized with markers of Golgi complex and ER and more weakly with marker of lysosomes *(Chapter 4, Figure 4)*. These organelles have relatively high cholesterol content, since transport of cholesterol occurs through them (Smart et al., 1996; Underwood et al., 1998). Specificity of our antibodies was further confirmed using cholesterol-modulating agents. Either cholesterol oxidase or filipin III could substantially reduce binding of AC8 to either treated cells or DRMs *(Chapter 4, Figure 5)*. These results all suggest that AC8 Ab is capable of marking cholesterol-rich lipid raft microdomains *(reviewed in Chapter 6)*. Binding properties of the new IgG ACHAs allow further possible applications in the study of lipid rafts in functions of immune cells, such as antigen presentation by APCs (Gombos et al., 2004; Poloso and Roche, 2004), receptor-mediated signal transduction in lymphocytes or myeloid cells (Pizzo and Viola, 2004) and the uptake of various pathogens and particles (e. g. influenza virus, apoptotic bodies) by phagocytes (Rosenberger et al., 2000; Yoshizaki et al., 2008). The question is whether binding of ACHAs to the membrane microdomains of these cells can modulate raft-dependent processes and, if so, how. However, such modulatory effects are most likely limited to those cells to which ACHAs can bind to a sufficient extent.

The ability of monoclonal IgG ACHAs to modulate immune functions was demonstrated by our collaboration partner, who found that target cell-bound AC1 and AC8 antibodies could inhibit *in vitro* HIV-1 (x4 T-tropic IIIB and R5 Ada-M strains) production *(Chapter 7, Figure 6)*. This inhibition might be dependent on cell type, the nature of the virus strain, and the assay conditions. The inhibitory effects of AC1

and AC8 cholesterol-specific antibodies on monocyte-derived macrophages and MT-4 T cells were comparable to those previously reported for anti-PIP antibody exhibiting neutralizing activity and blocking infection of PBMCs by two primary isolates of HIV-1 (Brown et al., 2007). Washing out of ACHAs prior to (or after) infection or their continuous supplementation throughout culturing did not significantly affect the final HIV-1 production. This suggests that the most likely phase that is inhibited is the attachment/anchorage of the virus to the target cell surface *(Chapter 7, Figure 7).*

Receptors, co-receptors in the cell membranes are usually not randomly distributed and, among others, their lipid environment can also control their movement and interactions. As shown by a body of data, cholesterol is indeed required for the interaction between gp120/gp41 trimers on the surface of HIV-1 and their receptor/co-receptor counterparts on the target cells. It seems that cholesterol is a critical lipid for stabilization of co-receptor protein clusters with multiple membrane-spanning helices in raft microdomains, such as most, but not all chemokine receptors (Pucadyil and Chattopadhyay, 2006).

In the plasma membrane of the investigated cell types, CD4 is constitutively and highly, whereas CXCR4 is much more weakly raft-localized *(Chapter 7, Figure 3).* Their localization and clustering in distinct membrane microdomains on HIV-1 permissive target cells was proposed earlier (Kozak et al., 2002). Binding of the cholesterol-specific mAb (AC8), but not of its Fab fragment or antibodies against non-raft membrane proteins, to the cells increased both CD4-CXCR4 colocalization and the raft-association of CXCR4 by approximately two-fold *(Chapter 7, Figure 4).* These observations, confirmed by FRET data *(Chapter 7, Figure 4)* and ganglioside staining *(Chapter 7, Figure 2),* together suggest a view that ACHAs may induce lateral clustering of cholesterol-rich lipid rafts (or caveolas) and thus modulate the interaction pattern between raft gangliosides, CD4 and CXCR4, which are all critical in membrane attachment/entry of the virus. Lateral diffusion features (assessed by FCS measurements) of the HIV-1 receptors, CD4 and CXCR4, gave further support to this view. In untreated control cells the CD4 diffused slower than the non-raft membrane protein CD2, and the diffusional rate of CXCR4 was significantly higher than that of CD4. The lateral mobility of CXCR4 but not of CD4 decreased substantially upon AC8 binding, having thereby these two recpetors similar diffusion coefficients *(Chapter 7, Figure 5 and Table 1).* The 2D diffusion of CD2 has been

left unchanged that substantiates the selectivity of AC8 effect on CXCR4 mobility *(Chapter 7, Figure 5)*. All these data are consistent with the picture that AC8 colocalizes (engages) the chemokine receptor and CD4 into the same compartment. It has been revealed earlier that the diffusion of CD4 could be restricted by elevated expression of G_{M3} ganglioside in a mouse T cell line (Rawat et al., 2008). This, in turn, reduced HIV-1 Env-mediated fusion by interfering with the lateral association of HIV-1 receptors (Rawat et al., 2004).

Based on these substantial changes in the dynamic membrane organization of HIV-1 receptors without masking the CD4 and CXCR4 HIV-1 receptors *(Chapter 7, Figure 1)*, it is postulated that the AC8 mAb can 'mimic' the action of viral glycoprotein gp120 in terms of co-aggregating HIV-1 receptors and co-receptors *(Chapter 7, Figure 8)*. These data also concur with the findings that gp120-CD4 engagement leads to a cholesterol-sensitive lateral redistribution of membrane microdomains and a subsequent assembly of the virus internalization complex (Manes et al., 2000). Furthermore, Nguyen et al. demonstrated that anti-CD4 beads occurred dynamic reorganization of chemokine receptors and lipid rafts to the site of CD4 engagement (Nguyen et al., 2005). Similarly, substantial reorganization of ErbB membrane proteins was reported upon cross-linking of gangliosides through cholera toxin B in breast tumor cells (Nagy et al., 2002).

Induction of broadly neutralizing antibodies is an essential prerequisite of an effective anti-HIV-1 vaccine. These antibodies can be specific to Env glycoproteins of the virus, such as 2F5, 4E10 or 2G12 (Calarese et al., 2003; Kunert et al., 2004; Zwick et al., 2004). However, alternative approaches for interfering with HIV-1 entry to target cells utilizing drugs or antibodies against cellular structures (CD4, chemokine receptors, HLA class I and II, adhesion molecules) involved in the entry process seem to be equally important (Phogat et al., 2007). Since cholesterol also has a major role in these processes, cholesterol-specific antibodies may also merit consideration.

Not just cholesterol, but several glycoconjugates in the mammalian cell membrane are also involved in the immune response. Sialic acid is frequently the glycan terminal sugar and it may modulate immune interactions. It can be found on both glycoproteins or glycolipids (Taylor and Drickamer, 2003). Siglecs are a growing family of lectins with selective binding to Sia-containing carbohydrate motifs and are thought to play an important role in immune regulation (Varki and

Angata, 2006). Most cells in the mouse and also in the human immune system express one or more siglecs. CD22, known to regulate B cell activation, is an α2,6-sialylated glycan binding siglec, preferring Neu5Gc (Walker and Smith, 2008). GL7, a rat monoclonal IgM was also shown to recognize α2,6-sialylated glycans, but in contrast to CD22, it binds to a Neu5Ac-containing epitope in mice (Naito et al., 2007). The CMAH enzyme, which converts Neu5Ac to Neu5Gc, may conversely regulate level of CD22 ligand and GL7 epitope. The other important enzyme that is implicated in the regulation of the GL7 epitope is the sialyltransferase ST6Gal I generating an α2,6-linkage of sialic acid to underlying N-acetyllactosamine (Weinstein et al., 1982). The amount of these and other enzymes, involved in sialic acid metabolism, is activation dependent. It has been demonstrated, that strong CMAH and moderate ST6Gal I repression occures in activated mouse B cells (Naito et al., 2007) that might contribute to the activation-dependent expression of GL7. Another workgroup found the upregulation of ST6Gal I gene expression upon B lymphocyte activation (Comelli et al., 2006), which also supports the appearance of the epitope. The inconsistency of the ST6GL I enzyme levels in the two experiments might be explained by the different assay conditions.

An exon deletion in the Cmah gene eliminated human expression of Neu5Gc (Chou et al., 1998). As a result of this mutation, in contrast to rodents, human lymphocytes constitutively and exclusively express the Neu5Ac-containing GL7 epitope among blood leukocytes *(Chapter 8, Figure 2)*. Contrary to mouse, human CD22 equally well binds either Neu5Ac or Neu5Gc but it prefers sulfated glycans (Kimura et al., 2007). This suggests that the preferential epitope in human is also different for GL7 Ab and for CD22. Expression of GL7 epitope cannot be regulated only by ST6Gal I and CMAH enzymes, since active CMAH is absent in human, and ST6Gal I is expressed by $GL7^-$ immune cells as well, like monocytes and DCs (Chou et al., 1998; Videira et al., 2008). Therefore, further yet unidentified enzymes should also be assumed to modulate the amount of the epitope.

In humans not only the glycosylation pattern (caused by changes in enzyme levels and activities) but the expression profile and the specificity of certain carbohydrate binding receptors show significant changes compared to rodents (Naito et al., 2007). Also, the structure of human secondary lymphoid organs shows detectable histological alterations (Cervenak et al., 2001). This finding is in good

correlation with our results showing weak GL7 staining of germinal center B cells but strong staining in the surrounding IgD^{hi} area *(Chapter 8, Figure 3)*, whereas in mice GL7 and IgD expression showed strong negative correlation in the spleen (Hennet et al., 1998). Interestingly, GL7 Ab and SNA lectin, known to be specific to α2-6 sialic acid, displayed an overlapping staining with their preferential binding to $CD19^+$ B cell regions over T lymphocytes *(Chapter 8, Figure 4)*. Nevertheless, SNA has a broader binding spectrum by intensive staining of whole germinal centers. This indicates that although GL7 Ab and SNA have α2-6 sialic acid epitope/ligand in common, but underlying sugar motifs or supposed amino acid or lipid moieties of the GL7 epitope determine binding of the Ab.

The characteristic signalling motifs (usually ITIM) in the intracellular part of most siglecs strongly suggest their role in cell signalling and they ligands may also mediate inverse signals. CD24 is a sialylated GPI-anchored membrane protein that is able to provide costimulatory signals to T cells (Hubbe, 1994, 24, 731). Moreover the newly identified siglec10 (siglec G in mice) was recently shown to bind CD24 (Chen, 2009, 323), although their signalling function is yet unknown. The high and constitutive raft-association of GL7 epitope observed on rodent and human lymphocytes *(Chapter 8, Figure 6)* suggest that GL7 epitope-containing proteins may receive and transmit signals through lipid rafts.

Although previous precipitation results suggested a 35 kDa membrane glycoprotein on activated mouse B cells (Laszlo et al., 1993), the nature of the GL7 epitope-bearing molecules is still unclear, consistent with the full neuraminidase- and partial papain-sensitivity shown by the present data *(Chapter 8, Figure 5)*. Therefore, the GL7 carbohydrate epitope can be linked to either a single protein or to a mixture of various cell surface glycosylated proteins and/or lipids.

In conclusion, the similarity between IgG ACHAs and GL7 antibody is that their specificity is unconventional, since both antibodies recognize epitopes other than amino acid residues of proteins. The monoclonal cholesterol-specific IgG antibodies are capable of marking lipid rafts and modulating cholesterol/raft-dependent functions of immune cells. One nice demonstration of it is that *in vitro* HIV-1 production of human T cells and macrophages could be inhibited by action of these antibodies on the plasma membrane and HIV-1 receptors of target cells. Therefore, the novel ACHAs, recognizing ’properly clustered membrane cholesterol only’, seem useful to

investigate the eventual role of cholesterol in the process of virus entry, as well as may serve as a molecular basis for the development of new, combined lipid raft-oriented approaches in HIV-1 therapy. Beside this inhibitory effect, IgG ACHAs may modulate other immune functions as well. In case of GL7 antibody, recognizing a Neu5Ac-containing epitope, the presented data clearly demonstrate that the expression profile of GL7 is different in human and rodents. Although, the presence of the epitope in human is also lymphocyte-restricted but it is constitutively expressed, while in mouse GL7 is a late activation antigen. The specific expression of the GL7 epitope and its high degree of raft-association on lymphocytes allow us to suggest a functional role for GL7 epitope and/or some supposed counterparts.

Reference list

Alving C. R., Swartz G. M., Jr. and Wassef N. M. (1989) Naturally occurring autoantibodies to cholesterol in humans. *Biochem Soc Trans* **17**, 637-9.

Alving C. R., Swartz G. M., Jr., Wassef N. M., Ribas J. L., Herderick E. E., Virmani R., Kolodgie F. D., Matyas G. R. and Cornhill J. F. (1996) Immunization with cholesterol-rich liposomes induces anti-cholesterol antibodies and reduces diet-induced hypercholesterolemia and plaque formation. *J Lab Clin Med* **127**, 40-9.

Biro A., Horvath A., Varga L., Nemesanszky E., Csepregi A., David K., Tolvaj G., Ibranyi E., Telegdy L., Par A., Romics L., Karadi I., Horanyi M., Gervain J., Ribiczey P., Csondes M. and Fust G. (2003) Serum anti-cholesterol antibodies in chronic hepatitis-C patients during IFN-alpha-2b treatment. *Immunobiology* **207**, 161-8.

Brown B. K., Karasavvas N., Beck Z., Matyas G. R., Birx D. L., Polonis V. R. and Alving C. R. (2007) Monoclonal antibodies to phosphatidylinositol phosphate neutralize human immunodeficiency virus type 1: role of phosphate-binding subsites. *J Virol* **81**, 2087-91.

Calarese D. A., Scanlan C. N., Zwick M. B., Deechongkit S., Mimura Y., Kunert R., Zhu P., Wormald M. R., Stanfield R. L., Roux K. H., Kelly J. W., Rudd P. M., Dwek R. A., Katinger H., Burton D. R. and Wilson I. A. (2003) Antibody domain exchange is an immunological solution to carbohydrate cluster recognition. *Science* **300**, 2065-71.

Cervenak L., Magyar A., Boja R. and Laszlo G. (2001) Differential expression of GL7 activation antigen on bone marrow B cell subpopulations and peripheral B cells. *Immunol Lett* **78**, 89-96.

Chou H. H., Takematsu H., Diaz S., Iber J., Nickerson E., Wright K. L., Muchmore E. A., Nelson D. L., Warren S. T. and Varki A. (1998) A mutation in human CMP-sialic acid hydroxylase occurred after the Homo-Pan divergence. *Proc Natl Acad Sci U S A* **95**, 11751-6.

Clarke M. S., Vanderburg C. R., Bamman M. M., Caldwell R. W. and Feeback D. L. (2000) In situ localization of cholesterol in skeletal muscle by use of a monoclonal antibody. *J Appl Physiol* **89**, 731-41.

Comelli E. M., Sutton-Smith M., Yan Q., Amado M., Panico M., Gilmartin T., Whisenant T., Lanigan C. M., Head S. R., Goldberg D., Morris H. R., Dell A. and Paulson J. C. (2006) Activation of murine CD4+ and CD8+ T lymphocytes leads to dramatic remodeling of N-linked glycans. *J Immunol* **177**, 2431-40.

Dijkstra J., Swartz G. M., Jr., Raney J. J., Aniagolu J., Toro L., Nacy C. A. and Green S. J. (1996) Interaction of anti-cholesterol antibodies with human lipoproteins. *J Immunol* **157**, 2006-13.

Egri G. and Orosz I. (2006) Elevated anti-cholesterol antibody levels in the sera of non-small cell lung cancer patients. *Interact Cardiovasc Thorac Surg* **5**, 649-51.

Gombos I., Detre C., Vamosi G. and Matko J. (2004) Rafting MHC-II domains in the APC (presynaptic) plasma membrane and the thresholds for T-cell activation and immunological synapse formation. *Immunol Lett* **92**, 117-24.

Hennet T., Chui D., Paulson J. C. and Marth J. D. (1998) Immune regulation by the ST6Gal sialyltransferase. *Proc Natl Acad Sci U S A* **95**, 4504-9.

Horvath A., Banhegyi D., Biro A., Ujhelyi E., Veres A., Horvath L., Prohaszka Z., Bacsi A., Tarjan V., Romics L., Horvath I., Toth F. D., Fust G. and Karadi I. (2001a) High level of anticholesterol antibodies (ACHA) in HIV patients. Normalization of serum ACHA concentration after introduction of HAART. *Immunobiology* **203**, 756-68.

Horvath A., Fust G., Horvath I., Vallus G., Duba J., Harcos P., Prohaszka Z., Rajnavolgyi E., Janoskuti L., Kovacs M., Csaszar A., Romics L. and Karadi I. (2001b) Anti-cholesterol antibodies (ACHA) in patients with different atherosclerotic vascular diseases and healthy individuals. Characterization of human ACHA. *Atherosclerosis* **156**, 185-92.

Kimura N., Ohmori K., Miyazaki K., Izawa M., Matsuzaki Y., Yasuda Y., Takematsu H., Kozutsumi Y., Moriyama A. and Kannagi R. (2007) Human B-lymphocytes express α2-6-sialylated 6-sulfo-N-acetyllactosamine serving as a preferred ligand for CD22/Siglec-2. *J Biol Chem* **282**, 32200-7.

Kozak S. L., Heard J. M. and Kabat D. (2002) Segregation of CD4 and CXCR4 into distinct lipid microdomains in T lymphocytes suggests a mechanism for membrane destabilization by human immunodeficiency virus. *J Virol* **76**, 1802-15.

Kruth H. S., Ifrim I., Chang J., Addadi L., Perl-Treves D. and Zhang W. Y. (2001) Monoclonal antibody detection of plasma membrane cholesterol microdomains responsive to cholesterol trafficking. *J Lipid Res* **42**, 1492-500.

Kunert R., Wolbank S., Stiegler G., Weik R. and Katinger H. (2004) Characterization of molecular features, antigen-binding, and in vitro properties of IgG and IgM variants of 4E10, an anti-HIV type 1 neutralizing monoclonal antibody. *AIDS Res Hum Retroviruses* **20**, 755-62.

Laszlo G., Hathcock K. S., Dickler H. B. and Hodes R. J. (1993) Characterization of a novel cell-surface molecule expressed on subpopulations of activated T and B cells. *J Immunol* **150**, 5252-62.

Manes S., del Real G., Lacalle R. A., Lucas P., Gomez-Mouton C., Sanchez-Palomino S., Delgado R., Alcami J., Mira E. and Martinez A. C. (2000) Membrane raft microdomains mediate lateral assemblies required for HIV-1 infection. *EMBO Rep* **1**, 190-6.

Matko J. and Szollosi J. (2005) Regulatory aspects of membrane microdomain (raft) dynamics in live cells. In *Membrane microdomain signaling: lipid rafts in biology and medicine* (Edited by Mattson M. P.), p. 15-46. Humana Press Inc., Totowa, NJ.

Nagy P., Vereb G., Sebestyen Z., Horvath G., Lockett S. J., Damjanovich S., Park J. W., Jovin T. M. and Szollosi J. (2002) Lipid rafts and the local density of ErbB proteins influence the biological role of homo- and heteroassociations of ErbB2. *J Cell Sci* **115**, 4251-62.

Naito Y., Takematsu H., Koyama S., Miyake S., Yamamoto H., Fujinawa R., Sugai M., Okuno Y., Tsujimoto G., Yamaji T., Hashimoto Y., Itohara S., Kawasaki T., Suzuki A. and Kozutsumi Y. (2007) Germinal center marker GL7 probes activation-dependent repression of N-glycolylneuraminic acid, a sialic acid species involved in the negative modulation of B-cell activation. *Mol Cell Biol* **27**, 3008-22.

Nguyen D. H., Giri B., Collins G. and Taub D. D. (2005) Dynamic reorganization of chemokine receptors, cholesterol, lipid rafts, and adhesion molecules to sites of CD4 engagement. *Exp Cell Res* **304**, 559-69.

Perl-Treves D., Kessler N., Izhaky D. and Addadi L. (1996) Monoclonal antibody recognition of cholesterol monohydrate crystal faces. *Chem Biol* **3**, 567-77.

Phogat S., Wyatt R. T. and Karlsson Hedestam G. B. (2007) Inhibition of HIV-1 entry by antibodies: potential viral and cellular targets. *J Intern Med* **262**, 26-43.

Pizzo P. and Viola A. (2004) Lipid rafts in lymphocyte activation. *Microbes Infect* **6**, 686-92.

Poloso N. J. and Roche P. A. (2004) Association of MHC class II-peptide complexes with plasma membrane lipid microdomains. *Curr Opin Immunol* **16**, 103-7.

Pucadyil T. J. and Chattopadhyay A. (2006) Role of cholesterol in the function and organization of G-protein coupled receptors. *Prog Lipid Res* **45**, 295-333.

Rawat S. S., Gallo S. A., Eaton J., Martin T. D., Ablan S., KewalRamani V. N., Wang J. M., Blumenthal R. and Puri A. (2004) Elevated expression of GM3 in receptor-bearing targets confers resistance to human immunodeficiency virus type 1 fusion. *J Virol* **78**, 7360-8.

Rawat S. S., Zimmerman C., Johnson B. T., Cho E., Lockett S. J., Blumenthal R. and Puri A. (2008) Restricted lateral mobility of plasma membrane CD4 impairs HIV-1 envelope glycoprotein mediated fusion. *Mol Membr Biol* **25**, 83-94.

Rosenberger C. M., Brumell J. H. and Finlay B. B. (2000) Microbial pathogenesis: lipid rafts as pathogen portals. *Curr Biol* **10**, R823-5.

Smart E. J., Ying Y., Donzell W. C. and Anderson R. G. (1996) A role for caveolin in transport of cholesterol from endoplasmic reticulum to plasma membrane. *J Biol Chem* **271**, 29427-35.

Swartz G. M., Jr., Gentry M. K., Amende L. M., Blanchette-Mackie E. J. and Alving C. R. (1988) Antibodies to cholesterol. *Proc Natl Acad Sci U S A* **85**, 1902-6.

Taylor M. and Drickamer K. (2003) *Introduction to glycobiology*. University Press, Oxford.

Underwood K. W., Jacobs N. L., Howley A. and Liscum L. (1998) Evidence for a cholesterol transport pathway from lysosomes to endoplasmic reticulum that is independent of the plasma membrane. *J Biol Chem* **273**, 4266-74.

Varki A. and Angata T. (2006) Siglecs--the major subfamily of I-type lectins. *Glycobiology* **16**, 1R-27R.

Videira P. A., Amado I. F., Crespo H. J., Alguero M. C., Dall'Olio F., Cabral M. G. and Trindade H. (2008) Surface α2-3- and α2-6-sialylation of human monocytes and derived dendritic cells and its influence on endocytosis. *Glycoconj J* **25**, 259-68.

Walker J. A. and Smith K. G. (2008) CD22: an inhibitory enigma. *Immunology* **123**, 314-25.

Weinstein J., de Souza-e-Silva U. and Paulson J. C. (1982) Purification of a Gal beta 1 to 4GlcNAc alpha 2 to 6 sialyltransferase and a Gal beta 1 to 3(4)GlcNAc alpha 2 to 3 sialyltransferase to homogeneity from rat liver. *J Biol Chem* **257**, 13835-44.

Yoshizaki F., Nakayama H., Iwahara C., Takamori K., Ogawa H. and Iwabuchi K. (2008) Role of glycosphingolipid-enriched microdomains in innate immunity: microdomain-dependent phagocytic cell functions. *Biochim Biophys Acta* **1780**, 383-92.

Zwick M. B., Komori H. K., Stanfield R. L., Church S., Wang M., Parren P. W., Kunert R., Katinger H., Wilson I. A. and Burton D. R. (2004) The long third complementarity-determining region of the heavy chain is important in the activity of the broadly neutralizing anti-human immunodeficiency virus type 1 antibody 2F5. *J Virol* **78**, 3155-61.

Summary

For their normal functions, cells require membrane integrity. Beside proteins, lipids and carbohydrates are also important cell membrane components. Using monoclonal antibodies, we studied the role of membrane cholesterol and sialic acid in the function of mammalian immunocytes.

The new cholesterol specific IgG mAbs (AC1 and AC8), generated by us, bound to intact mouse and human immunocytes and they strongly colocalized with different lipid rafts markers, reflecting recognition of clustered cholesterol in live cells. A medium affinity binding of AC8 mAb to cholesterol-rich liposomes was estimated by surface plasmon resonance. The new monoclonal IgG ACHAs may thus serve as novel probes of membrane microdomains. This implicates further on the potential of ACHAs to modulate various raft-dependent functions of immune cells. In collaboration we have shown that these mAbs were able to inhibit *in vitro* HIV-1 infection/production of virus permissive human cells. In human T cells or monocytes, AC8 mAb induced lateral lipid raft clustering and promoted the association of CXCR4 co-receptor with both CD4 HIV-receptor and the lipid rafts. Thus, the IgG ACHAs can alter the receptor/microdomain architecture at the surface of human macrophages and T cells. Further investigations are required to elucidate the modulatory role of IgG ACHAs in other immune functions.

Using GL7 antibody that recognizes a sialic acid-containing epitope (GL7), our results show that this epitope is exclusively expressed by lymphocytes among human blood cells. In contrast to rodents, where GL7 is a late activation antigen, in human the epitope is constitutively expressed. In human tonsil, the GL7 epitope shows the highest expression in the B cell follicles by naïve B lymphocytes. Furthermore, in both B and T cells the epiotpe strongly colocalized with lipid rafts. The heterogeneous expression of GL7 on different B lymphocyte subsets and its lymphocyte-restricted presence indicate a role in lymphocyte function possibly *via* recognition by some Sia-binding proteins. Additional studies are needed to find the GL7-bearing molecules and their supposed receptors.

Hungarian Summary – Összefoglalás

A sejtek membránját fehérjék, lipidek, és szénhidrátok alkotják, melyek mind szükségesek a normális sejtműködéshez. Monoklonális ellenanyagok segítségével vizsgáltuk a membrán koleszterin és sziálsav szerepét az immunsejtek működésében.

Kutatásaink során a munkacsoportunk által létrehozott új koleszterin-specifikus ellenanyagokat (ACHA) alkalmaztuk. Ezen ellenanyagokról (AC1 és AC8) kimutattuk, hogy kötődnek a sejtmembránhoz. Antitestjeink a koleszterinben gazdag lipid raftokat és sejten belül is a lokálisan koleszterinben dús membrán struktúrákat (ER, Golgi-vezikulák) ismerik fel. Az AC8 ellenanyag közepes affinitással kötődik koleszterin-dús liposzómákhoz. Az AC1 és AC8 antitestek a jövőben a lipid tutajok új markerévé válhatnak. További eredményeink szerint az új IgG ACHA-k képesek gátolni az *in vitro* HIV-fertőzést/termelődést. A gátlás hátterében az antitesteknek a célsejtek membránjához való kötődése áll. Ennek következtében a HIV-1 receptorok (főként a CXCR4) egymáshoz, valamint lipid raftokhoz való helyzete megváltozik: a lipid raftok mérete növekedik, a CXCR4 raft-asszociációja fokozódik, membránban való mozgása lelassul. A vírus így nem képes a bonyolult, több lépéses horgonyzásra és ezáltal a célsejtbe való bejutásra. További kísérletek hivatottak feltárni ellenanyagaink moduláló szerepét más immunfolyamatokban.

Egy sziálsav-tartalmú epitópot felismerő antitest (GL7) kötődési tulajdonságait is vizsgáltuk humán immunsejteken, melyről korábban kimutatták, hogy aktivált egér T- és B-sejtekhez kötődik. Méréseink szerint a GL7 epitóp jelenléte emberben is limfocita-specifikus, azonban, egerekkel ellentétben, expressziója nyugvó, naív limfocitákon is kimutatható. Emberi mandulában a B-sejt follikulusok szélén elhelyezkedő naiv B-sejtek mutatják a legerősebb GL7 pozitivitást. Más B-sejt populációk és T-sejtek kisebb mértékben expresszálják az epitópot. Továbbá kimutattuk, hogy a GL7 epitóp a limfocita membrán raftokban nagy gyakorisággal fordul elő. A limfocita-korlátozott expresszió és az erős raft-asszociáltság arra utal, hogy a GL7 epitópnak szerepe lehet a T- és B-sejtek funkciójában, mely feltételezhetően valamely sziálsavat felismerő receptoron keresztül valósul meg. Az epitópot tartalmazó molekulá(k)nak és a felismreő receptor(ok)nak az azonosítása és jellemzése még további kísérleteket igényel.

Acknowledgements

I wish to thank all my friends and colleagues who worked with me during the period of my PhD training.

First of all I would like to thank my supervisors, Prof. János Matkó and Dr. Glória László for the confidence placed in me and their continous support during these projects. I also thank Prof. Anna Erdei, head of the Department of Immunology, for allowing me to join to the research running at the department.

I thank my friends and colleagues for their good advices and the friendly atmosphere: Mónika Ádori, Krisztián Papp, Zsuzsanna Szekeres, Endre Kiss, Helga Látos, Imre Gombos, Emese Izsépi, Noémi Sándor, Máté Maus, Adrienn Angyal, Hajna Péterfy, Nóra Terényi, Leonóra Himer, Emese Kemény, Andrea Isaák, József Prechl, András Lőrincz, Gabriella Sármay, Imre Kacskovics, Zsuzsa Bajtay, Prof. János Gergely, Erzsébet Veres (Böbe), Pásztor Márta, Árpád Mikesy (Papa), Zsuzsanna Greff and many others.

Last but not least I thank my family the help and support they provided me.

List of Publications

Papers:

1. Adrienn Bíró*, László Cervenak*, Andrea Balogh*, András Lőrincz, Katalin Uray, Anna Horváth, László Romics, János Matkó, George Füst, Glória László: **„Novel anti-cholesterol monoclonal immunoglobulin G antibodies as probes and potential modulators of membrane raft-dependent immune functions"**
   Journal of Lipid Research 2007. 48(1):19-29. ***IF: 4.336***

2. Imre Gombos, Gábor Steinbach, István Pomozi, Andrea Balogh, György Vámosi, Alexander Gansen, Glória László, Győző Garab, János Matkó: **„Some new faces of membrane microdomains: a complex confocal fluorescence, differential polarization, and FCS imaging study on live immune cells"**
   Cytometry A 2008. 73(3):220-229. ***IF: 3.259***

3. Endre Kiss, Péter Nagy, Andrea Balogh, János Szöllősi, János Matkó: **"Cytometry of raft and caveola membrane microdomains: from flow and imaging techniques to high throughput screening assays"**
   Cytometry A. 2008. 73(7):599-614. ***IF: 3.259***

4. Zoltán Beck*, Andrea Balogh*, Andrea Kis, Emese Izsépi, Adrienn Bíró, Glória László, László Cervenak, Károly Liliom, Gábor Mocsár, György Vámosi, George Füst, János Matkó: **"New cholesterol-specific antibodies remodel HIV-1 target cells' surface and inhibit their *in vitro* virus production"**
   Journal of Lipid Research 2010. 51(2):286-296. ***IF: 4.409***

5. Andrea Balogh*, Mónika Ádori*, Katalin Török, János Matkó, Glória László: **"Closer look into the GL7 antigen: Its spatio-temporally selective differential expression and localization in lymphoid cells and organs in human"**
   Immunology Letters 2009. doi: 10.1016/j.imlet.2009.12.008 ***IF: 2.858***

*Authors contributed equally to the work.

Conference abstracts:

1. Pozsgai M., Balogh A., Prechl J., László G.: **"A Ly77 (GL7) molekula szerkezeti és funkcionális vizsgálata scFv konstrukció segítségével"** *XXXIV. MIT Vándorgyűlés, Sopron, 2004*

2. M. Ádori, A. Balogh, Zs. Weiszhár, J. Prechl, J. Matko, G. László: **"Studies on Cell Specific Expression, Structure and Membrane Localization of a Late Lymphoid Activation Antigen Ly77 (GL7)"** *13th Symposium on Signal and Signal Processing in the Immune System, Balatonőszöd, Hungary, 2005*

3. M. Ádori, A. Balogh, Zs. Weiszhár, J. Prechl, J. Matko, G. László: **"Expression, Structure and Membrane Localization of Ly77 (GL7), a Supposed Adhesion Molecule, on Lymphoid and Myeloid Cells"** *XXXV. Congress of Hungarian Scociety for Immunology, Sopron, Hungary, 2005*

4. Balogh A., Lőrincz A., Cervenak L. László G., Matkó J.: **"Új monoklonális IgG anti-koleszterin ellenanyagok: koleszterin-gazdag membránok markerei és raft-függő immunfolyamatok potenciális modulátorai"** *V. Magyar Sejtanalitikai Konferencia, Budapest, 2006*

5. Balogh A., Lőrincz A., Cervenak L., Füst Gy., László G., Matkó J.: **"Új monoklonális IgG anti-koleszterin ellenanyagok: koleszterin-gazdag membránok markerei és raft-függő immunfolyamatok potenciális modulátorai"** *XXXVI. Membrán-transzport Konferencia, Sümeg, 2006*

6. A. Balogh, A. Lőrincz, L. Cervenak, G. Füst, G. László, J. Matko: **"Anti-cholestreol IgG-s: Probes and Functional Modulators of Cholesterol-rich Membrane Micordomains"** *1st European Congress of Immunology, Paris, France, 2006*

7. A. Balogh, A. Lőrincz, G. László, J. Matko: **"Anti-cholesterol IgG antibodies: novel probes of clustered membrane cholesterol (microdomains) in intact cells"** *10th Conference on Methods and Applications of Fluorescence, Salzburg, Austria, 2007*

8. A. Balogh, A. Lőrincz, L. Cervenak, G. Füst, G. László, J. Matko: **"Anti-cholesterol IgG antibodies: novel probes and potential modulators of cholesterol-rich membrane microdomains"** *14th Symposium on Signal and Signal Processing in the Immune System, Balatonőszöd, Hungary, 2007*

9. A. Balogh, A. Lőrincz, G. László, J. Matko: **"Anti-cholesterol IgG antibodies: novel probes and modulators of cholesterol-rich membrane microdomains"** *ISAC XXIV International Congress, Budapest, Hungary, 2008*

10. A. Balogh, Z. Beck, G. Mocsár, G. László, G. Füst, J. Matko: **"Cholesterol-specific IgG monoclonal antibodies inhibit *in vitro* HIV production by remodeling plasma membrane of target cells"** *XXXVII. Congress of Hungarian Scociety for Immunology, Budapest, Hungary, 2008*

11. A. Balogh, E. Izsépi, G. Mocsár, G. Vámosi, G. László, J. Matko: **"Effect of new cholesterol-specific IgG antibodies on distribution and lateral mobility of HIV-receptors assessed by confocal and FCS imaging"** *11th Conference on Methods and Applications of Fluorescence, Budapest, Hungary, 2009*

12. Balogh, M. Adori, J. Matko, G. László: **"Comparative study of GL7 expression in mouse and human"** *2nd European Congress of Immunology, Berlin, Germany, 2009*